

GEOLOGY OF THE PASSIVE MARGIN OFF NEW ENGLAND

by

JAMES ALBERT AUSTIN, JR.

B.A., Amherst College
(1973)

SUBMITTED IN PARTIAL FULFILLMENT
OF THE REQUIREMENTS FOR THE
DEGREE OF

DOCTOR OF PHILOSOPHY

at the

MASSACHUSETTS INSTITUTE OF TECHNOLOGY

and the

WOODS HOLE OCEANOGRAPHIC INSTITUTION

(December, 1978)

(i.e. February 1979)

Signature of Author _____

Joint Program in Oceanography, Massachusetts
Institute of Technology-Woods Hole Oceanographic
Institution, and the Department of Earth and
Planetary Sciences, Massachusetts Institute of
Technology, December, 1978.

Certified by _____

Thesis Supervisor, _____

Accepted by _____

Chairman, Joint Oceanography Committee in Earth
Sciences, Massachusetts Institute of Technology-
Woods Hole Oceanographic Institution

WITHDRAWN
FROM

GEOLOGY OF THE PASSIVE MARGIN OFF NEW ENGLAND

by

James Albert Austin, Jr.

Submitted to the Department of Earth & Planetary Sciences, Massachusetts Institute of Technology, and to the Department of Geology and Geophysics, Woods Hole Oceanographic Institution, on December 1, 1978, in partial fulfillment of the requirements for the Degree of DOCTOR OF PHILOSOPHY.

ABSTRACT

The results of a detailed geophysical investigation conducted by the Woods Hole Oceanographic Institution in 1975 have been used in conjunction with other available information to reconstruct the geologic history of the passive continental margin off New England. Rifting between northeastern North America and Morocco during the Middle-Late Triassic produced a complex series of horsts and grabens in Precambrian/Paleozoic crust. Intra-rift sediments consist of clastics, evaporites, and volcanics. Continental separation occurred and sea-floor spreading began 195-190 my B.P. The boundary between "normal" continental crust and crust radically altered by fracturing and intrusion may be represented by a pronounced basement "hinge zone". Prior to margin subsidence, extensive sub-

aerial erosion carved a "break-up unconformity"-reflector "K" which truncated pre-existing rift structures and which must be approximately the same age as the oldest oceanic crust. Within the overlying "drift" sediments, six acoustic horizons have been regionally traced and correlated with strata sampled by a well drilled on the western Scotian Shelf. The total sediment thickness of both rift and drift sequences beneath Georges Bank may be 13 km, of which more than 80% is Jurassic in age. A Mesozoic reef/carbonate platform complex situated on the outer shelf-upper slope was an effective sediment barrier until the early Late Cretaceous, when prograding clastics buried the complex. This carbonate build-up and its basement foundation of altered continental or oceanic crust are responsible for the geographic position and steepness (5-8°) of the present continental slope south of Georges Bank.

Name and Title of Thesis Supervisor: Dr. Elazar Uchupi,
Associate Scientist, Woods Hole Oceanographic Institution,
Woods Hole, Mass. 02543

TABLE OF CONTENTS

	<u>Page</u>
ABSTRACT	2
TABLE OF CONTENTS	4
LIST OF FIGURES	7
LIST OF TABLES	10
BIOGRAPHICAL NOTE	11
LIST OF PUBLICATIONS	12
ACKNOWLEDGEMENTS	14
CHAPTER I	17
A. Introduction	17
1. Previous work	18
2. Present investigation	23
a. Scientific objectives	23
b. Data collection	25
CHAPTER II	29
A. Acoustic Stratigraphy	29
1. Introduction	29
2. Shell Mohawk B-93: Correlation of Well Logs and Reflection Profiles	29
a. Basement/Reflector "K"	32
b. Sediments/Reflectors "Z" to "1"	36
1) Reflector "Z"	36
2) Reflector "4"	40
3) Reflector "3"	44
4) Reflector "2"	46
5) Reflector "X"	48
6) Reflector "1"	49

	<u>Page</u>
3. Regional Correlations	51
a. Continental Shelf: Correlation of Acoustic Stratigraphy from from the Scotian Shelf to the New England Margin	51
1) LaHave Platform/Scotian Shelf	53
2) Georges Bank	55
3) Long Island Platform	64
b. Continental Rise	67
1) Nova Scotia	67
2) Georges Bank	71
c. Continental Slope: The Problem of Shelf-Rise Correlations	72
B. Geologic Maps: New England Passive Continental Margin	75
1. Introduction	75
2. Basement Tectonic Structures	79
3. Isopach Maps	84
a. Pre - "K"	84
b. "K" - "Z"	87
c. "Z" - "3"	91
d. "3" - "2"	94
e. "2" - "X"	97
f. "X" - Present	99
4. Structure Maps	103

	<u>Page</u>
a. Depth to acoustic basement	103
b. Depth to "K" unconformity	106
c. Depth to Jurassic-Cretaceous boundary	109
5. Velocity-lithofacies maps	111
CHAPTER III - Discussion of Results	123
A. Introduction	123
B. Models of passive margin formation	125
C. Geologic history of the New England passive continental margin	130
1. Rifting	130
a. Evolution of observed crustal structures	130
b. Pre - "K" stratigraphy	136
c. Continental separation and the development of the "K" unconformity	140
2. Drifting: Evolution of observed stratigraphy	141
a. "K" - "Z" (190-160 my B.P.)	141
b. "Z" - "3" (160-136 my B.P.)	148
c. "3" - "2" (136-~95 my B.P.)	149
d. "2" - "X" (~95-~75 my B.P.)	153
e. "X" - Present (~75-0 my B.P.)	155
SUMMARY	160
REFERENCES	163
APPENDICES	185

LIST OF FIGURES

	<u>Page</u>
Figure 1. Track chart, New England passive continental margin	22
Figure 2. Underway configuration, Woods Hole Oceanographic Institution multi-channel system . . .	27
Figure 3. Shell Mohawk B-93 - sonic and lithologic logs, acoustical correlations	30
Figure 4. Multi-channel seismic reflection profiles, Scotian Shelf and Georges Bank	33
Figure 5. Interpretation, Line 42, Scotian Shelf and Georges Bank	35
Figure 6. Stratigraphic nomenclature, Scotian Shelf	37
Figure 7. Regional extent of reflector "4" .	43
Figure 8. Interpretations, Lines 38 and 34, Scotian Shelf	54
Figure 9. Interpretation, Lines 23 and 21, Georges Bank	56
Figure 10. Interpretations, U.S.G.S. 4 and Line 17-19, Georges Bank	57
Figure 11. Interpretations, U.S.G.S. 1 and Lines 2 and 12/46, Georges Bank . . .	58
Figure 12. Single-channel seismic reflection profile, part of Line 26	61
Figure 13. Interpretations, U.S.G.S. 5 and Line 50, Long Island Platform	65
Figure 14. Interpretation, Line 45, Georges Bank continental rise off Nova Scotia	68

	<u>Page</u>
Figure 15. Basement tectonic structures	80
Figure 16. Pre - "K" isopach	86
Figure 17. "K" - "Z" isopach	88
Figure 18. "Z" - "3" isopach	92
Figure 19. "3" - "2" isopach	95
Figure 20. "2" - "X" isopach	98
Figure 21. "X" - Present isopach	100
Figure 22. Depth to acoustic basement	104
Figure 23. Depth to the "K" unconformity	107
Figure 24. Depth to the Jurassic-Cretaceous boundary	110
Figure 25. Tables relating lithology and velocity to density and depth of burial	113
Figure 26. "K" - "Z" velocity-lithofacies map	116
Figure 27. "Z" - "3" velocity-lithofacies	118
Figure 28. "3" - "Z" velocity-lithofacies	119
Figure 29. "2" - "X" velocity-lithofacies	120
Figure 30. North Atlantic plate reconstruc- tion at the time of the Blake Spur Anomaly	124
Figure 31. Stress patterns, New England margin	131
Figure 32. Model of passive margin forma- tion	134

	<u>Page</u>
Figure 33. Flow chart describing multi-channel seismic reflection processing procedures	192
Figure 34. Sonobuoy 36, Scotian Shelf	194
Figure 35. Sonobuoy 1, continental rise off Georges Bank	195
Figure 36. Sonobuoy results, continental shelf, New England margin	198
Figure 37. Sonobuoy results, continental rise, New England margin	199
Figure 38. Sonobuoy results, continental slope, New England margin	200

LIST OF TABLES

APPENDIX III: Time-To-Depth Conversions

Table I. Time-to-depth conversions,
U.S.G.S. CDP Lines 1, 4,
and 5

Table II. Time-to-depth conversions,
AII-91 CDP Profiles

Table III. Time-to-depth conversions,
Average AII-91 CDP/
sonobuoy results

Biographical Note

James Albert Austin, Jr. (that's me!) was born in White Plains, New York on September 24, 1951. For the first seventeen years of his life, he wintered in Scarsdale, New York and summered on Martha's Vineyard. He attended Edgemont High School in Scarsdale, and graduated with high honors in June, 1969. That same year he entered Amherst College in Amherst, Massachusetts, where he earned a B.A. magna cum laude in geology. Since June, 1973, he has been enrolled as a doctoral candidate in the Woods Hole Oceanographic Institution/Massachusetts Institute of Technology Joint Program in Oceanography, and has lived in Boston and Falmouth, Massachusetts. Besides marine geology, his interests include women, drinking, scuba diving, sailing, jogging, squash, and tennis. He has never been married (no one would have him).

LIST OF PUBLICATIONS

- Austin, James A., Bruce F. Molnia, and H. Allen Curran,
1973, Stratigraphy of marine and estuarine Pleis-
tocene beds exposed along the Pamlico River, North
Carolina: Geol. Soc. America Abs. with Programs,
v. 5, p. 375.
- Austin, J.A., Jr., E. Uchupi, D. Shaughnessy, and R.D.
Ballard, 1977, Stratigraphy and structure of the
Georges Bank region: EOS, v. 58, p. 404.
- Uchupi, E., J.A. Austin, Jr., D.R. Shaughnessy, III.,
D. Gever, and T.F. O'Brien, 1977, Geology of the
Laurentian Fan: EOS, v. 58, p. 1160.
- Austin, James A., Jr., Elazar Uchupi, and D.R. Shaughnessy,
III., 1978, Geology of the Georges Bank region:
Geol. Soc. America Abs. with Programs, v. 10, p. 30.
- Uchupi, Elazar, J.A. Austin, and D.R. Shaughnessy, III.,
1978, Sedimentary framework of the Laurentian Fan:
Geol. Soc. America Abs. with Programs, v. 10, p. 90.
- Austin, James A., Jr., 1978, Geology of the passive margin
off New England: EOS, v. 59, p. 1104.
- In press:
- Uchupi, Elazar, and James Albert Austin, Jr., in press,
The geologic history of the passive margin off New
England and the Canadian Maritime Provinces:
Tectonophysics.

In press (cont.):

Uchupi, E., J.A. Austin, Jr., and D. Ross, in press,
Stratigraphy and structure of the Laurentian Cone
region: Canadian Jour. Earth Sci.

Uchupi, E., J.P. Ellis, J.A. Austin, Jr., G.H. Keller,
and R.D. Ballard, in press, Mesozoic-Cenozoic
regressions and the development of the margin
off northeastern North America: Lamont-Doherty
Geological Observatory Memorial Volume to Bruce
Heezen.

In preparation:

Austin, J.A., Jr., and E. Uchupi, in preparation,
The geology of the passive margin off New England:
Ph.D. dissertation, Massachusetts Institute of
Technology-Woods Hole Oceanographic Institution
Joint Program in Oceanography.

Acknowledgements

First and foremost, thanks must go to the many sources of funds which were necessary to initiate and conduct the investigation of the New England passive continental margin. Cruise #91 of the R/V ATLANTIS II was sponsored by the National Science Foundation, Office of the International Decade of Ocean Exploration (ID074-04094). Support for subsequent data analyses and interpretation came from the Ocean Industry Program of the Woods Hole Oceanographic Institution, the U.S. Department of State (1722-620214), the National Science Foundation (OCE77-09421), and Sea Grant (04-7-158-44104 and 04-8-M01-149).

The successful completion of this work also required the assistance of many, many people. The following deserve special thanks for their contributions: K.E. Prada and A.B. Baggeroer for the development of the multi-channel seismic reflection system; R.D. Ballard, K.O. Emery, and E. Uchupi for their scientific leadership during AII-91; S. Leverette for the development of essential processing software; D.R. Shaughnessy, III and D. Gever for their diligent processing efforts; and T.F. O'Brien, K. von der Heydt, and M. Flora for their efficient handling of data acquisition. The

Captain and crew of the R/V ATLANTIS II did an excellent job of ship handling in very crowded waters.

M. Flora, S. Romaine, S.T. Knott, and H. Hoskins made the analyses of the sonobuoy data possible and profitable. F.J. Paulus of The Superior Oil Company supplied the sonic and lithologic logs of Shell Mohawk B-93.

R. Davis and H. Hays did a fine job of drafting the figures and A. Sousa typed the manuscript flawlessly.

A.L. Peirson, III ("Jake"), Assistant Dean of Education at Woods Hole, set an outstanding example of "laissez-faire" excellence in the administration of occasionally unruly doctoral candidates like myself.

J. Grow, U.S. Geological Survey, always made himself available for consultation.

E.T. Bunce of Woods Hole never let me get away with anything, but never gave up on me either.

My warmest regards go to all of my cohorts in the D.E.S.C. building (they know who they are), who provided me with a working atmosphere which can only be described, in retrospect, as relaxed.

E. Uchupi, R.D. Ballard, A.B. Baggeroer, J. Grow, and E.T. Bunce read the manuscript. Their criticisms vastly improved the final product.

During my tenure at Woods Hole, I was supported as a Research Fellow and a Graduate Research Assistant by the Woods Hole Oceanographic Institution. I am thankful for that financial assistance.

Last, but by no means least, I wish to express my deepest gratitude to Elazar Uchupi, who inspired fresh motivation when it was required, provided knowledge and insight when it was lacking, and furnished an occasional lunch/dinner and cigar, free-of-charge. This thesis is as much his as it is mine.

CHAPTER I

Introduction

During the past 15 years, the hypotheses concerned with earth behavior, now collectively referred to as "plate tectonics" (LePichon, 1968; Isacks et al., 1968; and many others), have been extensively tested and substantially verified. As a result, geologists studying the evolution of both continents and ocean basins can now compare and contrast their results on a common theoretical basis. Despite the advent of plate tectonics, however, the exact nature of the continent-ocean transition remains an unsolved problem. So-called passive or "Atlantic-type" (Mitchell and Reading, 1969, p. 631) continental margins overlie this transition when it occurs within a lithospheric plate. Because passive margins overlie both continental and oceanic crust, they have been sites of large vertical displacements and the consequent development of complex crustal structures. Overlying, and often masking these structures, are enormous accumulations of sediment. The development of advanced geophysical techniques like multi-channel seismic reflection profiling enabled the stratigraphy and structure of passive continental margins to be examined regionally for the first time. Such detailed

examinations are important, both for an understanding of the evolution of passive margins within the framework of plate tectonics, and for an accurate assessment of their possible economic potential.

Previous work

Using the northern Appalachians as a model, Kay in 1951 produced the classic, if somewhat overworked, cross-section of a mio-eugeosynclinal couplet. Kay did not consider the nature of the crust beneath geosynclines, nor did he relate his model to the structural elements composing modern continental margins. Such tasks would have been difficult in the early 1950's because little coordinated research had been carried out in the marine environment.

Drake et al. (1959) made the first attempt to pinpoint modern analogs for ancient geosynclines exposed on land. Using seismic refraction, magnetic, and gravity data collected off the east coast of North America, these authors equated Kay's geosynclines with two major sediment prisms underlying the continental shelf and the lower slope-upper rise. Separating these prisms was a shelf-edge basement high presumably equivalent to Kay's "tectonic borderland". Emery et al. (1970) later concluded that this buried high was, at least in part, a basement "ridge complex" related

to the early opening of the western North Atlantic. However, controversy over the composition and genesis of the "ridge complex" still continues (Dietz, 1964; Watkins and Geddes, 1965; Burk, 1968; Ballard and Uchupi, 1975; Schlee et al., 1976, 1977; Uchupi and Austin, in press; and others).

Dietz (1963) used plate tectonic theory in an attempt to relate modern and ancient geosynclinal deposits. In this and subsequent papers (Dietz and Holden, 1966; Dietz, 1972, 1974; Dietz and Holden, 1974), he developed a model whereby shelf and rise sediment prisms (deposited on continental and oceanic crust, respectively) were eventually deformed by subduction and plate collision to create mountain belts. This accretionary process was effectively continuous, eliminating the apparent non-uniformitarian aspects of geosynclinal sedimentation which had perplexed earlier researchers. According to the model, continental slopes were primarily structural expressions of the flanks of previously deformed continental rise prisms. With time, these flanks were modified by sedimentation, faulting, and isostatic compensation.

Building on Dietz's ideas, others began to use plate tectonics to explain the geological development of various types of continental margins. For example, Mitchell and Reading (1969) defined an "Atlantic-type"

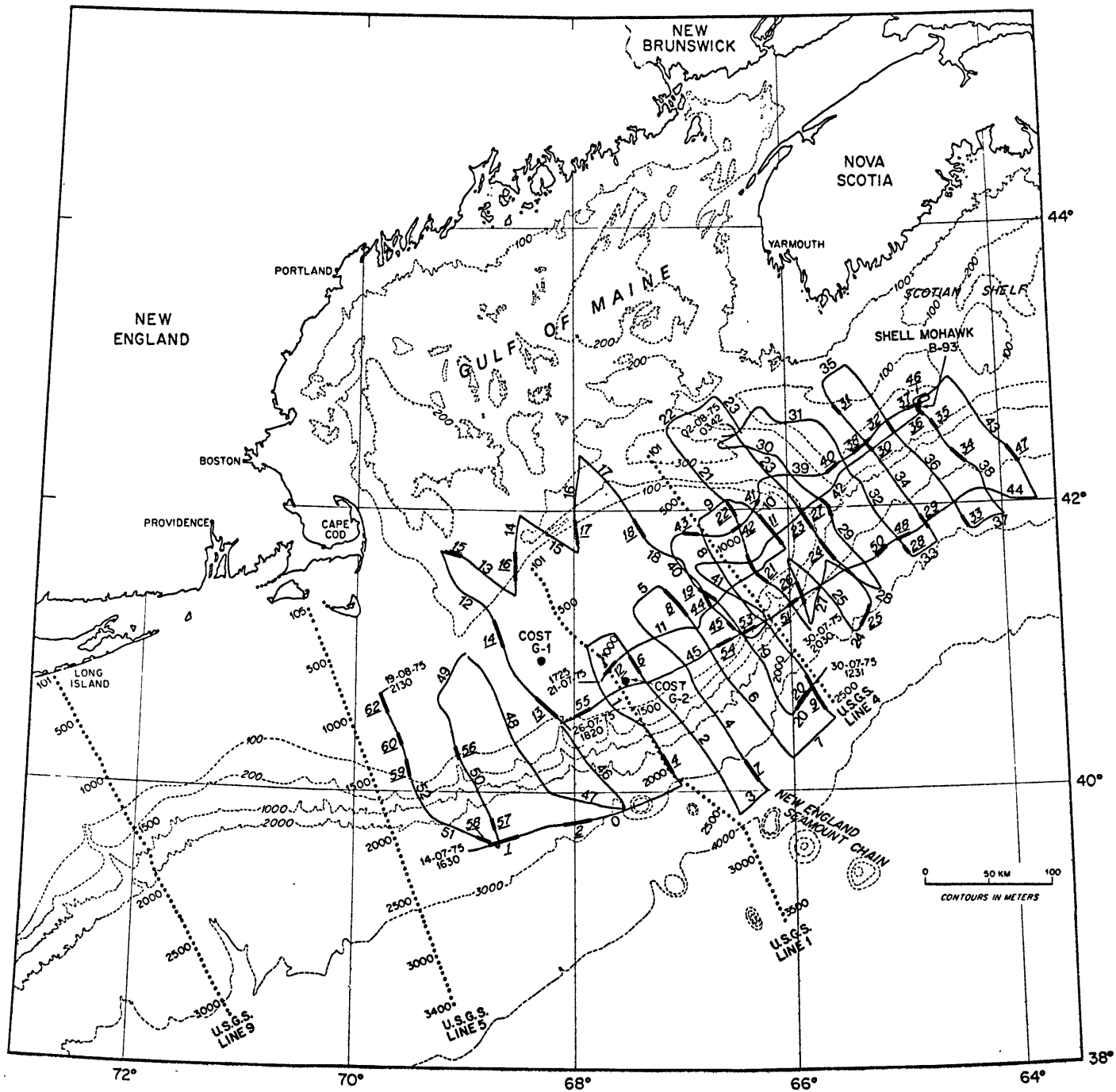
margin as one exhibiting complete coupling of continental and oceanic crust with little or no seismic and volcanic activity. Dewey and Bird (1970a, b) went a step further, and described the tectonic processes necessary to convert an Atlantic-type margin into a mountain belt. To substantiate their arguments, the authors compared stratigraphic sequences from a number of mountain belts with those available both from passive margins and the deep ocean, and found them to be similar.

During the 1960's, the huge quantities of sediment characterizing passive margins began to attract a great deal of attention as potential sources of oil and gas. In response to widespread commercial interest, many general reviews of available information on the continental margin off the east coast of the United States were published (Mayhew, 1974; Schultz and Grover, 1974; Mattick et al., 1974; Minard et al., 1974; Perry et al., 1975; Mattick et al., 1978; and others). Regional syntheses of the geology of the eastern Canadian margin were particularly instructive, as they could incorporate well data collected during exploratory drilling south of Nova Scotia and on the Grand Banks (Howie, 1970; McIver, 1972).

Since 1973, a great deal of new geological and geophysical information from the New England passive margin

has been collected. The United States Geological Survey, as part of a broad inspection of the entire east coast continental margin, has contracted for a number of multi-channel seismic reflection lines in the Georges Bank region. The lines which are currently in the public domain are shown in Figure 1. In addition, the U.S.G.S. has compiled detailed gravity and magnetic maps of the entire east coast margin (Grow et al., 1976; Klitgord and Behrendt, 1977). New syntheses of well information and multi-channel profiles from the adjacent Canadian margin (Jansa and Wade, 1975; Wade, 1977; Given, 1977; Wade, 1978; Uchupi and Austin, in press; Uchupi et al., in press) also have shed new light on the history of the margin off New England. Finally, submersible operations in several of the submarine canyons south of Georges Bank have led to the recovery of the first samples of Lower Cretaceous reef material from this part of the east coast margin (Ryan et al., 1978). These samples are important additions to Upper Cretaceous and younger rocks recovered previously by dredging (Weed et al., 1974), and underscore this margin's stratigraphic complexity.

Figure 1. Locations of single and multi-channel seismic reflection profiles used in this study. Solid lines: AII-91 track lines. Heavy short lines: locations of sonobuoy profiles. Dotted lines: U.S. Geological Survey multi-channel seismic reflection lines. (Note: Some proprietary multi-channel information used during this investigation which covers the central part of Georges Bank has been omitted.)



Present Investigation

Scientific objectives

Until rather recently, geophysical methods were inadequate for more than a general picture of margin stratigraphy and structure. Single-channel seismic reflection profiling systems were not powerful enough to resolve fully the complexities exhibited by passive margin depocenters. However, with the development of multi-channel seismic reflection profiling techniques, comprehensive geophysical surveys began to be used by commercial concerns, government agencies, and research laboratories to study passive margins in detail. In 1975, a group of scientists at the Woods Hole Oceanographic Institution selected a small part of the east coast continental margin as the subject of such a survey. The major objectives of the proposed examination were the following:

1. To attempt to locate and characterize the transition from continent to ocean basin.
2. To delineate the crustal structures which characterized the margin, and to determine their age and the extent to which they reflect the crustal response to rifting processes.

3. To estimate the lithologies and thicknesses of the sediments underlying the continental shelf, slope, and upper rise, and to ascertain by what processes and under what environmental conditions they were deposited.
4. To determine the extent to which a small area is typical or atypical of either the east coast margin as a whole, or of other passive margins which had been investigated.
5. To reconstruct the margin's evolution through time within the broad framework of plate tectonics.

The passive margin off New England (Figure 1) was an obvious choice as the location for the study for the following reasons. First, it adjoined two well-studied areas: the Scotian Shelf (King, 1967a, b; Uchupi, 1970; McIver, 1972; Jansa and Wade, 1975) and the Gulf of Maine (Drake et al., 1954; Uchupi, 1965, 1966, 1970; Malloy and Harbison, 1966; Knott and Hoskins, 1968; Tucholke, Oldale, and Hollister, 1972; Oldale, Uchupi, and Prada, 1973; Ballard and Uchupi, 1972, 1974, 1975; Oldale et al., 1974; and others). Second, early geophysical work (Officer and Ewing, 1954; Drake et al., 1959; Drake et al., 1968) indicated that

a major depocenter existed beneath Georges Bank. This and subsequent data collected on the "Georges Bank trough" (Maher, 1965, p. 6; Maher and Applin, 1971) supported the working hypothesis that this basin incorporated the complex crustal structure and thick Mesozoic-Cenozoic sediments considered characteristic of the entire east coast margin (Emery and Uchupi, 1965; Mayhew, 1974; Mattick et al., 1974; Minard et al., 1974; Schultz and Grover, 1974; Perry et al., 1975).

The Woods Hole Oceanographic Institution conducted the field investigation of the New England margin during July-August, 1975, aboard the R/V ATLANTIS II. During this cruise (AII-91), approximately 6,200 line km of single and 6-channel seismic reflection and magnetic profiles were collected, supplemented by 55 unreversed seismic refraction profiles (Figure 1). The study area extended from the site of the Shell Mohawk B-93 well on the Scotian Shelf to the eastern side of the Long Island Platform (Figure 1).

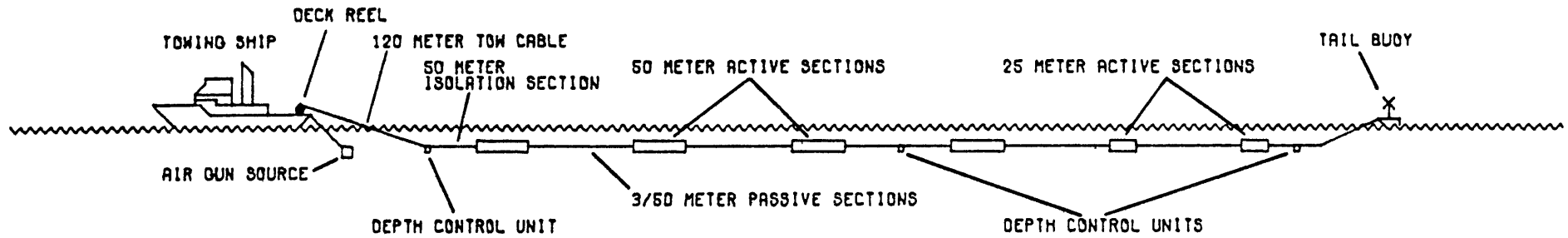
Data collection

Ship speed was maintained at roughly 4.0 knots for a shot spacing of 37.5 m (see Appendix I). A sound source consisting of four air guns (300, 120,

80, 40 cu. in.) operating at 1850 psi fired simultaneously at intervals of either 16 or 18 sec. The receiving array, approximately 1.2 km long, consisted of six active elements or channels, each containing 150 elements (Figure 2). Signals from one of the channels (usually channel 1, located nearest the sound source) were band-pass filtered and monitored in real time on two W.H.O.I.-modified X-Y graphic recorders. These recorders were operated simultaneously at different sweep speeds: 2.0 sec (band-pass generally 30-160 Hz) and 5.0 sec (band-pass generally 10-80 Hz). Signals from all channels were digitally recorded on magnetic tape for subsequent "common-reflection-point" (Mayne, 1962) processing ashore. (Appendix I is a detailed description of the processing procedures).

The seismic refraction profiles were collected using expendable radio sonobuoys. Signals transmitted from the buoys were displayed unfiltered on an X-Y recorder. At the same time, those signals, along with coincident normal incidence data, trigger impulses, and voice annotations, were recorded on magnetic tape using a four-channel FM tape recorder. (A full description of the analyses of the sonobuoy data is included in Appendix II, along with a compilation of results).

Figure 2. Underway configuration of the Woods Hole Oceanographic Institution's 6-channel seismic reflection profiling system.



Air gun source: a tapered array of 4 guns (300 in. ³/₁₂₀ in. ³/₈₀ in. ³/₄₀ in. ³).

Active seismic sections: 3 hydrophones/m.

Average towing speed: 4.0 knots.

Array length: approximately 1.2 km.

TYPICAL 6-CHANNEL ARRAY CONFIGURATION

The total geomagnetic field intensity was measured using a Varian proton precession magnetometer system. The sensor was towed approximately 250 m behind the ship, and the data recorded on analog chart recorders and digitally (at one-minute intervals) on magnetic tape. The noise level of the system was $\pm 2\%$. The 1975 version of the International Geomagnetic Reference Field (Leaton, 1976) was used to remove regional magnetic gradients, and the resulting anomalies were plotted as profiles along the tracks together with the seismic reflection and refraction information.

Precise navigation of survey lines was achieved by means of satellite and Loran A and C. Errors in geographic position of the cruise tracks probably do not exceed 0.5 km (R. Groman, personal communication).

Acoustic Stratigraphy

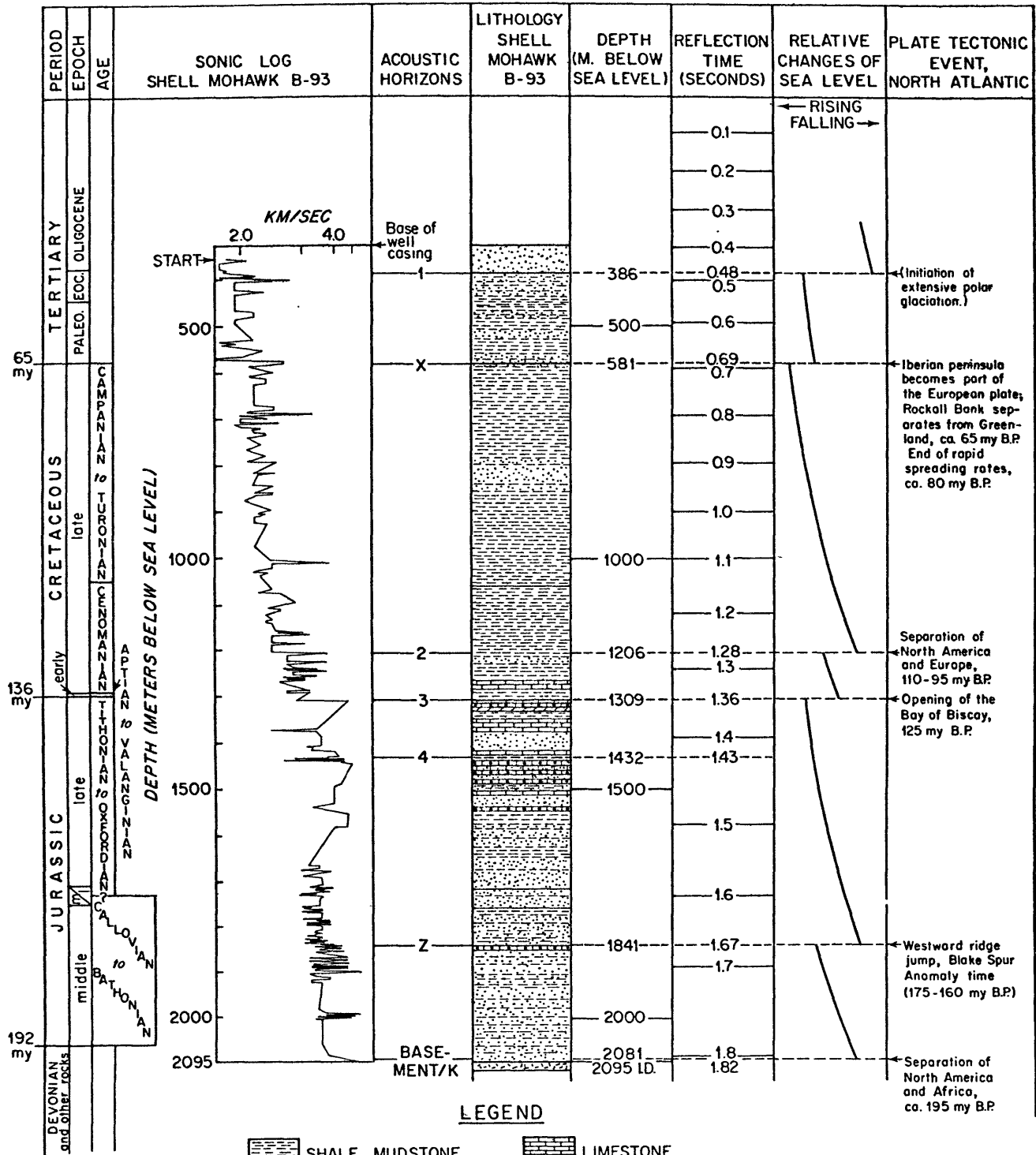
Introduction

If either single or multi-channel seismic reflection profile interpretations are to be used in mapping regional geology, the relationship of acoustic horizons to geologic horizons must be established, and their age and lithology determined as accurately as possible. Therefore, in order to establish a chronostratigraphic framework within which the AII-91 multi-channel seismic profiles could be interpreted geologically, tie-lines were run between the New England margin and Shell Mohawk B-93, an exploratory well drilled on the Scotian Shelf in 1970 (Figure 1). Based on a prior Canadian synthesis (McIver, 1972), it appeared that the stratigraphic succession characterizing the western part of the Scotian margin might be similar to that in the Georges Bank Basin.

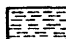

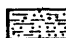



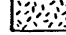
Shell Mohawk B-93: Correlation of Well Logs and Reflection Profiles

Both lithologic and sonic (continuous velocity) logs are available for the Shell Mohawk B-93 well (Figure 3). Because the sonic log provides a continuous record of both interval velocity and vertical one-way travel-time as a function of depth in a borehole

Figure 3. Sonic and lithologic logs, Shell Mohawk B-93, southwestern Scotian Shelf. Acoustical correlations with AII-91 multi-channel seismic reflection profiles are shown, along with major plate tectonic events in the North Atlantic and qualitative sea-level curves for the Late Triassic to the Present. Supplementary data from Shell Canada Ltd., Jansa and Wade (1975), van Hinte (1976a,b), Given (1977), Sclater et al. (1977), Klitgord and Schouten (1977), and Vail et al. (1977).



LEGEND

-  SHALE, MUDSTONE
-  LIMESTONE
-  SILTSTONE, SANDY SILTSTONE, SANDY SHALE
-  DOLOMITIC LIMESTONE
-  SANDSTONE
-  OOLITIC LIMESTONE
-  GRANITE

(Dobrin, 1976), it can be used in conjunction with lithologic information to establish interval velocity/lithology relationships and in the calibration of acoustic (time) horizons with depth.

With this in mind, the lithologic and sonic logs of Shell Mohawk B-93 were studied to pinpoint the travel-times and depths of velocity discontinuities associated with discernible lithologic changes. Then, the multi-channel seismic profiles collected over the well-site were examined for reflections coinciding with the velocity/lithology contrasts noted in the logs (Figure 3).

The sonic log did not provide any information above the base of the well-casing (Dobrin, 1976) which, in Shell Mohawk B-93, was 319 m below sea-level. Consequently, in order to calibrate the sonic log with the multi-channel seismic reflection profiles, which used sea-level as a permanent datum, a correction factor of .193 sec (one-way travel-time) was added to all of the log measurements. This factor was calculated by assuming an interval velocity of 1.5 km/sec for a 117 m-thick water layer, and 1.76 km/sec for an underlying 202 m-thick sediment blanket. The sediment velocity is from Officer and Ewing (1954), who reported a seismic refraction measurement of $1.76 \pm .08$ km/sec for unconsolidated sediments underlying the southwestern Scotian Shelf.

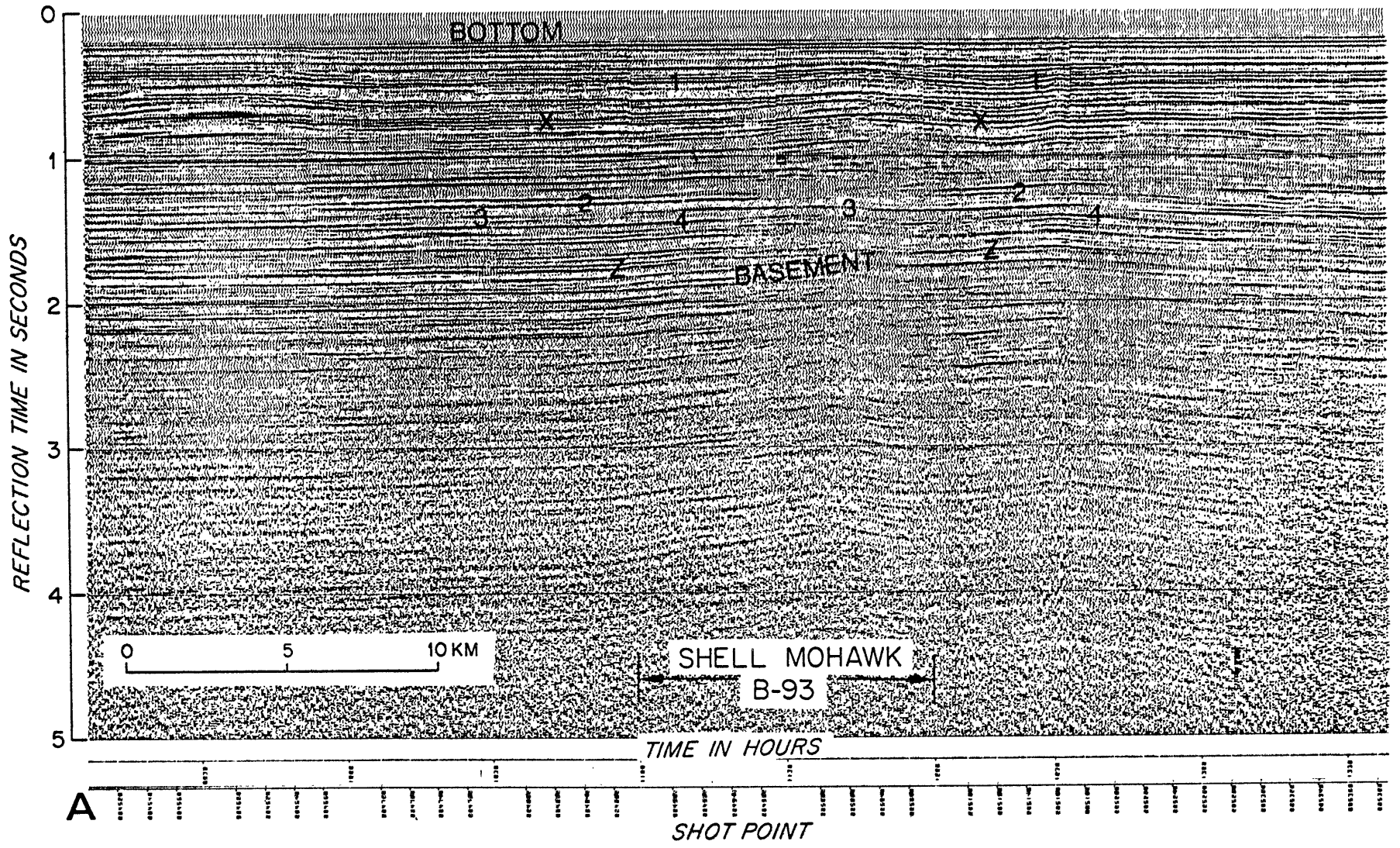
By using the well logs, seven reflectors were identified and correlated with pronounced velocity discontinuities and lithologic changes (Figures 3 and 4).

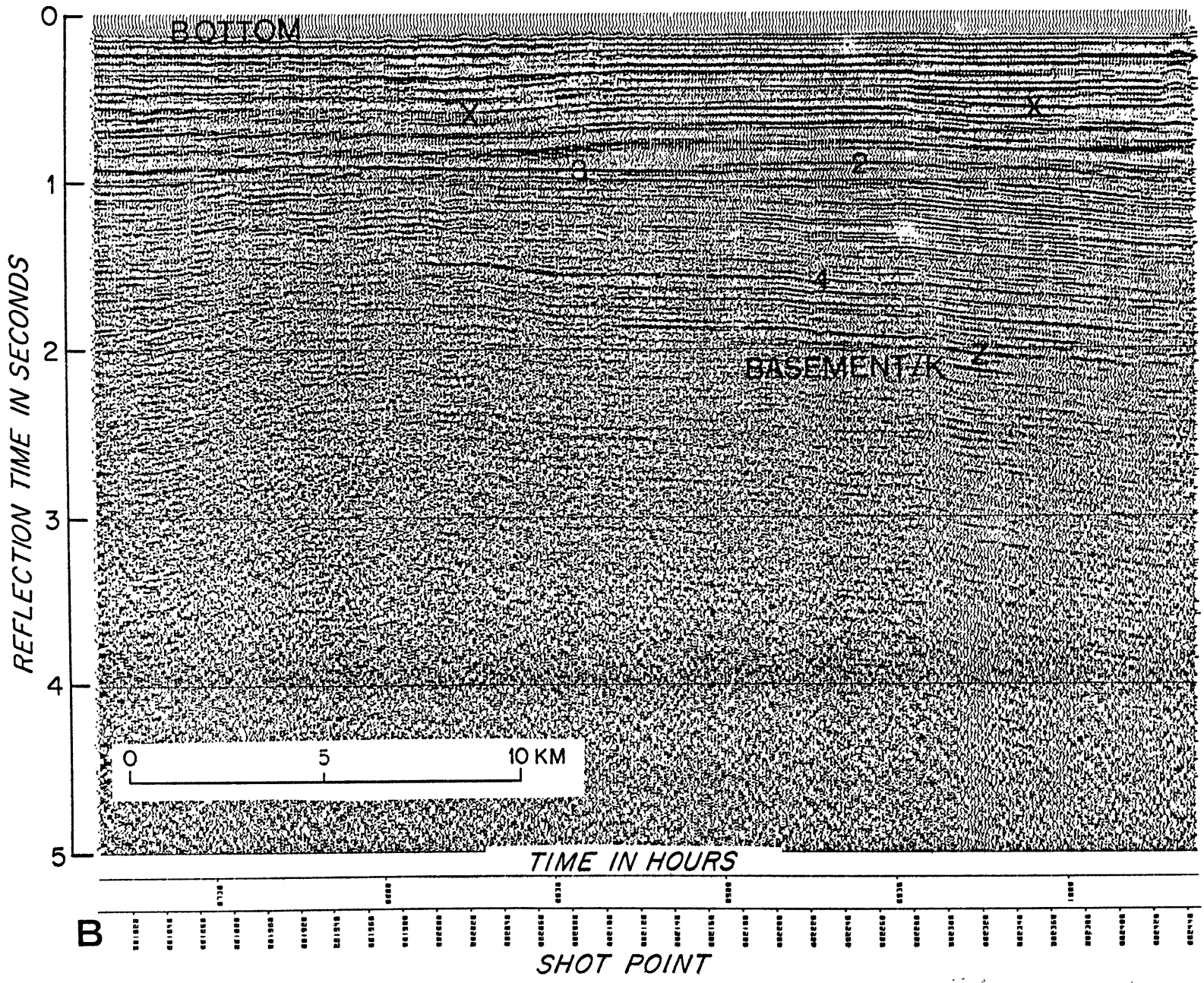
Basement/Reflector "K"

The Shell Mohawk B-93 well was drilled on a broad anticline to test the structure's potential as a trap for hydrocarbons. The well bottomed out in orthoclase granite at a depth of -2095 m (Figure 3). The sediment-granite contact is marked on the sonic log by an abrupt increase in interval velocity (from 3.6 to 5.86 km/sec) at a two-way or reflection time of 1.82 sec (Figure 3). The interpreted basement reflector occurs at approximately 1.74 sec (Figure 4A, 1145 hours). The discrepancy of .08 sec (roughly 150 m at the average sediment interval velocity of 3.6 km/sec) in the travel-times could be the result of one or both of the following factors: 1) The cruise track along which the profile was recorded did not pass directly over the well-site (local relief on the basement event is on the order of 0.1 sec), or 2) the initial velocity assumption for log correlation is slightly in error. Whatever the explanation, the discrepancy is so small that it approaches the limit of resolution of these profiles.

Figure 4. Two 6-channel seismic reflection profiles collected during AII-91. CDP processing has been carried out on both profiles. Both profiles are part of Line 42 (Figure 5). Reflector identifications are discussed in the next text. Vertical exaggeration of bottom topography 4:1.

- A. Collected near the site of the Shell Mohawk B-93 well, southwestern Scotian Shelf.
- B. Collected on the east-central part of Georges Bank. U.S.G.S. 4, shot-point 1100 (see Figure 10). crosses this profile at approximately 0820 hours.

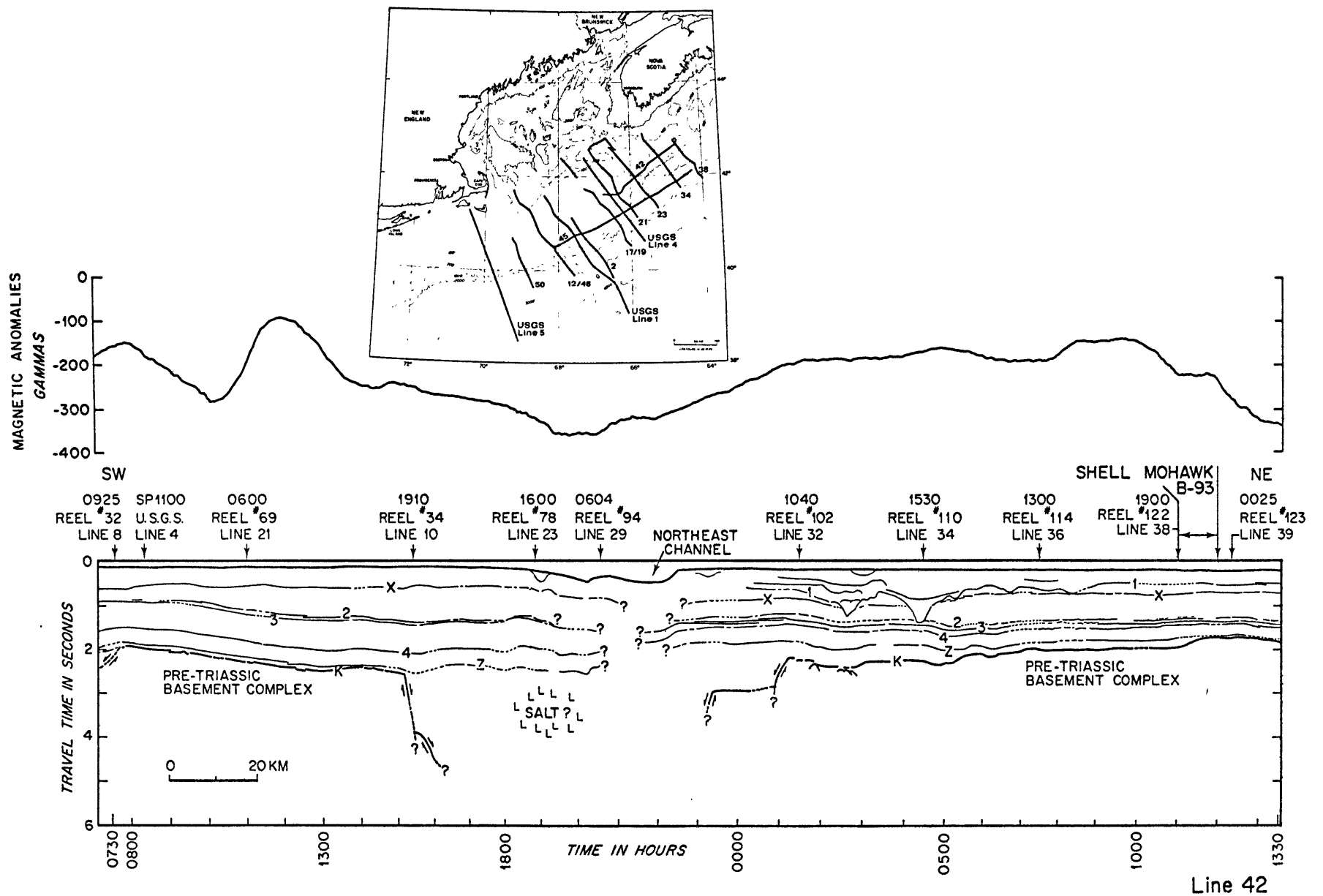




Away from the well-site, the basement reflector is generally characterized by a zone of low-amplitude hyperbolic echoes. Because of its relief, and regional dip approximating that of the overlying sediments, the basement horizon is occasionally masked (see the left side of Figure 5, and Figure 4B). Where such masking occurs, the trend of the reflector has been extrapolated. All available geophysical information from the Scotian Shelf indicates that basement is smooth, with a general seaward tilt (Emery and Uchupi, 1972; Jansa and Wade, 1975; Given, 1977).

In contrast, the geology of the basement is complex. King and MacLean (1976) have summarized geologic evidence indicating that the Shell Mohawk B-93 granite is probably part of a batholith emplaced beneath southern Nova Scotia and the Scotian Shelf during the Devonian Acadian orogeny. A Carboniferous date of 329 ± 14 m.y.B.P. reported by Given (1977) for this granite may record the last thermal event which affected the intrusive. Grabens and half-grabens filled with material of presumed Carboniferous and/or Triassic age are entrained into the granites and associated Cambro-Ordovician metasediments (King and MacLean, 1976). The graben structures are bounded by normal faults discernible on seismic profiles as lineated diffraction patterns.

Figure 5. Interpretation of Line 42, a processed 6-channel seismic reflection profile which runs from the Scotian Shelf across Northeast Channel to Georges Bank. Vertical exaggeration of bottom topography 13:1. Cross-ties with other profiles are shown. Reflector identifications are discussed in the text. Magnetic anomalies calculated from total field measurements by systematically removing the 1975 IGRF (Leaton, 1976). For exact location of this profile, refer to the location diagram. The "L" pattern on this and subsequent figures indicates evaporites.



A post-rifting erosional event bevels the block-faulted terrain where it can be discerned, creating an unconformity and a regional seismic marker which has been termed reflector "K" beneath Georges Bank (Schlee et al., 1976). Except where "K" is superimposed on graben-fill (see the extreme left side of Figure 5), the basement event beneath the Scotian Shelf and reflector "K" underlying Georges Bank are indistinguishable. The basement/"K" surface can be traced throughout the New England margin except beneath the southeastern part of Georges Bank, where massive basement down-faulting associated with high-amplitude reflections from overlying sediment somewhat obscure the acoustic picture.

Sediments/Reflectors "Z" to "1"

Formation names initially proposed by McIver (1972) for the stratigraphic succession underlying the Scotian Shelf are used during the ensuing discussion concerning the acoustic signatures of sediments sampled by Shell Mohawk B-93. His nomenclature, supplemented with ages supplied as a result of his and subsequent investigations by Jansa and Wade (1975), Given (1977), and Wade (1977, 1978), is reproduced as Figure 6.

Reflector "Z"

At -1841 m/1.67 sec (two-way travel-time), a velocity discontinuity occurs where sandstones with

Figure 6. Stratigraphic terminology proposed by McIver (1972) for sediments underlying the Scotian Shelf. McIver's Table 1 has been supplemented by ages taken from McIver (1972), Jansa and Wade (1975), Given (1977), and Wade (1977, 1978).

	GROUP	FORMATION	MEMBER	DOMINANT LITH.	MAXIMUM THICKNESS	
	QUATERNARY	* SABLE ISLAND		SAND AND GRAVEL		
		* LA HAVE		CLAY		
		* SAMBRO		SAND		
		* EMERALD		SILT		
		* SCOTIAN SHELF		GLACIAL DRIFT		
TERTIARY		BANQUEREAU		MUDSTONE	4000'	
CRETACEOUS	THE GULLY GROUP	WYANDOT		CHALK	750'	
		DAWSON CANYON	LST. MARKER	SHALE	3000'	
	NOVA SCOTIA GROUP	LOGAN CANYON			SANDSTONE & SHALE	800'
			SABLE SHALE		SHALE	500'
					SANDSTONE & SHALE	2000'
		NASKAPI		SHALE	750'	
		MISSISAUGA	LST. MARKER	SANDSTONE	3700'	
JURASSIC	WESTERN BANK GROUP	MIC MAC		CALCAREOUS SHALE	4000'	
		VERRILL CANYON		SHALE	> 2000'	
		BACCARO		LIMESTONE	2500'	
		MISAINÉ		CALCAREOUS SHALE	300'	
		SCATARIE		LIMESTONE	400'	
		MOHAWK		SANDSTONE & SHALE	3500'	
		IROQUOIS		DOLOMITE	650'	
		ARGO		SALT	> 3000'	

interfingering dolomitic limestone stringers (exhibiting interval velocities of approximately 4.1 km/sec) come into contact with overlying sandstones (with interval velocities of 3.4 km/sec) in the Mohawk well (Figure 3). On the seismic reflection profiles, an intermittent reflector, "Z" (Schlee et al., 1976), occurs which correlates with this discontinuity (Figure 4A). The reflector becomes more continuous away from the well-site, and beneath the southern part of Georges Bank it is one of the most prominent acoustic horizons in the entire sediment section (Figure 4B). Schlee et al. (1976) felt that horizon "Z" might represent the Jurassic-Cretaceous boundary within the Georges Bank Basin. However, correlation with Shell Mohawk B-93 stratigraphy as it has been dated by Gradstein et al. (1975) would make this horizon Bathonian (Middle Jurassic) in age (Figure 3).

The sediments within which "Z" occurs have been the object of controversy among Canadian researchers. McIver (1972) designated the sandstone/shale/limestone unit sampled between -1578 m and -2081 m in the Shell Mohawk B-93 well as the type section of the Mohawk Formation (Figure 6), and dated the formation as Middle Jurassic. Jansa and Wade (1975) concurred

with McIver, but Given (1977) split the Mohawk formation into an Early and Middle Jurassic Mohican Formation and a Middle and Late Jurassic Mohawk Formation (with the type section of the redefined Mohawk Formation remaining in Shell Mohawk B-93). According to Given, the sandstones of the two formations could not be shown to interfinger, and ought, therefore, to be treated separately. However, an examination of the sonic log (Figure 3) and the Jurassic sediments sampled in the Mohawk well does not reveal any good reason to separate the sequence in question into two formations. First, no apparent hiatuses occur in the section prior to the end of the Jurassic (Gradstein et al., 1975). Second, the oolitic limestones sampled between -1416 m and -1619 m (Figure 3) are of uncertain age. They could represent either the Scatarie (Callovian) or the Baccaro (Middle-Late Jurassic) members of the same Abenaki Formation, or the up-dip equivalent of the Baccaro Member known as the Mic Mac Formation (McIver, 1972; Figure 6).

The regional correlation of reflector "Z" accomplished during the present investigation may help to resolve the disagreement. The acoustic prominence of "Z" beneath Georges Bank must be caused by a large velocity contrast (Schlee et al., 1976), which suggests

a major lithologic change. If the oolitic limestones belong to the Scatarie Member, then the entire sequence beneath them would have to be Middle Jurassic or older. Concomittantly, "Z" could represent the contact between clastics of the Mohawk Formation as it was originally defined by McIver and dolomites of the Early Jurassic Iroquois Formation (Figure 6). Wade (1977) suggested this possibility. A lithologic contact of this type would produce both a highly reflective acoustic horizon and a large increase in interval velocity with depth. This is exactly what occurs across reflector "Z" in the Georges Bank Basin. In this regard, it is interesting to note that Wade (1977, 1978) renames the Mohawk Formation the Mohican Formation, without changing its stratigraphic position beneath the Middle Jurassic Scatarie limestone. Wade (personal communication) still considers "Z" to lie within the Mohawk Formation as it was originally defined by McIver (1972), thereby dating it as a Middle Jurassic horizon.

Reflector "4"

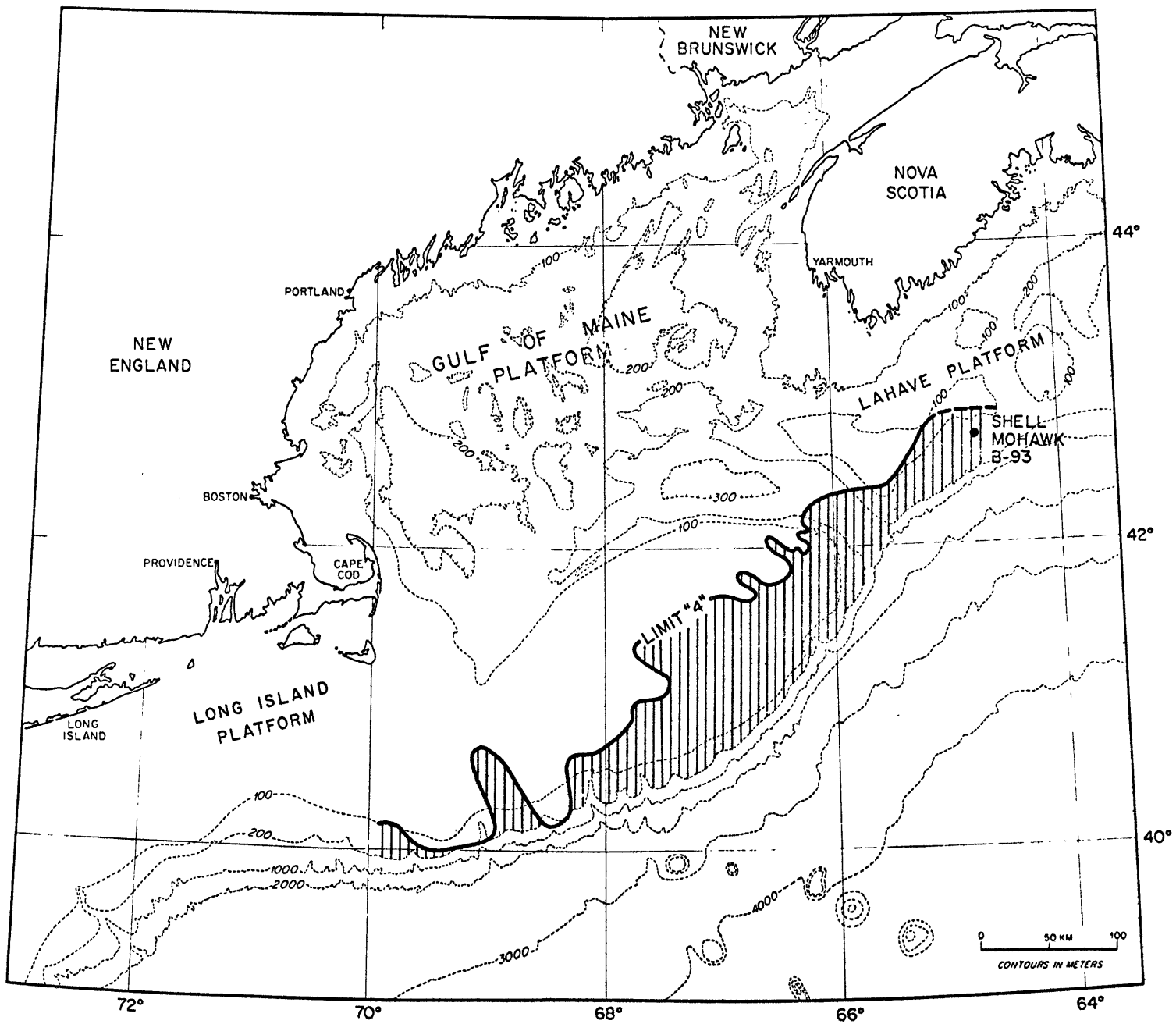
Another velocity discontinuity is apparent on the Shell Mohawk B-93 sonic log at -1432 m/1.43 sec (two-way travel-time). It occurs at the contact between sandstones/calcareous shales (average

interval velocity 3.8 km/sec) and oolitic limestones with interbedded sandstones and shales (average interval velocity 4.7 km/sec) (Figure 3). The corresponding acoustic horizon, here designated "4", is discontinuous but of high amplitude (Figure 4A). Reflector "4" is correlative with a horizon recognized by Schlee et al. (1976) as the possible boundary between Early and Late Cretaceous sediments. Beneath south-central Georges Bank, "4" is as prominent as "Z", and consists of a packet of continuous, high-amplitude reflectors (Figure 4B). Along U.S. Geological Survey CDP-Line #1 (Figure 6), reflectors "4" and "Z" mark the largest vertical changes in interval velocity which occur in this part of the Georges Bank Basin (Schlee et al., 1976, Figure 6). Wade (1977) identifies a horizon "J_S", which approximates reflector "4", during his discussion of acoustic correlations between the Scotian and Georges Bank basins. According to Wade, "J_S" represents the Scatarie limestone. However, based on dates available from Shell Canada Limited and Gradstein et al. (1975), the oolitic limestones which produce reflector "4" look to be younger than the Callovian age ascribed to the type section of the Scatarie in Shell Oneida 0-25 (McIver, 1972; Figure 3). According to McIver and subsequent researchers on the stratigraphy

of the Canadian margin, the Scatarie and Baccaro members of the Abenaki Formation are separated by the Middle Jurassic Misaine shale. A calcareous shale of uncertain age does occur at -1564 m in the Shell Mohawk well (Figure 3), perhaps lending some support to the argument that "4" is not the Scatarie Member, but is rather the Baccaro Member or part of its up-dip equivalent, the Mic Mac Formation (Figure 6).

Whatever its exact age, reflector "4" cannot be traced everywhere beneath the New England passive margin. The horizon is confined to the southern part of the Scotian Shelf and Georges Bank (Figure 7), suggesting that some kind of lithologic change may occur along its northern or landward limit. That such a lithologic change does occur is supported by interval velocities calculated during common-depth-point processing of both U.S.G.S. and W.H.O.I. multi-channel seismic reflection profiles collected over Georges Bank. The velocities clearly indicate a seaward increase, both laterally and with depth, in the Georges Bank Basin. These velocity trends and their significance for the stratigraphic history of the New England continental margin will be discussed later.

Figure 7. Regional extent of reflector "4".



Reflector "3"

One of the largest velocity discontinuities present in the Shell Mohawk B-93 hole is encountered at -1309 m/1.36 sec (two-way travel-time). At this depth, calcareous siltstones (average interval velocity 3.0 km/sec) overlie dolomitic limestones (average interval velocity 4.7 km/sec). (Figure 3). A strong generally continuous reflector, which occurs at 1.36 sec on Figure 4A, is presumed to correspond to the lithologic change. Reflector "3" can be followed regionally, and does not appreciably change its acoustic character beneath Georges Bank (Figure 4B). Age information supplied by Shell Canada Limited indicates that the limestone-siltstone contact marks the boundary between the Jurassic Abenaki/Mic Mac formations and the Cretaceous Mississauga Formation (McIver, 1972; Figure 6). According to Gradstein et al. (1975), the contact also represents a hiatus separating latest Jurassic from Valanginian sediments (Figure 3).

From an examination of the seismic profiles near Shell Mohawk (Figure 4A), it is clear that reflectors "4" and "3" are closely spaced in travel-time (.07sec, two-way time). According to the well logs, the geologic events interpreted as being responsible for the two acoustic horizons are only 123 m apart. At this point,

the question must be raised as to whether or not it is possible to resolve geology on this scale using "low-frequency" acoustic data.

The limit of seismic resolution is considered to be approximately a quarter-wavelength of the sound pulse encountering a reflecting surface at a given depth (Sheriff, 1976; Dobrin, 1976). Because higher frequencies and, correspondingly, shorter wavelengths are attenuated more rapidly with depth, resolution depends both on the bandwidth of the sound source and the depth of penetration desired. Unfortunately, no source monitoring of the air gun array was carried out during AII-91. However, the tapered array of four guns (see Figure 2) was fired simultaneously to maximize the amount of energy concentrated in the initial pulse and to reduce the length of subsequent bubble oscillations. Using a similar array consisting of three guns, Kramer et al. (1968) showed that the amplitude spectrum of the array signature peaked at 8 Hz, with very little energy concentrated at frequencies less than 4.5 Hz. Even though most of the AII-91 multi-channel profiles were filtered during CDP processing with a bandpass of 2-40 Hz, it is reasonable to assume from Kramer et al.'s results that the frequency of incident sound energy at the Shell Mohawk

B-93 well-site was centered approximately around 8 Hz. At the relatively shallow depths penetrated here, attenuation of such frequencies is small (McDonal et al., 1958; Sheriff, 1976). So, because the relationship between frequency, velocity, and wavelength is known ($v=f\lambda$), and because the frequency and velocity (derived from the sonic log for the interval between reflectors "4" and "3") have been determined, a representative wavelength can be calculated: $f = 8$ Hz, average interval velocity - 2.8 km/sec, $\lambda = 2.8/8 \approx .350$ km. Therefore, $\lambda/4 \approx 87.5$ m. It would appear that the geologic events at -1432 m and -1309 m in the Shell Mohawk B-93 well are theoretically resolvable as reflectors "4" and "3", respectively. This kind of resolution is possible only where well data are available. Beneath Georges Bank, the "4" - "3" interval thickens considerably (Figure 5), thereby increasing the confidence in the identification of these acoustic horizons as separate geologic events.

Reflector "2"

Another velocity discontinuity occurs at -1206 m/1.28 sec (two-way travel-time) in the well, only 103 m above the event interpreted to be responsible for reflector "3". Another simple $v = f\lambda$ calculation

based on the same assumptions indicates that resolution of these two events is also possible: $f = 8$ Hz (assumed) $v \approx 2.3$ km/sec (although the sonic log shows considerable scatter in the range 2.1-2.8 km/sec), $\lambda = 2.3/8 \approx .288$ km and $\lambda/4 \approx 71.9$ m. However, the "3" - "2" interval remains thin beneath Georges Bank, reaching a maximum of only .61 sec on U.S.G.S. line #1 near the shelf-break. Consequently, some uncertainty exists about the consistent resolution of the two acoustic horizons. Nonetheless, for the purposes of this discussion they are considered separate events, and they have been regionally correlated for later treatment of the stratigraphic succession underlying the New England margin.

The geologic event which appears to produce the reflector designated as "2" is the gradual transition from calcareous sandstones and silty shales (average interval velocity 2.9 km/sec, but with large fluctuations) to less calcareous siltstones, mudstones, and shales (average interval velocity 2.4 km/sec). Available information from the well logs and from Given (1977) date "2" beneath the Scotian Shelf as approximately Cenomanian. Reflector "2" may represent the contact between McIver's (1972) Logan Canyon and Dawson Canyon formations (Figure 6). According to Given (1977),

the Dawson Canyon is considered to be a fine-grained equivalent of the Logan Canyon, with the contact between the two transgressing landward until the end of the Cretaceous. All of the Cretaceous sediments sampled in the Shell Mohawk well can be attributed to these two formations.

According to Gradstein et al. (1975), a hiatus separates Aptian from Cenomanian sediments in the Mohawk well. Wade (1977) identified a seismic marker "K_a" on the Scotian Shelf, which he correlated with this mid-Cretaceous unconformity, but his interpretation presents a problem. Acoustically, "K_a" and reflector "3" (Jurassic-Cretaceous boundary) appear to be identical at the Mohawk well, perhaps because the Early Cretaceous section here is only 4 m thick (Figure 3). However, "K_a" and reflector "2" are more closely related geologically. "K_a" represents a late Early Cretaceous regression, while "2" could mark either that regression or the initiation of the ensuing transgression. If this identification of reflector "2" is correct, it could be time-transgressive.

Reflector "X"

Late Cretaceous sedimentation on the Scotian Shelf is characterized by the widespread deposition of marine shales and associated pelagic

chalks (Given, 1977). No Late Cretaceous chalk was sampled in Shell Mohawk B-93, but a velocity fluctuation at -581 m/.69 sec (two-way travel-time) (Figure 3) is interpreted as either a shallow-water equivalent of the Campanian Wyandot chalk (McIver, 1972; Wade's (1977) seismic horizon "K_w"), or the Maestrichtian-Paleocene hiatus which occurs in the well (Gradstein et al., 1975). A reflector corresponding to the velocity discontinuity was identified and correlated beneath Georges Bank with horizon "X" of Schlee et al. (1976), who considered it to mark the base of the Tertiary section (Figure 5). Reflector "X" is not continuous, and its amplitude varies considerably (Figures 4A and 4B). Nonetheless, it is possible to trace "X" regionally, and it can be considered as the approximate boundary between the clastics of the Cretaceous Dawson Canyon Formation and the Tertiary Banquereau Formation (McIver, 1972; Figure 6).

Reflector "1"

The shallowest reflector identified and correlated beneath the Scotian Shelf exhibits more relief than any other acoustic horizon within the sedimentary section (Figure 5). In this instance, the reflector was picked first, and then tied to the

well to establish its geologic character. Reflector "1" is generally of low amplitude and locally discontinuous, particularly where it exhibits structure. It lies at -386 m/0.48sec (two-way travel-time) in the Mohawk well, and correlates with the largest velocity fluctuation on the sonic log above the one producing reflector "X" (Figure 3). The reflector's depth corresponds to the disconformable contact between Eocene and Oligocene sediments (Gradstein et al., 1975) at the well-site. To the west along Line 42 (Figure 5), reflector "1" traces an unconformity exhibiting almost 1.0 sec of relief which outlines several buried submarine canyons. Similar structures were identified by King and MacLean (1976) beneath the eastern part of the Scotian Shelf.

Savin et al. (1975), Ingle et al. (1976, 1977), and Haq et al. (1977) have all pointed out the potential worldwide significance of a major regression during the Oligocene. Such a regression probably caused the erosion which created the now-filled submarine canyons on the Scotian Shelf. Interestingly, "1" cannot be traced across Northeast Channel (Figure 5). Either depositional conditions on the Scotian Shelf and Georges Bank differed during the Oligocene regression, or subsequent events on Georges Bank obliterated all seismic evidence of Oligocene erosion.

Regional Correlations

Continental Shelf: Correlation of Acoustic
Stratigraphy from the Scotian Shelf to
the New England Margin

During the foregoing development of the chronostratigraphic framework for the interpretation of seismic reflection profiles collected over the New England continental margin, frequent reference was made to Line 42 (Figure 5), one of two AII-91 6-channel profiles connecting the Scotian Shelf with Georges Bank. These tie-lines were examined first in order to assess the feasibility of correlating the acoustic horizons identified at Shell Mohawk B-93 over many kilometers. Figure 5 shows that such correlations were possible except in the immediate vicinity of Northeast Channel, where a combination of bottom topography (creating seismic processing difficulties) and the presence of deep-seated structure combined to cause acoustic disturbances resulting in a general deterioration of reflection quality. From a variety of geophysical evidence summarized by Keen and Keen (1974), Jansa and Wade (1975), Given (1977), Uchupi et al. (1977), and Wade (1977, 1978), the structures which create the acoustic disturbance beneath Northeast Channel are believed to be part of a diapiric zone

called the Sedimentary Ridge Province (Jansa and Wade, 1975), which extends along the entire Nova Scotian margin in water depths of 1,500-4,000 m. Evaporites of Early Jurassic age have been drilled on the Scotian Shelf, and they are now referred to as the Argo Formation (McIver, 1972; Figure 6). Based on data available at present, it is reasonable to conclude that the structures composing the Sedimentary Ridge Province (hereafter called the SRP) are indeed sedimentary. Obviously, the exact nature of the material will remain a question until deep-water drilling off Nova Scotia takes place. The presence of a fault-bounded trough in acoustic basement (associated with a broad negative magnetic anomaly) substantiates a sedimentary origin for the structures beneath Northeast Channel (Figure 5). Fortunately, the acoustic disruption here was confined to a narrow zone, allowing for the reasonable extrapolation of reflecting horizons.

Southeast of Northeast Channel, a general thickening of the sediment section occurs, particularly in the "z" - "3" and "2" - "x" intervals (Figure 5). Basement cannot be traced beneath Northeast Channel, but reappears on Line 42 beneath Georges Bank. As noted above, reflector "1" cannot be discerned on

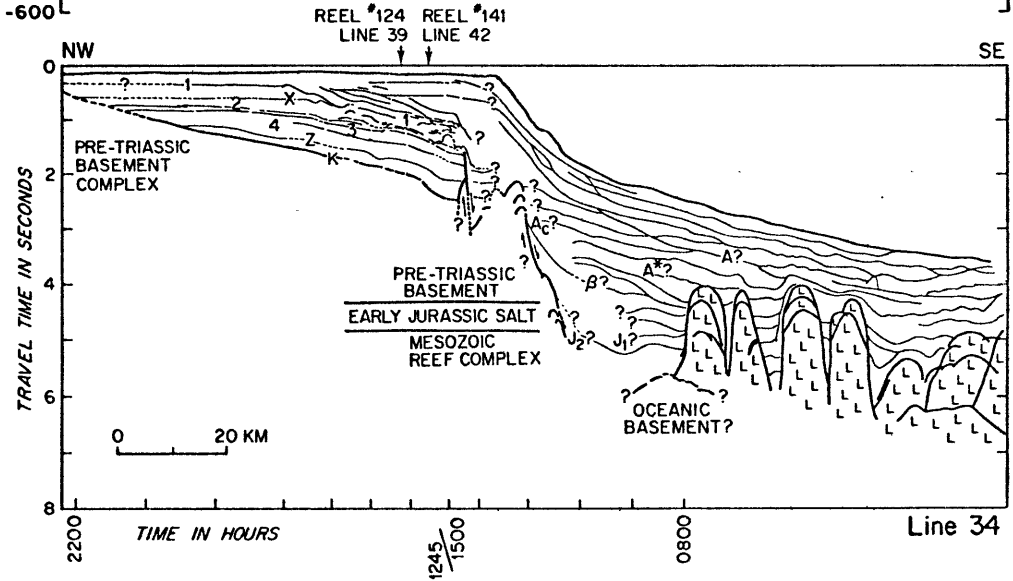
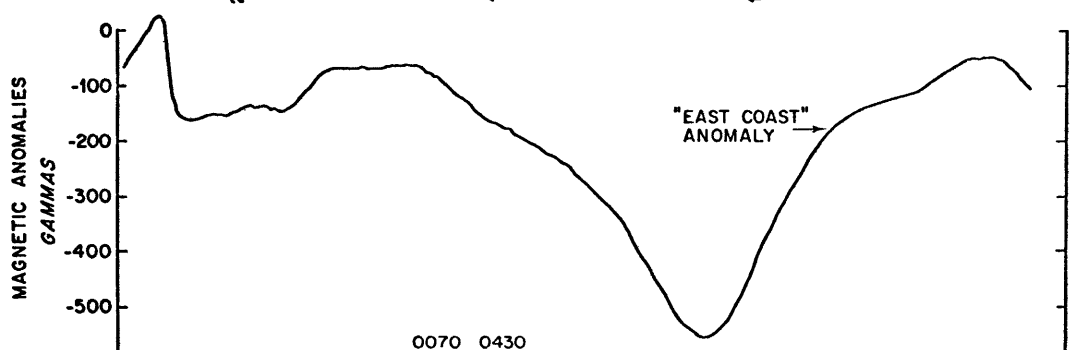
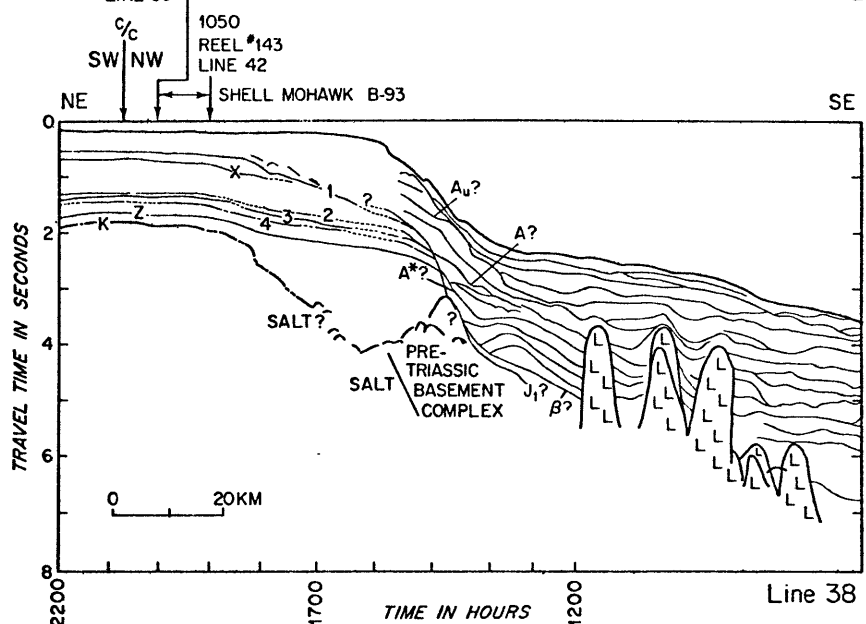
the Georges Bank side of the channel. This horizon may persist, but its lack of relief precludes its identification away from well-control data.

After completing the examination of the tie-lines, the rest of the available multi-channel information (Figure 1) was interpreted sequentially from northeast to southwest. The interpreted tie-lines were used for cross-reference. Line drawings (Figures 8-13) of a number of the profiles are presented along with accompanying magnetic anomalies.

LaHave Platform/Scotian Shelf

Lines 38 and 34 (Figure 8) show an interpretation of the acoustic stratigraphy underlying the Scotian Shelf, part of the LaHave Platform (Jansa and Wade, 1975). The basement/"K" surface is generally smooth and dips seaward. Along Line 38, however, a rapid thickening of the "K" - "Z" (Early-Middle Jurassic) interval accompanies a plunging basement surface, which culminates in a ridge-like feature beneath the shelf-break. The ridge exhibits an acoustic signature of confused hyperbolic echoes. It could represent a basement structure, but at this location the magnetics do not support the presence of a basement high. The presence of Early Jurassic salt

Figure 8. Interpretations of Lines 38 and 34 on the Scotian Shelf, the western part of the LaHave Platform. Landward of the shelf-break, these and the following line drawings are CDP-processed 6-channel recordings. The slope-upper rise portions are single-channel interpretations published in Uchupi et al. (1977). For these and all subsequent line drawings, vertical exaggeration of topography is approximately 13:1. Reflector identifications and accompanying magnetics are discussed in the text. For exact locations of the lines on this and the following figures, refer to the location map on Figure 5.



of the Argo Formation (Figure 6) at -4333 m in the Shell Mohican I-100 well drilled near the shelf-break about 200 km east of Line 38 prompted Given (1977) to postulate the existence of salt all along the shelf-break south of Nova Scotia. Perhaps the ridge is a landward extension of the SRP. Whatever its composition, the feature may have constituted a partial barrier during pre-"Z" sedimentation. On Line 34, a gently dipping basement/"K" surface also abuts a buried shelf-edge high. In this instance, the structure appears faulted on the seismic profile, which would tend to support a non-sedimentary origin. Unfortunately, the magnetics do not corroborate such an interpretation.

Sediment reflectors onlap the basement surface along Line 34, and they dip gently seaward. The cross-cutting nature of reflector "1" is clear. Inclined horizons above "1" indicate Neogene progradation of the shelf, resulting in thick wedges of post-"1" material near the shelf-break.

Georges Bank

Seven lines illustrate the acoustic structure and stratigraphy of the Georges Bank Basin: 23 and 21 (Figure 9), U.S.G.S. 4 and 17-19 (Figure 10), and 2, U.S.G.S. 1, and 12/46 (Figure 11). On Figures 9 and 10, a pronounced down-faulting of basement beneath the southern part of the bank can be discerned,

Figure 9. Interpretations of Lines 21 and 23 Northeast Channel and the eastern part of Georges Bank.

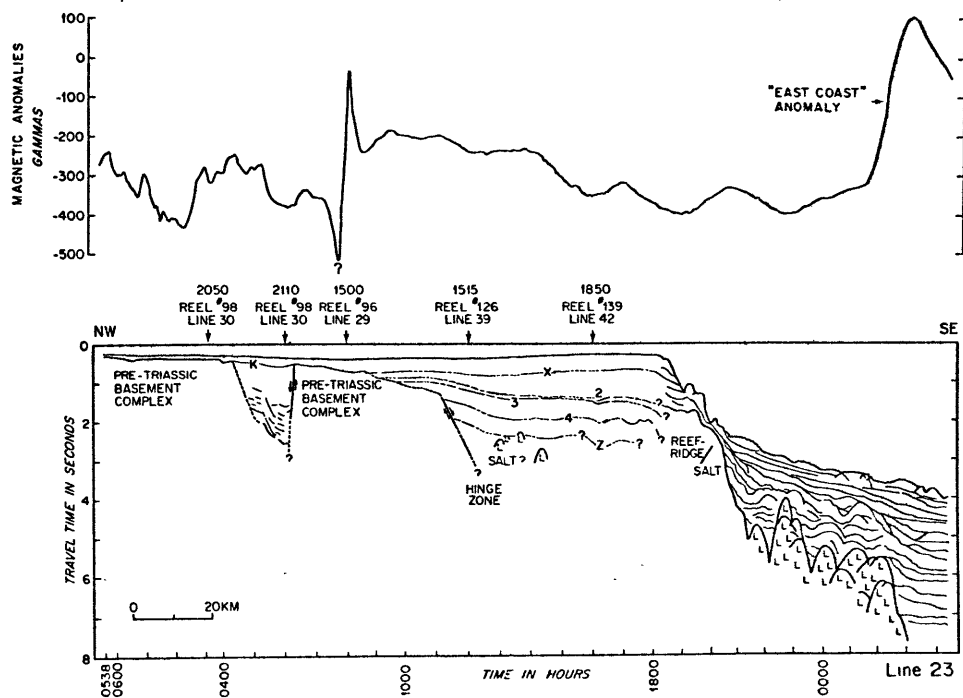
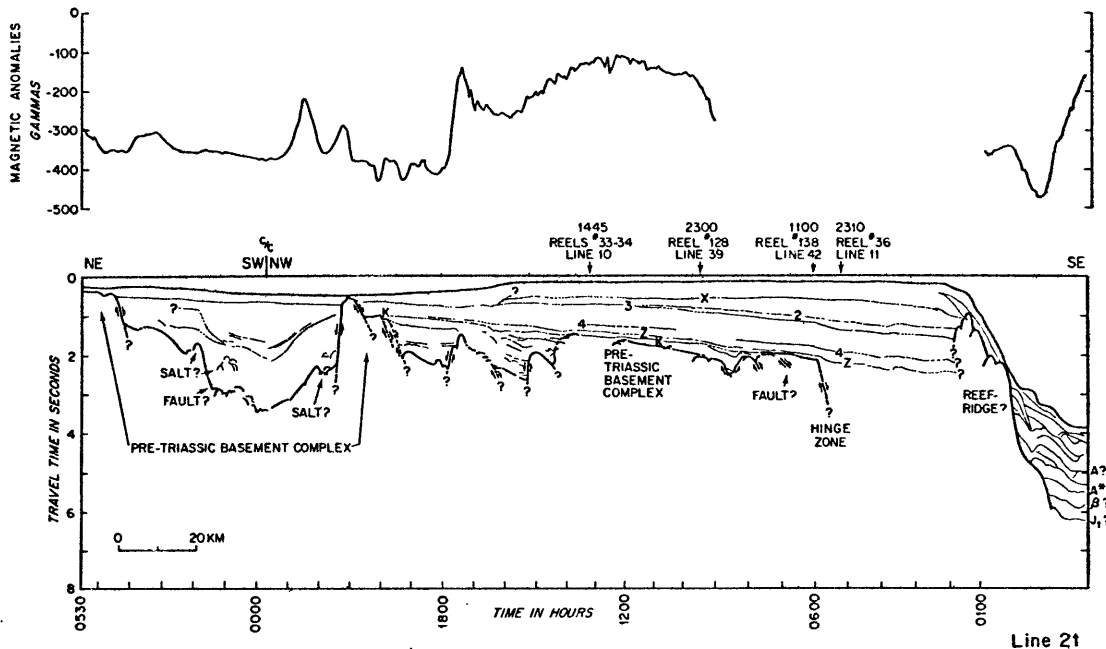
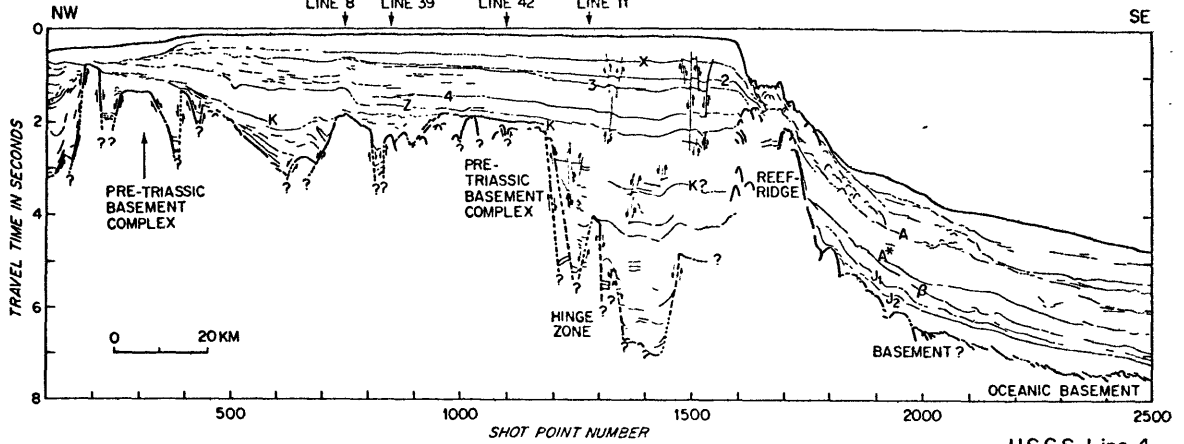
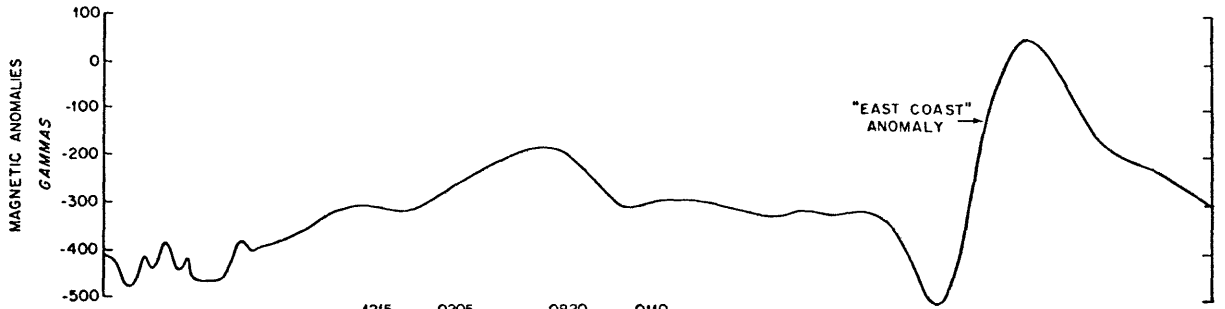
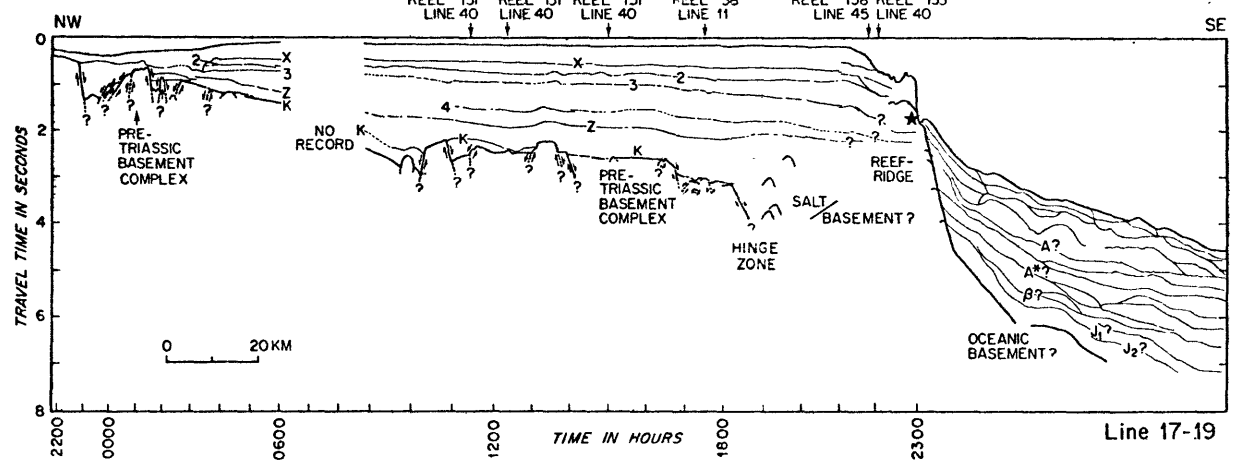
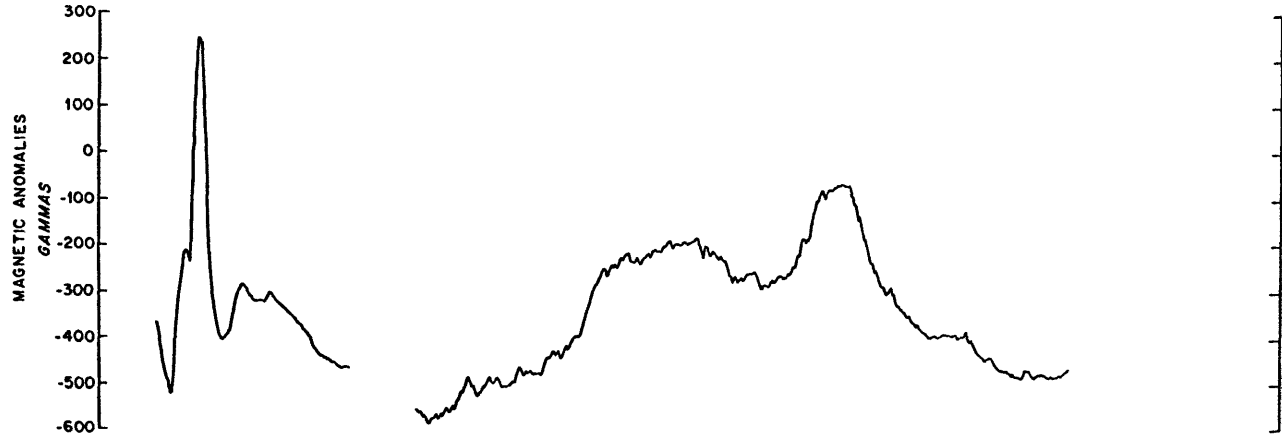


Figure 10. Interpretations of U.S.G.S. Line 4 (48-channel) and Line 17-19, the central part of Georges Bank. The "*" on the upper continental slope on 17-19 is the approximate location of the site from which Neocomian reefal limestone was collected by Ryan et al. (1978) in Heezen Canyon.

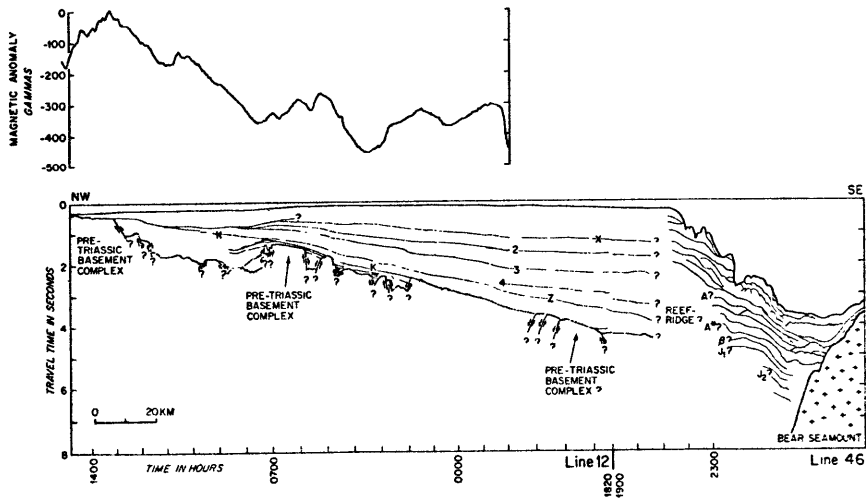
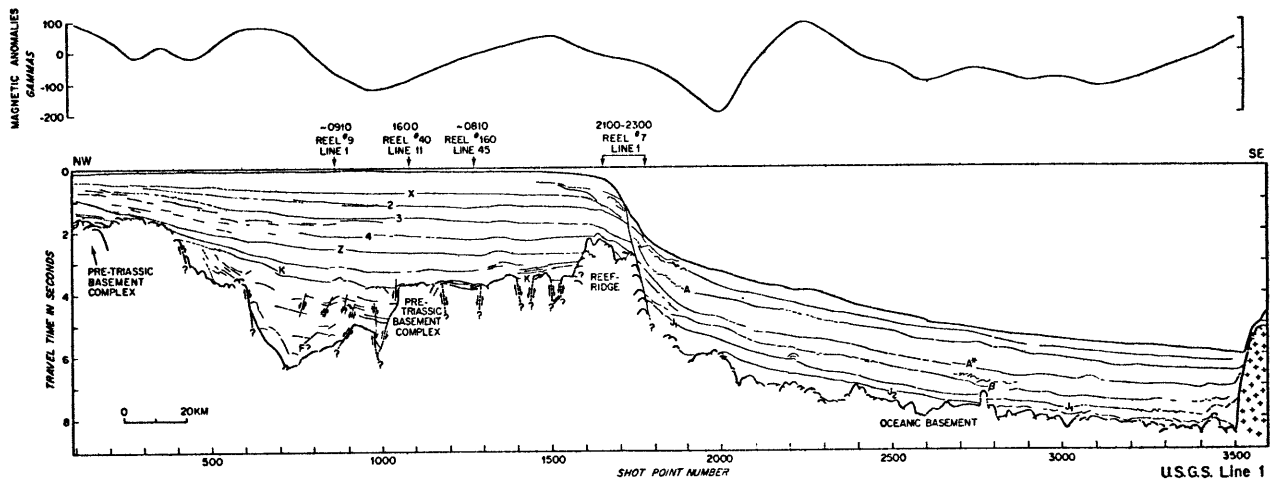
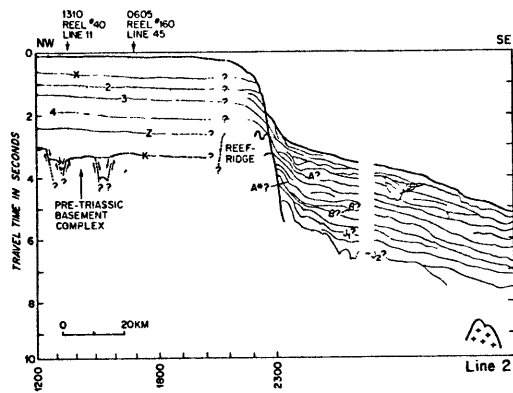
Figure 11. Interpretations of Lines 2, U.S.G.S. 1
(24-channels), and 12/46, the central
and western parts of Georges Bank.



U.S.G.S. Line 4



Line 17-19



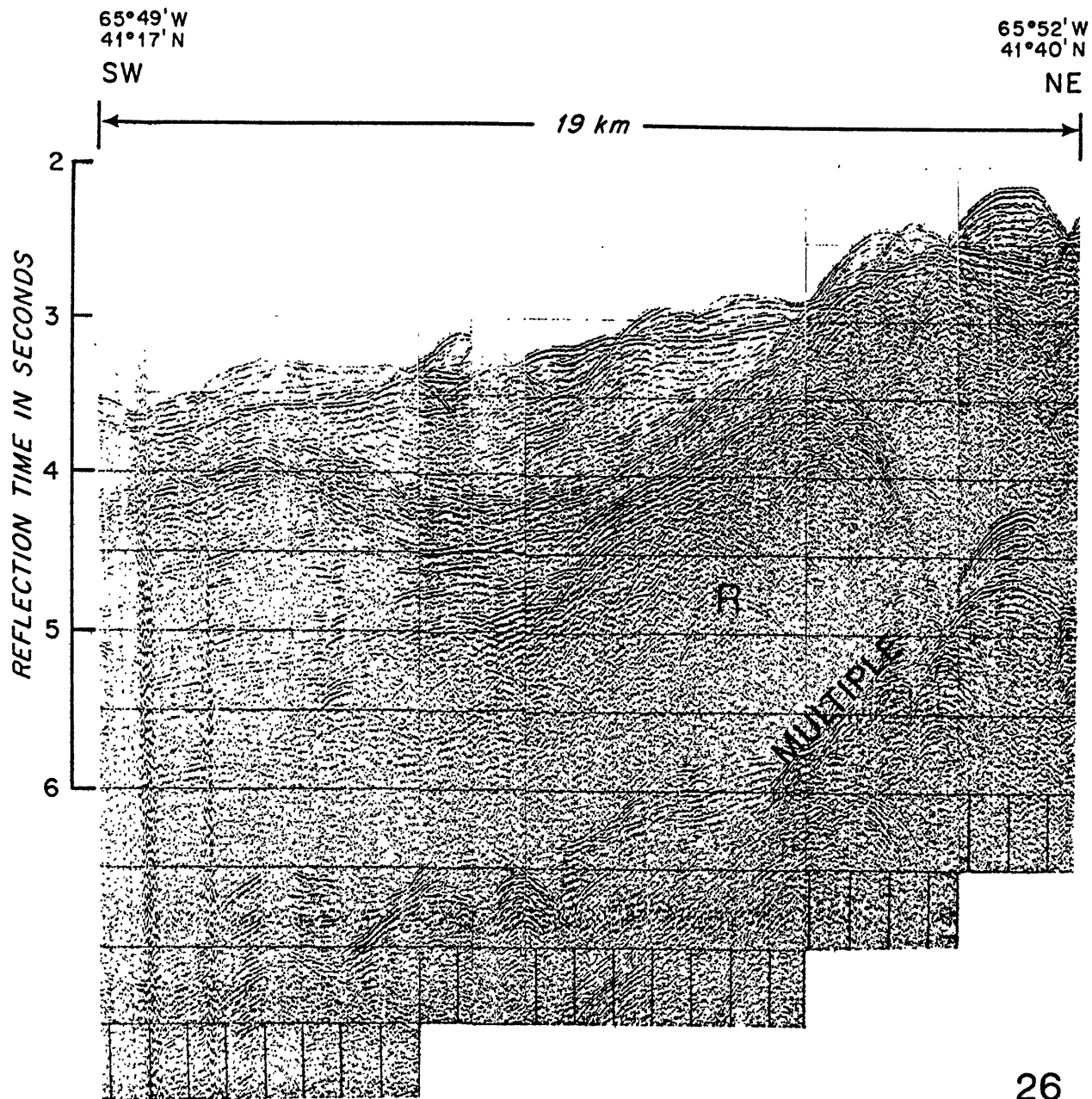
which is here termed the "hinge zone". The "hinge zone" is not observed on Figure 16, but it may be masked beneath the "reef-ridge", which is now known to consist, at least in part, of Mesozoic reef carbonate (Ryan et al., 1978).

On all of these profiles, basement appears as a block-faulted terrain truncated by the "K" unconformity. Similar structures have been observed on land within the Triassic rift system of New England and Nova Scotia, and offshore beneath the Gulf of Maine (Ballard and Uchupi, 1975). Reflector "K" is easily followed across the tops of blocks, but is occasionally difficult to trace over troughs (see U.S.G.S. 4, shot points 500-800, Figure 10). In general, "K" tilts seaward at varying dips. Normal faults are abundant and dip both landward and seaward. One of the largest graben structures of the New England margin underlies Georges Basin in the Gulf of Maine (left side of Line 21, Figure 9). Ballard and Uchupi (1975) have identified a possible diapiric structure within the fill of this graben, and there are several structures exhibiting no magnetic activity along Line 21 which could also be sedimentary. If evaporites do exist beneath the gulf, they are pre-"K" and have significance for the early development of this margin.

Diapirs may also be present seaward of the "hinge zone" on Line 23 (Figure 9) along the west side of Northeast Channel. Vague, isolated hyperbolae are discernible on the profile which do not appear to be associated with a significant positive magnetic anomaly (Figure 9). However, where similar acoustic structures occur along Line 17-19 (Figure 10), they do coincide with such an anomaly.

West of Line 17-19, the "hinge zone" is no longer visible (Figure 10). It may be masked by the shelf-edge high described by Drake et al. (1959). This so-called "reef-ridge" (Schlee et al., 1976) is acoustically identified as a zone of hyperbolic echoes accompanied by general deterioration in reflection amplitude (Figure 12). Reflectors can be traced seaward to their contact with this feature, but no further. From Northeast Channel to Line 17-19, the ridge appears to be continuous, and must have been at least a partial barrier to the seaward transport of sediment until reflector "2" time (early Late Cretaceous). Farther west, the ridge is buried more deeply, and could not have been a structural barrier beyond reflector "4" time (Middle-Late Jurassic). Throughout its length, this feature forms the foundation of the continental slope south of Georges Bank. Its position effectively

Figure 12. A single-channel profile, part of Line 26, published in Uchupi et al. (1977). The "reef-ridge" discussed in the text is labeled "R". Vertical exaggeration is approximately 9:1. For an exact location, refer to Figure 1.



prevents the correlation of acoustic horizons from the continental shelf to the continental rise. In this study, the "reef-ridge" is interpreted as a Mesozoic carbonate platform/reef complex. This interpretation is based upon available geophysical evidence and recent sampling operations by DSRV ALVIN in Heezen Canyon, which recovered algal reef carbonate of Neocomian age from near the top of the feature (Ryan et al., 1978). (The approximate sampling site is noted with a "*" on Line 17-19, Figure 10). Although the nature of the foundation of the carbonate build-up is still a matter of conjecture, recent modeling of magnetic data by Klitgord and Behrendt (in press) indicates the existence of a magnetic basement high at depths of 6-8 km below sea-level.

All of the sediment reflectors in the Georges Bank Basin exhibit gentle seaward dips. Across the "hinge zone", "K" - "Z" (Early-Middle Jurassic) thicknesses increase rapidly. The thickness of pre-"K" sediments (seaward of the "hinge zone") is unknown, primarily because "K" cannot be recognized with certainty in this region (see U.S.G.S. 4, Figure 10). The overall thickness of the sediment section is much larger here than beneath the LaHave Platform, owing to greater subsidence of basement.

A significant change in the acoustic nature of the pre-"3" (Jurassic) sediments is associated with the landward termination of reflector "4" (see U.S.G.S. Lines 4 and 1, Figures 10 and 11). Fairly continuous reflectors of high amplitude are generally replaced with discontinuous, bifurcating horizons exhibiting variable amplitude. This is accompanied by a systematic decrease in interval velocities. Schlee et al. (1976) postulated a major facies change from carbonate (seaward) to clastics as the cause of this major acoustic transition.

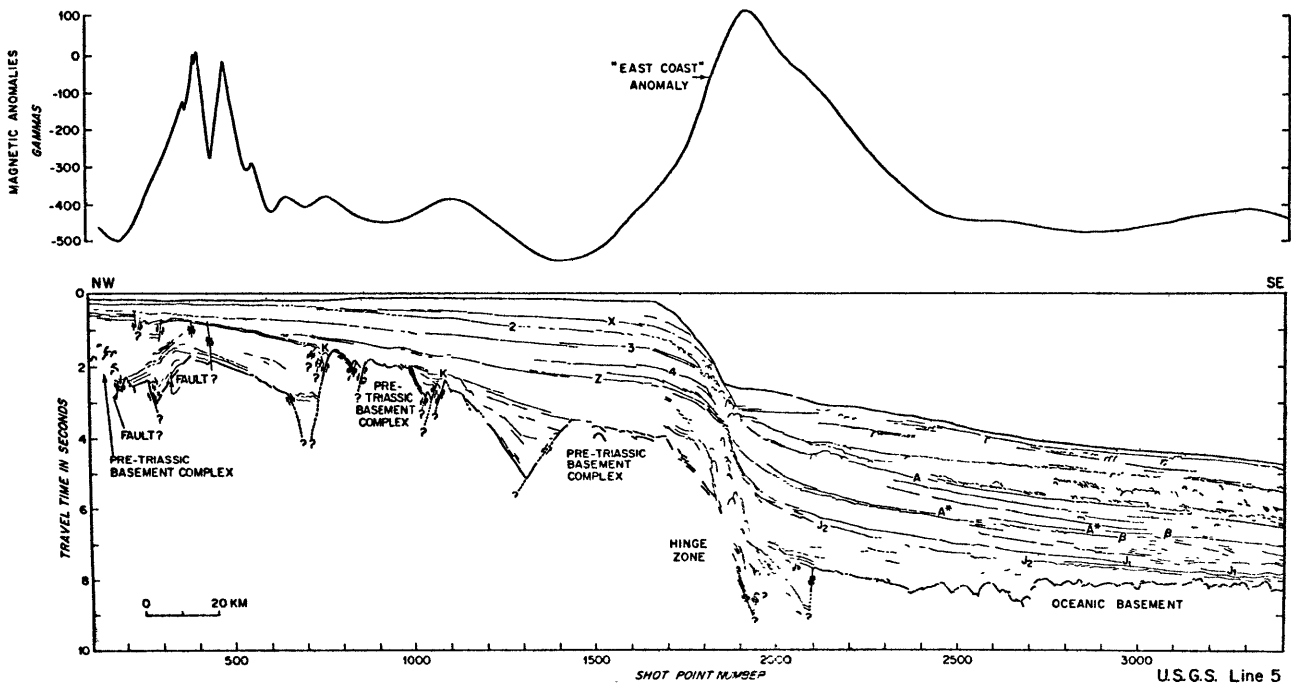
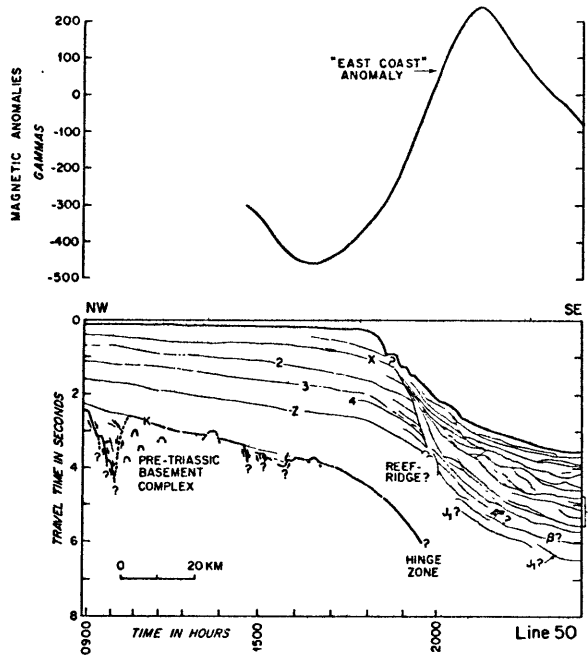
Reflector "X", the approximate Cretaceous-Tertiary boundary, is the uppermost acoustic horizon which can be followed beneath Georges Bank. Evidence for Tertiary progradation of the shelf is not abundant except near the shelf-break, where some inclined horizons resemble foreset beds (U.S.G.S. 1, Figure 11). Although reflector "1", which was interpreted as an Oligocene unconformity beneath the Scotian Shelf, cannot be traced beneath Georges Bank, Oligocene erosion may, in part, be responsible for the submarine canyons indenting the continental slope there. A Tertiary unconformity, perhaps correlative with "1", is observed on Lines 21 (Figure 9), U.S.G.S. 4 and 17-19 (Figure 10), and on U.S.G.S. 1 and 12/46 (Figure 11) beneath

the Gulf of Maine. It truncates all post-"K" reflectors, and is responsible for the present cuesta morphology of Georges Bank postulated by Johnson (1925). According to Lewis and Sylwester (in press), who used high-resolution seismic reflection techniques to study the uppermost sediments of Georges Bank and the Gulf of Maine, the unconformity probably formed as a result of Pleistocene modification of a middle to late Tertiary coastal plain drainage system. The present submarine canyons south of Georges Bank could represent part of that drainage system.

Long Island Platform

The Long Island Platform is that part of the shelf south of Long Island which forms the structural divide between the Georges Bank Basin and the Baltimore Canyon Trough (Schultz and Grover, 1974). Two lines, 50 and U.S.G.S. 5 (Figure 13), illustrate the platform's acoustic character. Geologically, basement is a complex mosaic of block-faulted horsts and grabens. A "hinge zone" is discernible, but no "reef-ridge" can be discerned west of U.S.G.S. 1. Magnetic depth-to-source estimates for U.S.G.S. 5 (Klitgord and Behrendt, in press) indicate a magnetic ridge beneath the slope at a depth of 8 km below sea-level. Apparently,

Figure 13. Interpretations of Lines 50 and U.S.G.S.
5, Long Island Platform.



the foundation for a reef structure exists here, but for some reason no reefal build-up occurred as it did on the eastern part of Georges Bank.

The stratigraphic succession on the Long Island Platform is similar to that underlying Georges Bank and, therefore, will not be discussed in detail. In the absence of any shelf-edge structures, acoustic horizons can be traced all the way to the upper continental slope, where they are truncated by an unconformity separating the shelf sequence from the overlapping continental rise prism. Unlike the profiles to the east, there is only minor evidence of shelf progradation during the Tertiary. In fact, the paleoshelf break outlined by reflector "Z" on U.S.G.S. 5 is approximately 20 km seaward of the present shelf-break. Examination of the profile indicates that net erosion of the shelf occurred from reflector "Z" to reflector "2" time, after which some net outbuilding took place. According to Folger et al. (in press), the shelf-break south of 40°N in the Baltimore Canyon Trough region retreated 20 km during the Oligocene regression inferred to have created reflector "1" beneath the Scotian Shelf.

On the magnetic profiles, the "slope anomaly" is clearly visible over the continental slope (Figure 13). The prominent double-peaked magnetic high present along

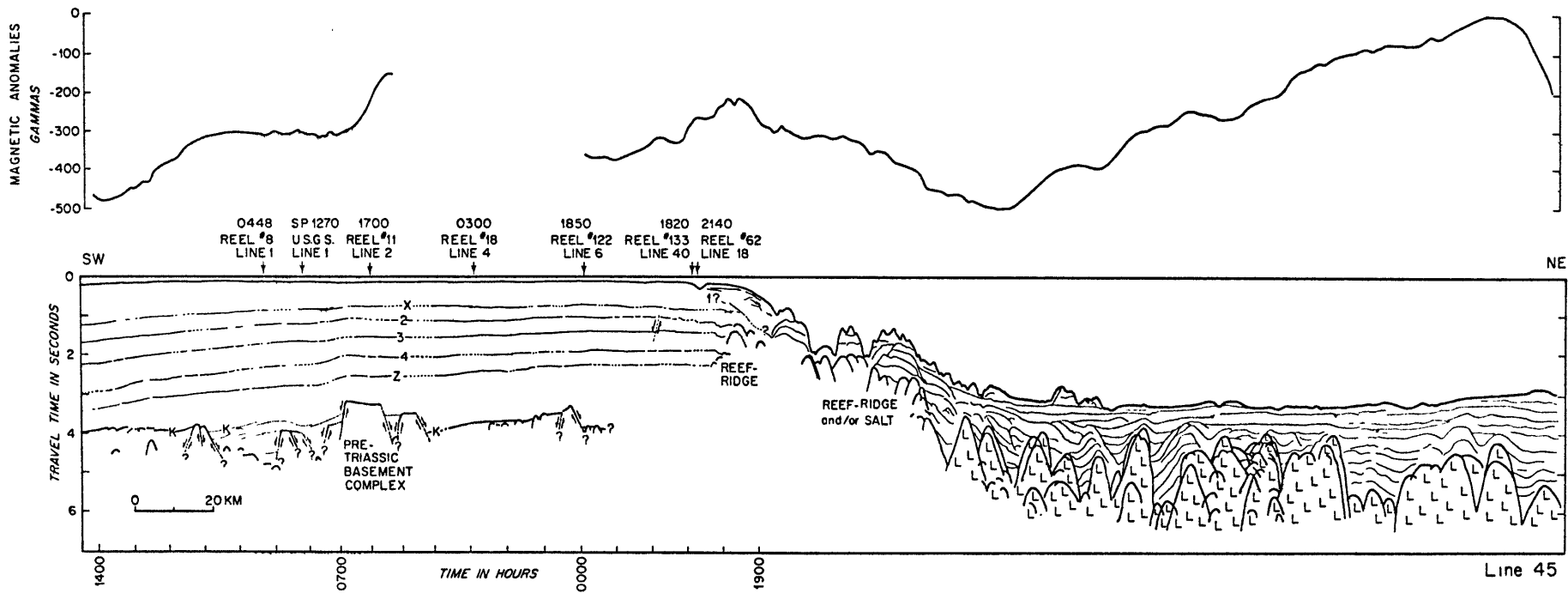
the landward part of U.S.G.S. 5 (centered about shot point 450) may be caused by a seaward extension of Early Jurassic (or older) volcanics sampled by a drill hole (U.S.G.S. #6001) on Nantucket Island south of Cape Cod (Figure 1). According to Valentine (1978), these volcanics are responsible for the prominent reflecting horizon designated as "K" on U.S.G.S. 5 landward of shot point 800 (Figure 13). The extent of these volcanics, and their exact relationship in time and space to the "K" unconformity, is presently unknown.

Continental Rise

Nova Scotia

Line 45 (Figure 14) extends from the continental rise south of Nova Scotia obliquely across the continental slope onto the southern part of Georges Bank. As can be seen from an examination of this line, the continental rise prism south of Nova Scotia is highly deformed by the SRP. Jansa and Wade (1975) inferred a sedimentary origin for the SRP on the basis of acoustic signature, the contact relationships with overlying sediments, and the recovery of Early Jurassic evaporites from similar structures drilled beneath the continental shelf. Thus far, geophysical studies of this "ridge complex" (Emery et al., 1970) have not proven the structures to be diapirs. Nonetheless, the

Figure 14. Interpretation of Line 45, which runs from the Scotian rise southwest obliquely across the continental slope to end on the central part of Georges Bank.



available evidence, summarized below, favors that hypothesis:

1) Seismic refraction velocities ranging from 3.45 - 5.29 km/sec (Keen and Keen, 1974). A typical anhydrite velocity (Gulf Coast) is 4.1 km/sec (Press, 1966), while rock salt exhibits velocities around 4.6 - 4.9 km/sec (Gardner et al., 1974; Sheriff, 1976). However, other rock types (i.e. basalt, granite, limestone) also yield similar velocities.

2) Elevated heat flow (L. Hyndman, personal communication). Heat flow measurements over known diapiric structures off West Africa (Von Herzen et al., 1972), Brazil (Leyden et al., 1978), and in the Gulf of Mexico (Epp et al., 1970) show higher than normal thermal gradients, presumably as a result of the high thermal conductivity of salt.

3) The acoustic similarities between these structures and proven diapirs off West Africa (Emery et al., 1974), Brazil (Leyden et al., 1976), in the Gulf of Mexico (Emery and Uchupi, 1972), and off the Laurentian Channel (Uchupi and Austin, in press). These similarities include: collapse structures piercements which have breached the sea-floor (presumably indicative of the rapid dissolution of the evaporites upon contact

with sea-water), and deformation of both overlying and flanking sediments and occasionally the sea-floor by these structures. This deformation is apparent on both 3.5 kHz and seismic reflection profiles, and is considered to be strong evidence for the vertical migration of evaporites.

4) Magnetic and gravity data indicating that the SRP structures are often nonmagnetic and associated with negative free-air gravity anomalies (Emery et al., 1970).

The SRP comes into contact with the "reef-ridge" previously discussed at the base of the continental slope (Figure 14). The exact nature of the contact is unclear on Line 45, but west of this line along the upper rise no diapiric structures can be discerned (Figures 10, 11, and 13; Uchupi et al., 1977). It is possible either that the Mesozoic reef or its basement foundation form one of the boundaries of the evaporite basin, or that competent sediments (i.e. fore-reef carbonates?) overlie and effectively prevent the vertical migration of salt south of Georges Bank.

Georges Bank

The acoustic stratigraphy of the continental rise south of Georges Bank is based on long-distance seismic correlations with prominent acoustic horizons identified in the western North Atlantic (Tucholke and Vogt, in press; Tucholke and Mountain, in press) made by B. Tucholke of Lamont-Doherty Geological Observatory in association with K. Klitgord of the U.S. Geological Survey. Their reflector "J₂" (see deep-water portions of Figures 10, 11, and 13) is recognized near the base of the continental rise section, and is presently interpreted to be correlative with the formation of the Blake Spur Anomaly (Klitgord and Schouten, 1977). The Jurassic-Cretaceous boundary is marked by reflector "J₁" (Figures 10, 11, and 13), coeval with reflector "3" beneath the shelf. Both the "3" - "K" interval beneath the shelf and the "J₁"-acoustic basement interval under the rise exhibit interval velocities in excess of 4.7 km/sec (Schlee et al., 1976; Grow and Schlee, 1976), but the "J₁"-acoustic basement interval is generally thinner. Along the rise portion of U.S.G.S. 4 (Figure 10), acoustic basement climbs smoothly to the base of the "reef-ridge". This "basement" surface could be either a landward extension of oceanic layer 2, or the top of competent

sediments. Perhaps such sediments, eroded during the formation of the "K" unconformity, reached the deep-sea through gaps in the basement foundation of the "reef-ridge" to fill depressions at the foot of the continental slope (an indication of such a depression may occur along U.S.G.S. 5, Figure 13). Unfortunately, little knowledge of the pre-"J₁" section will be ascertained until deep-drilling takes place on the continental rise.

Where it has been sampled by the Deep Sea Drilling Project, Horizon "β" overlying "J₁" separates Neocomian limestones from Aptian-Albian black shales. Horizon "A*" is produced as a result of the contact between the black shales and an overlying calcareous unit deposited during a late Maestrichtian depression of the CCD (Tucholke and Mountain, 1977, in press). Finally, the Horizon "A" complex consists of a packet of reflectors caused both by the deposition of upper-lower to lower-middle Eocene cherty turbidites and by the development of a late Eocene-early Miocene regional unconformity ("A^u") (Tucholke and Mountain, 1977, in press).

Continental Slope: The Problem of Shelf-
Rise Correlations

The continental slope along the New England continental margin is steep (5-8°) and highly irregular

(Figure 1). Because of the rapid change in water depth, seismic profiles collected across the slope exhibit a water multiple which cuts across and often obscures sub-bottom structure (see Figure 12 for an example). Despite the advent of multi-channel profiling and various processing techniques, the adverse effects of these multiples on seismic resolution have not been completely eliminated.

To further compound the problems, the geology of this feature is very complex. The "reef-ridge" underlying part of the shelf-break has maintained a steep slope for much of the margin's history. Along this natural ramp, sediments have moved in response to turbidity currents (particularly associated with submarine canyons, Uchupi et al., 1977; Ryan et al., 1978) and mass-wasting or gravitational tectonics (slumping, sliding, and creep, MacIlvaine, 1973). Consequently, unconformities beneath the slope are common (Figures 11 and 13). They often prevent the straight-forward correlation of acoustic horizons from the shelf to the rise.

Where the slope is not being controlled structurally, the position of the shelf-break is a complicated interaction of changes in sedimentation, subsidence, and eustatic sea-level (King and Young, 1977). U.S.G.S. 5 (Figure 13) illustrates this stratigraphic complexity.

According to Ryan et al. (1978), the submarine canyons south of Georges Bank are products of numerous erosional episodes. Uchupi et al. (1977) recognized at least two such episodes on single-channel profiles collected over Corsair Canyon, while three are discernible beneath the continental slope along Line 45 (Figure 14).

It is not yet known whether or not all or part of the continental slope off New England has fundamental structural significance as the ocean-continent transition zone. The location of the "east coast magnetic anomaly" (Drake et al., 1963) implies that some kind of basement structure forms the slope's foundation, but magnetic modeling of the so-called "slope anomaly" does not yield a unique solution as to its exact nature (Klitgord and Behrendt, in press). In this context, the opinion has even been expressed that slope structures are in many instances merely phantoms created by sloppy multi-channel processing techniques (Taner, Cook, and Neidell, 1970). While this is possible, an examination of Figure 12, which is an unprocessed single-channel profile, leaves little doubt that the feature labeled "R" is a physically real entity.

The presence of a steep continental slope has been a help, as well as a hindrance, because outcrops on

the slope which have been sampled by dredge and submersible have supplied virtually all of our stratigraphic knowledge of the New England margin. Available lithologic information from the slope south of Georges Bank will be summarized and used in conjunction with the regional acoustic correlations already developed to make inferences about the paleogeographic history of the region.

Geologic Maps: New England Passive Continental Margin

Introduction

Reliable interval velocities are necessary to convert reflection travel-times to actual sediment depths and thicknesses, and therefore they are essential for the construction of geologically meaningful isopach and structure maps from seismic reflection data. For the most part, the reliability of interval velocities derived from "common-depth-point" (CDP) processing depends upon the degree to which simplifying assumptions made about the nature of the geology being examined are accurate (see Appendix I). Fortunately, the sediments underlying Georges Bank are essentially undeformed and flat-lying. However, this is not the case near the shelf-break, and consequently CDP interval velocities for this region must be treated with caution. The length

of the receiving array is a second inherent limitation of the CDP technique. The 6-channel streamer used during AII-91 could not resolve differences in rms velocities (see Appendix I) below a travel-time depth of approximately 2.8 sec. Because NMO (see Appendix I) drops to zero at roughly this depth, returns from deeper than 2.8 sec are effectively averaged over all six channels of the array, producing a single-channel result. A third factor is the subjective nature of picking rms velocities from velocity spectra. According to Taner and Koehler (1969), peaks in reflection coherency as continuous functions of normal incidence travel-times ($T_{O,N}$) characterize primary over secondary or multiple reflection returns. Unfortunately, hyperbolic velocity-time functions (see Appendix I) are not sensitive to many geologic phenomena (i.e. velocity inversions). Furthermore, multiples may produce peaks in coherency which may be erroneously picked as primaries by the unwary or inexperienced interpreter. Finally, the Dix (1955) formula (see Appendix I) for calculating interval velocities from rms velocities is subject to large errors where layers are thin, even if derivation of the rms velocities using the Taner and Koehler (1969) technique has been carried out correctly (Sheriff, 1976).

As is the case for CDP processing, the reliability of interval velocities calculated from expendable sonobuoy profiles depends primarily on a geology which conforms to a simple layered-earth model. Fortunately, the Georges Bank region is a good natural example of such a model. Because regional dips beneath the New England continental shelf are constant and very small, and because concurrent normal incidence profiles were available to estimate dips where they did occur, unreversed sonobuoy profiles collected on this margin (All of the AII-91 sonobuoy runs were unreversed) should yield velocities which are neither systematically high nor low. Both LINFT and SLOWI (Appendix II) assume an increase of compressional wave velocity with depth. Unfortunately, this is not always true in nature. Moreover, SLOWI carries out a vertical average of both high and low-velocity thin layers to arrive at an oblique reflection interval velocity solution for the thicker composite layer, while LINFT calculates an interval velocity based upon a refraction arrival which follows the fastest paths from source to receiver. Consequently, discrepancies between refraction and oblique reflection velocities for the same interval may occur in an area characterized by diverse lithologies. This is the case beneath Georges Bank, where refraction velocities are

systematically higher than oblique reflection interval velocities calculated from sonobuoys and CDP processing (Grow et al., 1978). Minor graphical inconsistencies (i.e. in drawing the hyperbolic curve approximations of the oblique reflection returns, see Figure 35B) are estimated by SLOWI, and incorporated into the interval velocity solution as a standard deviation (all of these deviations are quoted in Appendix II). LINFT does not calculate standard deviations, and consequently there is no way to estimate, quantitatively, the errors in refraction velocities for the shallow-water buoys (Appendix II).

In order to achieve an even coverage of time-to-depth conversion points, at least one CDP-pick from each reel (representing approximately 35-40 line km) of AII-91 multi-channel data was chosen for interval velocity information. Where a sonobuoy run occurred, interval velocities from the sonobuoy and from a CDP velocity analysis made along or near the sonobuoy profile were averaged over the same or similar travel-time intervals. Wherever possible, these intervals coincided with major subdivisions of the region's acoustic stratigraphy. Obviously, the CDP/sonobuoy velocity comparisons were subjective, but whenever averaging occurred, standard deviations were calculated. In certain instances,

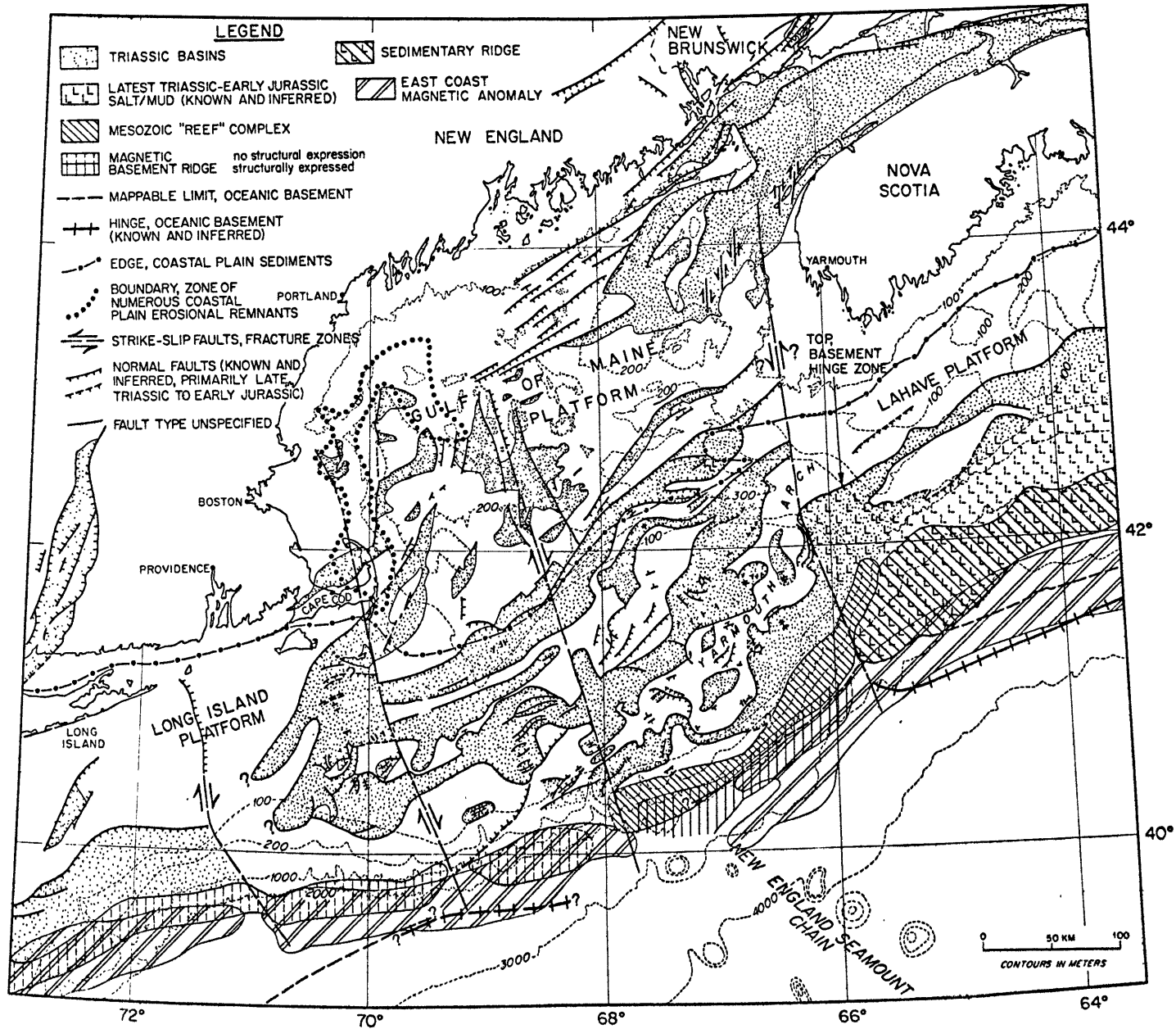
as, for example, in areas where acoustic basement could not be discerned, extrapolations of layer thicknesses and velocities were made (Appendix III). Only the U.S.G.S. interval velocity results were used to estimate thicknesses and depths on the continental slope and upper rise. The identification of reflectors on the AII-91 single-channel profiles off the shelf was uncertain because of too few ties with the U.S.G.S. multi-channel lines (Figure 1).

Ultimately, averaged interval velocities at more than 200 points (Appendix III) were used to calculate layer thicknesses and depths to the major acoustic horizons underlying the New England passive margin.

Basement Tectonic Structures

Based on previously published information (Ballard and Uchupi, 1975; Given, 1977) and all of the multi-channel seismic reflection data available (including some proprietary CDP lines collected by a geophysical contracting company over northern and central Georges Bank which are not shown on Figure 1), a map of tectonic structures characterizing the acoustic basement of the New England margin was compiled (Figure 15). Acoustic basement is block-faulted. The structural grain trends generally NE-SW at a slight angle (approximately 25°) to the regional strike of the shelf-break. As far as can be determined from the profiles, all of

Figure 15. Basement tectonic structures. Information compiled from Ballard and Uchupi, 1975 (Gulf of Maine), King and MacLean, 1976 (Bay of Fundy), Given, 1977 (Scotian Shelf), and Uchupi et al., 1977 (Sedimentary Ridge Province).



the faults are normal, with individual throws varying from less than a kilometer to several kilometers. Because the "K" unconformity bevels basement structure and makes an estimate of original basement relief impossible, these throws are minimum figures. One of the large horsts separates two major graben complexes underlying the southeastern and central parts of the bank. This high causes regional warping of post-"K" sediments referred to as the "Yarmouth arch" (Schultz and Grover, 1974). The southeastern side of the arch is formed by the basement "hinge zone". The basement low southeast of the arch appears to be a southwestern extension of the Scotian Basin (Jansa and Wade, 1975), the depocenter which contains the Sedimentary Ridge Province (SRP). If the SRP is composed of Early Jurassic evaporites, the possibility exists that salt was also deposited along the southeastern flank of the Yarmouth arch. The nature of the crust southeast of the arch is, as yet, undetermined, but the magnitude of the vertical tectonism (approximately 10 km) inferred at the basement "hinge zone" (Figure 15) implies a crustal transition of some kind. The "hinge zone" is here interpreted as the boundary between normal continental crust and continental crust drastically affected by fracturing and intrusion during the initial rifting process.

Unfortunately, seismic resolution of basement structures seaward of the "hinge zone" is hampered by overlying sediments which are highly reflective (Figure 10).

The "reef-ridge" is shown on this map for schematic purposes, but it is not a tectonic structure, except insofar as it must sit on some kind of basement foundation. The sharp contact between this feature and the SRP is clear, which supports the contention that the interpreted Mesozoic reef-complex/carbonate bank sits on a topographic high.

Schouten and Klitgord (1977) have extensively mapped Mesozoic magnetic anomalies in the western North Atlantic basin. They have isolated fracture zones in Cretaceous/Jurassic oceanic crust which they have extrapolated to the outer edge of the margin off the east coast of North America. As a result of this investigation, zones of weakness in the continental crust which may have controlled subsequent fracture zone development have been recognized in the New England margin. The zones are potentially tied to older basement structures. Inferred movement along the trends of these zones of weakness is based on either proven displacements along aligned margin structures or apparent offsets in the

Mesozoic spreading anomalies or the continental slope magnetic basement ridge postulated by Klitgord and Behrendt (in press) (Figure 15). The westernmost trend intersects a N-S striking dislocation in basement east of Long Island called the New Shoreham fault (McMaster, 1971). Although there is no evidence for translational motion along the New Shoreham fault, right-lateral motion along the trend is interpreted from offsets of the Mesozoic spreading anomalies and the magnetic slope ridge. A second zone of weakness intersects the shelf between 69°W and 70°W, and is associated with a gap in the magnetic basement ridge. It is extended northward to correlate with parallel basement structures identified east of Boston (Ballard and Uchupi, 1975). This zone of weakness also apparently modifies several Georges Bank graben structures located southeast of Cape Cod (Figure 15). Right-lateral motion is again inferred based on offsets in the magnetics. A third trend bounds the "reef-ridge" at 68°W, and enters the margin through another gap in the magnetic basement ridge (presumably created by the magnetic disturbance of the New England Seamount Chain (Klitgord and Behrendt, in press)). Its shelf extension is not well-documented on Georges Bank, although it could be responsible for the western boundary of the large graben discernible on U.S.G.S. 1 (Figures 11 and 15). In the Gulf of

Maine, the extension parallels large NNW-SSE trending normal faults (Ballard and Uchupi, 1975). Right-lateral displacement is inferred both from offsets in the deep-sea Mesozoic magnetic anomalies and from a structural analysis of the Gulf of Maine fault system made by Ballard and Uchupi (1975). Finally, an easternmost trend intersects the shelf-break at approximately 66°W, coinciding with the part of the basement "hinge zone" which forms the western side of the structural embayment underlying Northeast Channel (Figure 5). North of the channel, this postulated zone of weakness lines up with a left-lateral strike-slip fault which offsets Triassic basalts and diabases in the Bay of Fundy (Goldthwait, 1924). However, the Mesozoic anomalies are offset in a right-lateral sense by the associated oceanic fracture zone, so the sense of movement along this easternmost trend is still a matter of conjecture.

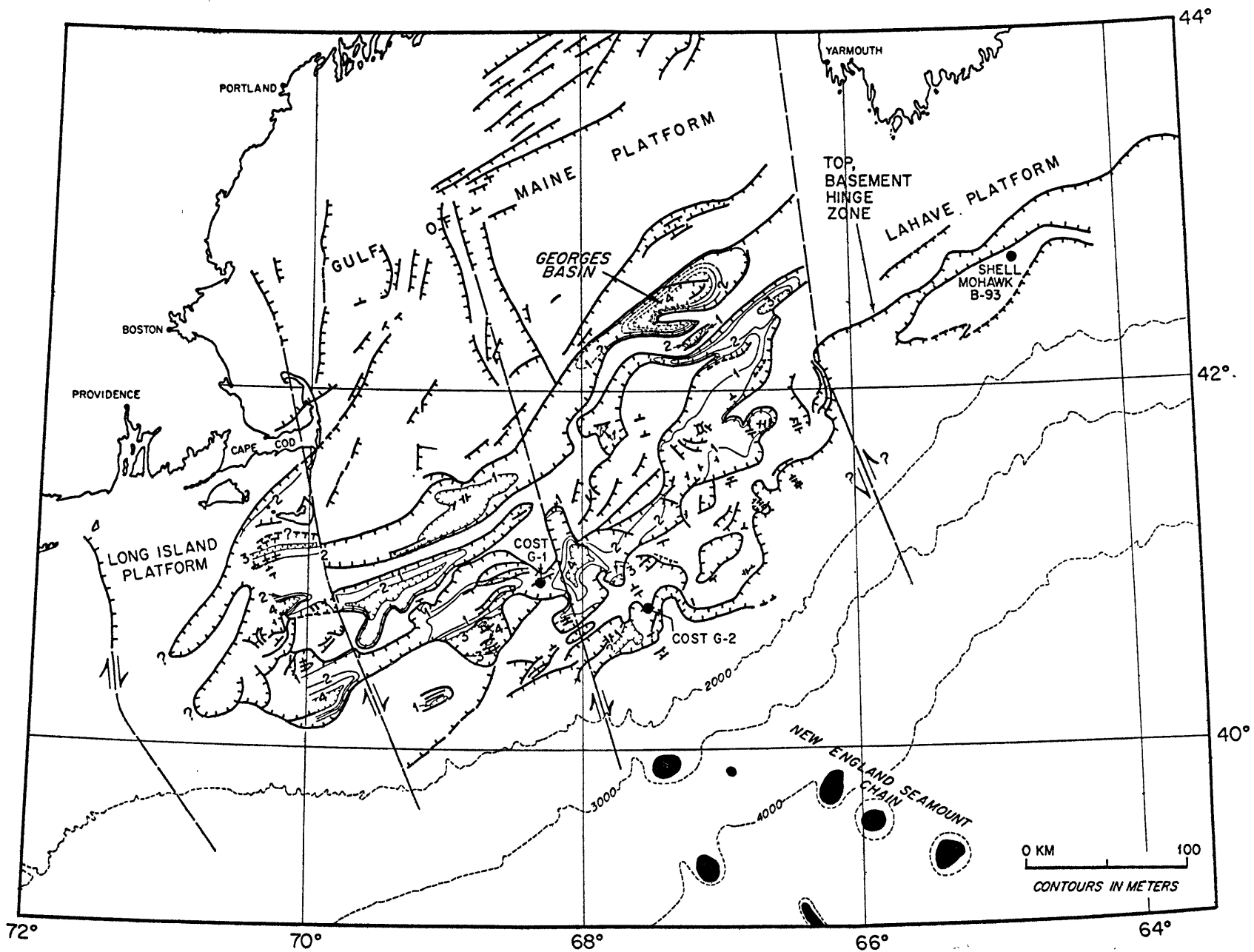
Isopach Maps

Pre-"K"

All pre-"K" sediments underlying the New England continental margin consist of graben-fill. Because little velocity information on the graben-fill section is presently available, all interval velocities used for the preparation of this

map (Figure 16) were obtained either from U.S.G.S. lines 4 and 5 (Grow and Schlee, 1976), or from Ballard and Uchupi (1975) (Appendix III). Maximum thicknesses of this interval are in excess of 4 km within several large grabens. The largest of these underlies Georges Basin in the southeastern part of the Gulf of Maine (Figure 9, Line 23; Figure 16). To date, these sediments have not been sampled except by a well drilled in the Orpheus graben off Nova Scotia (Jansa and Wade, 1975). There, the graben-fill sequence consisted of Late Triassic-Early Jurassic redbeds (Eurydice Fm; Jansa and Wade, 1975; Given, 1977). On land in New England, sediments filling the structurally similar Triassic rifts also consist of Late Triassic-Early Jurassic redbeds, including fanglomerates, flood-plain deposits, and lacustrine sediments (Hubert et al., 1976). Ground-water wells indicate that the New England graben-fill attains thicknesses of 5 km (R.M. Foose, personal communication). Some of the graben-fill on the New England continental margin may consist of evaporites. Halite of inferred pre-"K" (i.e. Late Triassic) age has been sampled in the Carson Subbasin on the eastern Grand Banks (Jansa et al., 1977), and evidence for possible diapiric activity has been reported by Ballard and Uchupi (1975), Uchupi et al. (1977), and Austin (this investi-

Figure 16. Isopach of pre-"K" sediments. Contour interval 1.0 km. Thicknesses are unknown beneath the Gulf of Maine north and west of Georges Basin, and are assumed to be zero southeast of the Yarmouth arch because of poor seismic resolution.



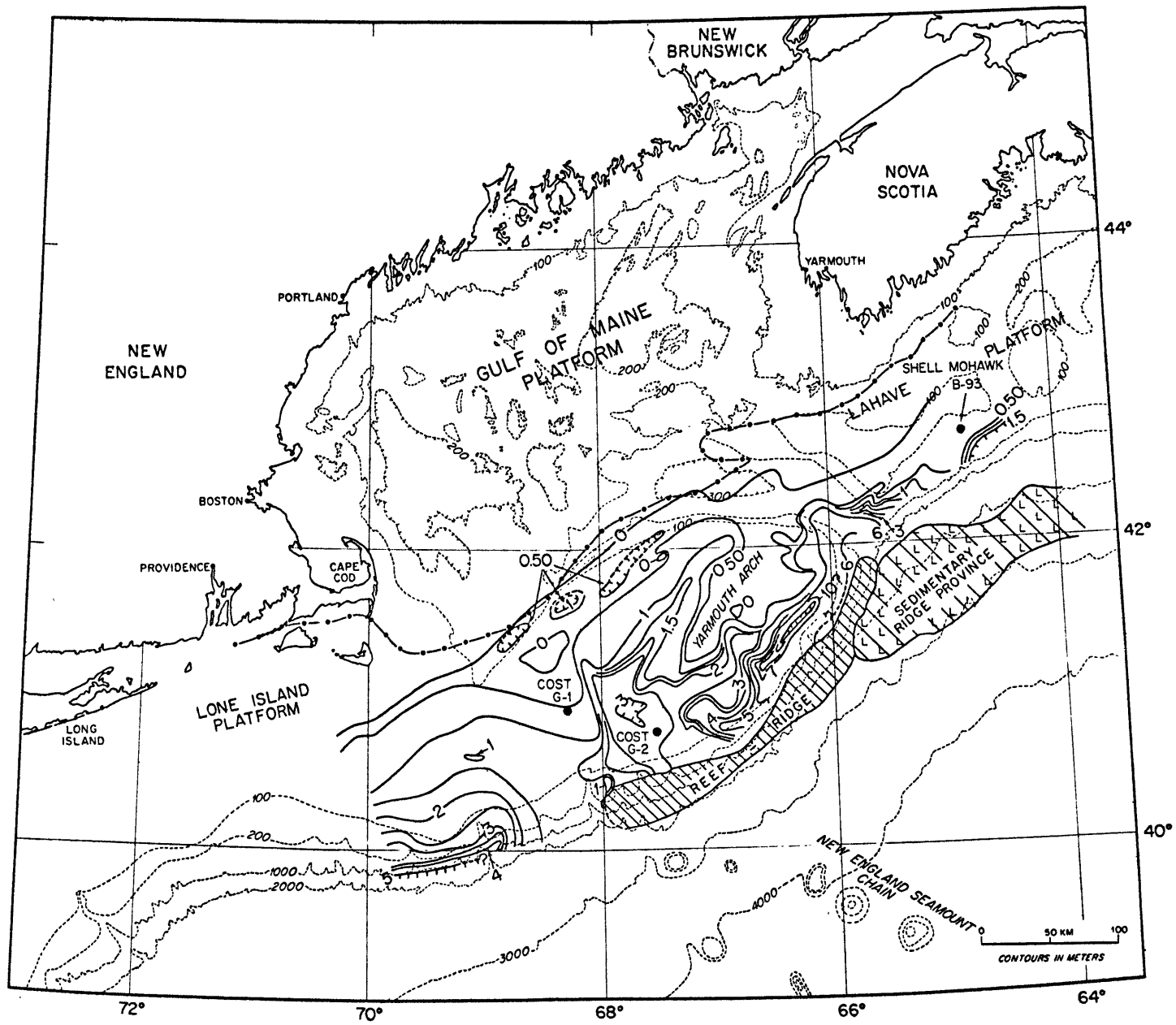
gation) within the Georges Basin graben in the Gulf of Maine (Figure 9, Line 23; Figure 16).

Southeast of the Yarmouth arch, seaward of the "hinge zone", the thickness of pre-"K" sediments is presently unknown because "K" cannot be traced beneath this part of Georges Bank (see U.S.G.S. 4, Figure 10). For the purposes of this map, "K" was assumed to coincide with the interpreted basement surface in this area, as it does beneath other parts of the region. Consequently, the pre-"K" thickness is inferred to be zero. The thickness of graben-fill is also uncertain beneath the Gulf of Maine north and west of Georges Basin. Ballard and Uchupi (1975) mapped the distribution of rift structures in the gulf, but did not determine the pre-"K" sediment thicknesses.

"K" - "Z"

Figure 17 illustrates thickness of the interval between the "K" unconformity and the "Z" reflector (Bathonian). The influence of the Yarmouth arch is evident. Generally less than 500 m of pre-"Z" sediments are present atop the arch. In one location, the "K" - "Z" interval pinches out completely against it, perhaps indicating that part of the arch was sub-aerial during the Early Jurassic. Parts of the northern

Figure 17. "K" - "Z" isopach. Contour interval 0.5 km to 4.0 km, then 1.0 km. Y.A. = Yarmouth arch. The equivalent continental rise sequence is not included, but is discussed in the text. In this and subsequent isopach maps, the "-●-●-" symbol marks the approximate edge of the coastal plain wedge as defined by Emery and Uchupi (1972), Ballard and Uchupi (1975), and King and MacLean (1976).



boundary of Georges Bank may also have been subaerial at this time. Maximum thicknesses occur southeast of the Yarmouth arch, where more than 10 km of pre-"Z" sediments are inferred from available travel-time and velocity information. Part of this section may consist of pre-"K" sediments, as well.

The "reef-ridge" is included for reference, but the presence of an Early Jurassic reef complex/carbonate bank can only be inferred at this time, as no samples have, as yet, been recovered to confirm its existence. If the SRP is cored with Early Jurassic salt, the evaporites were being deposited during the "K" - "Z" interval. The present extent of the SRP is shown to indicate the minimum extent of the original basin of deposition. Seismic evidence compiled during the present investigation implies that evaporites also may be present in the structural embayment underlying Northeast Channel, in the basement low southeast of the Yarmouth arch and seaward of the "hinge zone", and as far seaward as the hinge in oceanic basement shown on the tectonic map (Figure 15). If the basement "hinge zone" marks the transition from normal continental to altered continental crust, then all of these evaporites were deposited on faulted and extended continental material. On the LaHave Platform, "K" - "Z" thicknesses are less than 1.5 km except near the shelf-break. For example,

at the Shell Mohawk B-93 well, this interval is only 240 m thick. To the southwest, rapid thickening occurs as a result of down-faulting associated with the structural embayment beneath Northeast Channel. Here, the "K" - "Z" thicknesses could exceed 9 km, although seismic resolution is extremely poor as a result of the presence of interpreted diapiric structures.

A NW-SE trending saddle separates the Georges Bank Basin (northwest of the Yarmouth Arch) and the Scotian Basin (southeast of the Yarmouth Arch) from a third depocenter centered below the continental slope SSE of Cape Cod. This saddle constitutes the eastern part of the Long Island Platform and lines up along one of the postulated zones of weakness crossing this margin (Figure 15). The depocenter west of the saddle may make the eastern terminus of the Baltimore Canyon Trough, the next major basin system to the southwest.

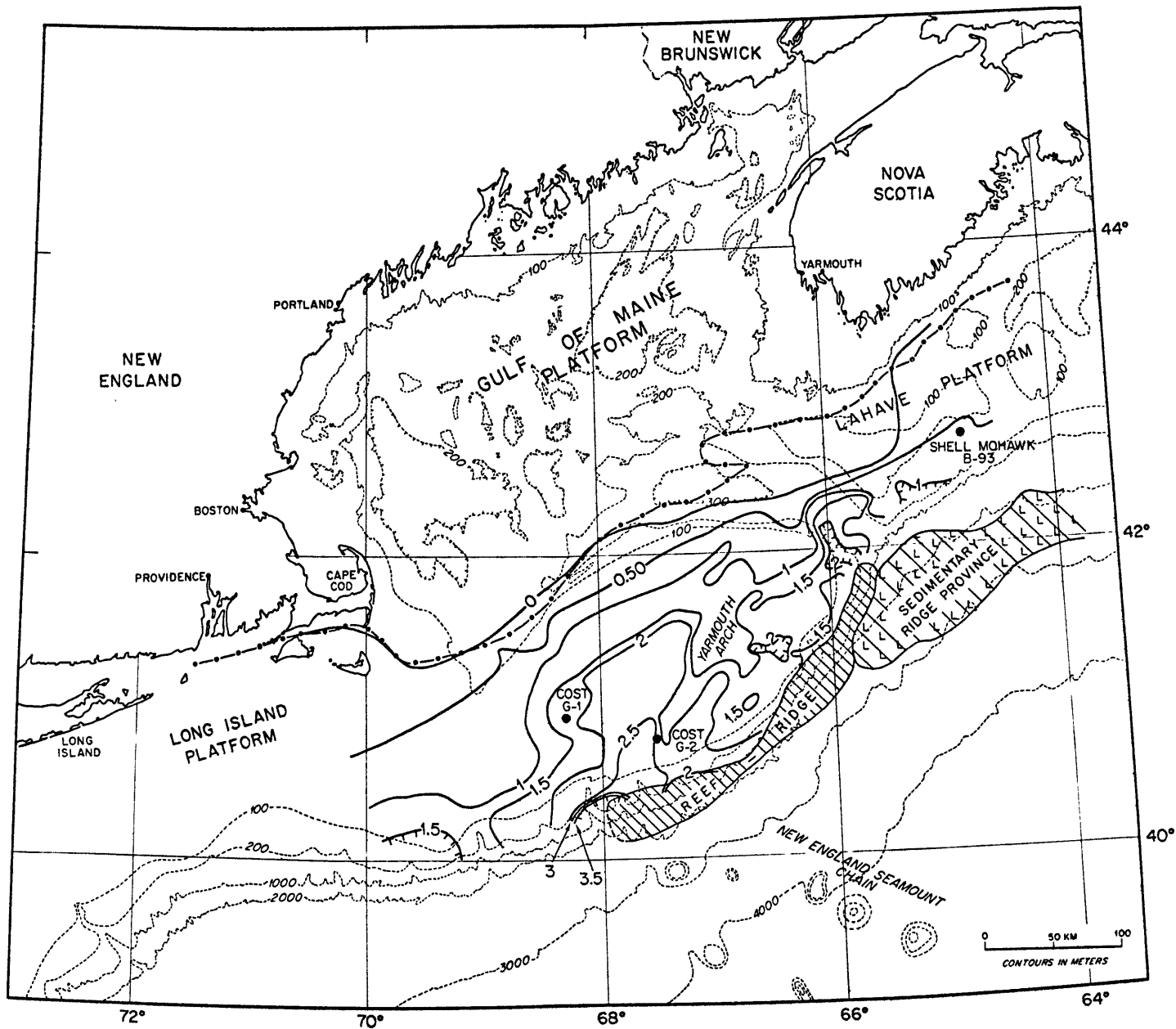
This isopach does not include a continental rise sequence equivalent to the "K" - "Z" interval beneath the shelf for two reasons. First, no acoustic horizon could be identified beneath the rise which was considered equivalent to reflector "Z". The "K" unconformity is interpreted as being correlative with acoustic basement beneath the rise for reasons to be discussed later. Second, the only high-quality seismic coverage available

(U.S.G.S. Lines 1, 4, and 5) was insufficient for regional correlation. However, several statements concerning the Early Jurassic sequence underlying the continental rise can be made. The acoustic horizon closest in postulated age to "Z" (approximately 160 my BP) is "J₂", believed to be 175 my old (Klitgord and Schouten, 1977). The calculated thickness of the basement-"J₂" interval along U.S.G.S. 5 (Figure 13) is inferred to be approximately 7 km, beneath the base of the continental slope. Thicknesses are considerably less, around 2 km, along U.S.G.S. 1 (Figure 11) because of the basement swell associated with the New England Seamount Chain. Farther to the east, along U.S.G.S. 4 (Figure 10), basement-"J₂" thicknesses are generally less than 2 km beneath the rise. However, there is a question as to whether or not the acoustic basement surface here is equivalent to oceanic basement. "True" or geologic basement could be masked by highly reflective sediments (i.e. fore-reef deposits) filling a trough similar to the one interpreted to underlie the slope on Line 5 (Figure 13).

"Z" - "3"

Figure 18 encompasses the section between the Bathonian and the Jurassic-Cretaceous boundary. Clearly, sedimentation rates across the entire margin are much reduced over what they were during the Early

Figure 18. "z" - "3" isopach. Contour interval 0.5 km.
For an explanation of map patterns and labels,
refer to Figure 17.



Jurassic. For the 24-my interval covered by this map, the maximum average sedimentation rate is 15 cm/1000 yrs. This compares with 21 cm/1000 yrs estimated for the "K" - "Z" interval. Averaging over the entire Jurassic and the Late Triassic (in order to take into account any uncertainty in age of reflector "K"), sedimentation rates of 16-17 cm/1000 yrs prevail. Paleobathymetric studies by Gradstein et al. (1975) of boreholes drilled on the Canadian margin indicate that, in many instances, sedimentation rates approximate basin subsidence rates, but whether or not this is true for the New England margin awaits drilling information. It should be kept in mind that the sedimentation rates calculated above are minimum estimates, because neither compaction nor erosion has been taken into account.

The influence of the Yarmouth arch continues to be reflected in the Middle-Upper Jurassic sediment distribution, and there is still the vague suggestion of two distinct depocenters (the Georges Bank Basin to the north and the Scotian Basin to the south) which merge beneath the southwestern part of Georges Bank. The "reef-ridge" is presumed to have existed during the Middle and Upper Jurassic, although no Jurassic sediments

have as yet been recovered from this margin. Whether or not it served as a sediment barrier during the "Z" - "3" interval is unknown.

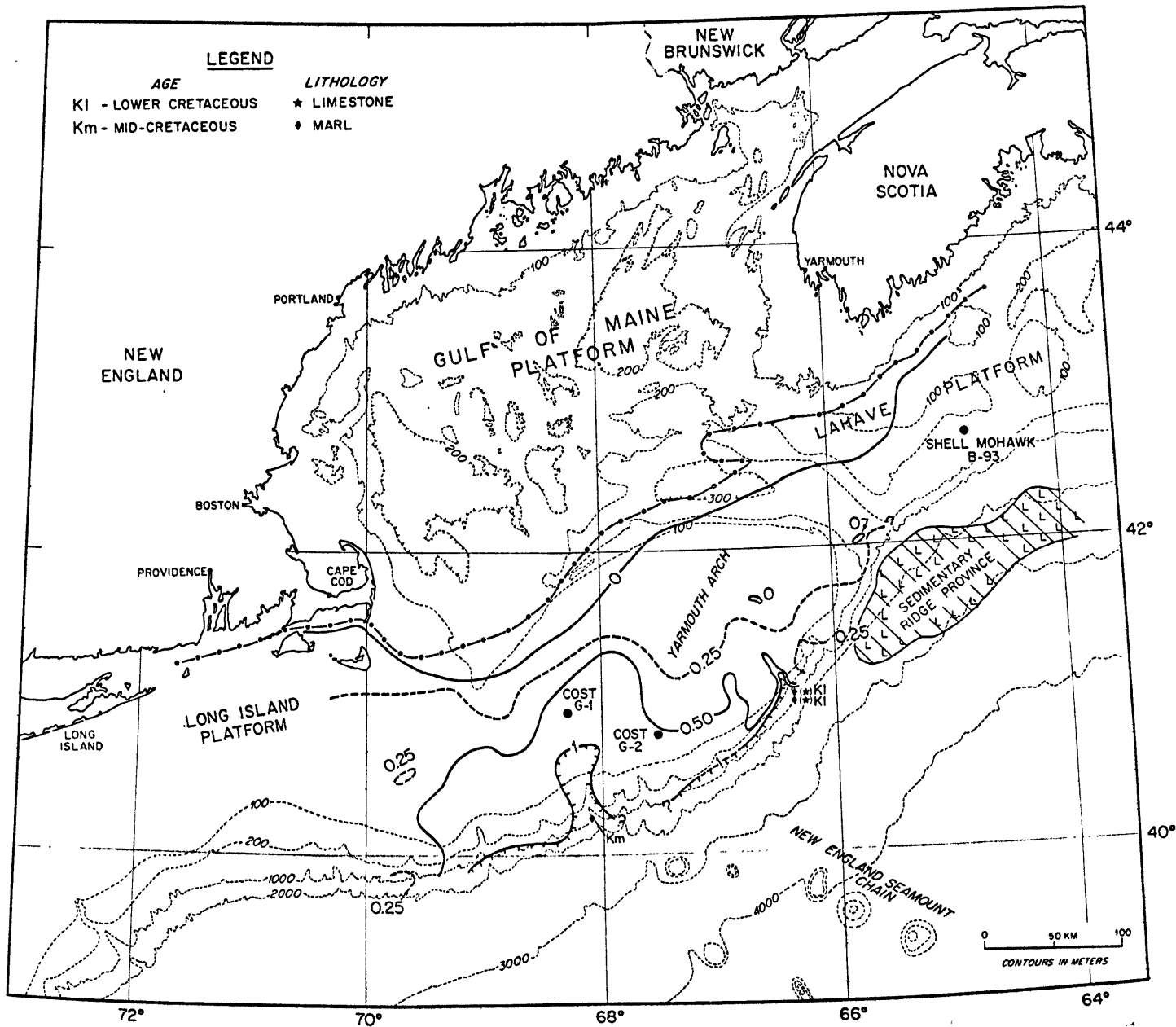
Beneath the LaHave Platform, "Z" - "3" thicknesses are less than one km except near the shelf-break. This interval is 532 m thick at Shell Mohawk B-93, yielding a sedimentation/subsidence rate of roughly 2 cm/1000 yrs. The slow rate of subsidence of the LaHave Platform throughout the Jurassic indicates significant decoupling between this feature and the foundation of the depocenters to the south and southwest.

Beneath the continental rise, the "Z" - "3" interval is roughly equivalent to the interval between reflectors "J₂" and "J₁". An inspection of U.S.G.S. lines 1 (Figure 11), 4 (Figure 10), and 5 (Figure 13) reveal that the "J₂" - "J₁" interval is thin, usually less than 1.5 km. Because of otherwise sparse seismic coverage, the actual distribution of "J₂" - "J₁" thicknesses was not mapped.

"3" - "2"

The thickness of the interval between reflector "3" (Jurassic-Cretaceous boundary) and reflector "2" (early Late Cretaceous) is illustrated by Figure 19. Except near the shelf-break, thicknesses of this unit

Figure 19. "3" - "2" isopach. Contour interval 0.25/0.5 km.
The symbols in the legend refer to samples
collected by Ryan et al. (1978). For other
symbols, refer to Figure 17.



rarely exceed 1 km. The recovery of Neocomian bioclastic limestones and marls from Heezen Canyon (Ryan et al., 1978; Figure 19) are the first geologic evidence that the so-called "reef-ridge" is indeed composed, at least in part, of a Mesozoic reef complex/carbonate platform. Dolomite-cemented arkosic sandstone of mid-Cretaceous age sampled in Oceanographer Canyon may represent beach rock associated with the carbonate bank (Ryan et al., 1978).

The "3" - "2" interval could not be mapped beneath the continental rise off Georges Bank because no prominent acoustic horizon equivalent to "2" occurs between horizons "β" and "A*". However, such is not the case everywhere beneath the east coast continental rise. Vail et al. (in press) identify a prominent acoustic horizon beneath the Blake-Bahama Outer Ridge which they tie to an Albian hiatus. Ryan et al. (1978) also recognize an erosional episode separating Neocomian from Maestrichtian sediments in submarine canyons south of Georges Bank.

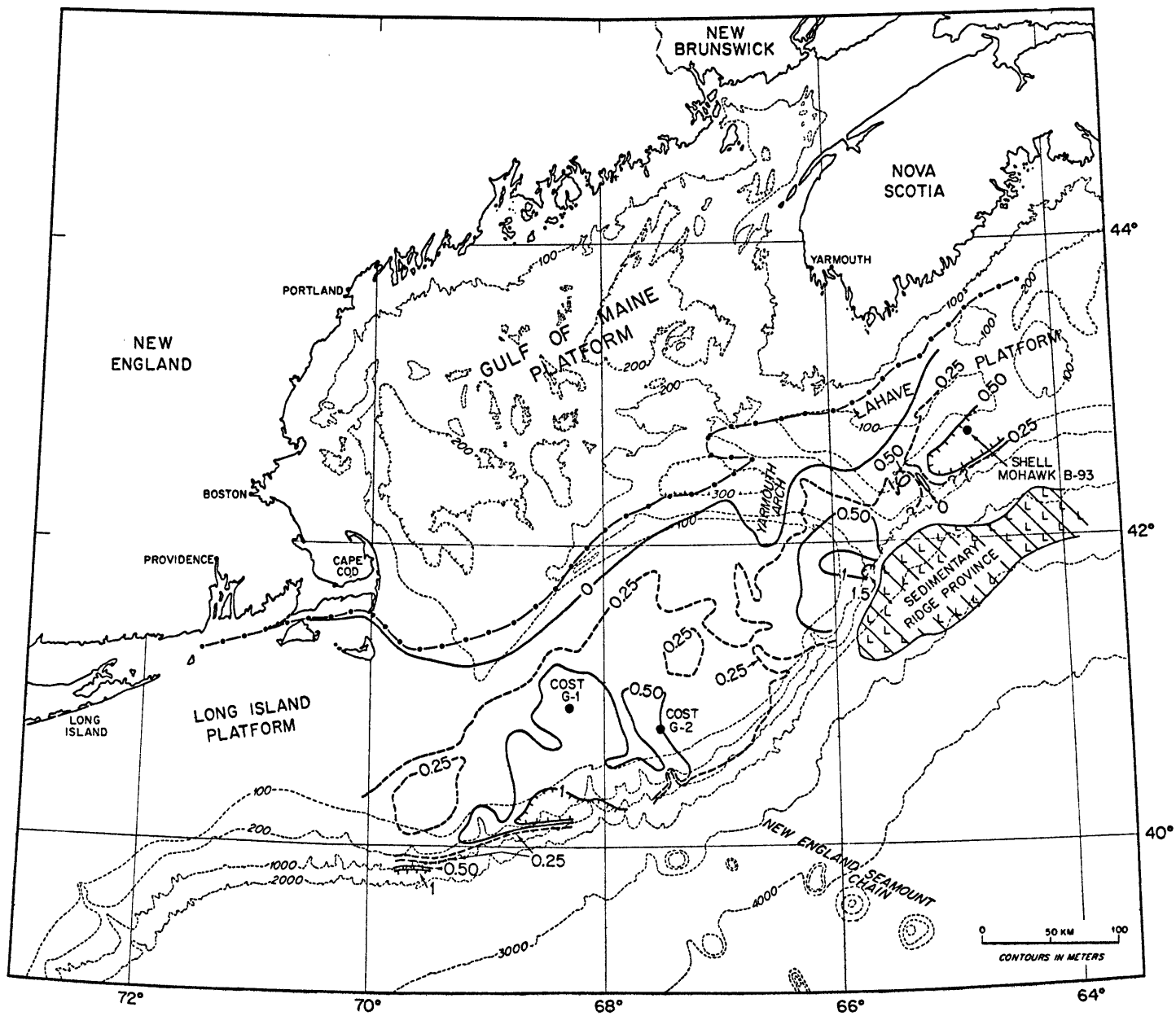
According to Jansa and Wade (1975), regional uplift associated with the separation of the North American and European plates began at the end of the Jurassic and extended until the end of the Albian. As both reflectors "3" and "2" are associated with hiatuses in the stratigraphic section sampled by Shell

Mohawk B-93, it seems likely that both acoustic horizons represent regional unconformities carved during this tectonism. The maximum "3" - "2" sediment thicknesses, which are located near the shelf-break (Figure 19), probably represent submarine canyons cut during the Early Cretaceous and subsequently filled by deltaic clastics of the Mississauga Formation (McIver, 1972; Figure 6). On the LaHave Platform and away from the shelf-break, conditions were apparently more stable, resulting in either non-deposition or erosion. This would explain the very thin Early Cretaceous interval (4 m) encountered in the Shell Mohawk B-93 well.

"2" - "X"

The early Late Cretaceous to latest Cretaceous interval (Figure 20) is not distinguished by significant regional trends. Maximum thicknesses exceed one km beneath the continental slope, perhaps representing fill of canyons cut during the Early Cretaceous. Erosion of the Scotian Shelf during the Oligocene (resulting in the formation of reflector"1") has completely removed the "2" - "X" interval in the axis of a filled shelf-edge canyon just northeast of Northeast Channel. The influence of the Yarmouth arch is still detectable, but it obviously exerts no significant

Figure 20. "2" - "X" isopach. Contour interval 0.25 km.
For an explanation of symbols, refer to
Figure 17.



influence on regional sedimentation after reflector "2" time. The "reef-ridge" continues to control the position of the continental slope east of 68°W, but is completely buried by the early Late Cretaceous.

During this period, maximum average sedimentation rates are approximately 1 cm/1000 yrs. Such rates imply that basin subsidence was very slow on the New England margin during the latter half of the Cretaceous.

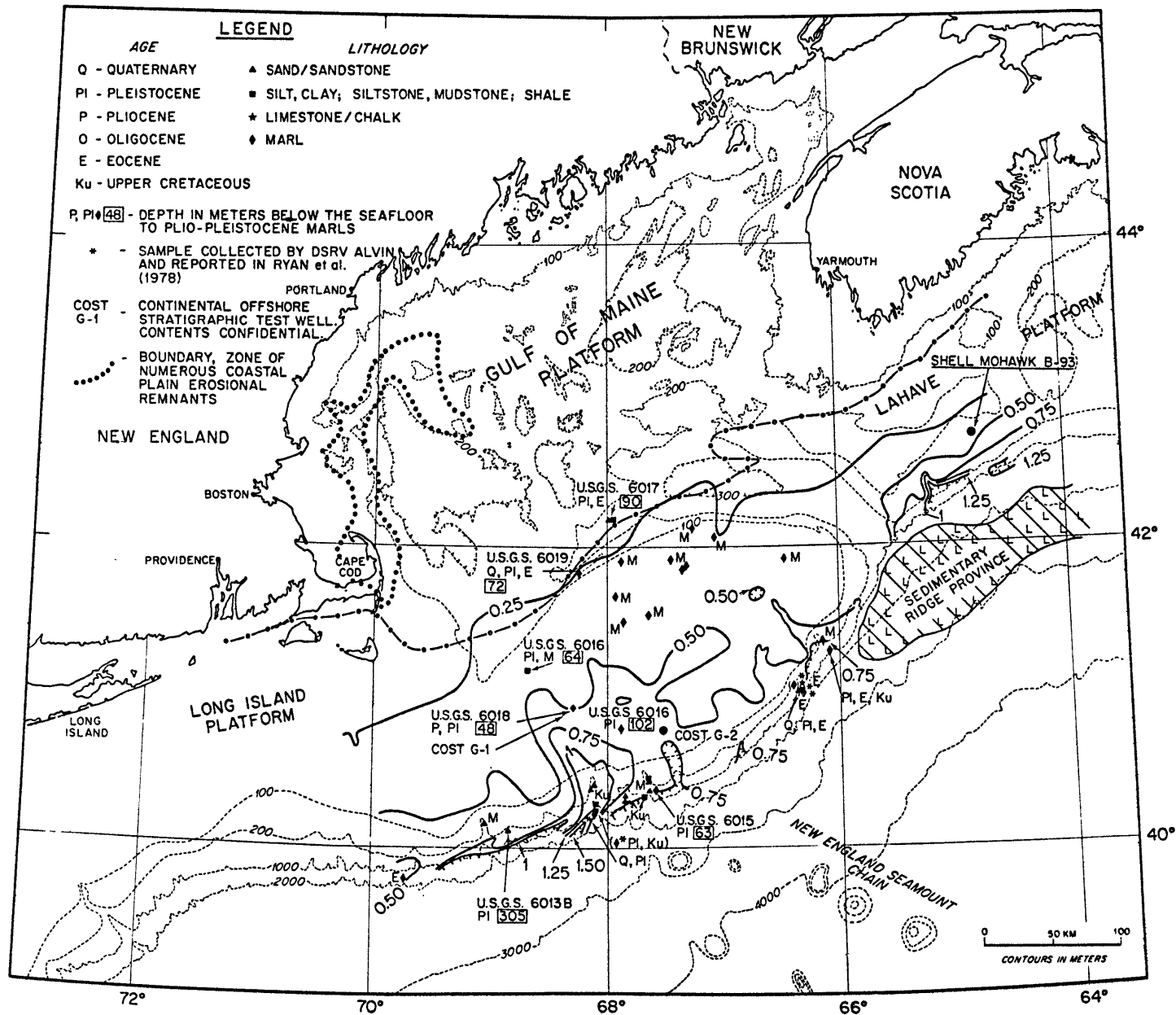
Using well information from the Scotian Basin, Gradstein et al. (1975) also have shown that the Late Cretaceous is characterized by uniformly slower rates of sedimentation and subsidence than the Early Cretaceous.

"X" - Present

The final isopach (Figure 21) concerns sediments of latest Cretaceous age and younger. Available geologic information on the Late Cretaceous to Quaternary sediments from Emery and Uchupi (1972), Oldale, Uchupi, and Prada (1973), Weed et al. (1974), Hathaway et al. (1976), and Ryan et al. (1978) also is included.

The most interesting feature of this map is the presence of filled submarine canyons near the shelf-break, both on the Scotian Shelf and on Georges Bank. In the axis of these canyons, the "X" - Present interval attains its maximum thicknesses. The largest of the paleocanyons underlies the present axis of Oceanographer Canyon (just west of 68°W), indicating that at least

Figure 21. "X" - Present isopach. Contour interval 0.25 km. Sample locations and ages after Emery and Uchupi (1972), Oldale, Uchupi, and Prada (1973), Weed et al. (1974), Hathaway et al. (1976), and Ryan et al. (1978). For an explanation of symbols not contained in the legend, refer to Figure 17.



one period of re-excavation has occurred. This fact is supported by the recent systematic stratigraphic sampling carried out by Ryan et al. (1978) which resulted in the recognition of at least four erosional episodes: the late Early Cretaceous (approximately reflector "2" time), the post-Eocene (approximately reflector "1" time), and two or more during the Plio-Pleistocene.

The waxing and waning of continental glaciers and associated eustatic changes in sea level during the Plio-Pleistocene modified the morphology of both the Gulf of Maine and Georges Bank. During the regressive phases, complex cut-and-fill structures were developed by stream erosion along the northern edge of Georges Bank. In many places, Miocene sediments were exposed (Knott and Hoskins, 1968; Emery and Uchupi, 1972; Figure 21). Direct glaciation of the Gulf of Maine and the northern edge of Georges Bank considerably modified the morphology of the region (Oldale and Uchupi, 1970). These glaciers appear to have reached the open sea by way of the Northeast and Great South channels, depositing their load on the continental slope and beyond. Considerable quantities of detritus also were transported seaward by streams running Georges Bank (Lewis and Sylwester, in press). More than 300 m of Pleistocene clastics were sampled at the shelf break southwest

of Georges Bank by a shallow drill hole (6013B, Hathaway et al., 1976; Figure 21).

In the interior lowland of the Gulf of Maine north of the 250 m line (Figure 21), sediment thicknesses in the "X" - Present interval vary. Within some of the closed basins, single-channel records have been used to estimate thicknesses reaching 150 m, most of which is believed to be the result of reworking of Coastal Plain and Pleistocene drift sediments during the early Holocene transgression (Austin, unpublished information). While Cretaceous and Tertiary coastal plain remnants have been mapped in the northwestern gulf (Oldale, Uchupi, and Prada, 1973) and in Cape Cod Bay (Hoskins and Knott, 1961), they probably lie scattered throughout the gulf in complex association with glacial and periglacial deposits.

Reflector "1" was cut during the "X" - Present interval. It can be followed as an angular unconformity beneath the Scotian Shelf (Figure 5), but because it exhibits no relief beneath Georges Bank it cannot be followed southwest of Northeast Channel. At the Shell Mohawk B-93 well, reflector "1" is dated as Oligocene, which coincides with the time of a worldwide regression associated with the onset of Antarctic glaciation (Savin et al., 1975; Ingle et al., 1976, 1977; Haq et al., 1977). An unconformity perhaps coeval with "1"

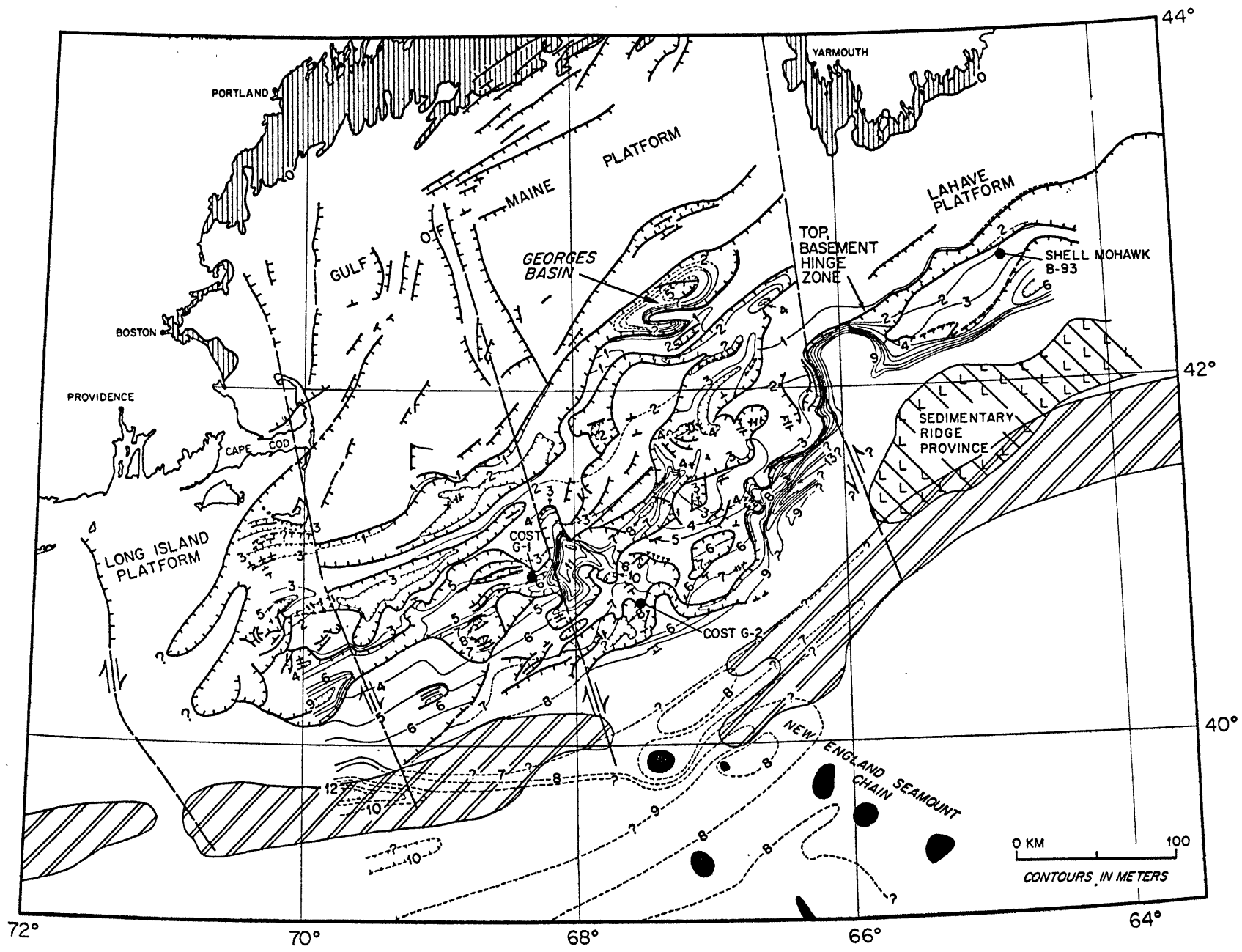
has been identified by Uchupi et al. (1977) on a series of single-channel profiles transecting Corsair Canyon. Work by Ryan et al. (1978) in the same canyon also supports the presence of at least one late Eocene or Oligocene unconformity there.

Structure Maps

Depth to Acoustic Basement

On the continental shelf, this map (Figure 22) effectively approximates total post-Paleozoic sediment thickness. The maximum shelf sediment thickness occurs southeast of the Yarmouth arch and seaward of the "hinge zone", and may be more than 13 km. The structural embayment beneath Northeast Channel is inferred to contain more than 9 km of sediment, but as basement cannot be traced across the embayment because of the probable presence of evaporites, greater or lesser thicknesses are possible. More than 12 km of sediment overlies a large graben structure along U.S.G.S. 1 (Figure 11). The Georges Basin graben in the Gulf of Maine contains the greatest thickness of pre - "K" sediments (Figure 16), but total sediment thickness there is only 5-6 km. An attempt to sample pre - "K" graben-fill just west of Georges Basin failed because of hard Eocene limestones (Hathaway et al., 1976; hole #6019). These limestones may be responsible for

Figure 22. Depth to acoustic basement. Contour interval 1.0 km. For an explanation of labels and symbols, refer to previous figures.



the acoustic horizon interpreted as a Tertiary or Pleistocene unconformity (perhaps equivalent to reflector "1") which truncates older strata along the northern part of Georges Bank (see Figures 10 and 11).

This map also indicates that the zones of crustal weakness discussed earlier may be sites of dip-slip, as well as strike-slip motion. Normal faults forming the western flank of the Northeast Channel low lie along one of these zone trends, as do normal faults forming the western boundary of the large graben visible on U.S.G.S. 1 (Figure 11). Sediment thicknesses appear to be thicker to the west than to the east of the zone of weakness which crosses the shelf-break near 70°W south of Cape Cod. Finally, some dip-slip motion has also been mapped along the New Shoreham fault (McMaster, 1971), which is here interpreted as the zone of weakness associated with a fracture zone which intersects the margin at 71°W. Dip-slip movement along postulated zones of weakness in the Gulf of Maine occurs, but its magnitude is unknown (Ballard and Uchupi, 1975).

On the LaHave Platform, sediment thicknesses range from 2-4 km landward of the basement "hinge zone". However, seaward of the "hinge zone", basement rapidly plunges to depths of more than 9 km. According to Keen and Keen (1974), seismic refraction results indicate that basement depths beneath the SRP exceed

12 km below sea-level.

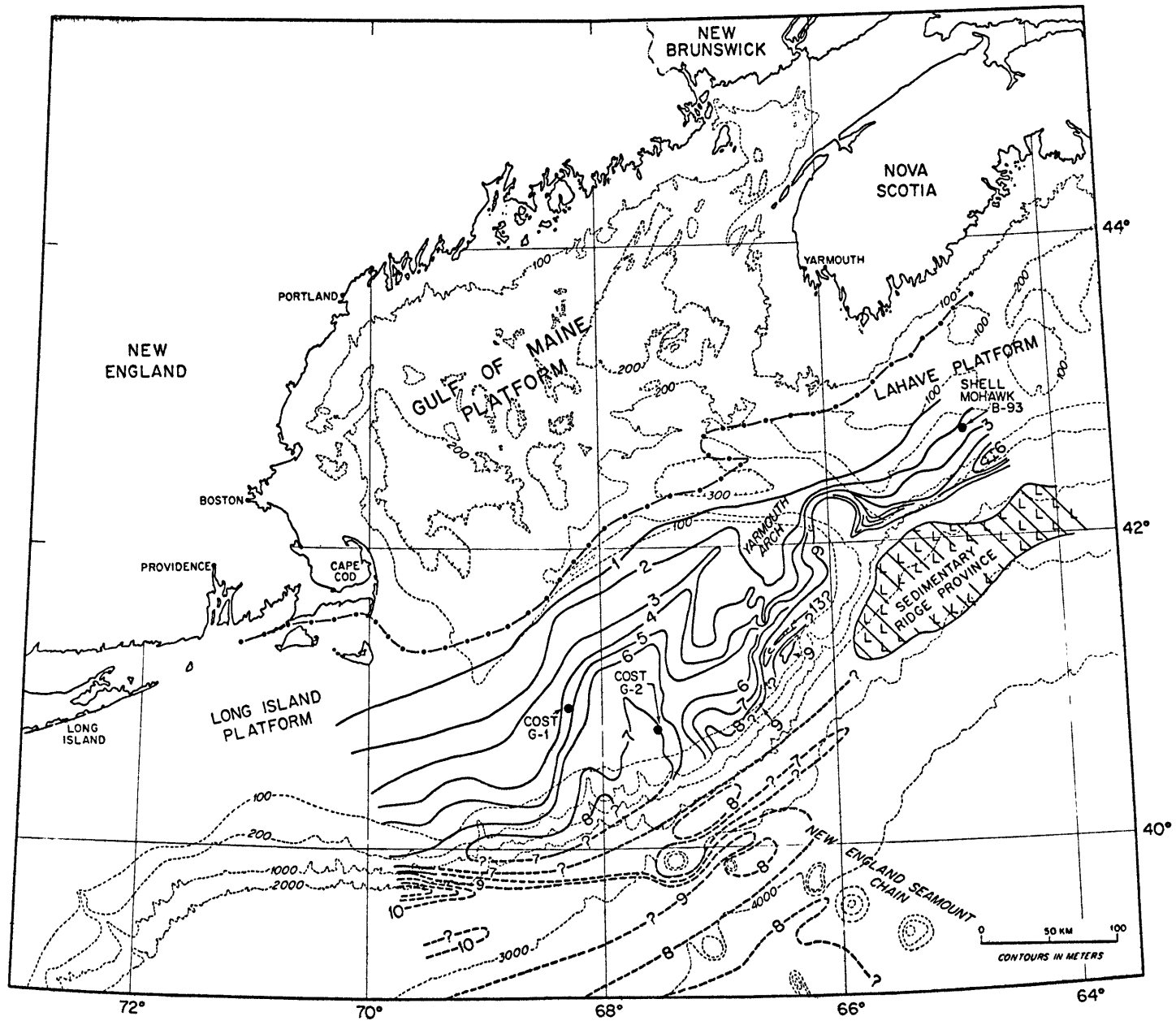
Depth to acoustic basement beneath the slope and rise is based on interpretations of the three U.S.G.S. multi-channel lines. In general, basement could not be traced on AII-91 single-channel profiles collected in deep-water. The maximum depth, more than 12 km, occurs over a buried trough underlying the base of the slope between 69°W and 70°W. Depths decrease to 7-9 km both seaward and to the east in the vicinity of the New England Seamount Chain. Contours around the seamounts, however, are of necessity generalized as a result of insufficient seismic coverage. East of the seamounts, there is no indication of a trough similar to that encountered to the west. However, as discussed earlier, the trough may exist but be masked by sediments.

Depth to "K" Unconformity

Seaward of the basement "hinge zone" and beneath the continental rise, the depth to reflector "K" (Figure 23) is the same as the depth to basement (Figure 22). The reasons for this will be discussed later on.

On the shelf, the Yarmouth arch forms a divide between one large trough to the northwest (Georges

Figure 23. Depth to the "K" unconformity. Contour interval 1.0 km. Beneath the rise, depth to interpreted acoustic basement as on Figure 22. For an explanation of labels and symbols, refer to previous figures.



Bank Basin) and another to the southeast (Scotian Basin). Along the axis of the Georges Bank Basin, reflector "K" plunges to the southwest from depths of less than 2 km to more than 8 km, where it appears to come into contact with the "reef-ridge". The western side of the Georges Bank Basin may be controlled by the zone of crustal weakness which cuts across the margin at 68°W (Figure 15). West of 68°W, smooth contours roughly parallel to the shelf-edge indicate the simple ramping of "K" to depths of more than 8 km which is characteristic of the Long Island Platform. The structural picture is similar on the LaHave Platform. At the extreme eastern edge of the study area, however, a shelf-edge basin more than 6 km deep occurs behind what might be either a basement horst or halokinetic structures (Figure 8). On this map, the Yarmouth arch as a simple extension of the LaHave Platform is evident.

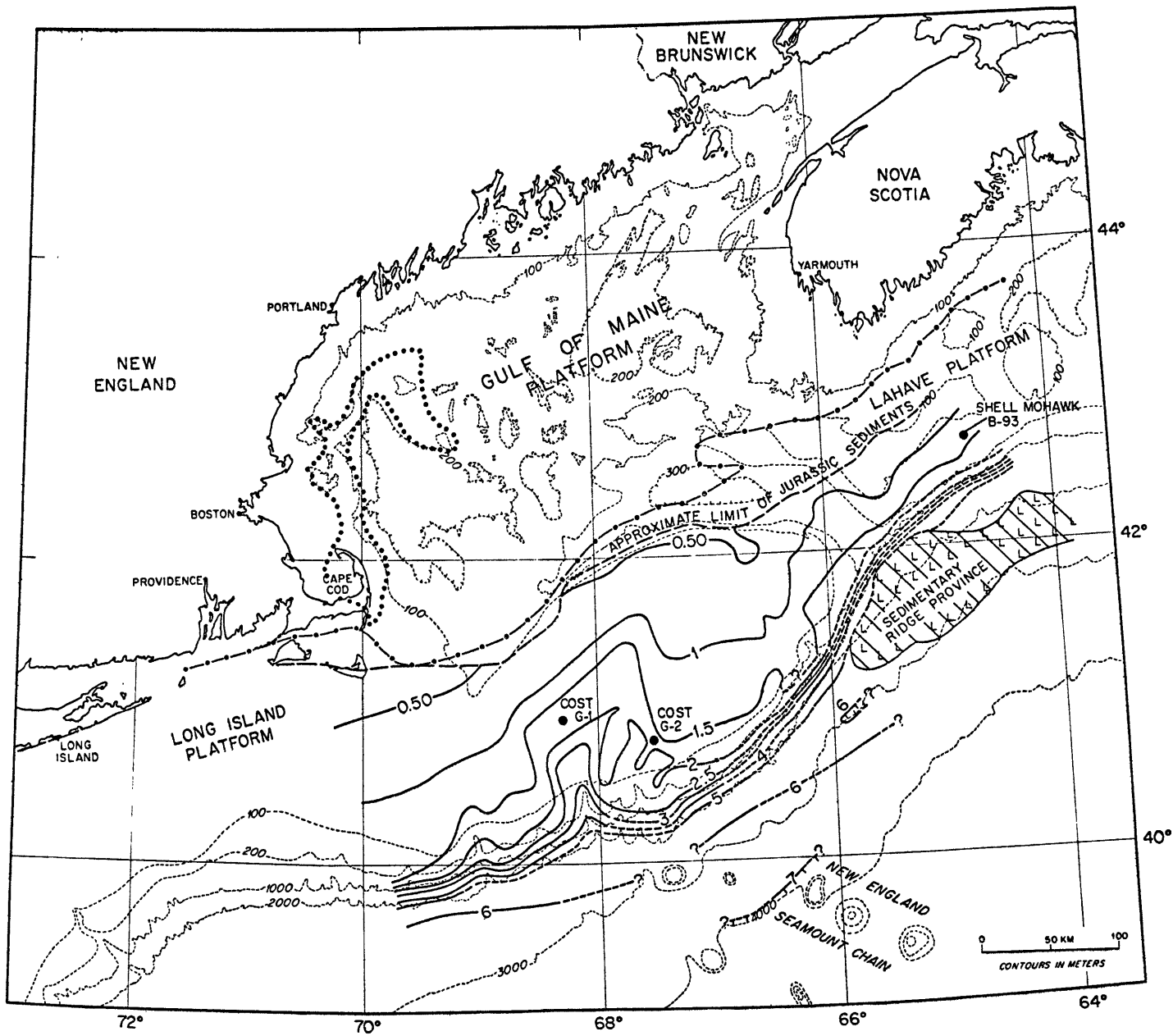
Beneath the Gulf of Maine, the "K" unconformity is everywhere less than one km below sea-level. North of the leading edge of the coastal plain sediment wedge, "K" probably has been re-excavated by one or more erosional episodes during the Tertiary and Quaternary (Lewis and Sylwester, in press).

Depth to Jurassic-Cretaceous Boundary

Figure 24 details the depth to reflector "3" beneath the shelf and upper slope, and the depth to "J₁" beneath the rise. On the shelf, this map approximates a Cretaceous-Tertiary isopach. The influence of the Yarmouth arch on reflector "3" morphology is evident, as is the continuing existence of the Georges Bank Basin as an actual depression at the end of the Jurassic. Since the beginning of the Cretaceous, however, subsidence and sedimentation rates have been low. Reflector "3" is never deeper than 2.5 km at the shelf-break, and comes to within 0.5 km of sea-level near the northern boundary of Georges Bank. On the Long Island and LaHave platforms, the Jurassic-Cretaceous boundary dips gently seaward from depths of less than 0.5 km to 1.5-2.0 km at the top of the continental slope. Beneath the slope, the rapid increase in depth to the boundary is predominantly the result of increasing water depth.

Under the rise, post-"J₁" sediment thicknesses average about 3 km. From the limited data available, depths to "J₁" are uniformly 5-7 km. Obviously, in the vicinity of the SRP, relief of the "J₁" reflector must increase, but no acoustic surface can be regionally mapped in the vicinity of the SRP piercement structures.

Figure 24. Depth to the Jurassic-Cretaceous boundary (reflector "3" beneath the continental shelf and upper slope, reflector "J₁" beneath the continental rise). Contour interval 0.5 km. For an explanation of labels and symbols, refer to previous figures.



The Cretaceous-Tertiary section remaining in the Gulf of Maine consists of isolated erosional remnants (Figure 24) which have been mapped seismically and occasionally sampled (Schlee and Cheetham, 1967). If reflector "3" ever extended north of Georges Bank, it has been removed by subsequent erosion during the development of the gulf's present morphology.

Velocity-Lithofacies Maps

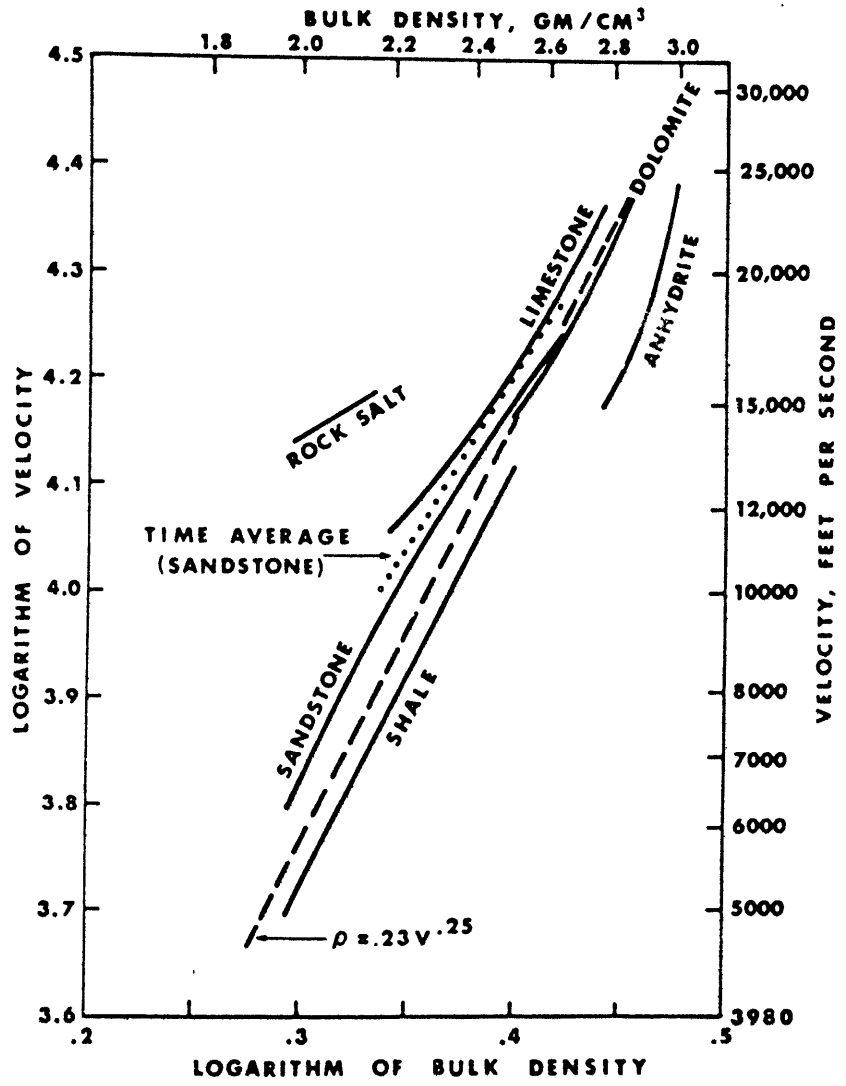
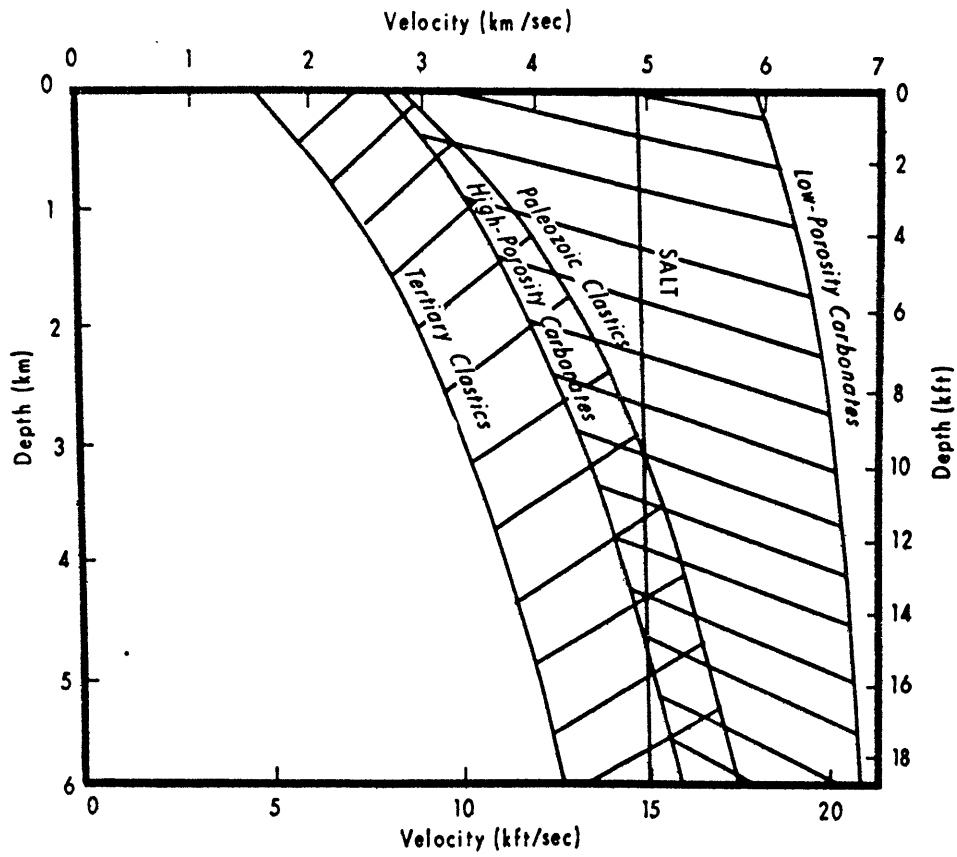
In order to use sound velocity as a geologic mapping tool, it must be related in some systematic way to lithology. Unfortunately, lithology is but one parameter affecting compressional wave velocity, V_p , which is defined for an isotropic elastic solid by the expression $(K + \frac{4}{3}\mu)^{1/2}$, where K = bulk modulus, μ = rigidity, and ρ = density. With increasing depth in the earth, K and μ generally grow faster than ρ , and hence V_p usually increases. Although this is the assumption most often used in seismic interpretation, it is not always valid geologically. All three variables affecting V_p are continuous functions of pressure and temperature. In addition, increases in V_p (and ρ) can be caused by increasing age and degree of cementation (with attendant decrease in porosity), while changes in mineralogy and associated structures may also have an effect (Töksoz et al., 1976).

In attempts to facilitate the identification of lithologies from velocities, laboratory measurements of the sound velocities "characteristic" of various rock types have been conducted, and empirical curves developed relating the various rock parameters to velocity.

Hamilton (1956), Laughton (1957), Nafe and Drake (1957), and others made extensive studies of marine sediments, while field and laboratory measurements of the velocity ranges of a wide variety of sediment and rock types were compiled (Press, 1966).

Despite the complexity, certain broad distinctions between major classes of sedimentary rocks began to emerge. These general relationships are summarized by Gardner et al. (1974) and Sheriff (1976) (Figure 25). Dolomites possess the highest velocity range, from approximately 4.3 km/sec (14,000 ft/sec) to 7.3 km/sec (24,000 ft/sec) with increasing depth of burial. Limestones range from 3.4 km/sec (11,000 ft/sec) to 7.0 km/sec (23,000 ft/sec). Porosity has an enormous effect on carbonate velocities, although the effect is greatly reduced at large depths (Figure 25). Sandstones and shales generally exhibit lower velocities (shales: 1.5 km/sec (5,000 ft/sec) to 4.1 km/sec (13,500 ft/sec); sandstones: 1.8 km/sec (6,000 ft/sec) to 5.5 km/sec (18,000 ft/sec), particu-

Figure 25. Tables relating lithology and velocity to density and depth of burial published by Gardner et al. (1974) and Sheriff (1976). The Gardner et al. table summarizes sediment data from a diverse spectrum of depositional basins and ages to depths up to 7.6 km. General relationships among the parameters are evident and are discussed in the text.



larly when they are young and not deeply buried (Figure 25). Differentiating sandstone from shale seismically is a difficult problem, but differentiating thick clastic (sandstone-shale) from thick carbonate sequences is possible if adequate velocity information of good quality is obtainable (Sheriff, 1976). Obviously, if subsurface control is available the chances of making a correct lithologic interpretation from velocity data are vastly increased.

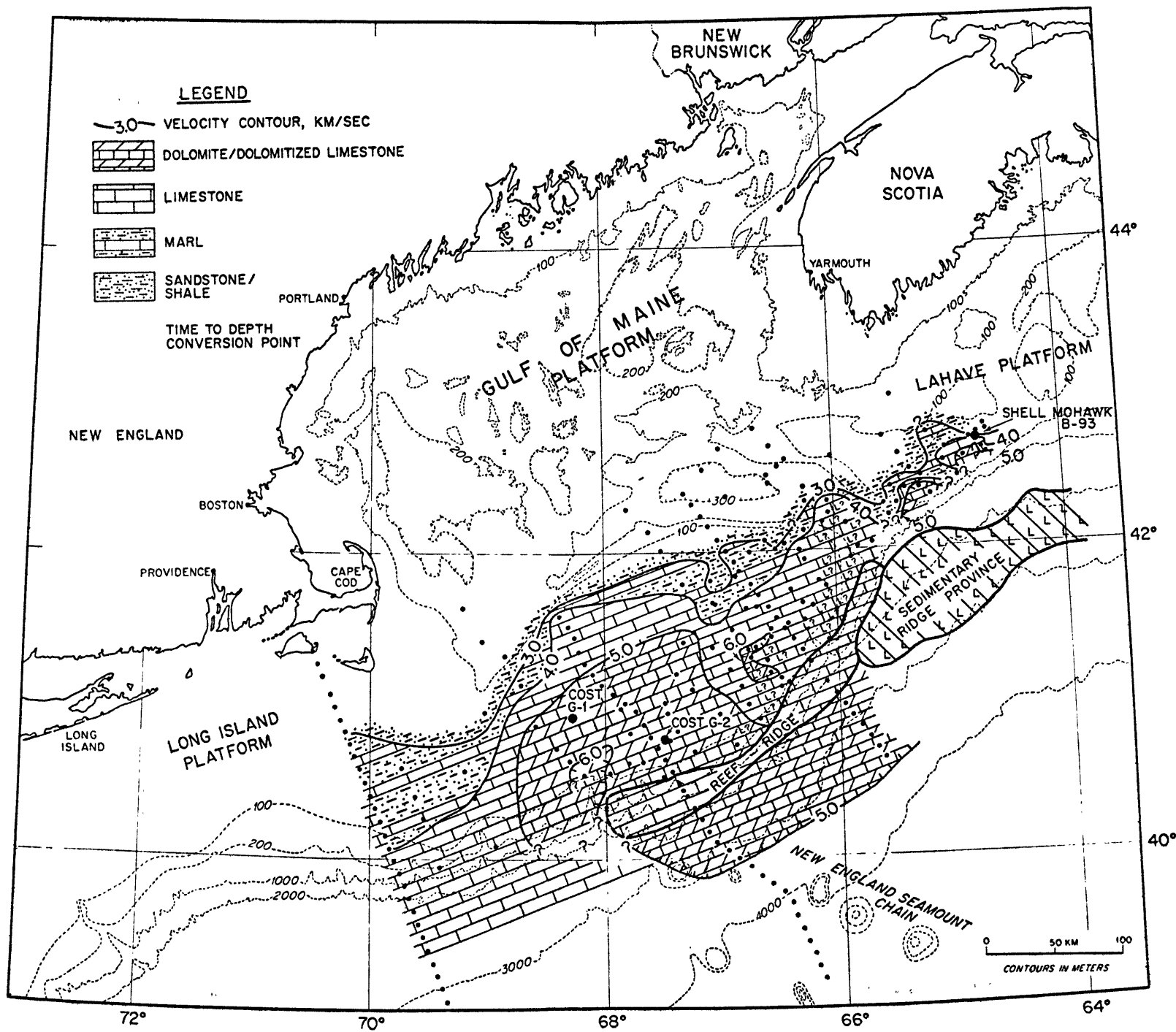
Until 1976, the only direct lithologic information available from the New England passive margin consisted of samples collected over a 30-year period with a dredge and occasionally a submersible (Emery and Uchupi, 1972; Weed et al., 1974). In 1976, the U.S. Geological Survey conducted a shallow drilling program on the east coast continental margin (Hathaway et al., 1976). The results of the program in the New England region are summarized on Figure 21. Ryan et al. (1978) carried out the first detailed stratigraphic mapping of the New England margin in 1977 through the use of DSRV ALVIN in several of the submarine canyons south of Georges Bank (see Figures 19, 20, and 21). For the first time, rocks of Early Cretaceous age were recovered from this margin. Even more important,

the Early Cretaceous samples were reefal limestone, strong evidence that at least part of the "reef-ridge" recognized on seismic reflection profiles consists of a Mesozoic reef complex/carbonate bank.

Even though most of the sediments filling the Georges Bank and Scotian basins are inferred to be Jurassic in age, no rocks older than Early Cretaceous have as yet been recovered from the New England margin. Fortunately, numerous drill-holes on the adjacent Canadian margin have led to the development of a recognized Jurassic stratigraphy which is acoustically correlative with that underlying Georges Bank. In the absence of any well-data (the C.O.S.T. G-1 and G-2 well-data are confidential at the present time), the acoustic correlations must be assumed to hold for stratigraphic correlation as well, particularly insofar as the majority of the reflectors which are identifiable regionally represent unconformities and therefore approximate time-stratigraphic boundaries.

In an attempt to develop lithofacies maps of the New England margin from the admittedly meagre lithologic data base described above, interval velocity maps of the area were prepared. Interval velocities calculated at the time-to-depth conversion points (Appendix III) were plotted and contoured in km/sec for each of the following intervals: "K" - "Z" (Figure 26),

Figure 26. "K" - "Z" velocity/lithofacies map. In this and subsequent figures, velocity contour interval is 1.0 km/sec. The locations of the velocity data base are shown. For actual values, see Appendix III. For an explanation of other labels and symbols, refer to previous figures.



"Z" - "3" (Figure 27), "3" - "2" (Figure 28), and "2" - "X" (Figure 29). The pre-"K" interval was not mapped because of insufficient velocity information. The "X"-Present interval was not mapped either, because all velocities plotted fell within the range 1.5 - 2.0 km/sec and did not exhibit any systematic trends. As had been noted previously (Schlee et al., 1976), all four maps were characterized by general seaward increases in interval velocity.

Once the velocity maps had been completed, a lithofacies interpretation was made based upon all available lithologic information and a general understanding of the relationship between sound velocity and lithology. All velocities greater than 5.0 km/sec were interpreted as evidence for dolomite or dolomitized limestone. These velocities were restricted to the outer-shelf parts of the Jurassic "K" - "Z" (Figure 26) and "Z" - "3" (Figure 27) intervals. Although volcanics also exhibit velocities in this range, no post-"K" volcanics have as yet been sampled on either the Scotian Shelf or New England margins. Velocities between 4.0 and 5.0 km/sec were inferred to represent limestones (Figure 25). Once again, such velocities were predominantly found in the seaward parts of Figures 26 and 27,

Figure 27. "2" - "3" velocity/lithofacies map. For an explanation of labels and symbols, refer to Figure 26 and previous figures. The outline of the "reef-ridge" is derived from seismic interpretation and is only approximate because of patchy coverage and generally poor resolution near the shelf-break.

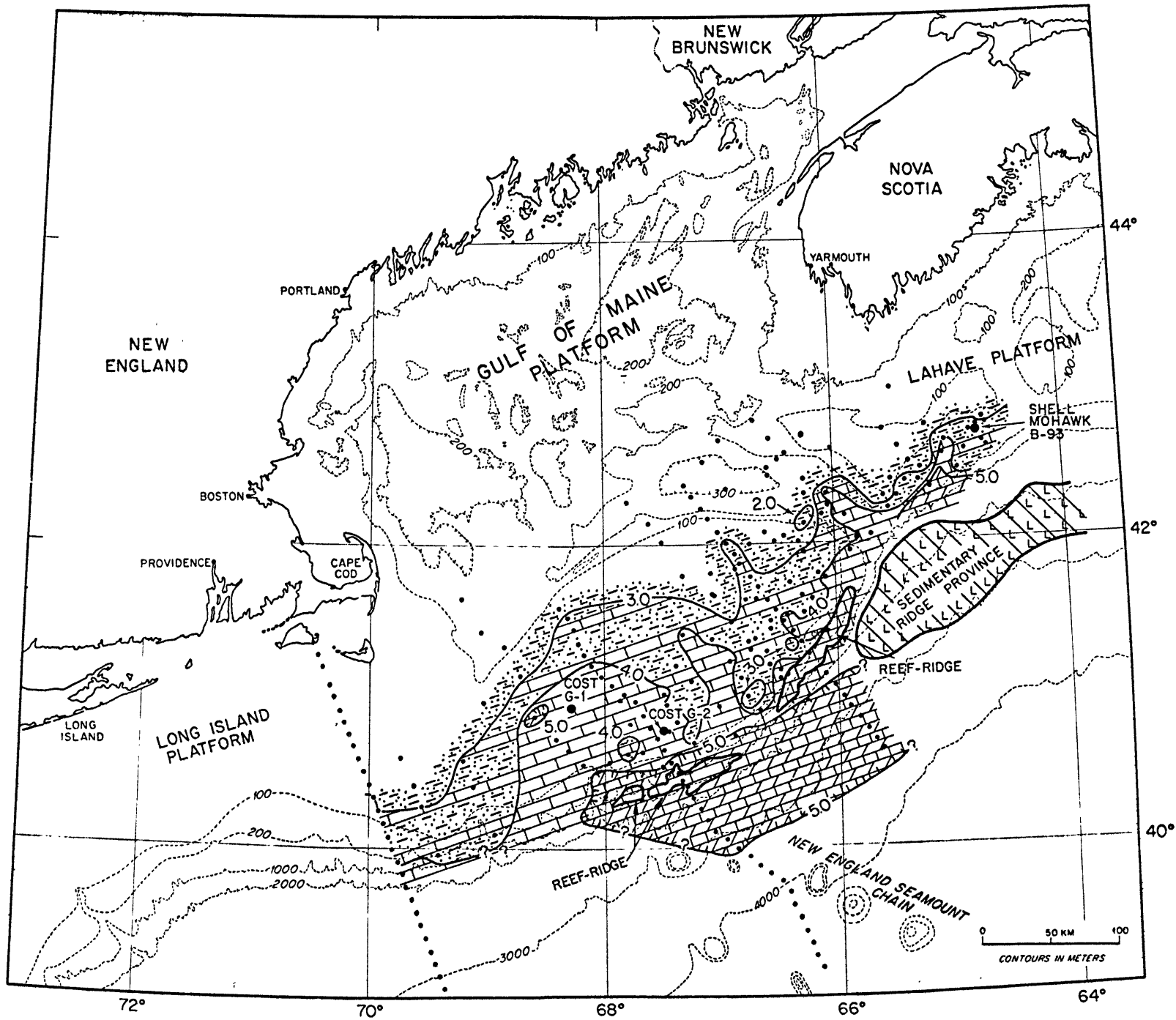


Figure 28. "3" - "2" velocity/lithofacies map. For an explanation of labels and symbols, refer to Figure 26 and previous figures. The outline of the "reef-ridge" is the same as that shown on Figure 27, but during this period (Early Cretaceous) its extent must have been reduced and very patchy.

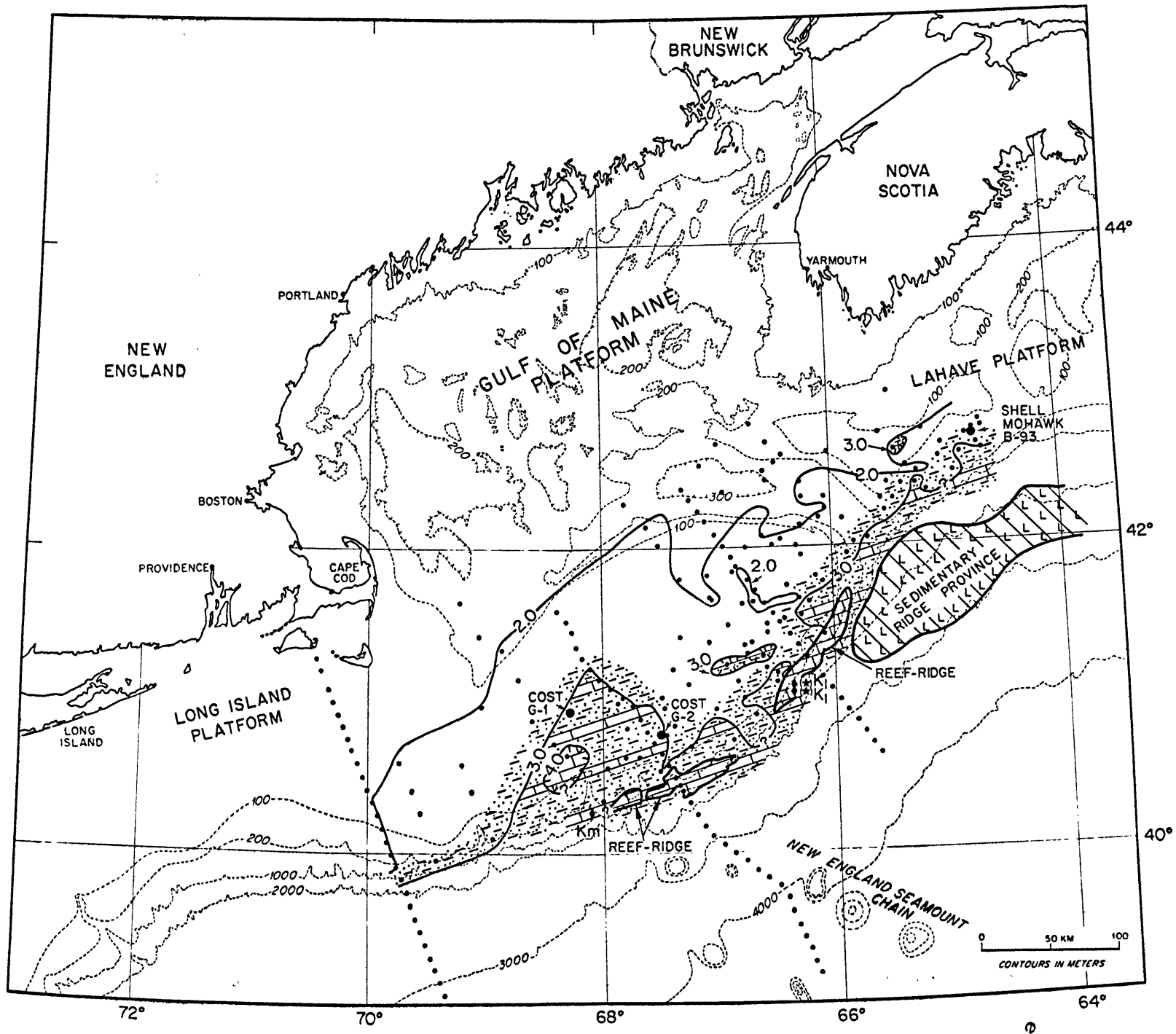
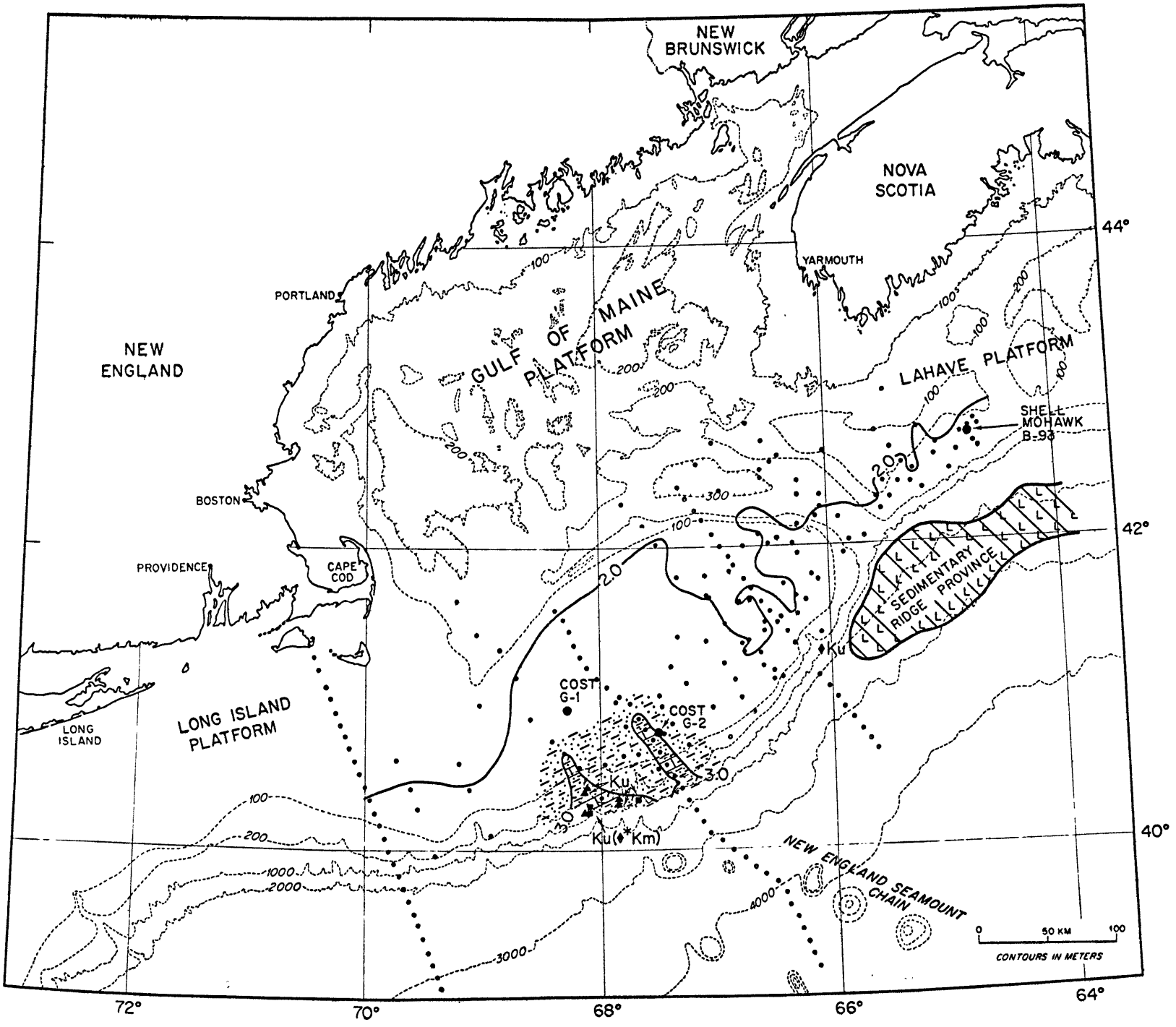


Figure 29. "2" - "X" velocity/lithofacies map. For an explanation of labels and symbols, refer to Figure 34 and previous figures.



tending to corroborate the Canadian experience that the Jurassic section underlying the outer shelf is predominantly carbonate (McIver, 1972). Velocities from 3.0 - 4.0 km/sec were interpreted as marls, often indicative of a facies transition from carbonates to clastics. Marl velocities occurred on all the maps, but their position appears to migrate seaward with time (Figures 26-29). This migration is supported by the geologic evidence, which suggests a gradual transition from carbonates to clastics by the end of the Early Cretaceous (reflector "2" time). Finally, velocities less than 3.0 km/sec were assumed to be a mixed sandstone-shale assemblage. No attempt was made to differentiate these low-velocity sediments, which dominate the section during the "2" - "X" interval (Figure 29). The geology of post - "X" sediments (Figure 21) supports the widespread existence of non-carbonate lithologies on the New England margin by the end of the Cretaceous.

Based on the findings of Ryan et al. (1978), the "reef-ridge" is interpreted as limestone. Little reliable velocity information exists to delineate its internal structure any further. It is assumed to have existed throughout the Jurassic and Early Cretaceous until its complete burial at about reflector "2" time (see Figure 10). The patchy nature of the reef on

Figures 27 and 28 is based on seismic interpretation of the structure's local relief, and is only an approximation based on available control.

The SRP is inferred to be the product of the vertical migration of salt belonging to the Early Jurassic Argo Formation (McIver, 1972). The compressional wave velocity of salt is reasonably constant at 4.6-4.9 km/sec (Figure 25), but collecting reliable velocity information over the SRP is extremely difficult because of rugged topography and complex geology. The hypothetical extension of evaporites beyond the SRP on Figure 26 is based upon a seismic interpretation of possible diapiric structures both beneath Northeast Channel and southeast of the Yarmouth arch. Their existence could not be proven or disproven on the basis of velocities alone.

The paleogeographic implications of Figures 26-29 will be examined in detail below as part of a reconstruction of the geologic development of the New England passive continental margin.

CHAPTER III

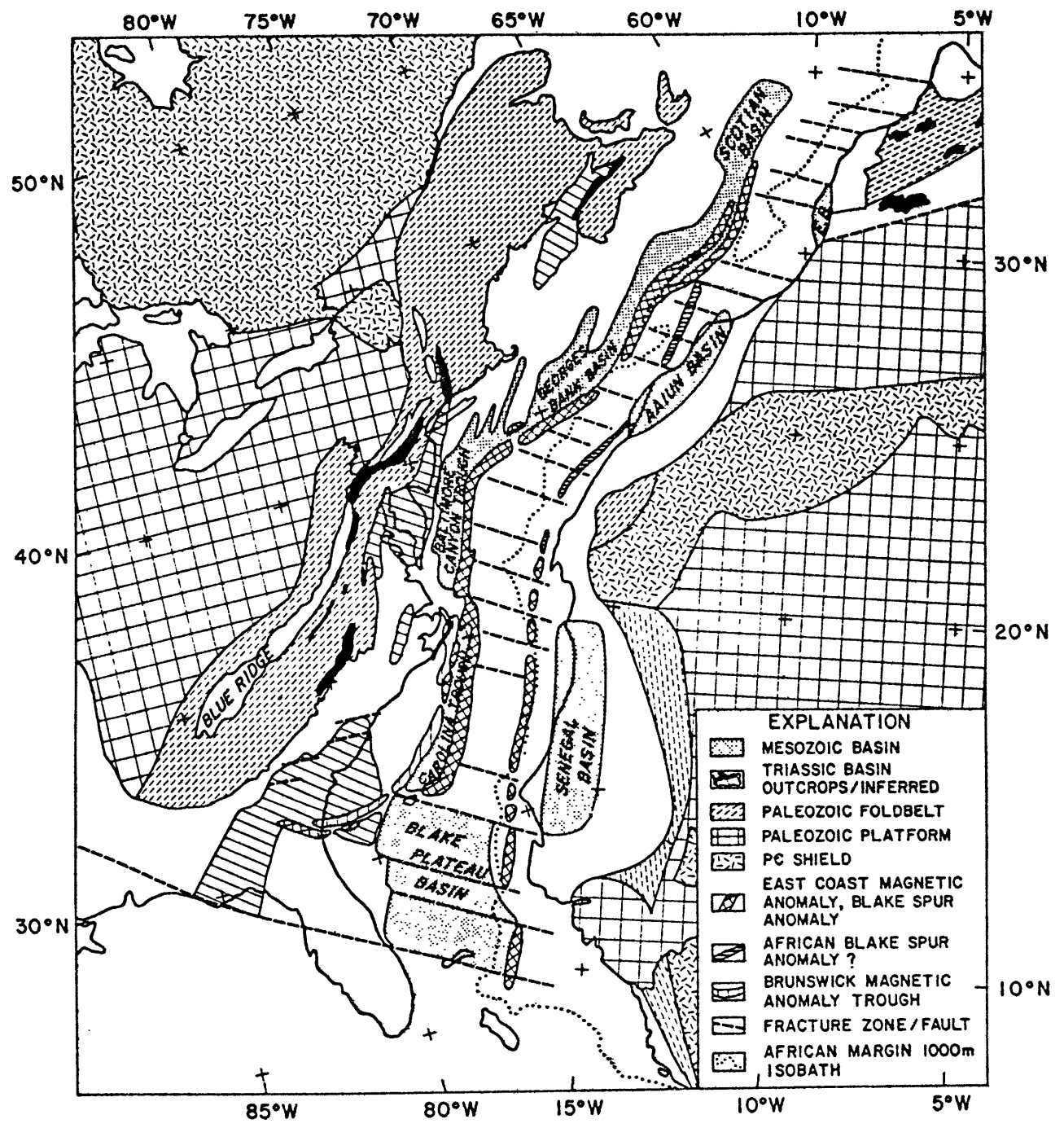
Discussion of Results

Introduction

It is now generally accepted that eastern North America and northwestern Africa were joined prior to the Late Triassic, although the exact fit of the two continents remains a matter of conjecture (LePichon et al., 1977; Sclater et al., 1977). One reason for this uncertainty has been and continues to be a lack of knowledge of the geology of the continental margins of Morocco and eastern North America. Another reason is that, landward of the Jurassic quiet zone boundaries, evidence both for sea-floor spreading and for a clear transition from oceanic to continental crust is lacking. Recent work by Schouten and Klitgord (1977) and Klitgord and Schouten (1977) has resulted in a plate reconstruction at the time of the Blake Spur Anomaly, which has been tentatively dated by van Hinte (1976a) at 160 my B.P. and by Klitgord and Schouten (1977) at 175 my B.P. (Figure 30). Unlike other reconstructions, which rely on an isobath as a continental edge (Bullard et al., 1965; LePichon et al., 1977; Sclater et al., 1977), the Klitgord and Schouten (1977) version does not recognize a unique relationship between water depth

Figure 30. North Atlantic plate reconstruction at the time of the Blake Spur Anomaly. After Klitgord and Schouten (1977).

BLAKE SPUR ANOMALY RECONSTRUCTION



- EXPLANATION**
- MESOZOIC BASIN
 - TRIASSIC BASIN
 - PALEOZOIC FOLDBELT
 - PALEOZOIC PLATFORM
 - PC SHIELD
 - EAST COAST MAGNETIC ANOMALY, BLAKE SPUR ANOMALY
 - AFRICAN BLAKE SPUR ANOMALY ?
 - BRUNSWICK MAGNETIC ANOMALY TROUGH
 - FRACTURE ZONE/FAULT
 - AFRICAN MARGIN 1000m ISOBATH

and crustal type. An examination of Figure 30 reveals that the Georges Bank Basin and the southwestern Scotian Basin border a proto-North Atlantic Ocean whose maximum width was already approximately 200 km at Blake Spur Anomaly time. Facing these North American depocenters are the Aaiun/Tarfaya and Essaouira basins, which underlie the Moroccan margin. While such a reconstruction facilitates trans-Atlantic correlations of the Mesozoic stratigraphy of these marginal basins, it does not shed any light on their formation. However, models do exist, and the theoretical and practical constraints on the genesis of a passive continental margin will now be considered.

Models of Passive Margin Formation

Armed with theory, imagination, and very little data, a number of investigators have addressed the question of crustal behavior during rifting and separation of continental plates (Dietz, 1963; Dewey and Bird, 1970; Sleep, 1971; Bott, 1971; Walcott, 1972; Falvey, 1974; Watts and Ryan, 1976; McKenzie, 1978; Veevers and Cotterill, 1978; Pegrum and Mounteney, 1978; Steckler and Watts, 1978; Royden et al., in press; and others). Watts and Ryan (1976) determined that subsidence of the margin off the east coast of the United States could not be the result of sediment loading alone.

The authors postulated that so-called "'driving forces'" were also involved, and that the observed subsidence could be modeled as an exponential decay similar to that governing the thermal contraction of oceanic lithosphere. The nature of the driving forces was discussed by Falvey (1974), who concluded that there were only three possible ways to develop an Atlantic-type passive margin and maintain isostatic equilibrium:

1. Change crustal thickness.
2. Change crustal density.
3. Change upper mantle density, i.e. by means of either phase changes or thermal expansion.

Bott (1971), McKenzie (1978), and Royden et al. (in press) have all discussed the first mechanism, that of lithospheric thinning and extension. Royden et al. (in press) found that this kind of crustal behavior would produce subsidence (neglecting the effects of sediment loading) which would follow an exponential decay curve similar to that derived by Watts and Ryan (1976). However, the extension required to produce the observed subsidence was very large. McKenzie (1978) estimated that continental crust would have to be stretched to twice its original length to produce a depression filled with only 4.5 km of sediment.

While the existence of block-faulted terrain beneath Georges Bank implies some extension, fault-plane dips there do not appear to decrease at depth (Figure 15), and block rotation along such faults would be essential to produce large amounts of crustal thinning (McKenzie, 1978; Royden et al., in press). Consequently, there is no evidence at present for hundreds of kilometers of extension on the New England margin. In this regard, Steckler and Watts (1978) estimate that only 20-25 km of extension have occurred in the vicinity of the C.O.S.T. B-2 well in the nearby Baltimore Canyon Trough.

Falvey's second mechanism produces subsidence by means of an increase in the density of rifted continental lithosphere achieved through the intrusion of mantle material. Once again, the subsidence would be exponential (Royden et al., in press). Only indirect data are currently available to indicate that the intrusion of mafic dikes is a primary mechanism of margin formation. For example, volcanics are associated with the Triassic grabens of eastern North America (Sanders, 1963) and Morocco (Van Houten, 1977; Manspeizer et al., 1978), and may also be present as part of the pre-"K" graben-fill underlying the New England margin (Valentine, 1978). Perhaps the so-called "transitional"

continental crust inferred to lie seaward of the basement "hinge zone" beneath the southeastern part of Georges Bank represents dike-injected continental crust. However, if that is the case, the intrusion process must have been highly localized to achieve the abrupt change in density necessary to produce the large vertical displacement observed.

Falvey (1974) himself favored changes in upper mantle density as an explanation of margin tectonics. He called upon thermal expansion to produce a density decrease and consequent uplift, then erosion of the uplifted arch and deep-crustal metamorphism to cause subsidence. Sleep (1971) had also used thermal expansion to produce uplift, but his model relied on large amounts of crustal erosion and cooling to engender subsidence. Neither cooling nor extensive erosion was necessary to Falvey's hypothesis, so it became an attractive explanation of syn-rifting and early post-rifting crustal phenomena.

Because all of these rifting models incorporate block-faulting as the characteristic response of the rigid upper part of the continental lithosphere, the faulting which is observed on the New England margin (Figure 15) cannot be used to differentiate between them. Nonetheless, several conclusions can be drawn.

First, crustal extension on the New England margin appears to have been small, not more than a few tens of kilometers. Second, the probable existence of volcanics within this margin's graben-fill (Valentine, 1978) lends some support to the dike-injection model, even though its importance to the margin formation process has not yet been fully established (Royden et al., 1978). Finally, the existence of the "K" unconformity, which truncates the margin's rifted basement terrain, implies both uplift and crustal erosion prior to margin subsidence. Some kind of thermal expansion is indicated by the uplift, but at present the models of Sleep (1971) and Falvey (1974) cannot be distinguished because the amount of pre- and syn-"K" erosion cannot be determined. If the basement troughs lying seaward of the basement "hinge zone" are partially or entirely filled with syn-"K" sediments, the erosion which created "K" could have been substantial.

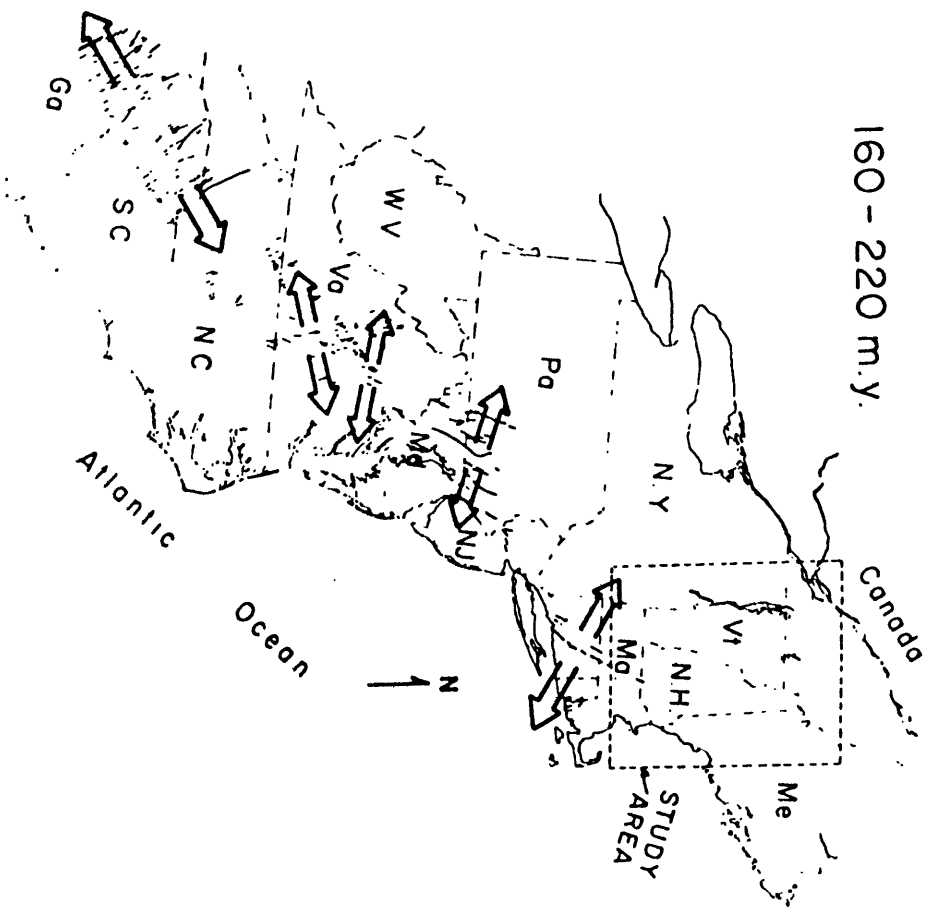
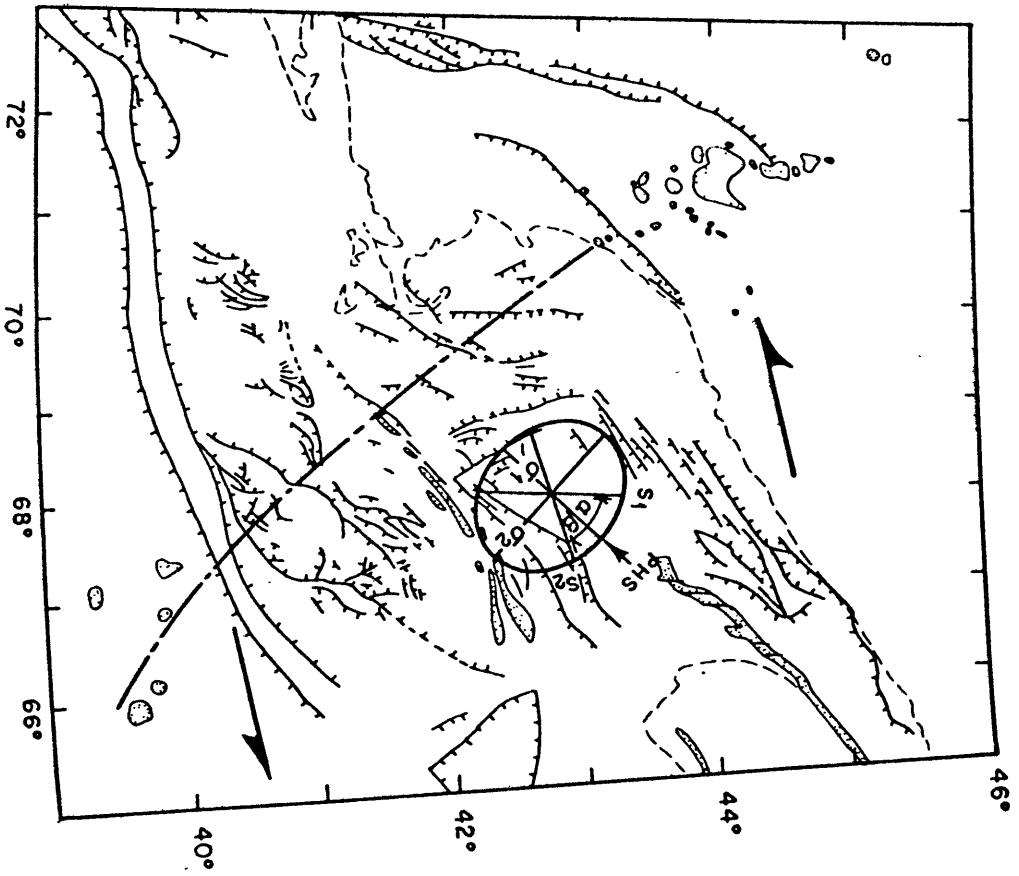
Geologic History of the New England Passive
Continental Margin

Rifting

Evolution of Observed Crustal Structures

The crustal structures exhibited by the New England margin are shown on Figure 15. Ballard and Uchupi (1975) attempted to explain the regional structural grain in the Gulf of Maine with a NE-SW oriented left-lateral shear couple (Figure 31A). DeBoer (1967) used a similar mechanism to account for the orientation of Mesozoic (predominantly Jurassic) dike swarms in the northern Appalachians. On the other hand, McHone (1978) has postulated NW-SE crustal extension to explain NNE-SSW-trending Late Triassic-Early Jurassic mafic dikes in central New England (Figure 31B). Figure 31 shows that McHone's dikes are oriented approximately parallel to one of the planes of tensional fractures (σ_1) defined by the sinistral shear couple of Ballard and Uchupi (1975). Therefore, the extension which favored the dike emplacement could have been caused by the same stress pattern inferred to have created the graben structures underlying the Gulf of Maine. In fact, an examination of Figure 31 does not reveal any crustal structures completely incompatible with a stress field dominated by left-lateral shear. Furthermore,

- Figure 31. A. Stress pattern used by Ballard and Uchupi (1975) to explain the orientation of observed Late Triassic (?) crustal structures in the Gulf of Maine.
- B. Proposed direction of extensional stress inferred by McHone (1978) from the NNE-SSW orientation of Triassic and Jurassic mafic dikes. The dike orientations coincide with the σ_1 direction postulated by Ballard and Uchupi (1975). Therefore, the extension which favored the emplacement of the dikes could have been caused by sinistral shear.



160 - 220 m.y.

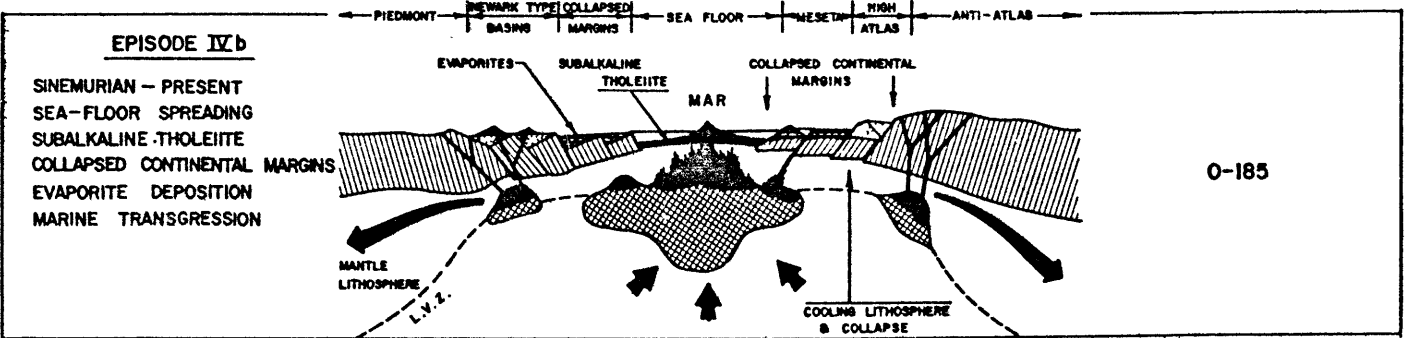
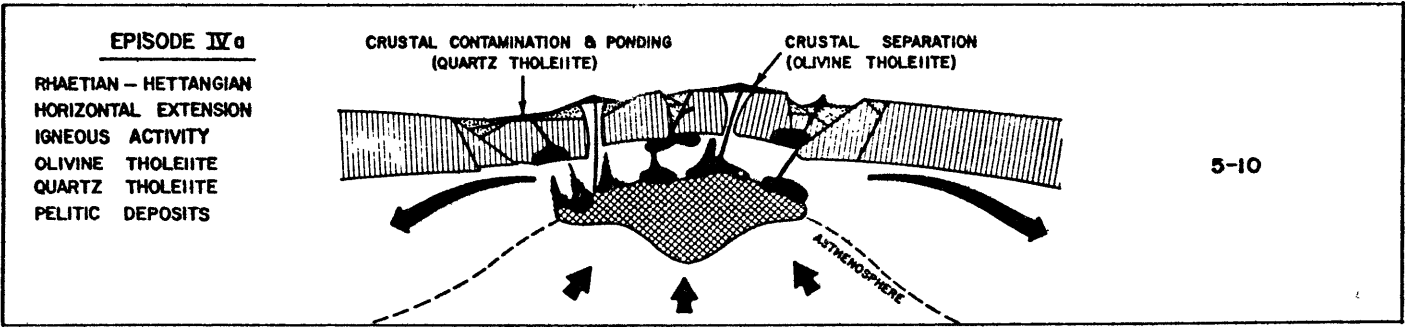
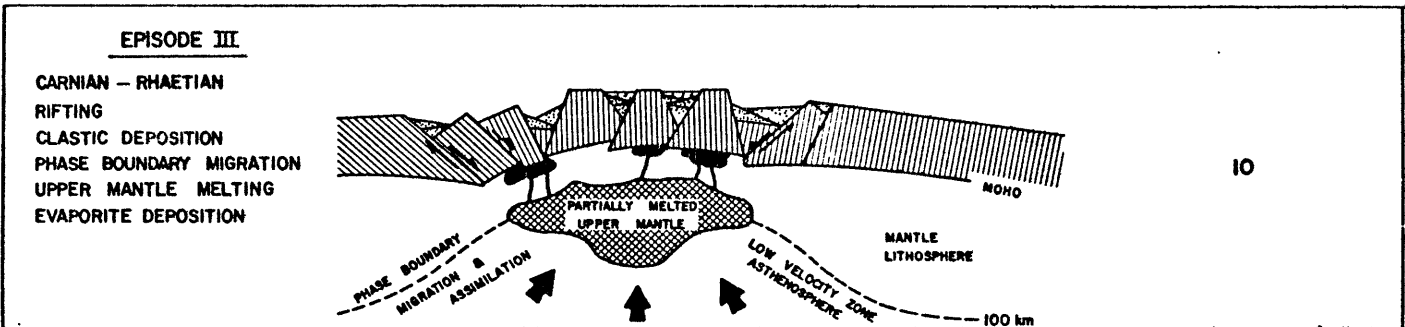
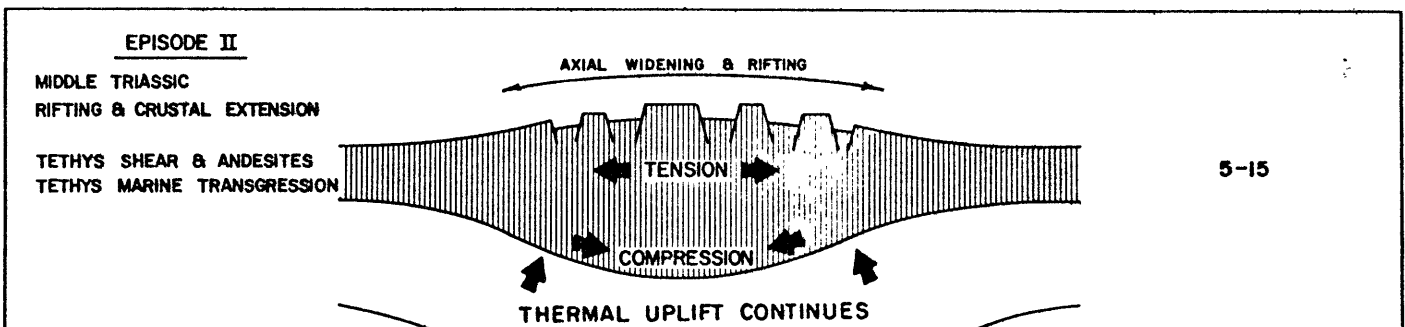
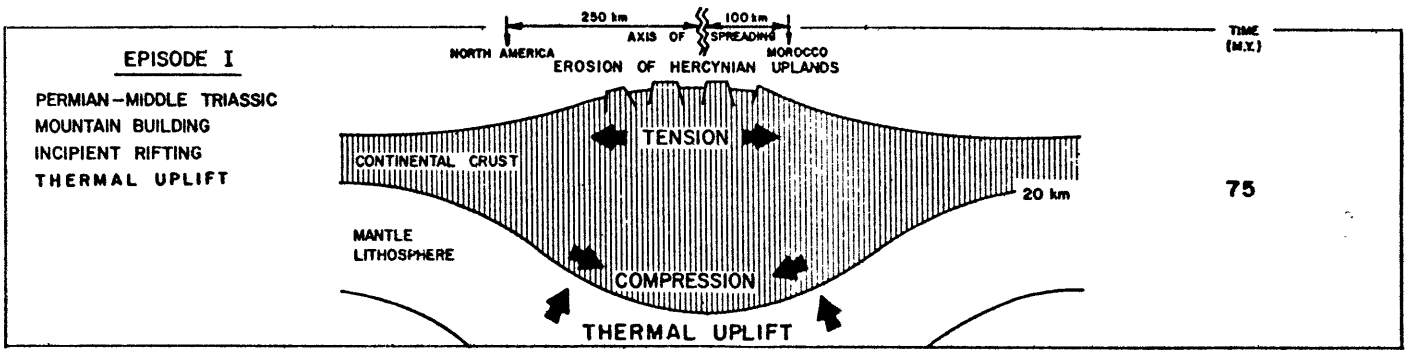
any early translational motion between the North American and African plates would have had to occur along either one or both of the shear fracture plane orientations (S_1 and S_2 , Figure 31A) predicted by the shear couple. Interestingly, all of the postulated zones of weakness in the New England margin (Figure 15) line up roughly parallel to S_1 . Perhaps the positions of oceanic fracture zones were controlled by pre-existing stresses in the rifting continental crust.

The orientations of fault planes created during the rifting process may also have been at least partially controlled by the structural foliation present in older rocks. Lindholm (1978) has examined many of the Triassic rift basins of eastern North America, and he found in all cases that border faults parallel the country rock foliation. Unfortunately, the foliation of the Precambrian/Paleozoic basement complex into which the rift structures of the New England margin have been entrained has not yet been mapped in detail. At present, all that can be said is that these structures generally parallel Appalachian trends (Wilson, 1966; King, 1977).

Recently, Van Houten (1977) and Manspeizer et al. (1978) attempted trans-Atlantic correlations of early Mesozoic geology based upon new stratigraphic and

radiometric data from the Late Triassic and Early Jurassic deposits of Morocco. Manspeizer and his colleagues developed a model for crustal distention and separation which is here reproduced as Figure 32. According to this model, the absence of Permian and Early-Middle Triassic rocks on both North Atlantic margins is the result of uplift and erosion of continental crust previously thickened during the Acadian/Hercynian orogenics (Figure 32, Episode I). Falvey (1974) interpreted the hiatus as a "rift-onset unconformity". Manspeizer and his colleagues (1978) postulated continuous upper crustal extension until the end of the Middle Triassic (Figure 32, Episode II), although there is no indication that a large amount of extension occurred during the formation of the New England margin (Figure 15). As previously discussed, a reasonable mechanism to explain the initial uplift was isostatically compensated thermal expansion associated with heating of the upper mantle. The source of this heat could have been the Paleozoic continental collision, although this cannot be proven. Deep-crustal heating would explain the carboniferous-Permian thermal event noted by Ballard and Uchupi (1975) in the Gulf of Maine, and the spurious Carboniferous

Figure 32. Model of passive margin formation. After
Manspeizer et al. (1978).



K-Ar date derived for Devonian granite sampled at the Shell Mohawk B-93 well on the Scotian Shelf (Given, 1977).

The model put forth by Manspeizer et al. (1978) agrees with previous estimates of the amount of time required for plate distention. As examples, Burke (1976) estimated that 20 ± 10 my of intra-continental rifting were necessary, while Dewey and Bird (1970) and Falvey (1974) hypothesized that the entire plate stretching and breaking process could take 50-150 my. However, the model does not explain why much of the western Appalachian region was undergoing compression during the Permian Allegheny orogeny (King, 1977). Ballard and Uchupi (1975) recognized this problem, and tried to explain simultaneous Carboniferous-Permian tensional rifting of northeastern North America and compressional deformation of the Appalachian miogeosyncline by means of an oblique, NE-to-SW continental collision during the late Paleozoic. The authors also used this mechanism to account for right-lateral motion on the Cobequid-Chedabucto fault system. Such right-lateral translation, when coupled with left-lateral displacement along the Tethys fracture zone, could have produced the uplift necessary for subsequent intra-continental

rifts on the North American and African margins (Manspeizer et al., 1978).

Pre-"K" Stratigraphy

The pre-"K" section constitutes the clastics, evaporites, and volcanics associated with intra-rift sedimentation (Figure 32, Episodes II, III, and IVa). Palynomorphs indicate that clastic graben-fill of the High Atlas in Morocco date is Carnian or older (Cousminer and Manspeizer, 1976; Manspeizer et al., 1978). In New England, the graben-fill ranges in age from Late Triassic to Early Jurassic (Cornet and Traverse, 1975). Apparently, intra-rift sedimentation did not cease with plate separation, but continued after the initiation of sea-floor spreading (and the formation of reflector "K"). This could be the reason why "K" is difficult to trace across troughs (Falvey, 1974), and why red-beds of the Late Triassic-Early Jurassic Eurydice Formation (Jansa and Wade, 1975; Given, 1977) straddle the ages proposed for North America-Africa plate decoupling.

On both margins, there is evidence for the deposition of evaporites during the continental distention phase. Triassic palynomorphs have been recovered from evaporites sampled beneath the Grand Banks (Walton

and Berti, 1976; Jansa et al., 1977), and incipient diapiric activity has been noted in the graben-fill of the Georges Basin (Ballard and Uchupi, 1975; Figure 9). In western and northwestern Morocco, thick evaporite sequences of Late Triassic age are present on the Oranian Meseta, in the Essaouira Basin/Argana Valley, and in the southwestern Aaiun/Tarfaya Basin (Van Houten, 1977; Manspeizer et al., 1978; Figure 30). Apparently, evaporites were deposited progressively from east to west as a result of a Tethyan marine transgression (Jansa and Wade, 1975; Van Houten, 1977; Manspeizer et al., 1978). Consequently, the deposits are generally Middle-Late Triassic in Morocco, latest Triassic-earliest Jurassic in southern Portugal (Zbyszewski and de Faria, 1971), and Late Triassic-Early Jurassic off eastern North America. Tethyan waters may have reached the New England region via the left-lateral Tethys and Newfoundland fracture zones and the right-lateral Cobequid-Chedabucto fault system north of Nova Scotia (Manspeizer et al., 1978).

Available paleogeographic information on the pre-"K" graben-fill sequences on both the North American and African margins suggests that the climate during the Late Triassic-Early Jurassic was tropical (Jansa

and Wade, 1975; Hubert et al., 1976; Van Houten, 1977; Manspeizer et al., 1978). Thick evaporite sequences appear to be restricted to outer-margin rift basins where early marine incursions were common (Van Houten, 1977). Wade (1978) has indicated that both restricted marine and playa evaporite deposition occurred on the northeastern North American margin during the Late Triassic. However, original thicknesses of evaporites deposited on these margins may never be ascertained because of subsequent diapiric activity.

The thickness of graben-fill exceeds 4 km in the Georges Basin graben, and has been reported to be as much as 9 km in parts of the Triassic system of northeastern North America (Sanders, 1963). The possible presence of large thicknesses of pre- and/or syn-"K" sediments seaward of the "hinge zone" beneath the southeastern part of Georges Bank cannot be dismissed. This would account for much of the sediment which must have been eroded during the formation of the "K" unconformity.

During the latest Triassic-earliest Jurassic (approximately 205-190 my B.P.), widespread tholeiitic volcanism and the intrusion of mafic dikes and sills began (Figure 32, Episode IVa). The exact time of opening of the present North Atlantic can be estimated

from radiometric dates on these syn-rift volcanics, which are present on both flanking continents. In eastern North America, Erickson and Kulp (1961) obtained what they considered to be reliable K-Ar dates on the Palisades basalt sill which ranged from 202 to 190 my B.P. K-Ar dates reported by deBoer (1968) from the Holyoke and Deerfield diabases of the Connecticut Valley were 193 ± 6 my B.P. and 191 ± 6 my B.P., respectively. Reesman et al. (1973) presented 14 more dates from Connecticut Valley flows. They ranged from 196 to 171 my B.P., with an average of 184 ± 8 my B.P. In his dike study, McHone (1978) found diabase ages to range from 180 ± 8 to 200 ± 9 my B.P., although the entire group of dikes examined spanned the interval from Late Triassic to Early Cretaceous.

In Morocco, Hailwood and Mitchell (1971) dated the Draa Valley dolerite sills and the Foun-Zguid-El Graara quartz dolerite dike in the Anti-Atlas at 187 and 181 my B.P., respectively. LeBlanc (1973) obtained slightly younger dates for the Foun-Zguid-El Graara dike (168 ± 5 and 152 ± 5 my B.P.), perhaps suggesting multiple injection of material along the same structural trend. The Foun-Zguid-El Graara dike, like the mafic dikes of similar age in New England (McHone, 1978), parallels the present coastline. Finally, Cousminer and Manspeizer

(1976) reported dates on lava flows from the High Atlas Mountains ranging from 218 ± 21 to 196 ± 20 my B.P.

To date, no pre- or syn-"K" volcanics have been sampled beneath the New England margin. Basalts sampled by a well on Nantucket Island southeast of Cape Cod at the same depth as "K" along the landward portion of U.S.G.S. 5 (Valentine, 1978; Figure 13) could represent a pre-separation eruptive episode similar to those documented in New England (deBoer, 1968; McHone, 1978) and Morocco (Cousminer and Manspeizer, 1976; Manspeizer et al., 1978).

Continental Separation and the Development of the "K" Unconformity

As suggested by Scrutton (1973), plate decoupling probably occurred near the peak of volcanic activity, 10-15 my after the onset of rifting and 75 my after the initial crustal uplift (Figure 32). On the northeastern North American margin, the basement "hinge zone" (Figure 15) is here interpreted as the boundary between "normal" continental crust and continental crust extensively altered by rifting. There is no consistent relationship between the trend and position of the "hinge zone" and that of the "east coast magnetic anomaly" (Figure 15). In fact, the "hinge zone" does

not seem to be associated with any lineated magnetic anomaly, a somewhat puzzling fact considering the magnitude of the basement tectonism involved there.

With the initiation of sea-floor spreading, margin subsidence began, first in response to dike injection (Royden et al., in press) and deep-crustal metamorphism (Falvey, 1974), then as a result of cooling and consequent contraction (Sleep, 1971; Royden et al., in press; Figure 32, Episode IVb). Prior to final margin collapse, subaerial erosion truncated pre-existing rift structures. Falvey (1974) called the resultant surface the "break-up unconformity". According to him, this unconformity ought to be about the same age as the oldest oceanic crust generated in the adjacent ocean basin. The "K" unconformity, recognized and mapped beneath the New England margin, must be equivalent to the "break-up unconformity". If its age correlates with the beginning of sea-floor spreading, then it formed approximately 195-190 my B.P. (Manspeizer et al., 1978).

Drifting: Evolution of Observed Stratigraphy

"K" - "Z" (190-160 my B.P.)

Based upon an examination of borehole data from the 25 my-old Gulf of Lion in the Mediterranean, Watts and Ryan (1976) estimated that initial basement

subsidence rates for a young passive margin could be as high as 20 cm/1000 yrs, much higher than the rates predicted for the thermal contraction of oceanic crust. Their estimate compares favorably with the 21 cm/1000 yrs rate calculated for the 30 my period (190-160 my B.P.) separating reflectors "K" (basement) and "Z". It must be remembered, however, that this rate incorporates the added effect of sediment loading seaward of the basement "hinge zone" (see Chapter II). A truly accurate assessment of basement subsidence rates cannot be made for the New England margin until borehole data for the region becomes available.

Following the initiation of sea-floor spreading and the carving of the "K" unconformity, rapid margin subsidence caused an Early Jurassic marine transgression which inundated pre-existing rift structures. In the southwestern parts of the Essaouira and Aaiun/Tarfaya basins, the sea transgressed eastward. Early Jurassic stratigraphy in both of these depocenters consists of sabkha tidal-flat deposits of dolomite, marl, and gypsum overlain by platform carbonates (Van Houten, 1977). A similar sequence has been sampled on the Grand Banks and the Scotian Shelf. Two transgressions may have occurred across the New England margin: the first

prior to actual continental separation (Late Triassic) which is responsible for the evaporites inferred to exist within Georges Basin, and the second following the initiation of sea-floor spreading (Early Jurassic) which resulted in the deposition of the Argo Formation (McIver, 1972; Jansa and Wade, 1975; Given, 1977; Figure 6). The Argo Formation is inferred to form the core of the Sedimentary Ridge Province (see previous figures). Uchupi and Austin (in press) have pointed out that the SRP could represent a seaward migration of salt in response to sediment loading on the outer shelf. If so, then Argo (Early Jurassic) evaporites could have moved from continental crust out across the basement "hinge zone" onto altered continental and/or oceanic crust to form the SRP (Uchupi and Austin, in press, Figure 8). The lack of a consistent relationship between the positions of the "east coast magnetic anomaly" and the seaward boundary of the SRP (Uchupi and Austin, in press, Figure 1) seems to support the hypothesis that the diapirs south of Nova Scotia are not controlled by the underlying basement configuration.

Evaporites of the Early Jurassic Argo Formation are overlain by dolomitic limestones of the Iroquois Formation (McIver, 1972; Figure 6). According to Given (1977) and Wade (1978), the Iroquois dolomites are indicative of progressively less restricted marine

circulation. Some researchers believe that the Iroquois Formation was deposited completely in an epicontinental sea prior to the formation of any oceanic crust (Jansa and Wade, 1975; Wade, 1978). Based upon evidence put forth here, and by Van Houten (1977) and Manspeizer et al. (1978), both the Argo and Iroquois formations must have been laid down at least in part on "transitional" continental crust highly altered by rifting.

Figure 26 is the lithofacies reconstruction of the New England margin for the 30 my interval between horizons "K" and "Z". The present boundary of the SRP is shown, although it is not yet known whether it has any resemblance to the limits of the original basin of evaporite deposition. An acoustic disturbance which may be a diapir has been recognized on multi-channel seismic reflection profiles collected across Northeast Channel, and halokinetic structures are also postulated beneath Georges Bank seaward of the "hinge zone" (Schlee et al., 1977; Figures 9 and 10). The rocks exhibiting interval velocities in excess of 5.0 km/sec (Figure 26) are interpreted as dolomitized limestones equivalent to those of the Iroquois Formation. Landward of the "reef-ridge", these limestones probably represent sabkha

deposits intercalated with marls, gypsum, and salt (Jansa and Wade, 1975; Given, 1977). Seaward of the "reef-ridge", coeval deposits on the upper rise are inferred to be open-marine carbonates deposited in a fore-reef environment. East of the New England Seamounts, these high-velocity sediments may fill troughs located at the base of the continental slope (compare U.S.G.S. 5, Figure 13, and U.S.G.S. 4, Figure 10).

The "reef-ridge" is assumed here to be a limestone reef complex/outer shelf carbonate platform, even though no Jurassic sediments have as yet been recovered from its seaward flank, which constitutes the continental slope south of New England. At present, all available geologic evidence supports this conclusion. Ryan et al. (1978) have recovered Neocomian reefal limestone from near the top of the feature (Figure 10), while ammonite-rich reefal limestone of middle Oxfordian (early Late Jurassic) age has been sampled from the Mazagan Escarpment northwest of the Essaouira Basin off Morocco (Renz et al., 1975). Recent modeling of the "east coast magnetic anomaly" (Klitgord and Behrendt, in press) suggests a basement foundation for the "reef-ridge" at depths of 6-8 km. Presumably, the reef complex or platform began to develop on a topographic high similar to the

tilted fault-block interpreted along the outer-shelf portion of U.S.G.S. 5 (Figure 13). The identity of basement in this region remains a mystery, although the position of the "reef-ridge" seaward of the "hinge zone" implies that its foundation is either transitional continental or oceanic crust.

The "reef-ridge" appears to constitute a boundary of the SRP, which could be additional evidence for basement control of both features (Figure 15). If evaporites of the SRP continue to the southwest along the seaward flank of the "reef-ridge", they are either too thinly bedded to produce diapirs, or are prevented from vertical migration by the presence of competent overlying sediments (i.e. fore-reef carbonates). Recent discoveries of diapiric structures along the trend of the "east coast magnetic anomaly" on the continental slope off Cape Hatteras (Grow and Markl, 1977) suggests the latter possibility.

Landward of the dolomitized limestones, a major facies change to limestones, marls, and clastics (probably red-beds) is inferred (Figure 26), based upon interval velocity data and similar transitions in the Morocco and eastern Canada margins. In the proximal part of the Essaouira Basin in Morocco, 3-4 km of Late Triassic to earliest Jurassic fanglomerates are overlain by

approximately 2 km of late Early Jurassic deltaic sediments whose distal equivalents are sabkha tidal flat deposits and salt (Van Houten, 1977). If Manspeizer and his colleagues (1978) are correct about the sequence of events in Morocco, then this salt is coeval with the Early Jurassic Argo Formation off Canada. On the North American side, red-beds of the Late Triassic-Early Jurassic Eurydice Formation and sands and sandstones of the Early-Middle Jurassic Mohican/Mohawk formations (Jansa and Wade, 1975; Given, 1977; Wade, 1977) are here interpreted as having continued to accumulate in and over inner-shelf basins during the outer-shelf deposition of both the Argo and Iroquois formations (Figure 26). Consequently, the Eurydice/Mohican-Mohawk clastics must interfinger with the Argo/Iroquois evaporites and carbonates across the north-central part of Georges Bank (Figure 26). This marked lateral change in lithology is considered responsible for both the decreases in interval velocities and the general deterioration of reflector amplitude and continuity northward across the bank. The Shell Mohawk B-93 well does not sample either the Argo or Iroquois formations because it is located landward of this facies transition (Figures 3 and 26).

"Z" - "3" (160-136 my B.P.)

In this report, the "Z" reflector is interpreted as marking the contact between Iroquois dolomites and prograded clastics of the Mohican/Mohawk formations. The contact is assigned a Bathonian (Middle Jurassic, approximately 160 my B.P.) age. Wade (1978) considers the facies change to be an indication of the initiation of sea-floor spreading, which resulted in uplift and the rejuvenation of sediment source areas. However, a ridge jump westward towards the continental margin would produce the same effects, and such a ridge jump has been postulated at the time of the Blake Spur Anomaly to account for the asymmetry of the Jurassic quiet zones of the North Atlantic (Luyendyk and Bunce, 1973; Sclater et al., 1977; H. Schouten, personal communication). Given that the Blake Spur Anomaly was formed at some time between 175 my B.P. (Klitgord and Schouten, 1977) and 160 my B.P. (van Hinte, 1976a), a ridge jump appears to be the most reasonable explanation for the origin of the "Z" horizon.

Following the ridge jump, margin subsidence continued, and the outer New England shelf became dominated by limestones of the Abenaki Formation (Figure 27). These open marine conditions prevailed on the outer shelf until the end of the Jurassic (Wade, 1978). Landward,

these carbonates grade to the deltaic clastics of the Mohican/Mohawk and Mic Mac Formations (Figures 6 and 27). Seaward, the carbonates are bounded by the "reef-ridge". During this period, the exact extent of the "reef-ridge" is unknown, but its discontinuous nature can be inferred from available seismic data (Figure 27). It could not have been a significant barrier to the seaward transport of sediments during the latter half of the Jurassic.

Reflector "4" is interpreted in this report as representing either the late Middle Jurassic Scatarie limestone or the Middle-Late Jurassic Baccaro limestone of the Abenaki Formation. This horizon records the marine transgression following the Blake Spur Anomaly ridge jump. The northern limit of reflector "4" (Figure 7) generally mimics the transition from limestones to marls shown on Figure 27, and its regional extent probably indicates the approximate area of the Middle or Late Jurassic carbonate platform.

"3" - "2" (136-~95 my B.P.)

Deltaic sediments began to prograde across the LaHave Platform/Georges Bank region during the latest Jurassic and Early Cretaceous in response to tectonism which is here attributed to the opening of the Bay of Biscay approximately 125 my B.P. (Jansa and Wade, 1975; Sclater et al., 1977) and to the

separation of Europe and North America 110-95 my B.P. (H. Schouten, personal communication; Sclater et al., 1977). Reflector "3", the acoustic horizon interpreted as marking the Jurassic-Cretaceous boundary, is associated with a hiatus separating latest Jurassic (Tithonian) from Early Cretaceous (Valanginian) sediments in the Shell Mohawk B-93 well (Figure 3). This hiatus was probably created when Abenaki carbonates were inundated by deltaic sands and shales of the Mississauga and Verill Canyon formations (McIver, 1972; Wade, 1978; Figure 6). The delta complex is characterized by a number of lobate accumulations which in some places transect the shelf completely (Figure 28).

The "reef-ridge" was so discontinuous during the Early Cretaceous that its distribution could not be accurately mapped seismically. It is shown on Figure 28 as it appeared on Figure 27 for schematic purposes, but it probably consisted of little more than a series of small patch reefs near the present shelf-break. When the sample locations of Neocomian reefal limestones recently recovered from Heezen Canyon (Ryan et al., 1978; see Figures 10 and 19) are plotted on Figure 28, they fall on the seaward flank of one of the inferred patch reefs, proof that some sporadic carbonate build-up continued during the Early Cretaceous despite the

influx of terrigenous material.

Early Cretaceous regression resulted in widespread erosion of the continental margin off the east coast of North America. The hiatus produced by this erosion separates Aptian from Cenomanian sediments in the Shell Mohawk B-93 well, resulting in an Early Cretaceous interval which is only 4 m thick (Figure 3). Reflector "2" occurs right above the Albian hiatus at the Shell Mohawk well (Figure 3), and is inferred to represent that unconformity beneath the rest of the New England continental margin. Downcutting associated with the carving of the unconformity is probably responsible for the regional thinness of the interval between reflectors "3" and "2" (Figure 19).

By the early Late Cretaceous, the remnants of the "reef-ridge" had been completely buried (Figure 10). Active erosion of the surviving patch reefs may account for the "beach rock" (dolomite-cemented subarkosic sandstone) of mid-Cretaceous age recently recovered from Oceanographer Canyon south of Georges Bank (Ryan et al., 1978; Figure 28).

On the continental rise, the Early Cretaceous is marked by the deposition of black clays atop Horizon β . These sediments are now thought to be the product of a rise in the CCD during Valanginian-Hauterivian time

associated with a restriction in the deep circulation of the North Atlantic. Tucholke and Mountain (in press) have mapped the distribution of black clays along the North American margin of the western North Atlantic, and they find lobes of thick accumulation which they feel are evidence for a terrigenous origin. One of the black clay lobes underlies the rise south of the Long Island Platform. According to the authors, black clays deposited on the rise may have been funneled through gaps in the remnants of an Early Cretaceous reef complex. Figure 28 supports such a conclusion.

By Cenomanian time, black clays were replaced by multi-colored clays on the rise, indicative of the introduction of oxygenated bottom waters (Tucholke and Vogt, in press). Perhaps the separation of Europe, Greenland, and North America at approximately this time (Sclater et al., 1977) was responsible for the marked change in deep-ocean circulation. The source for the multi-colored clays may have been terrigenous detritus eroded during the formation of the reflector "2" unconformity and carried to the continental rise by turbidity currents. After reflector "2" time, there was no longer any significant reefal barrier to the off-shelf transport of sediment on the New England margin.

"2" - "X" (~95-~75 my B.P.)

Margin subsidence continued at a much reduced rate during the Late Cretaceous. Figure 29 shows that almost the entire New England margin was blanketed by sandstones and shales during this period. Available evidence from the Canadian margin suggests that slow transgression of the region continued until the Maestrichtian (Jansa and Wade, 1975; Given, 1977; Wade, 1978). Coarse clastics of the Logan Canyon Formation interfingered with and were overlain by finer-grained terrigenous sediments of the Dawson Canyon Formation (Given, 1977; Figure 6). In general, Late Cretaceous sediment thicknesses and sedimentation/subsidence rates averaged 0.5 km and 2.5 cm/1000 yrs, respectively (Figure 21). Based upon seismic and well data, Given (1977, p. 80) described the Late Cretaceous Scotian Shelf as "a large coastal area of multiple streams, marine embayments, marine bars, shelly beds, tidal channels and estuaries".

From Turonian to Campanian time, a deep-water basin occupied at least part of the southwestern Scotian Shelf and the adjacent New England margin. First limestone and then chalk, which are responsible for regionally identifiable acoustic horizons, was

deposited. Reflector "X" is produced by either the Turonian Petrel limestone or the Turonian-Campanian chalks of the Wyandot Formation (Wade, 1978). The close proximity of the "X" reflector to a hiatus separating lower Campanian from Paleocene sediments in the Shell Mohawk B-93 well suggests a correlation with the Wyandot chalk and the Cretaceous-Tertiary boundary. Because "X" can be traced regionally across the New England margin, the presence of chalk there can be inferred even though Figure 29 does not indicate its presence. Given (1977) reports that Late Cretaceous water depths on this margin ranged from middle neritic to bathyal. Apparently, subsidence exceeded sedimentation during this transgression.

Hays and Pitman (1973) have argued that the Late Cretaceous transgression was a response to an increase in ridge volume associated with faster spreading rates in the Atlantic during the interval 110-85 my B.P. However, based upon information from the northeastern North American margin, transgression did not begin until the Cenomanian (approximately 95 my B.P.), and it continued until the lower Campanian (approximately 75 my B.P.). Consequently, if Hays and Pitman are correct, a time lag of 10-15 my is involved between

the change in ridge volume and the related transgressive episode on the flanking margins. This discrepancy is not resolved by the new Cretaceous time-scale put forth by van Hinte (1976b). It extends the period of rapid spreading from 120 to 80 my B.P., which still does not correlate with the duration of the transgression as it was recorded by the margin's sediment cover.

"X" - Present (~75-0 my B.P.)

Whatever its cause, the Late Cretaceous transgression had ended by the lower Campanian. A lower Campanian-Paleocene hiatus in the Shell Mohawk B-93 well points to renewed erosion of the inner parts of the Scotian Shelf. The onset of the regressional phase coincides with a major North Atlantic plate reorganization (The Iberian peninsula becomes part of the European plate, and Rockall Bank starts to separate from Greenland; Sclater et al., 1977), a decrease in spreading rates (van Hinte, 1976b), and a noticeable decline in bottom water temperatures perhaps indicative of high-latitude cooling (Savin et al., 1975).

The majority of the geologic evidence supports the contention that prograding sandstones and siltstones of the Banquereau and younger formations (Figure 6) have dominated the New England margin since the Campanian,

even though Eocene chalks sampled in Heezen Canyon (see Figure 21) prove that carbonate deposition extended into the Tertiary at least in some places.

The most spectacular erosional episode of the Tertiary occurred in the middle Oligocene, when a major regression perhaps accompanying the onset of Antarctic glaciation (Savin et al., 1975; Ingle et al., 1976, 1977; Haq et al., 1977) resulted in massive downcutting of the central and outer portions of the Scotian Shelf (see Figures 5 and 8). This Paleogene erosional event has been recognized on many margins around the world (Vail et al., 1977, in press). Reflector "1" marks the angular unconformity associated with it (see Figures 5 and 8). According to Vail and his colleagues, sea-level may have dropped some 250 m below its present level at this time. If their figure is correct, the present shelf was exposed, and the now-filled canyons along Line 42 (Figure 5) were cut at least in part subaerially.

The Tertiary unconformity present beneath the Gulf of Maine may also have been carved during the Oligocene (see Figures 9-11). In fact, it is possible that much of the erosion which left the Gulf of Maine as an interior lowland took place at this time (Lewis and

Sylwester, in press). Apparently, little of the sediment eroded from the inner shelf remained on the shelf. Most of it must have been transported by turbidity currents down the continental slope via submarine canyons and deposited on the continental rise and adjacent abyssal plains. To date, large thicknesses of Oligocene sediment have not been identified by drilling in the western North Atlantic, but extensive sampling of the continental rise off eastern North America has not yet taken place. Furthermore, all indications point to extensive bottom current activity in the western North Atlantic since the Eocene (Tucholke and Mountain, in press). These "contour currents" may have effectively redistributed Oligocene sediments, thereby preventing the build-up of thick local accumulations on the continental rise.

Apparently, Georges Bank underwent less erosion than the Scotian Shelf during the Oligocene regression because reflector "1" does not exhibit any relief beneath the bank. Extensive outcrops of Eocene rocks in the submarine canyons south of the bank (Ryan et al., 1978) suggest that most or all of the erosion was restricted to near the present shelf-break and on the upper continental slope (Figure 14). Perhaps Georges Bank was partially submerged at this time, while the adjacent Scotian Shelf was emergent and subject to extensive subaerial erosion.

Savin et al. (1975) reported paleotemperature work on benthonic foraminifera which indicated that cooling events in the middle Miocene and late Pliocene might be related to increases in the extent of polar glaciation. With the onset of widespread continental glaciation during the Pleistocene, the New England margin underwent considerable modification (Pratt and Schlee, 1969; Oldale and Uchupi, 1970; Lewis and Sylwester, in press; and others). The Gulf of Maine was actively eroded by ice and meltwater, and pre-existing fluvial drainage patterns were scoured. Ice may have reached the present shelf-break via Northeast and Great South channels, which acted as conduits for the seaward transport of sediments. Such transport explains both the large thickness of Pleistocene material sampled by U.S.G.S. hole 6013B at the shelf-break south of Great South Channel (Figure 21), and the filling of Tertiary submarine canyons on the Scotian Shelf east of Northeast Channel (Figure 5). Georges Bank was emergent and ice-free, but fluvial drainage along its northern and eastern parts created complex cut-and-fill structures which in some cases exposed Miocene sediments (Knott and Hoskins, 1968; Lewis and Sylwester, in press; and others; Figure 21).

During the Holocene transgression, reworking of glacial and periglacial sediments caused the winnowing of fine-grained material, leaving behind the sands

which compose the shoals now veneering Georges Bank and adjacent areas. Rising sea-level prevented the continued off-shelf transport of sediment, although some down-slope movement continues sporadically in the submarine canyons south of Georges Bank (Ryan et al., 1978). By 2000 yrs B.P., the New England passive continental margin had assumed virtually its present form (Oldale and O'Hara, 1978).

Summary

The geologic history of the New England margin has been traced by means of seismic reflection and refraction data supplemented by geologic information available from the North American and African continental margins.

That history can be briefly summarized as follows:

1. Permian to Triassic (270-195 my B.P.):

Intra-continental rifting in response to thermal uplift. The development of complex block-faulted terrain with little attendant extension of continental crust. Intra-rift clastic and evaporite deposition, with minor volcanism.

2. Latest Triassic to Earliest Jurassic (195-190

my B.P.): Initiation of sea-floor spreading, with actual continental separation occurring between the basement "hinge zone" on the shelf and the "east coast magnetic anomaly". Peak volcanic activity. Carving of the "K" or "break-up" unconformity.

3. Earliest Jurassic to Middle Jurassic (190-160

my B.P.): Rapid margin subsidence in response to cooling and/or dike injection. Establishment of fully marine conditions, with attendant deposition of first evaporites and later on platform and reef carbonates. Clastic deposition continues in proximal rift basins. Age of "Z"

horizon: 160 my B.P.

4. Middle Jurassic to latest Jurassic (160-136 my B.P.) Westward ridge jump at Blake Spur Anomaly time (175-160 my B.P.) with resultant uplift and widespread progradation of clastics across the inner margin. Ensuing subsidence produces transgression. Age of "4" horizon: 155-140 my B.P. (?). Age of "3" horizon: 136 my B.P.
5. Latest Jurassic-early Late Cretaceous (136-~95 my B.P.): Regression associated with the opening of the Bay of Biscay, 125 my B.P., and the separation of Europe and North America, 110-95 my B.P. Progradation of clastics with resultant cessation of shelf-edge reef growth, Georges Bank. Deposition of black clays on the continental rise. Georges Bank reef complex buried by clastics. Carving of the reflector "2" unconformity. Age of "2" horizon: approximately 95 my B.P.
6. Early Late Cretaceous-middle Late Cretaceous (~95-~75 my B.P.) Transgression, with deposition of shales, limestones, and chalks. Slow margin subsidence. Age of "X" horizon: approximately 75 my B.P.

7. Middle Late Cretaceous-Present (~75-0 my B.P.); Regression, with continuous progradation of clastics. Extensive shelf erosion during eustatic sea-level lows in the middle Oligocene and Plio-Pleistocene. Final reworking of surficial sediments during the Holocene marine transgression.

REFERENCES

- Ballard, R.D., and E. Uchupi, 1972, Carboniferous and Triassic rifting; a preliminary outline of the tectonic history of the Gulf of Maine: *Geol. Soc. America Bull.*, v. 83, p. 2285-2301.
-
- _____ 1974, Geology of Gulf of Maine: *AAPG Bull.*, v. 58, p. 1156-1158.
-
- _____ 1975, Triassic rift structure in Gulf of Maine: *AAPG Bull.*, p. 1041-1072.
- Bott, M.H.P., 1971, Evolution of young continental margins and formation of shelf basins: *Tectonophysics*, v. 11, p. 319-327.
- Burk, C.A., 1968, Buried ridges within continental margins: *New York Acad. Sci. Trans.*, ser. 2, v. 30, p. 397-409.
- Burke, K., 1976, Development of graben associated with the initial ruptures of the Atlantic Ocean: *Tectonophysics*, v. 36, p. 93-112.
- Cornet, B., and A. Traverse, 1975, Palynological contributions to the chronology and stratigraphy of the Hartford Basin in Connecticut and Massachusetts: *Geoscience and Man*, v. 11, p. 1-33.
- Cousminer, H.L., and W. Manspeizer, 1976, Triassic pollen date Moroccan High Atlas and the incipient rifting of Pangaea as middle Carnian: *Science*, v. 191, p. 943-945.

- deBoer, J., 1967, Paleomagnetic study of Mesozoic dike swarms in the Appalachians: *Jour. Geophys. Research*, v. 72, p. 2237-2250.
- _____ 1968, Paleomagnetic differentiation and correlation of the Late Triassic volcanic rocks in the central Appalachians (with special reference to the Connecticut Valley): *Geol. Soc. America Bull.*, v. 79, p. 609-626.
- Dewey, J.F., and J.M. Bird, 1970a, Plate tectonics and geosynclines: *Tectonophysics*, v. 10, p. 625-638.
- _____ 1970b, Mountain belts and the new global tectonics: *Jour. Geophys. Research*, v. 75, p. 2625-2647.
- Dietz, R.S., 1963, Collapsing continental rises: an actualistic concept of geosynclines and mountain building: *Jour. Geology*, v. 71, p. 314-333.
- _____ 1964, Origin of continental slopes: *Am. Scientist*, v. 52, p. 50-69.
- _____ 1972, Geosynclines, mountains and continent building: *Sci. American*, v. 226, p. 30-38.
- _____ and J.C. Holden, 1966, Miogeoclines (miogeosynclines) in space and time: *Jour. Geology*, v. 74, pt. 1, p. 566-583.
- _____ and J.C. Holden, 1974, Collapsing continental rises: actualistic concept of geosynclines - a review, in *Modern and ancient geosynclinal sedimentation*: *SEPM Spec. Pub.* 19, p. 14-25.

Dix, C.H., 1955, Seismic velocities from surface measurements: *Geophysics*, v. 20, p. 68-86.

Dobrin, M.O., 1976, Introduction to geophysical prospecting, 3rd ed: New York, McGraw-Hill, 630 p.

Drake, C.L., J.L. Worzel, and W.C. Beckman, 1954, Geophysical investigations in the emerged and submerged Atlantic coastal plain. Part IX, Gulf of Maine: *Geol. Soc. America Bull.*, v. 65, p. 957-970.

_____ M. Ewing, and G.H. Sutton, 1959, Continental margin and geosynclines: the east coast of North America, north of Cape Hatteras, in *Physics and Chemistry of the Earth*: London, Pergamon Press, v. 3, p. 110-198.

_____ J.R. Heirtzler, and J. Hirshman, 1963, Magnetic anomalies off eastern North America: *Jour. Geophys. Research*, v. 68, p. 5259-5275.

_____ J.I. Ewing, and H. Stockard, 1968, The continental margin of the eastern United States: *Canadian Jour. Earth Sci.*, v. 5, p. 993-1010.

Emery, K.O., and E. Uchupi, 1965, Structure of Georges Bank: *Marine Geology*, v. 3, p. 349-358.

_____ 1972, Western North Atlantic Ocean: Topography, rocks, structure, water, life, and sediments: *AAPG Mem.* 17, 532 p.

J. Phillips, C. Bowin, and

J. Mascle, 1974, The continental margin off western Africa: Angola to Sierra Leone: W.H.O.I. Ref. No. 74-99, 152 p.

E.T.

Bunce, and S.T. Knott, 1970, Continental rise off eastern North America: AAPG Bull., v. 54, p. 44-108.

Epp, D., P.J. Grim, and M.G. Langseth, Jr., 1970, Heat flow in the Caribbean and Gulf of Mexico: Jour. Geophys. Research, v. 75, p. 5655-5669.

Erickson, G.P., and J.L. Kulp, 1961, Potassium-argon dates on basaltic rocks: New York Acad. Sci. Annals, v. 91, p. 321-323.

Ewing, J.I., 1963, Elementary theory of seismic refraction and reflection measurements, in The sea, ideas and observations on progress in the study of the seas: New York, Interscience Publ., v. 3, p. 1-19.

Falvey, D.A., 1974, The development of continental margins in plate tectonic theory: The Australian Petroleum Exploration Assoc. Jour., v. 14, p. 95-106.

Folger, D.W., W.P. Dillon, J.A. Grow, K.D. Klitgord, and J.S. Schlee, in press, Evolution of the Atlantic continental margin of the United States: Am. Geophysical Union Maurice Ewing Series 2.

- Gardner, G.H.F., L.W. Gardner, and A.R. Gregory, 1974, Formation velocity and density - the diagnostic basics for stratigraphic traps: *Geophysics*, v. 39, p. 770-780.
- Given, M.M., 1977, Mesozoic and Early Cenozoic geology of offshore Nova Scotia: *Bull. Canadian Petroleum Geology*, v. 25, p. 63-91.
- Goldthwait, J.W., 1924, *Physiography of Nova Scotia*: Geol. Surv. of Canada Mem. 140, 179 p.
- Gradstein, F.M., G.L. Williams, W.A.M. Jenkins, and P. Ascoli, 1975, Mesozoic and Cenozoic stratigraphy of the Atlantic continental margin, eastern Canada, in *Canada's continental margins and offshore petroleum potential*: CSPG Mem. 4, p. 103-132.
- Grow, J.A., and J. Schlee, 1976, Interpretation and velocity analysis of U.S. Geological Survey multi-channel reflection profiles 4, 5, and 6, Atlantic continental margin: *U.S. Geol. Surv. Misc. Field Studies Map MF-808*.
- _____ and R.G. Markl, 1977, IPOD-USGS multichannel seismic reflection profile from Cape Hatteras to the Mid-Atlantic Ridge: *Geology*, v. 5, p. 625-630.
- _____ B.L. Jaworski, and C.A. Meeder, 1978, Sedimentary rock velocity trends across Georges Bank: *Geol. Soc. America Abs. with Programs*, v. 10, p. 45-46.

- _____ C.O. Bowin, D.R. Hutchinson, and K.M. Kent,
1976, Preliminary free-air gravity anomaly map along
the Atlantic continental margin between Virginia and
Georges Bank: U.S. Geol. Survey Misc. Field Studies
Map MF-795, scale: 1=1,200,000.
- Hailwood, E.A., and J.G. Mitchell, 1971, Paleomagnetic and
radiometric dating results from Jurassic intrusions in
South Morocco: *Geophys. Jour. Royal Astr. Soc.*, v. 24,
p. 351-364.
- Hamilton, E.L., 1956, Low sound velocities in high porosity
sediments: *Jour. Acoust. Soc. America*, v. 28, p. 16-
19.
- Haq, B.U., I. Premoli-Silva, and G.P. Lohmann, 1977,
Calcareous plankton paleobiogeographic evidence for
major climatic fluctuations in the early Cenozoic
Atlantic Ocean: *Jour. Geophys. Research*, v. 82,
p. 3861-3876.
- Hays, J.D., and W.C. Pitman, III., 1973, Lithospheric
plate motion, sea level changes and climatic and
ecological consequences: *Nature*, v. 246, p. 18-22.
- Hill, M.N., 1963, Single-ship seismic refraction shooting,
in *The sea, ideas and observations on progress in the
study of the seas*: New York, Interscience Publ.,
v. 3, p. 39-46.
- Hoskins, H., and S.T. Knott, 1961, Geophysical investiga-
tion of Cape Cod Bay, Massachusetts, using the

continuous seismic profiler: Jour. Geology, v. 69,
p. 330-339.

Howie, R.D., 1970, Oil and gas exploration - Atlantic
coast of Canada: AAPG Bull., v. 54, p. 1989-2006.

Hubert, J.F., A.A. Reed, and P.J. Carey, 1976, Paleo-
geography of the East Berlin Formation, Newark
Group, Connecticut Valley, Am. Jour. Sci., v. 276,
p. 1183-1207.

Ingle, J.C., Jr., 1977, Evidence of global late Paleo-
gene climatic and eustatic events and the Oligocene
hiatus, in The new uniformitarianism: events on a
Cenozoic scale, or, "What's so unusual about a
catastrophe?": Woods Hole Symposium no. 2, Woods
Hole Oceanographic Institution Graduate Education
Program, 3 p.

S.A. Graham, and W.R. Dickinson, 1976,
Evidence and implications of worldwide late Paleogene
climatic and eustatic events: Geol. Soc. America
Abs. with Programs, v. 8, p. 934-935.

Isacks, B., J. Oliver, and L.R. Sykes, 1968, Seismology
and the new global tectonics: Jour. Geophys.
Research, v. 73, p. 5855-5899.

Jansa, L.F., and J.A. Wade, 1975, Geology of the continent-
al margin off Nova Scotia and Newfoundland,

in Offshore geology of eastern Canada; v. 2,
Regional geology: Geol. Survey of Canada Paper
74-30, p. 51-105.

- _____ F.M. Gradstein, G.L. Williams, and W.A.M.
Jenkins, 1977, Geology of the Amoco Imp Skelly A-1
Osprey H-84 well, Grand Banks, Newfoundland:
Geol. Survey of Canada Paper 77-21, 17 p.
- Johnson, D.W., 1925, The New England - Acadian shoreline:
New York, John Wiley & Sons, Inc., 584 p.
- Kay, M., 1951, North American geosynclines: Geol.
Soc. America Mem. 48, 143 p.
- Keen, C.E., and M.J. Keen, 1974, The continental margins
of eastern Canada and Baffin Bay, in The geology
of continental margins: New York, Springer-Verlag,
p. 669-682.
- King, L.H., 1967a, Use of a conventional echo-sounder
and textural analyses in delineating sedimentary
facies, Scotian Shelf: Canadian Jour. Earth Sci.,
v. 4, p. 691-708.
- _____ 1967b, On the sediments and stratigraphy
of the Scotian Shelf: Geol. Assoc. Canada Spec.
Paper no. 4, p. 71-92.
- _____ 1975, Geosynclinal development on the con-
tinental margin south of Nova Scotia and Newfound-

land, in Offshore geology of eastern Canada; v. 2, Regional geology: Geol. Survey of Canada Paper 74-30, p. 199-206.

_____ and B. MacLean, 1976, Geology of the Scotian Shelf: Geol. Survey of Canada Paper 74-31, 31 p.

_____ and I.F. Young, 1977, Paleo-continental slopes of East Coast Geosyncline (Canadian Atlantic Margin): Canadian Jour. Earth Sci., v. 14, p. 2553-2564.

King, P.B., 1977, The evolution of North America: Princeton, Princeton University Press, 197 p.

Klitgord, K., and J.C. Behrendt, in press, Basin structure of the U.S. Atlantic continental margin, in Geological investigations of continental margins: AAPG Mem.

_____ and H. Schouten, 1977, The onset of sea-floor spreading from magnetic anomalies, in Symposium on the geological development of the New York Bight: Palisades, Lamont-Doherty Geol. Observatory, p. 12-13.

Knott, S.T., and H. Hoskins, 1968, Evidence of Pleistocene events in the structure of the continental shelf off northeastern United States: Marine Geology, v. 6, p. 5-43.

- _____ and H. Hoskins, 1975, Collection and analysis of seismic wide angle reflection and refraction data using radio sonobuoys: W.H.O.I. Ref. No. 75-33, 86 p.
- Kramer, F.S., R.A. Peterson, and W.C. Walter, eds., 1968, Seismic Energy Sources, 1968 Handbook: United Geophysical Corporation, 57 p.
- Leaton, B.R., 1976, International Geomagnetic Reference Field, IAGA Division I Study Group: EOS, v. 57, p. 120-121.
- LeBlanc, M., 1973, Le grand dyke de dolérite de l'Anti-Atlas et le magmatisme jurassique du Sud marocain: C.R. Acad. Sci. Paris, v. 276, ser. D, p. 2943-2946.
- LePichon, X., 1968, Sea-floor spreading and continental drift: Jour. Geophys. Research, v. 73, p. 3661-3697.
- _____ J.I. Ewing, and R.E. Houtz, 1968, Deep-sea sediment velocity determination made while reflection profiling: Jour. Geophys. Research, v. 73, p. 2597-2614.
- _____ J.C. Sibuet, and J. Francheteau, 1977, The fit of the continents around the North Atlantic Ocean: Tectonophysics, v. 38, p. 169-209.
- Lewis, R.S., and R.E. Sylwester, Shallow sedimentary framework of Georges Bank: in preparation.

Leyden, R., H. Asmus, S. Zembruski, and G. Bryan, 1976,
South Atlantic diapiric structures: AAPG Bull.,
v. 60, p. 196-212.

_____ J.E. Damuth, L.K. Ongley, J. Kostecki,
and W. Van Stevenick, 1978, Salt diapirs on São
Paulo Plateau, southeastern Brazilian continental
margin: AAPG Bull, v. 62, p. 657-666.

Lindholm, R.C., 1978, Triassic-Jurassic faulting in
eastern North America - A model based on pre-
Triassic structures: Geology, v. 6, p. 365-368.

Luyendyk, B.P., and E.T. Bunce, 1973, Geophysical study
of the northwest African margin off Morocco:
Deep-Sea Res., v. 20, p. 537-549.

MacIlvaine, J.C., 1973, Sedimentary processes on the
continental slope of New England: W.H.O.I. Ref.
No. 73-58, 211 p.

Maher, J.C., 1965, Correlations of subsurface Mesozoic
and Cenozoic rocks along the Atlantic coast:
AAPG, Cross Section Pub. 3, 18 p.

_____ and E.R. Applin, 1971, Geologic framework
and petroleum potential of the Atlantic Coastal
Plain and continental shelf: U.S. Geol. Survey
Prof. Paper 659, 98 p.

- Malloy, R.J., and R.N. Harbison, 1966, Marine geology of the northeastern Gulf of Maine: U.S. Coast and Geodetic Survey Tech. Bull., no. 28, 15 p.
- Manspeizer, W., J.H. Puffer, and H.L. Cousminer, 1978, Separation of Morocco and eastern North America: A Triassic-Liassic stratigraphic record: Geol. Soc. America Bull., v. 89, p. 901-920.
- Mattick, R.E., R.Q. Foote, N.L. Weaver, and M.S. Grim, 1974, Structural framework of United States Atlantic outer continental shelf north of Cape Hatteras: AAPG Bull., v. 58, p. 1179-1190.
- _____ O.W. Girard, Jr., P.A. Scholle, and J.A. Grow, 1978, Petroleum potential of U.S. Atlantic slope, rise, and abyssal plain: AAPG Bull., v. 62, p. 592-608.
- Mayhew, M.A., 1974, "Basement" to east coast continental margin of North America: AAPG Bull., v. 58, p. 1069-1088.
- Mayne, W.H., 1962, Common reflection point horizontal data stacking techniques: Geophysics, v. 27, p. 927-938.
- McDonal, F.J., F.A. Angona, R.L. Mills, R.L. Sengbush, R.G. van Nostrand, and J.E. White, 1958, Attenuation of shear and compressional waves in Pierre Shale: Geophysics, v. 23, p. 421-439.

- McHone, J.G., 1978, Distribution, orientations, and age of mafic dikes in central New England: *Geol. Soc. America Bull.*, v. 89, p. 1645-1655.
- McIver, N.L., 1972, Cenozoic and Mesozoic stratigraphy of the Nova Scotia Shelf: *Canadian Jour. Earth Sci.*, v. 9, p. 54-70.
- McKenzie, D., 1978, Some remarks on the development of sedimentary basins: *Earth and Planetary Sci. Letters*, v. 40, p. 25-32.
- McMaster, R.L., 1971, A transverse fault on the continental shelf off Rhode Island: *Geol. Soc. America Bull.*, v. 82, p. 2001-2004.
- Minard, J.P., W.J. Perry, E.G.A. Weed, E.C. Rhodehamel, E.I. Robbins, and R.B. Mixon, 1974, Preliminary report on geology along Atlantic continental margin of northeastern United States: *AAPG Bull.*, v. 58, p. 1169-1178.
- Mitchell, A.H., and H.G. Reading, 1969, Continental margins, geosynclines, and ocean floor spreading: *Jour. Geology*, v. 77, p. 629-646.
- Nafe, J.E., and C.L. Drake, 1957, Variation with depth in shallow water and deep water marine sediments of porosity, density, and the velocities of compressional and shear waves: *Geophysics*, v. 22, p. 523-552.

Officer, C.B., and M. Ewing, 1954, Geophysical investigations in the emerged and submerged Atlantic Coastal Plain Pt. VII: Continental shelf, continental slope, and continental rise south of Nova Scotia: Geol. Soc. America Bull., v. 65, p. 653-670.

Oldale, R.N., and C.J. O'Hara, 1978, New radiocarbon dates from the inner continental shelf off southeastern Massachusetts and a local sea-level rise curve for the last 12,500 years, in A marine geology symposium dedicated to K.O. Emery by his colleagues and former students: Woods Hole, Woods Hole Oceanographic Institution, 4 p.

_____ and E. Uchupi, 1970, The glaciated shelf off northeastern United States: U.S. Geol. Survey Prof. Paper 700-B, p. B167-B173.

_____ and K.E. Prada, 1973, Sedimentary framework of the western Gulf of Maine and the southeastern Massachusetts offshore area: U.S. Geol. Survey Prof. Paper 757, 10 p.

_____ J.D. Hathaway, W.P. Dillon, J.D. Henricks, and J.M. Robb, 1974, Geophysical observations on northern part of Georges Bank and adjacent basins of Gulf of Maine: AAPG Bull., v. 58, p. 2411-2427.

- Peacock, K.L., and S. Treitel, 1969, Predictive deconvolution: theory and practice: *Geophysics*, v. 34, p. 155-169.
- Pegrum, R.M., and N. Mounteney, 1978, Rift basins flanking North Atlantic Ocean and their relation to North Sea area: *AAPG Bull.*, v. 62, p. 419-441.
- Perry, W.J., Jr., J.P. Minard, E.G.A. Weed, E.I. Robbins, and E.C. Rhodehamel, 1975, Stratigraphy of Atlantic coastal margin of United States north of Cape Hatteras: *AAPG Bull.*, v. 59, p. 1529-1548.
- Pratt, R.M., and J. Schlee, 1969, Glaciation on the continental margin off New England: *Geol. Soc. America Bull.*, v. 80, p. 2335-2341.
- Press, F., 1966, Seismic velocities, in *Handbook of physical constants*: *Geol. Soc. America Mem.* 97, p. 195-218.
- Reesman, R.H., C.R. Filbert, and H.W. Krueger, 1973, Potassium-argon dating of the Upper Triassic lavas of the Connecticut Valley, New England: *Geol. Soc. America Abs. with Programs*, v. 5, p. 211.
- Renz, O., R. Imlay, Y. Lancelot, and W.B.F. Ryan, 1975, Ammonite-rich Oxfordian limestones from the base of the continental slope off northwest Africa: *Eclogae geol. Helv.*, v. 68, p. 431-448.

- Robinson, E.A., 1967, Multichannel time series analysis with digital computer programs: San Francisco, Holden-Day.
- Royden, L., J.G. Sclater, and R.P. Von Herzen, in press, Continental margin subsidence and heat flow: important parameters in formation of petroleum hydrocarbons: Jour. Geophys. Research.
- Ryan, W.B.F., M.B. Cita, E.L. Miller, D. Hanselman, W.D. Nesteroff, B. Hecker, and M. Nibbelink, 1978, Bedrock geology in New England submarine canyons: Oceanologica Acta, v. 1, p. 233-254.
- Sanders, J.E., 1963, Late Triassic tectonic history of the northeastern United States: Am. Jour. Sci., v. 261, p. 501-524.
- Savin, S.M., R.G. Douglas, and F.G. Stehli, 1975, Tertiary Marine paleotemperatures: Geol. Soc. America Bull., v. 86, p. 1499-1510.
- Schlee, J.S., R.G. Martin, R.E. Mattick, W.P. Dillon, and M.M. Ball, 1977, Petroleum geology on the United States Atlantic-Gulf of Mexico margins, in Exploration and Economics of the Petroleum Industry, v. 15, p. 47-93.
-
- J.C. Behrendt, J.A. Grow, J.M. Robb, R.E. Mattick, P.T. Taylor, and B.J. Lawson, 1976, Regional geologic framework off northeastern United States: AAPG Bull., v. 60, p. 926-951.

- Schouten, H., and K.D. Klitgord, 1977, Mesozoic magnetic anomalies, western North Atlantic: U.S. Geol. Surv. Misc. Field Studies Map MF-915, Scale: 1:2,000,000.
- Schultz, L.K., and R.L. Grover, 1974. Geology of Georges Bank Basin: AAPG Bull., v. 58, p. 1159-1168.
- Sclater, J.G., S. Hellinger, and C. Tapscott, 1977, The paleobathymetry of the Atlantic Ocean from the Jurassic to the present: Jour. Geology, v. 85, p. 509-552.
- Scrutton, R.A., 1973, The age relationship of igneous activity and continental break-up: Geol. Mag., v. 110, p. 227-234.
- Sheriff, R.E., 1973, Encyclopedic dictionary of exploration geophysics: Tulsa, The Society of Exploration Geophysicists, 266 p.
- _____ 1976, Inferring stratigraphy from seismic data: AAPG Bull., v. 60, p. 528-542.
- Sleep, N.H., 1971, Thermal effects of the formation of Atlantic continental margins by continental break-up: Geophys. Jour. Royal Astr. Soc., v. 24, p. 325-350.
- Steckler, M.S., and A.B. Watts, 1978, Subsidence of the Atlantic-type margin off New York: Earth Planet. Sci. Letters, v. 41, p. 1-13.

Taner, M.T., and F. Koehler, 1969, Velocity spectra - digital computer derivation and applications of velocity functions: *Geophysics*, v. 34, p. 859-881.

E.E. Cook, and N.S. Neidell, 1970, Limitations of the reflection seismic method; lessons from computer simulations: *Geophysics*, v. 35, p. 551-573.

Toksöz, M.N., C.H. Cheng, and A. Timur, 1976, Velocities of seismic waves in porous rocks: *Geophysics*, v. 41, p. 621-645.

Tucholke, B.E., and G. Mountain, 1977, The Horizon-A complex: lithostratigraphic correlation and paleo-oceanographic significance of reflectors in the western North Atlantic: *EOS*, v. 58, p. 406.

_____ and P.R. Vogt, in press, Western North Atlantic: Sedimentary evolution and aspects of tectonic history, in Initial Reports of the Deep Sea Drilling Project: Washington, D.C., U.S. Government Printing Office.

_____ R.N. Oldale, and C.D. Hollister, 1972, A 3.5 kHz acoustic penetration map of the Jeffreys Ledge quadrangle: U.S. Geol. Survey Misc. Geol. Inv. I-716, scale: 1: 260,000.

- Uchupi, E., 1965, Basins of the Gulf of Maine: U.S. Geol. Survey Prof. Paper 525-D, p. 175-177.
- _____ 1966, Structural framework of the Gulf of Maine: Jour. Geophys. Research, v. 71, p. 3013-3028.
- _____ 1970, Atlantic continental shelf and slope of the United States: shallow structure: U.S. Geol. Survey Prof. Paper 529-I, 44 p.
- _____ and J.A. Austin, Jr., in press, The geologic history of the passive margin off New England and the Canadian Maritime Provinces: Tectonophysics.
- _____ R.D. Ballard, and J.P. Ellis, 1977, Continental slope and upper rise off western Nova Scotia and Georges Bank: AAPG Bull., v. 61, p. 1483-1492.
- Ulrych, T.J., 1971, Application of homomorphic deconvolution to seismology: Geophysics, v. 36, p. 650-660.
- Vail, P.R., R.M. Mitchum, Jr., and S. Thompson, III., 1977, Seismic stratigraphy and global changes of sea level, part 4: Global cycles of relative changes in sea level, in Seismic stratigraphy - applications to hydrocarbon exploration: AAPG Mem. 26, p. 83-97.

- Walcott, R.I., 1972, Gravity, flexure, and the growth of sedimentary basins at a continental edge: Geol. Soc. America Bull., v. 83, p. 1845-1848.
- Walton, H.S., and A.A. Berti, 1976, Upper Triassic and Lower Jurassic palynology of the Grand Banks area: Am. Assoc. Stratigraphic Palynologists and Commission Internat. Microflore du Paléozoïque Abs. with Program, p. 27-28.
- Watkins, J.S., and W.H. Geddes, 1965, Magnetic anomaly and possible orogenic significance of geological structure of the Atlantic Shelf: Jour. Geophys. Research, v. 70, p. 1357-1361.
- Watts, A.B., and W.B.F. Ryan, 1976, Flexure of the lithosphere and continental margin basins: Tectonophysics, v. 36, p. 25-44.
- Weed, E.G.A., J.P. Minard, W.J. Perry, Jr., E.C. Rhodehamel, and E.I. Robbins, 1974, Generalized pre-Pleistocene geologic map of the northern United States Atlantic continental margin: U.S. Geol. Surv. Misc. Geol. Inv. Series Map I-861, Scale: 1:1,000,000.
- Wilson, J.T., 1966, Did the Atlantic close and then reopen?: Nature, v. 211, p. 676-681.
- Woods, L.C., and S. Treitel, 1975, Seismic signal processing: IEEE Proceedings, v. 63, p. 649-661.

Zbyszewski, G., and J.B. de Faria, 1971, O sal-gema em Portugal metropolitano sus jazidas, caracteristicas e aproveitamento: Portugal Serv. Fom. Mineiro, Estud., Notas Trab., v. 20, p. 5-105.

APPENDIX I

Data Analyses: Laboratory Methods, Seismic Reflection
Multi-Channel Seismic Reflection Processing

The purpose of the "common-reflection-point" or "common-depth-point" (CDP) technique is to increase signal-to-noise ratios by combining travel-time data from a single sub-surface reflection point acquired using a multiplicity of source/receiver locations (Mayne, 1962). All of the AII-91 seismic profiles were collected with the system shown in Figure 2. Shots were generally fired every 18 sec at tow speeds of approximately 4.0 knots, allowing for an interval between shots of 37.5 m. In order to provide an elevated signal-to-noise ratio (roughly 2.45/1) without overstepping the system's ability to resolve rapid lateral variations in geology, 6-fold "multiplicity" [a term defined by Mayne (1962) as the number of travel paths with a common reflection point] was decided upon. Every two successive shots were numerically combined, yielding an effective time-average over 0.5 the channel-spacing of the array (75 m). Then, according to Mayne's (1962) formula for multiplicity, M:

$M = NS/2n$, where M = path multiplicity (6)

N = number of array channels (6)

S = number of shot positions
for each array configuration
(1)

n = number of channel spacings
by which the array is advanced/
shot (0.5)

$$M = (6)(1)/2(0.5) = 6$$

Most of the CDP processing of the profiles was carried out ashore. A brief synopsis of the procedures used is given below:

1) Single-channel Profiles

The first step in data handling is the production of single-channel normal-incidence profiles. Even though sub-bottom resolution on many parts of the shelf is severely limited by water multiple interference, these profiles are useful for the following reasons:

a) They are generated in real time aboard ship, allowing quick evaluation of the upper part of the section. Such an evaluation aids in selecting points for subsequent velocity analyses (see below).

b) In parts of the study area either blanketed by a thin veneer of sediment (i.e. the Gulf of Maine) or in deep water, subsequent processing is unnecessary and an interpretation of the data can be made immediately (Uchupi et al., 1977).

2) Deconvolution

In simplest terms, deconvolution is the process by which the various filtering effects of the earth are removed, thereby enhancing the resolution of reflection events. General reviews of this process have been published by Robinson (1967), Peacock and Treitel (1969), Ulrych (1971), Wood and Treitel (1975), and Dobrin (1976, p. 186-192), and new procedures are still being developed (P. Stoffa, personal communication). Various types of deconvolution are possible, depending upon the data set and the desired result (Sheriff, 1973). One of the types most commonly used is called "dereverberation", whereby the ringing effects of the water column are removed using knowledge both of the depth of water and the nature of the source signature. On all of the shelf profiles collected during AII-91, dereverberation was carried out.

3) Normal-move-out (NMO) corrections

Woods and Treitel (1975, p. 652) define NMO as "the increase in reflection time due to an increase in distance from source to receiver for a horizontal reflecting interface in a homogeneous medium of constant velocity". They provide the following expression for an NMO time-correction:

$$\Delta T_{\text{NMO}} = T_x - T_o = \frac{1}{v} (4z^2 + x^2)^{1/2} - T_o$$

ΔT_{NMO} = NMO time-correction

T_x = Two-way reflection time for a trace of offset distance X

T_o = Two-way reflection time for the zero-offset (normal incidence) trace

v = velocity of the medium

z = depth to the reflecting horizon

x = source-receiver separation, or offset distance

NMO corrections help to align reflections prior to final summing of the traces by systematically compensating for changes in X, source-receiver separation. In order to apply these corrections properly, velocities must be determined as a function of reflection time.

4) Velocity Analysis

Enhancement of the deconvolved single-channel returns is both possible and desirable. First, the six pieces of data from each common reflection point are corrected for NMO (at more than one rms velocity, see below) and summed, thereby increasing signal-to-noise ratios and allowing more reliable identification of primary (geologically produced) reflections. Second, if the geology of the subsurface under consideration does not seriously violate the following assumptions:

- a) a finite number of horizontal or near-horizontal layers separated by plane interfaces, and
- b) each layer composed of a homogeneous medium of constant compressional wave velocity, then the rms ("root-mean-square") velocities characterizing that geology can be closely approximated by using the following equation:

$$T_{X,N}^2 = T_{O,N}^2 + \frac{X^2}{V_{rms}^2} + \dots \text{(Taner and Koehler, 1969)}$$

X = offset distance (or the distance between source and receiver)

N = number of layers overlying the reflecting interface

$T_{O,N}$ = two-way travel time to the bottom of the Nth layer for the normal incidence trace (for which X=0)

$T_{X,N}$ = two-way travel time to the bottom of the Nth layer for an obliquely incident trace (for which the X values are non-zero but known)

V_{rms} = rms velocity to the bottom of the Nth layer

Velocity analyses were normally conducted at approximately 30-minute intervals, but occasionally more often in regions of complex geology.

After all of these procedures have been completed, final compositing of the traces results in a CDP "stack". If the velocity analyses and NMO corrections are accurate, primary reflections will be enhanced while multiples

will be attenuated. Figures 4A and 4B are examples of stacked profiles. Beneath Georges Bank, coherent returns from as deep as 4.0 sec (two-way travel-time) can be discerned.

Calculation of Interval Velocities

Interval velocities (the average velocity between two flat, parallel interfaces) can be calculated from the rms velocities by using the following equation:

$$V_{int,N}^2 = \frac{V_{rms,N}^2 T_{0,N} - V_{rms,N-1}^2 T_{0,N-1}}{T_{0,N} - T_{0,N-1}} \quad (\text{Dix, 1955})$$

$V_{rms,N}$ = rms velocity to the bottom of the Nth layer

$V_{rms,N-1}$ = rms velocity to the top of the Nth layer

$T_{0,N}$ = two-way travel time to the bottom of the Nth layer for the zero offset or normal incidence trace

$T_{0,N-1}$ = two-way travel time to the top of the top of the Nth layer for the zero offset or normal incidence trace

$V_{int,N}$ = interval velocity for the Nth layer

If the geologic assumptions are reasonably valid, interval velocities should aid in the geologic interpretation of multi-channel reflection data. However, the Dix formula is insensitive to very thin layers (where $T_{0,N} - T_{0,N-1}$ is very small). Consequently, interval velocities derived for these layers must be used with caution.

Interval velocities were calculated at more than 200 points on the New England margin using both the CDP and sonobuoy velocity data (Appendix II). These calculations are summarized in Appendix III.

Figure 33 is a flow chart describing in detail the sequence of multi-channel seismic reflection processing procedures.

Figure 33. Flow chart describing multi-channel seismic reflection processing procedures. Courtesy D.R. Shaughnessy, Woods Hole Oceanographic Institution.

APPENDIX II

Data Analyses: Laboratory Methods, Seismic Refraction
Sonobuoy Processing

The practice of using expendable radio sonobuoys in the collection of seismic refraction data was developed in the 1940's and 50's and summarized by Hill (1963). All of the refraction information was collected and stored on magnetic tape for subsequent processing.

The basic theory behind seismic refraction and oblique seismic reflection measurements has been clearly summarized by Ewing (1963). Because no theoretical advances or equipment modifications were made during this study, the voluminous literature available on this subject will not be reviewed here. Methods of sonobuoy data reduction developed at Woods Hole by Knott and Hoskins (1975) were employed to assign compressional wave velocities to measured travel-time sections. The ultimate goal was to relate the acoustic stratigraphy of the New England continental margin to its actual stratigraphy by using the velocities as general indicators of lithology. Figures 34 and 35 are representative examples of actual sonobuoy profiles and their interpretation for the continental shelf and continental rise, respectively. Three buoys (#24, #26, and #51; see Figure 1) were run on the continental

Figure 34. A representative sonobuoy profile collected during AII-91 over the continental shelf. This is sonobuoy 36, taken near the Shell Mohawk B-93 well-site on the Scotian Shelf (see Figure 3). Only refractions are discernible.

A. Actual record of the refracted arrivals.

The direct wave is not visible on this profile, filtered at 0-20 Hz.

B. A line interpretation of the record on a time-distance plot. The results of the analysis (see the discussion in the text) are as follows:

<u>Velocity, Km/sec</u>	<u>Depth to refracting horizon</u>		
	<u>Seconds</u> (2-way travel-time)	<u>Kilometers</u>	
G ₁	1.82	0.16	.075
G ₂	3.07	1.06	.951
G ₃	4.33	1.57	1.728
G ₄	5.12	1.99	2.638
G ₅	5.92	2.36	3.589

Slope corrections were not made on this profile.

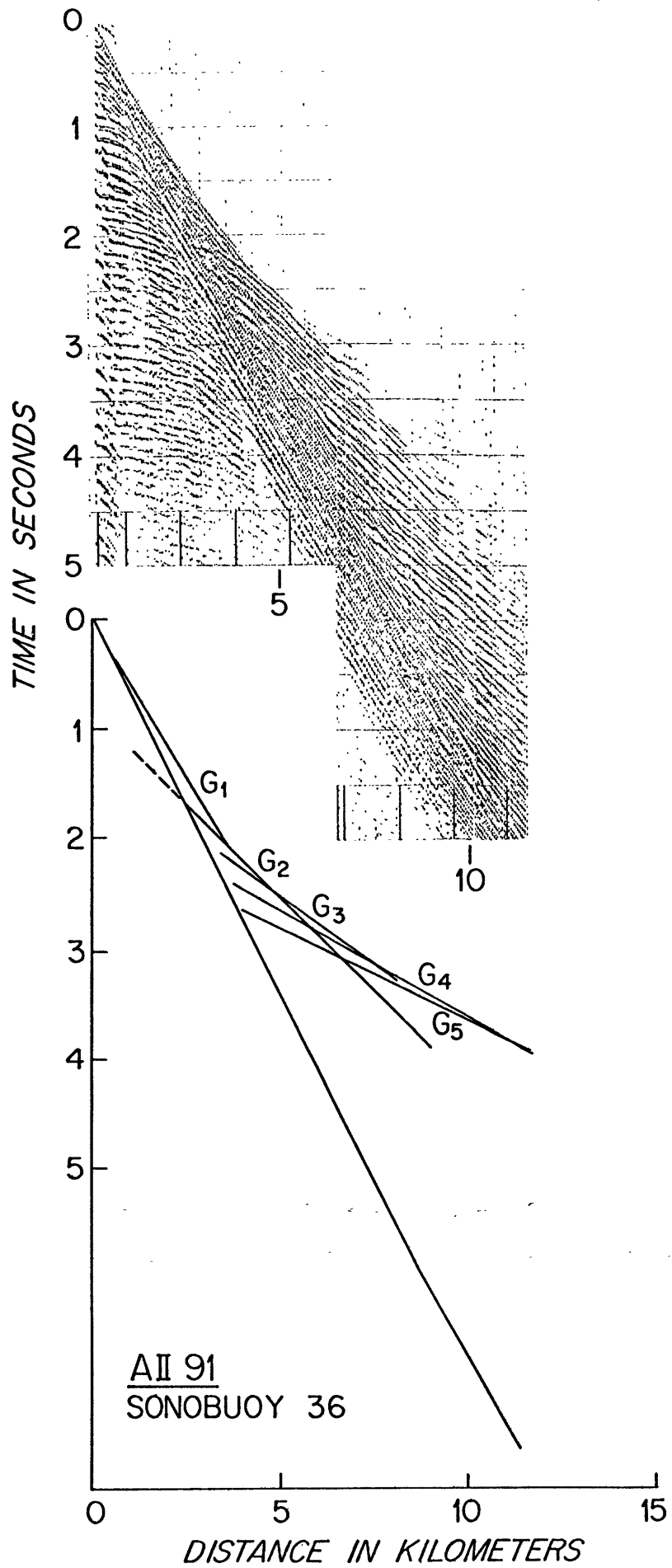


Figure 35. A representative sonobuoy profile collected during AII-91 over the upper continental rise. This is sonobuoy 1, taken on the rise southwest of Georges Bank (see Figure 1). Both oblique reflection and refraction arrivals are discernible.

- A. Actual record of arrivals. The direct wave is visible on this profile, filtered at 0-30 Hz. Also shown is a short segment of single-channel normal-incidence profile collected just prior to buoy launch in order to aid in the correlation of reflecting horizons.
- B. A line interpretation of the record on a time-distance plot. The results of the analysis (see the discussion in the text) are as follows:

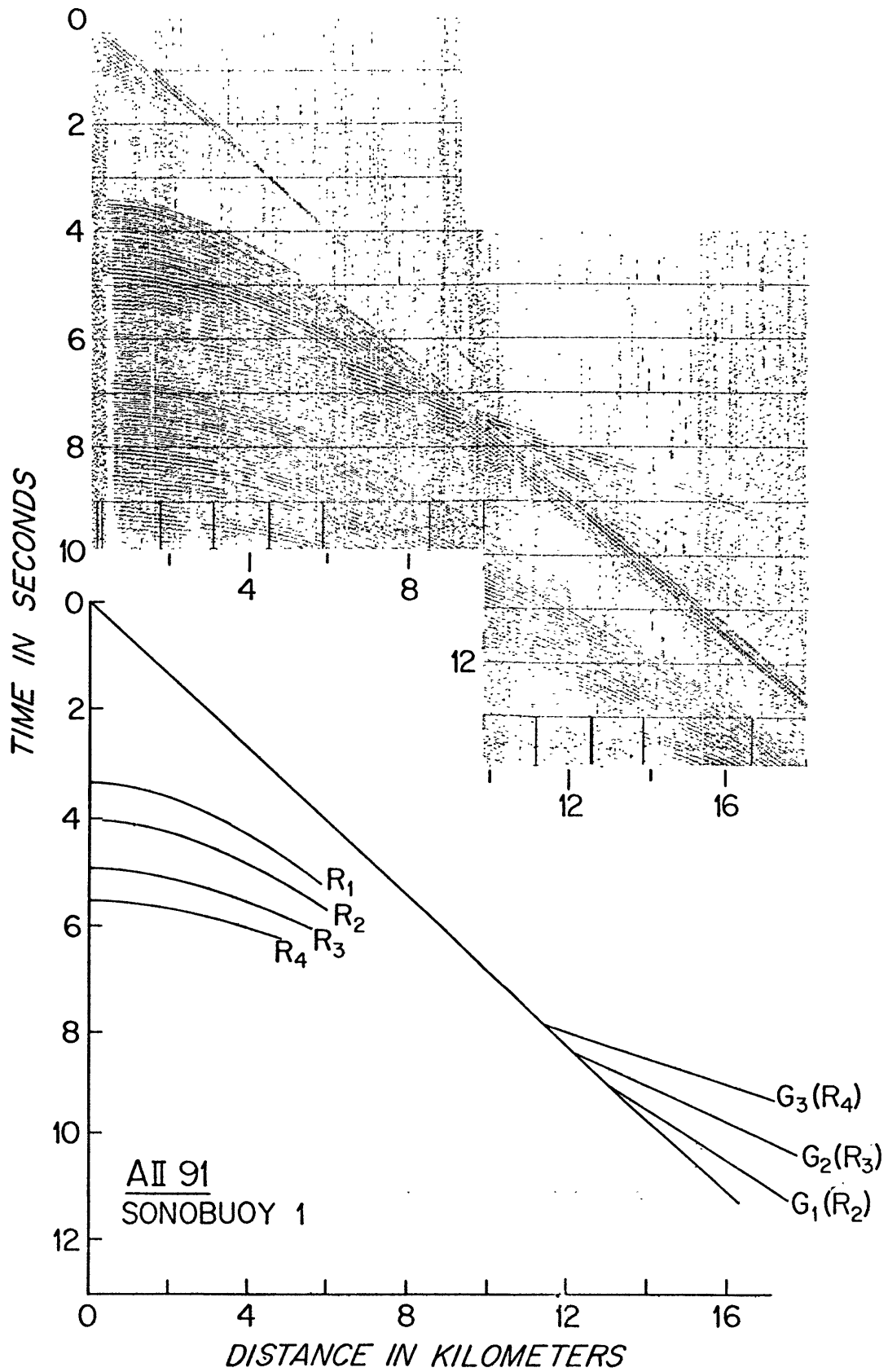
Oblique Reflections

	Interval velocity, km/sec	Layer thickness		Depth to layer base		Dip, degree
		Seconds (two-way travel- time)	Kilo- meters	Seconds (two-way travel- time)	Kilometers	
R ₁ (water)	1.48±.01	3.40	2.52	3.40	2.52	0
R ₂	1.59±.08	0.68	0.54	4.08	3.06	0
R ₃	1.94±.10	0.90	0.87	4.97	3.93	0
R ₄	2.20±.60	0.59	0.65	5.56	4.58	0

Refractions

	Interval velocity, km/sec	Depth to refracting horizon	
		Seconds (two-way travel-time)	Kilometers
G ₁ (R ₂)	2.15	3.98	2.98
G ₂ (R ₄)	2.95	5.07	4.16
G ₃ (below R ₄)	4.04	5.56	4.87

7



slope, but rugged topography and complicated structure along the line of the profiles rendered the results of little value.

On the shelf profiles (Figure 1), only refracted arrivals were considered, as no primary reflections could be distinguished due to multiple interference (Figure 34A). All of the shallow-water runs were bandpass filtered either at 0-20 Hz to bring out refractions or at 600-1200 Hz to enhance direct-wave arrivals. Some playbacks from magnetic tape were made at sea, but the majority were carried out ashore. Time-distance graphs of both direct (D) and refracted (G_1 , G_2 , etc.) arrivals were plotted (Figure 34B), and X-Y measurements made on each trace (usually a minimum of five points/refraction). Then, these time-distance data were fed to a computer program (LINFT, Knott and Hoskins, 1975) which computed a velocity for each refracted arrival. Given an estimate of the average velocity above the shallowest refractor (which was usually a water velocity, as the shallowest refractor most often approximated the sediment-water interface), this program could also calculate the travel-time and depth to each refracting horizon (Figure 34B).

Refraction velocity determinations are known to

be quite sensitive to bottom and sub-bottom slopes (Ewing, 1963; Knott and Hoskins, 1975). In order to compensate for such slopes, sonobuoy profiles are usually reversed (run end-to-end in both directions along the same track). This was not done during AII-91, but the refraction velocities calculated for the shelf and rise are considered valid because of the generally low slopes (less than 1°) encountered.

On the rise, both oblique reflection and refraction returns could be traced (Figure 35A). Filter settings were occasionally set as high as 50 Hz to pick up oblique reflections during playbacks ashore. In the same manner as for the shelf profiles, time-distance graphs were constructed (Figure 35B). Hyperbolic approximations of the interpreted reflection arrivals (R_1 , R_2 , etc.) were made and sampled (a minimum of seven times/hyperbola). These points were fed to another computer program (SLOWI, Knott and Hoskins, 1975) which employed a reduced travel-time technique developed by LePichon et al. (1968) to calculate interval velocities, layer thicknesses and depths, and regional dips of reflection interfaces given an initial approximation of these dips estimated from concurrent normal incidence reflection profiles (Figure 35B).

Figures 36-38 tabulate the results of the AII-91 sonobuoy data analyses.

Figure 36. AII-91 sonobuoy results, continental shelf:

- A. LaHave Platform
- B. Gulf of Maine
- C. Georges Bank
- D. Long Island Platform

For locations of profiles, refer to Figure 1.

Sonobuoy Results: LaHave Platform

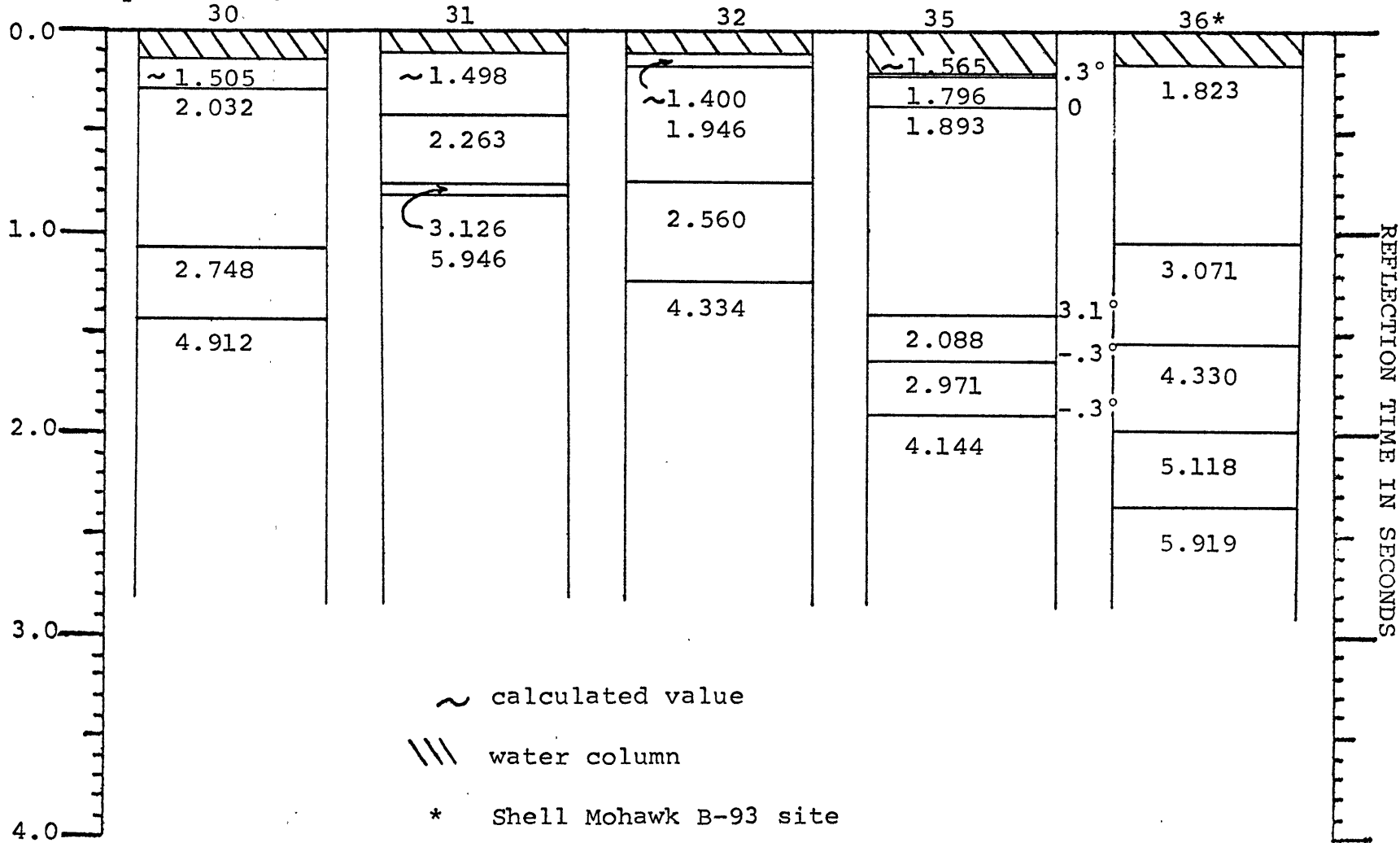


Figure 36A.

Quoted slopes are incremental (see Knott and Hoskins, 1975).
 Numbers are refraction velocities in km/sec.

Sonobuoy Results: LaHave Platform (cont.)

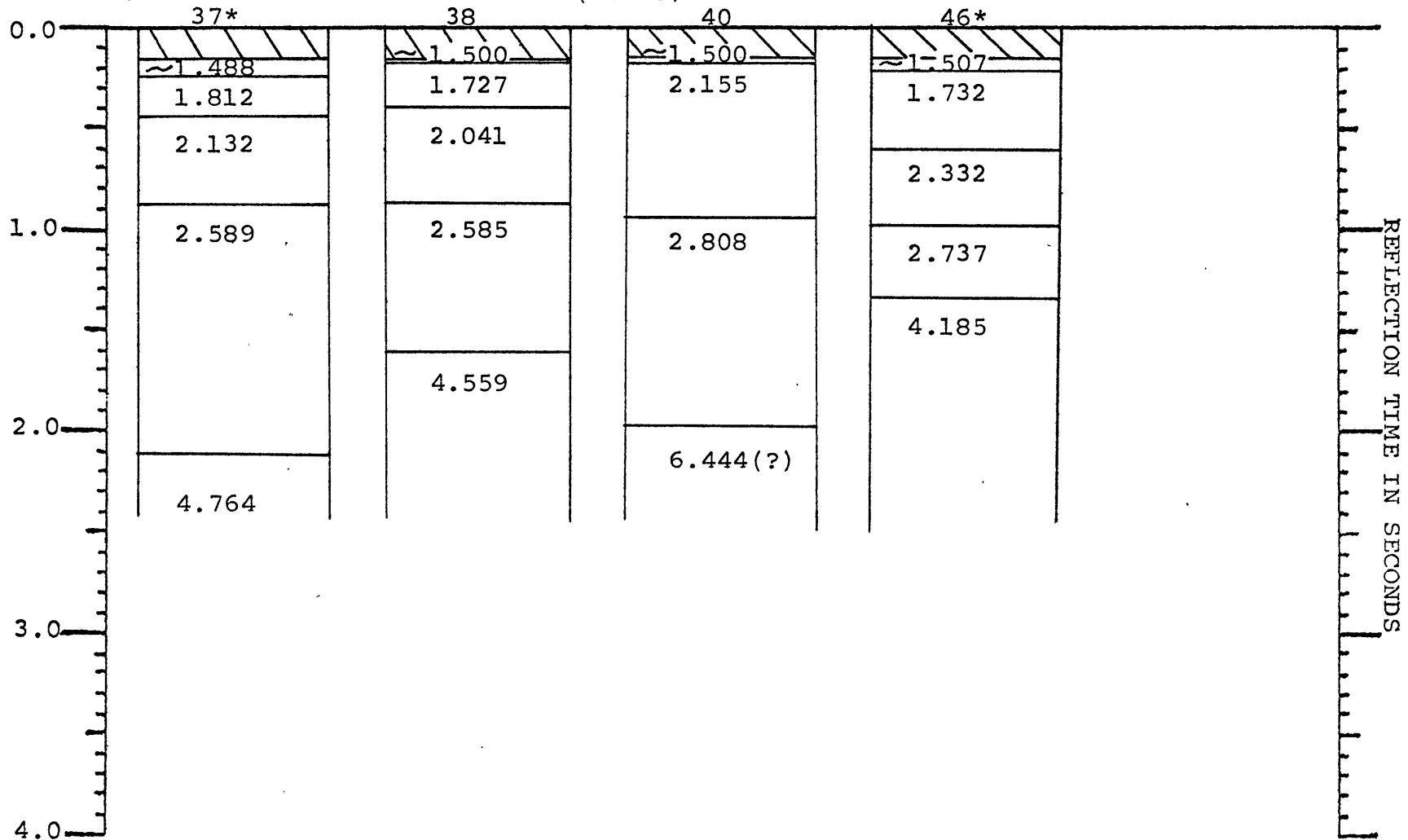


Figure 36A. (cont.)

Sonobuoy Results: Gulf of Maine

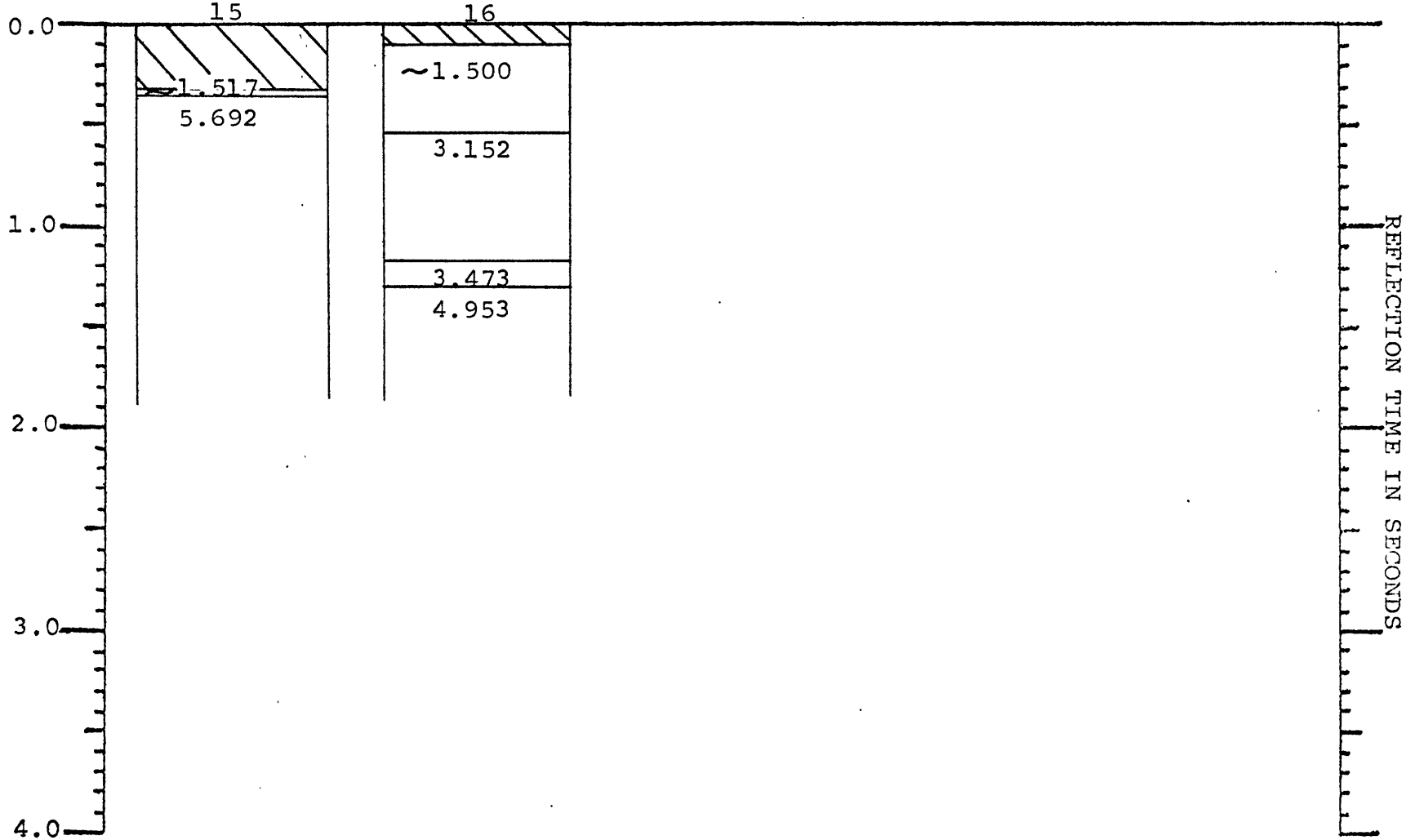


Figure 36B.

Sonobuoy Results: Georges Bank

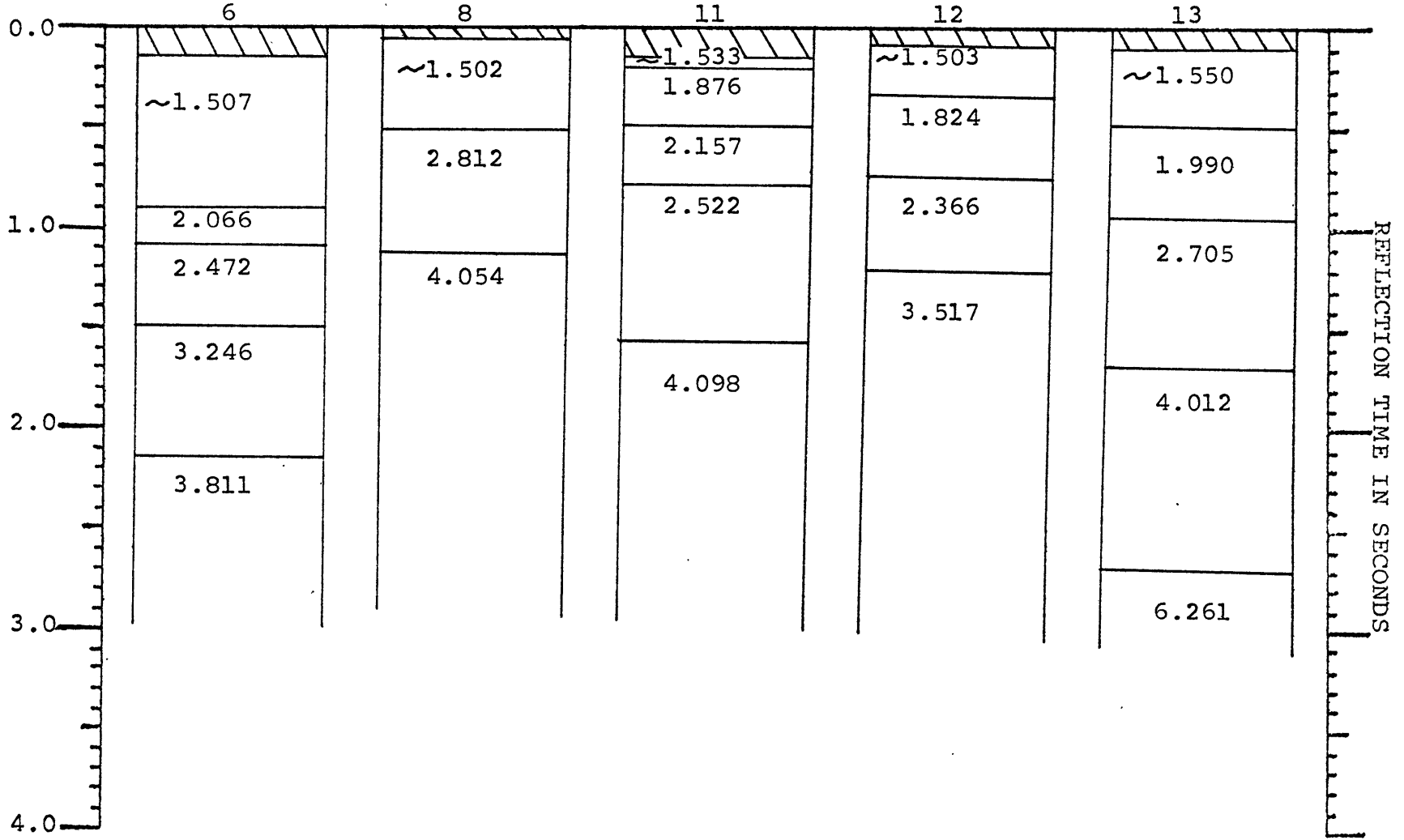


Figure 36C.

Sonobuoy Results: Georges Bank (cont.)

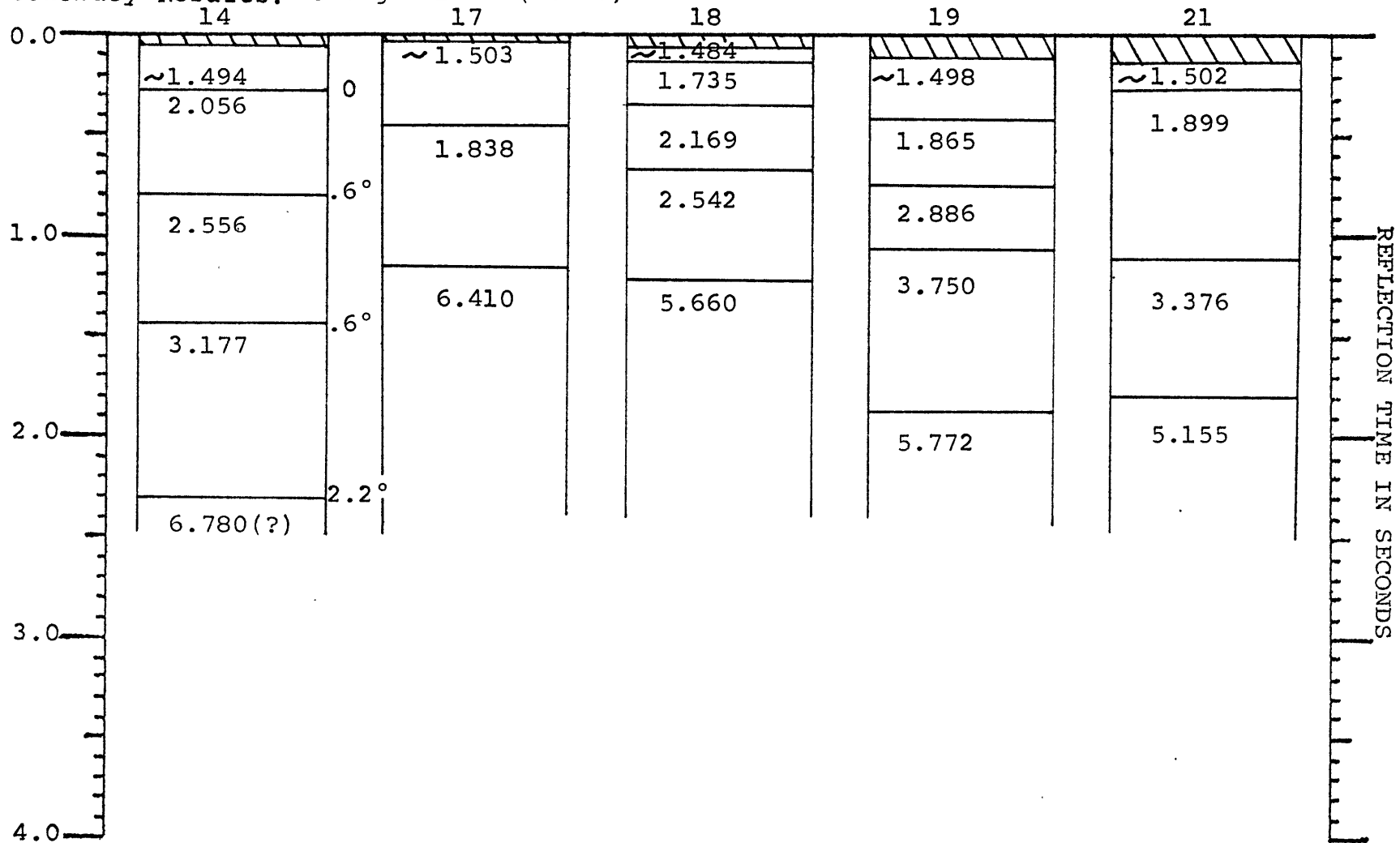


Figure 36C. (cont.)

Sonobuoy Results: Georges Bank (cont.)

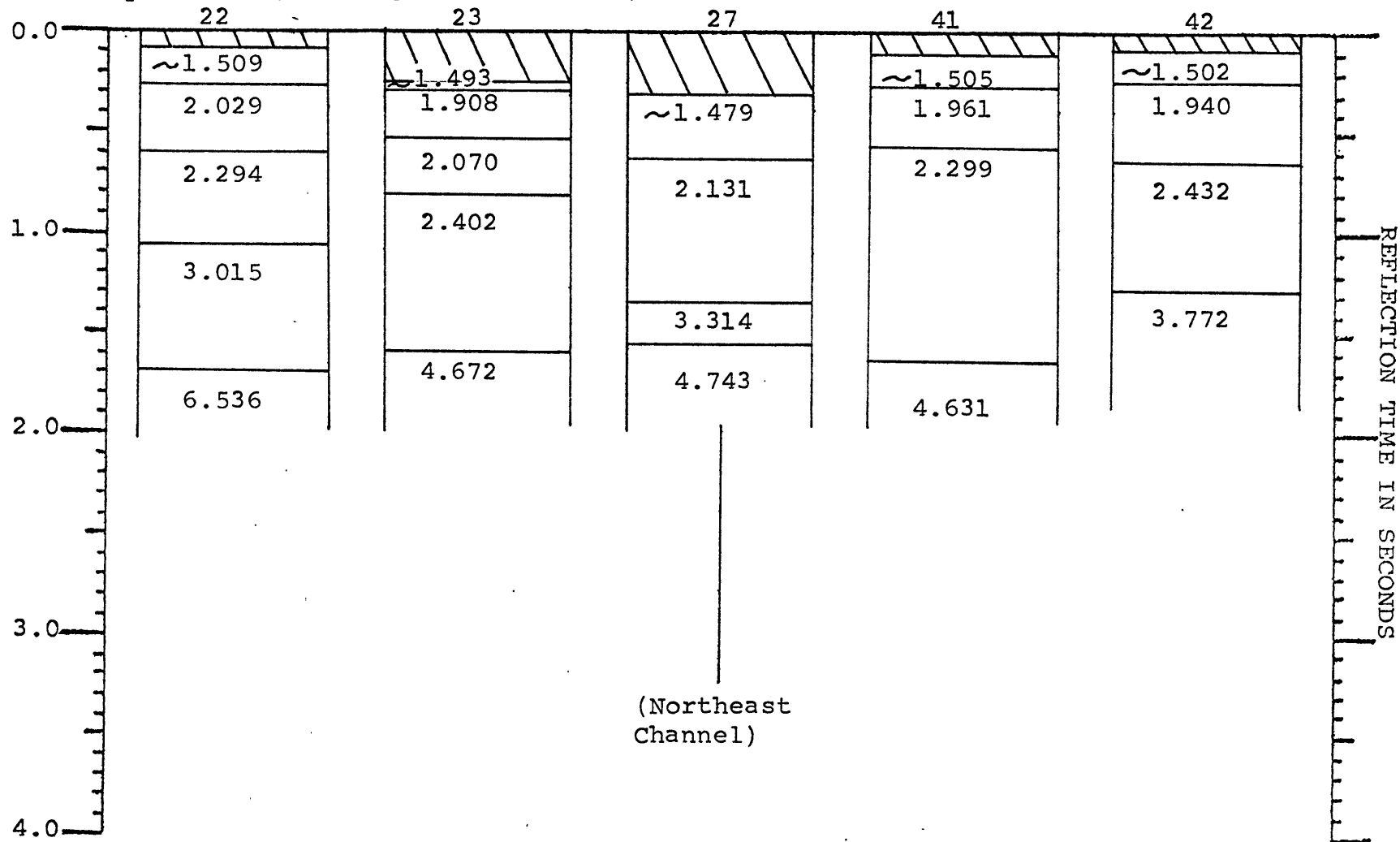


Figure 36C. (cont.)

Sonobuoy Results: Georges Bank (cont.)

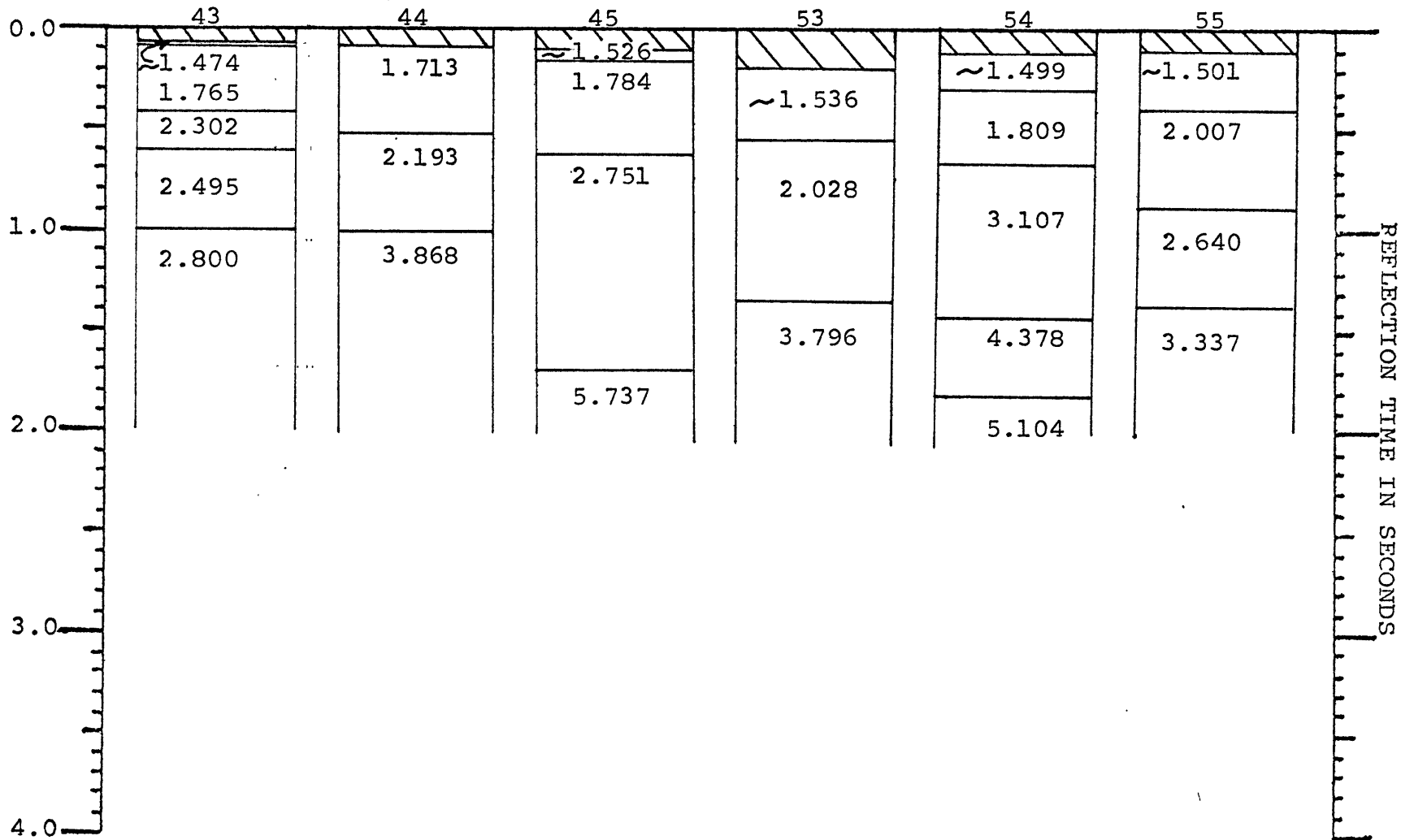


Figure 36C. (cont.)

Sonobuoy Results: Long Island Platform

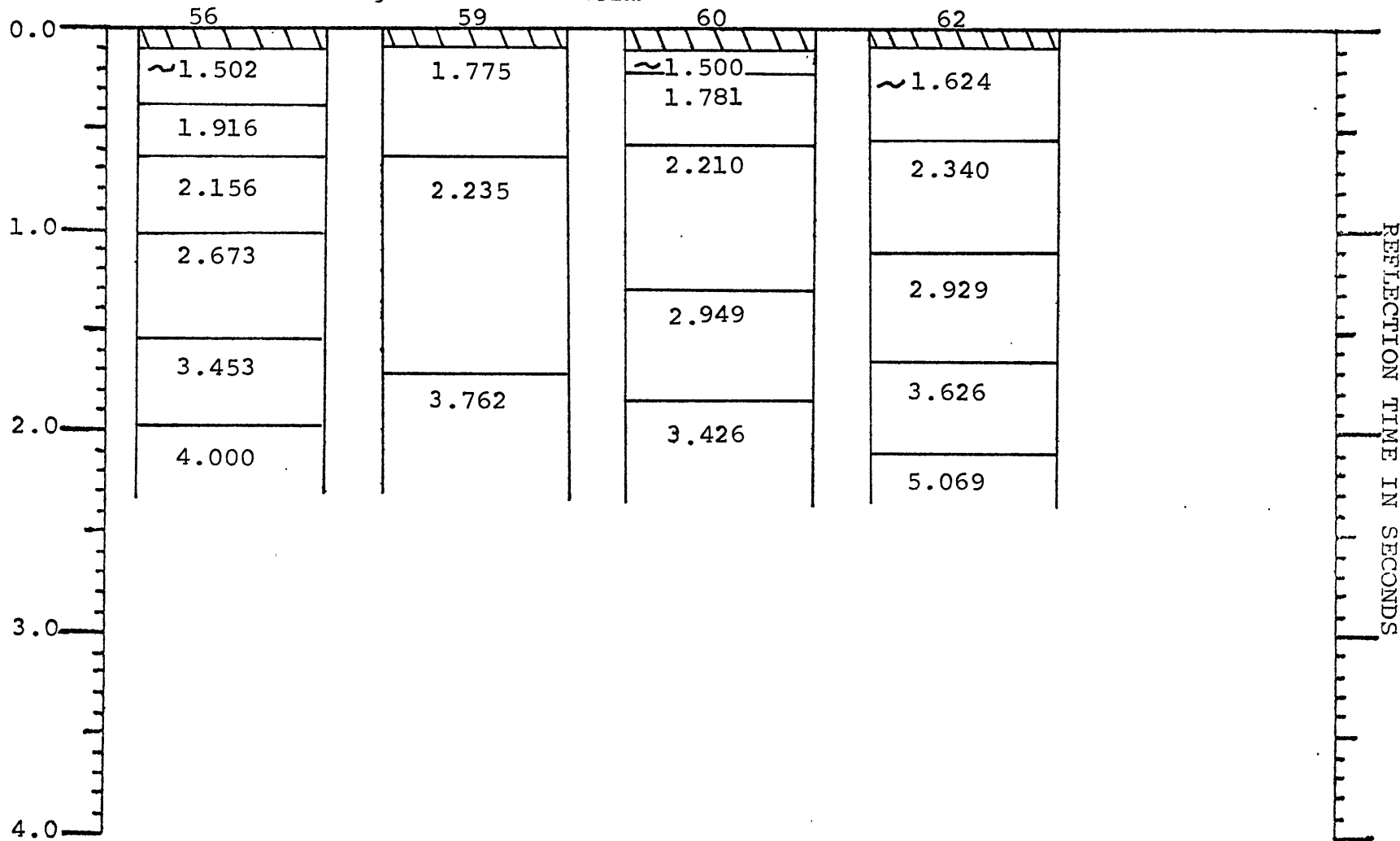


Figure 36D.

Figure 37. AII-91 sonobuoy results, continental
rise:

- A. Off Nova Scotia
- B. Off Georges Bank

For locations of profiles, refer to
Figure 1.

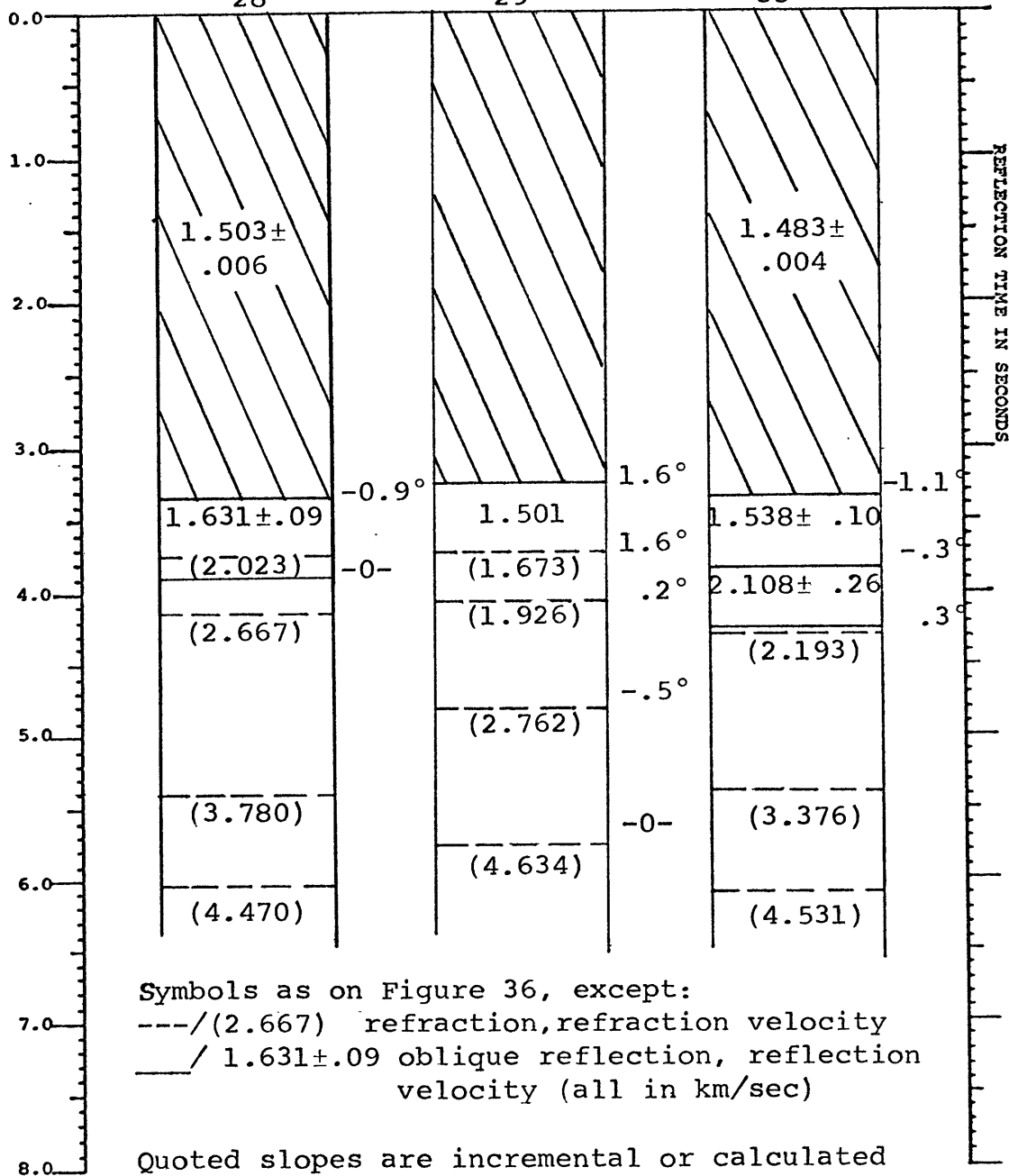
Continental rise off Nova Scotia

Sonobuoy Results:

28

29

33



Symbols as on Figure 36, except:
 ---/(2.667) refraction, refraction velocity
 ___/ 1.631±.09 oblique reflection, reflection velocity (all in km/sec)

Quoted slopes are incremental or calculated
 Figure 37A. by program SLOWI (see Knott and Hoskins, 1975).

Continental rise off Nova Scotia (cont.)

Sonobuoy Results:

34

47

48

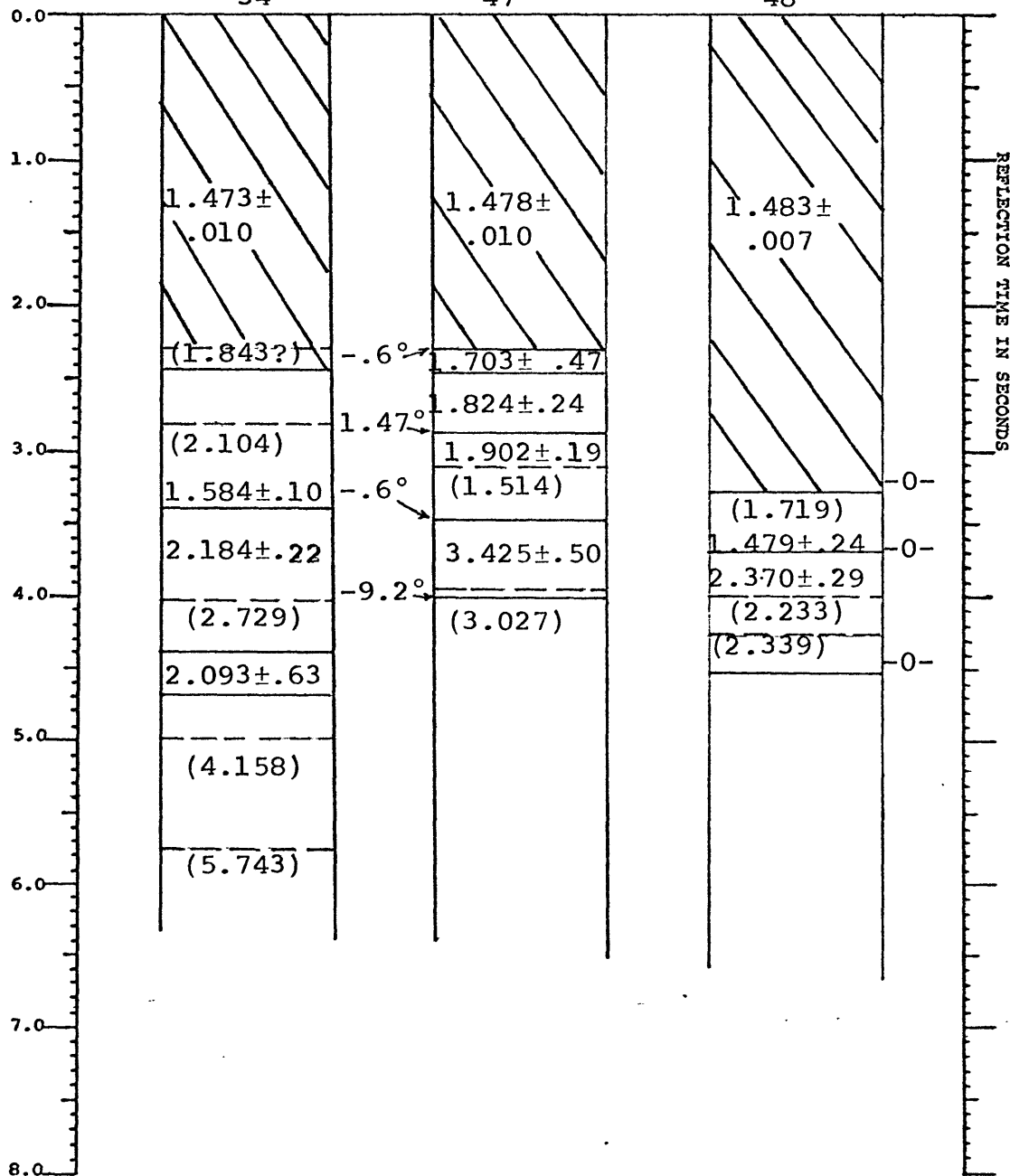


Figure 37A. (cont.)

Continental rise off Georges Bank

Sonobuoy Results: 1

2

4

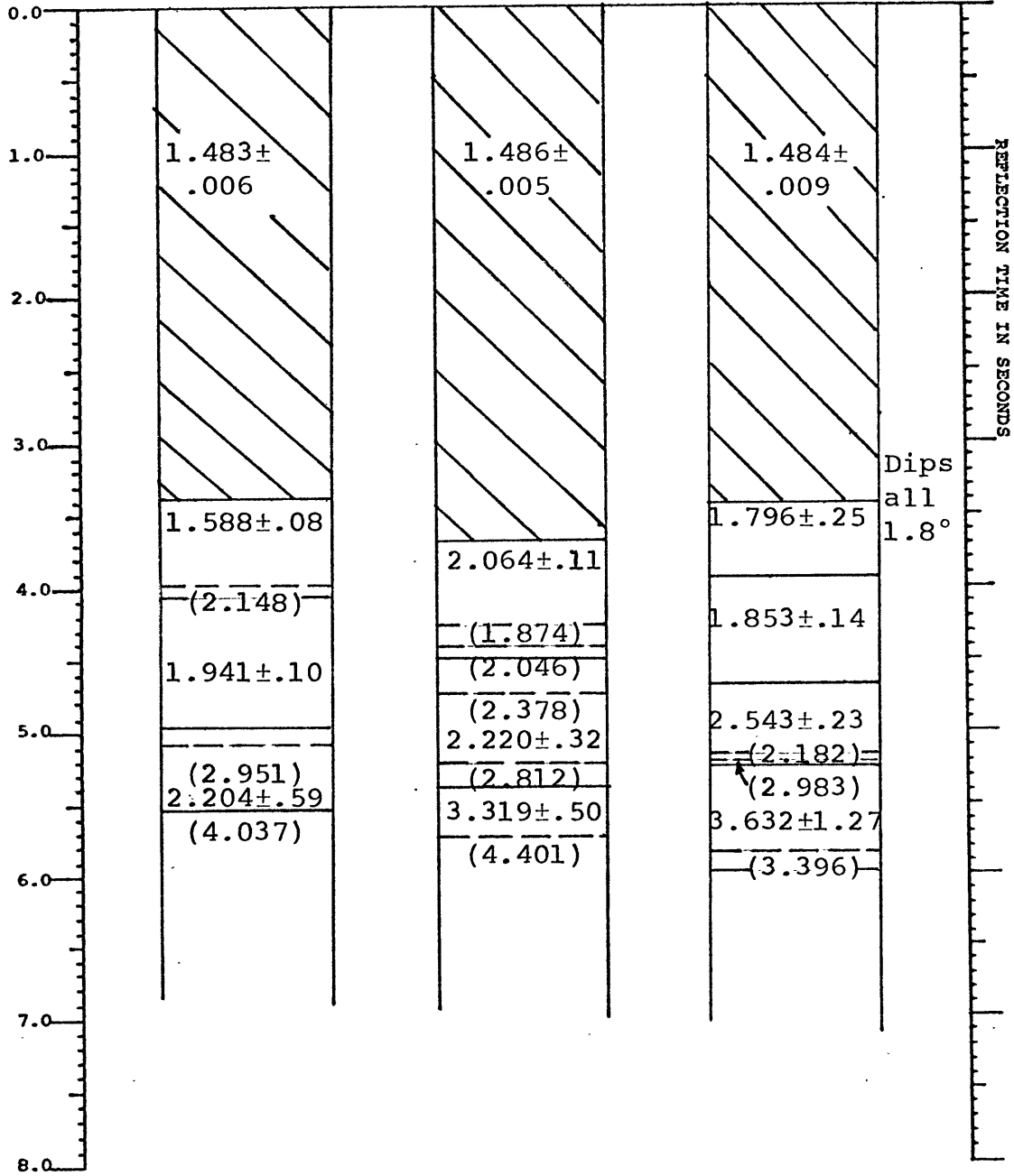


Figure 37B.

Continental rise off Georges Bank (cont.)

Sonobuoy Results:

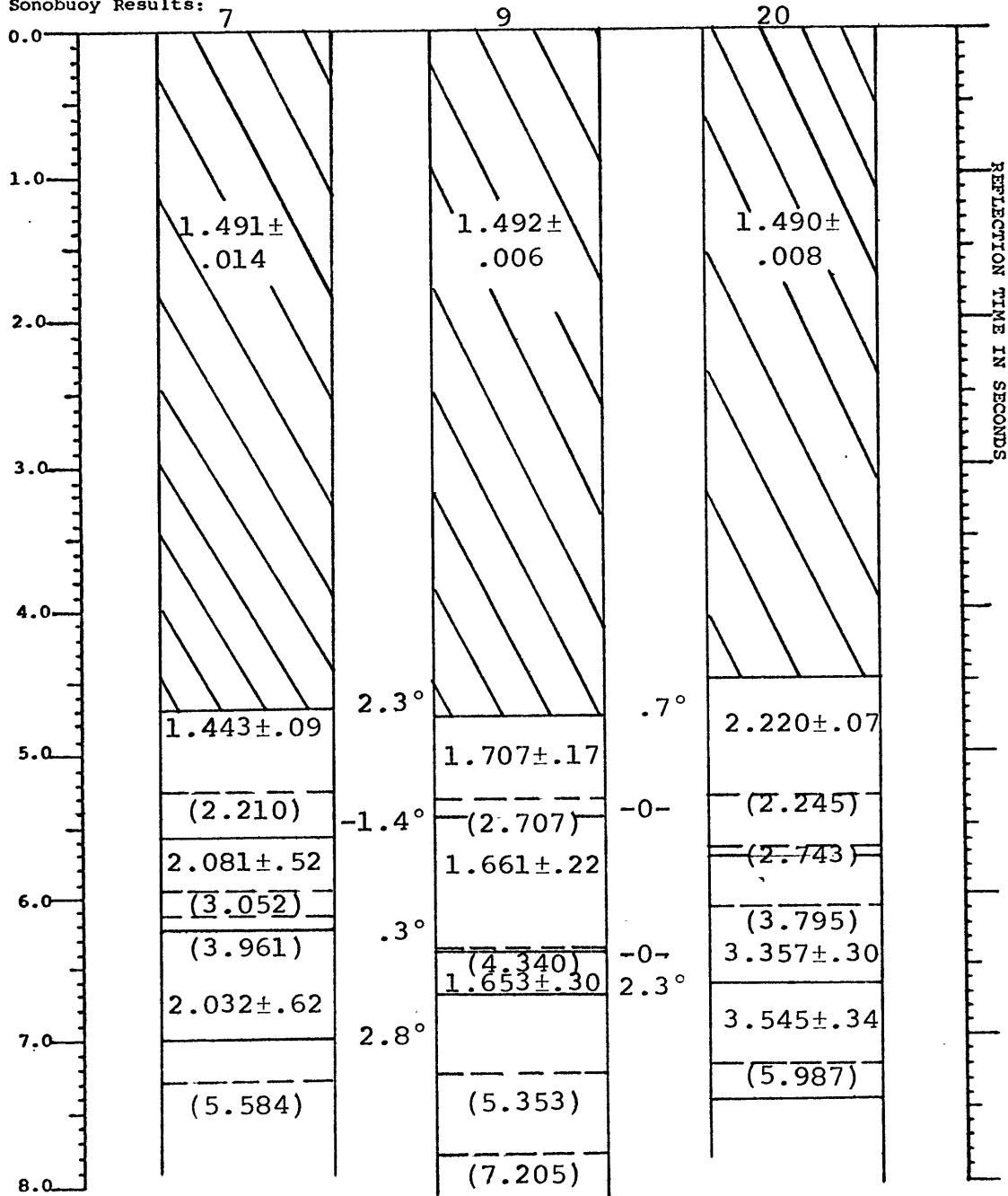


Figure 37B. (cont.)

Continental rise off Georges Bank (cont.)

Sonobuoy Results:

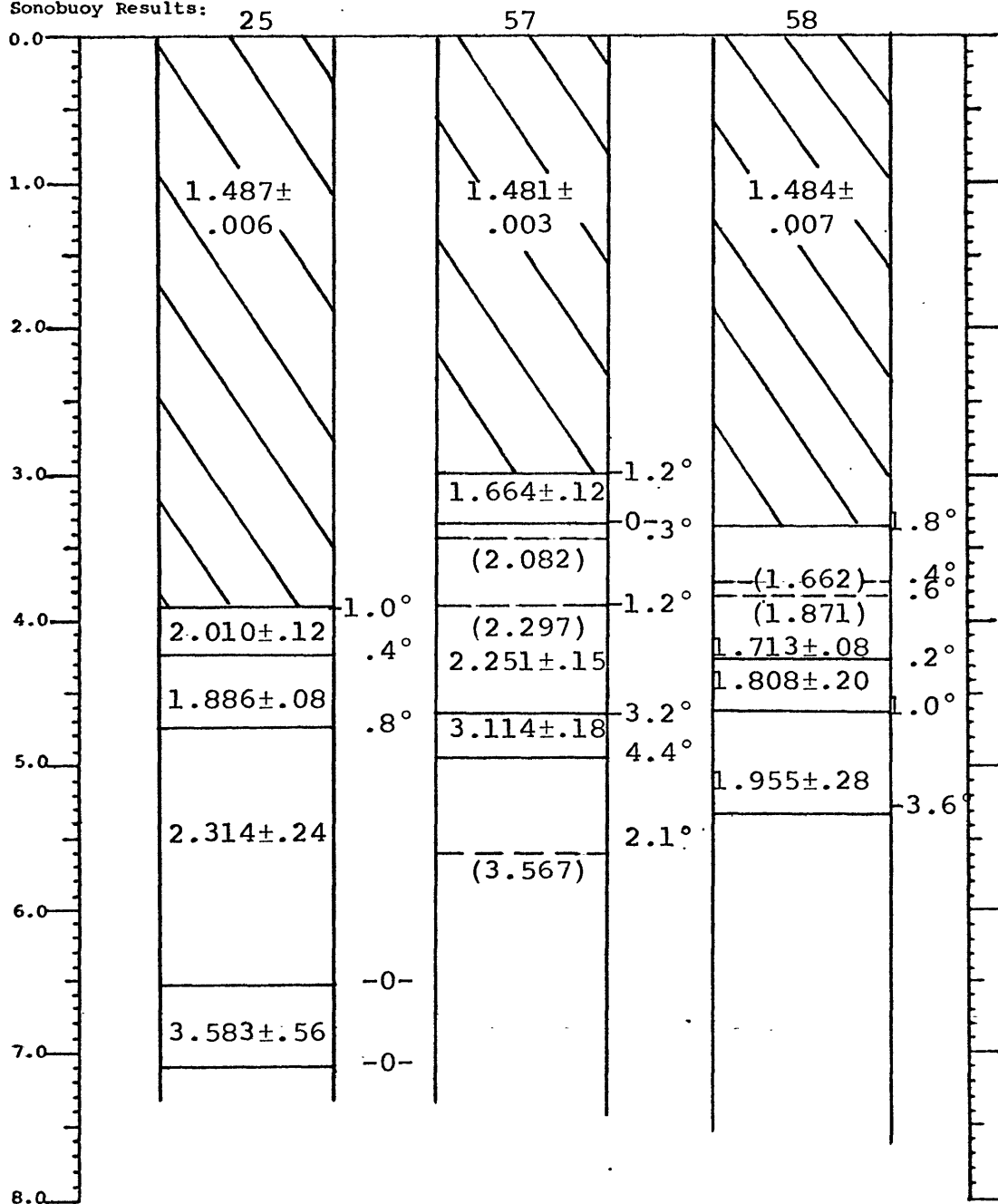
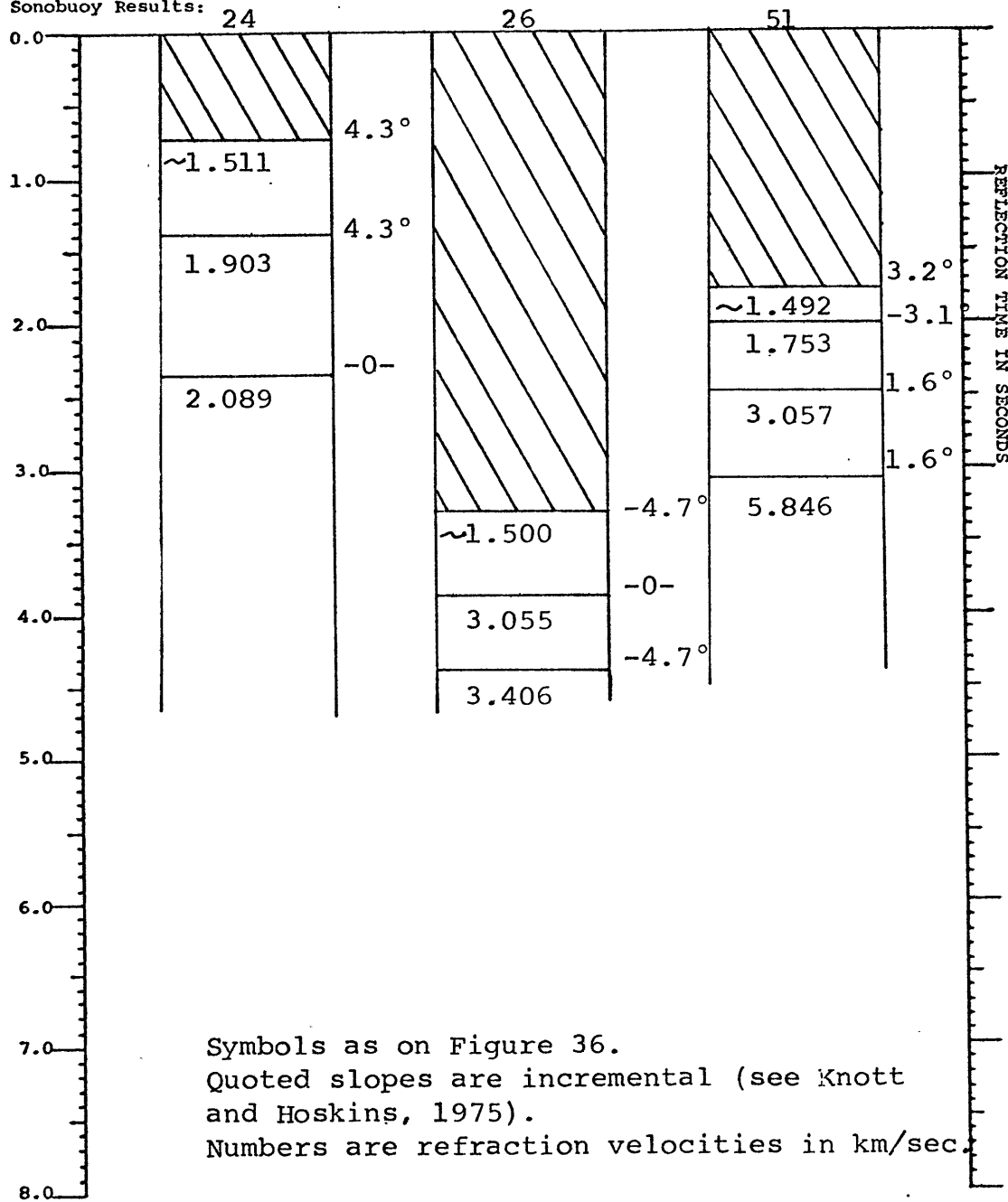


Figure 37B. (cont.)

Figure 38. AII-91 sonobuoy results, New England continental slope. For locations of profiles, refer to Figure 1.

Continental slope south of Georges Bank

Sonobuoy Results:



Symbols as on Figure 36.

Quoted slopes are incremental (see Knott and Hoskins, 1975).

Numbers are refraction velocities in km/sec.

Figure 38.

APPENDIX III

TIME-TO-DEPTH

CONVERSIONS

Table I. Time-To-Depth Conversions, U.S.G.S. CDP Lines 1, 4, and 5.

Line/ Reel (SB)	Time (SF)	Bottom- "X" 1 to "X"	"X" - 3 "X" - 2 (1-2)	2 - 3	"X" - "2" 3 - "2"	3 - 4	4 - "2"	"2" - "K"	"K" - Basement
1	100	1.92±.08 (.31sec/298m)	-	-	*2.75±.35 (.56sec/770m)	-	-	4.1±.4 (.40sec/820m) Tot. to "K"= 1,888m	*3.8±.8 (.43sec/817m) Tot. to "B"= 2,705m
1	200	1.92±.08 (.41sec/394m)	*2.4±.14 (.18sec/216m)	-	3.1±.4 (.63sec/976m)	-	-	4.1±.4 (.22sec/451m) Tot. to "K"= 2,037m	*3.8±.8 (.25sec/475m) Tot. to "B"= 2,512m
1	300	1.92±.08 (.42sec/403m)	2.4±.14 (.07sec/84m)	2.4±.14 (.17sec/204m)	3.1±.4 (.77sec/1,194m)	-	-	4.1±.4 (.06sec/123m)	-0- Tot. to "B"=2,008m
1	400	1.92±.08 (.47sec/451m)	2.4±.14 (.16sec/192m)	2.4±.14 (.20sec/240m)	3.1±.4 (.92sec/1,426m)	-	-	4.1±.4 (.38sec/779m)	-0- Tot. to "B"=3,038m
1	500	1.92±.08 (.48sec/461m)	2.4±.14 (.23sec/300m)	2.4±.14 (.34sec/408m)	3.1±.4 (.92sec/1,426m)	-	-	4.1±.4 (.43sec/882m) Tot. to "K"= 3,477m	*3.8±.8 (1.02sec/1,938m) Tot. to "B"= 5,415m
1	600	2.05±.05 (.55sec/564m)	3.0±.15 (.29sec/435m)	3.0±.15 (.41sec/615m)	4.2±.3 (.97sec/2,037m)	-	-	5.6±.8 (.60sec/1,680m) Tot. to "K"= 5,331m	*3.8±.8 (.83sec/1,577m) Tot. to "B"= 6,908m
1	700	2.05±.05 (.64sec/656m)	3.0±.15 (.31sec/465m)	3.0±.15 (.43sec/645m)	4.2±.3 (.96sec/2,016m)	-	-	5.6±.8 (.99sec/2,772m) Tot. to "K"= 6,554m	*3.8±.8 (2.61sec/4,959m) Tot. to "B"= 11,513m
1	800	2.05±.05 (.67sec/687m)	3.0±.15 (.31sec/465m)	3.0±.15 (.50sec/750m)	-	4.2±.3 (.57sec/1,197m)	4.2±.3 (.43sec/903m)	5.6±.8 (1.00sec/2,800m) Tot. to "K"= 6,802m	*3.8±.8 (2.28sec/4,332m) Tot. to "B"= 11,134m
1	900	2.05±.05 (.70sec/718m)	3.0±.15 (.38sec/570m)	3.0±.15 (.45sec/675m)	-	4.2±.3 (.59sec/1,239m)	4.2±.3 (.61sec/861m)	5.6±.8 (1.00sec/2,800m) Tot. to "K"= 6,863	*3.8±.8 (1.64sec/3,116m) Tot. to "B"= 9,979
1	1000	2.05±.05 (.68sec/697m)	3.0±.15 (.41sec/615m)	3.0±.15 (.41sec/615m)	-	4.2±.3 (.53sec/1,113m)	4.2±.3 (.56sec/1,134m)	5.6±.8 (1.09sec/3,052m) Tot. to "K"= 7,226m	*3.8±.8 (1.85sec/3,515m) Tot. to "B"= 10,741m
1	1100	2.05±.06 (.67sec/687m)	3.4±.1 (.41sec/697m)	3.4±.1 (.40sec/680m)	-	4.7±.4 (.59sec/1,386m)	4.7±.4 (.61sec/1,434m)	5.9±.6 (.99sec/2,920m)	-0- Tot. to "B"=7,804m
1	1200	2.05±.06 (.69sec/707m)	3.4±.1 (.41sec/697m)	3.4±.1 (.43sec/731m)	-	4.7±.4 (.60sec/1,410m)	4.7±.4 (.49sec/1,152m)	5.9±.6 (1.00sec/2,950m)	-0- Tot. to "B"=7,667
1	1300	2.05±.06 (.72sec/738m)	3.4±.1 (.40sec/680m)	3.4±.1 (.55sec/935m)	-	4.7±.4 (.50sec/1,175m)	4.7±.4 (.55sec/1,292m)	5.9±.6 (.93sec/2,744m)	-0- Tot. to "B"=7,564m
1	1400	2.05±.06 (.75sec/769m)	3.4±.1 (.35sec/595m)	3.4±.1 (.55sec/935m)	-	4.7±.4 (.53sec/1,246)	4.7±.4 (.47sec/1,104m)	5.9±.6 (.77sec/2,272m) Tot. to "K"= 6,921m	*3.8±.8 (.30sec/570m) Tot. to "B"= 7,491m
1	1500	2.16±.1 (.72sec/778m)	3.3±.3 (.37sec/610m)	3.3±.3 (.56sec/924m)	-	5.2±.3 (.46sec/1,196m)	5.2±.3 (.50sec/1,300m)	5.9±.6 (.86sec/2,537m) Tot. to "K"= 7,345m	*3.3±.8 (.71sec/1,349m) Tot. to "B"= 8,694m
1	1600	2.16±.1 (.73sec/788m)	3.3±.3 (.32sec/528m)	3.3±.3 (.51sec/841m)	-	5.2±.3 (.39sec/1,014m)	5.2±.3 (.28sec/728m) Tot. to "K"= 3,899m	-	-0-(?)
1	1700	2.16±.1 (.67sec/724m)	3.3±.3 (.08sec/132m)	3.3±.3 (.61sec/1,006m)	-	5.2±.3 (.25sec/650m)	5.2±.3 (.48sec/1,248m) Tot. to "K"= 3,760 m	-	-0-(?)

Table I (continued)

Line	Shot Point	Depth of Water	Bottom - "Ac" Depth to "Ac"	"Ac" - "J ₁ " Depth to "J ₁ "	"J ₁ " - Basement Depth to Basement
1	1800	2.48sec/1.484/1,840m 1,840m	.84sec/2.05±.34 (SB#4) /861m 2,701m 2.04±.11(1)	1.13/3.63±1.271(SB#4) /2,051m 4,752m 3.6± 5(1)	~.55sec/5.5±.9(1)/1,513m (?) 6,265m
1	1900	3.00sec/same/2,226m 2,226m	.90sec/same/923m 3,149m	1.31sec/same/2,378m 5.527m	1.04sec/same/2,860 8,387m
1	2100	3.69sec/same/2,738m 2,738m	.78sec/same/800m 3,538m	1.46sec/same/2,650m 6,188m	.96sec/same/2,640m 8,828m
1	2000	3.33sec/same/2,471m 2,471m	.85sec/same/871m 3,342m	1.37sec/same/2,487m 5,829m	.42sec/same/1,155m 6,984m
1	2200	3.91sec/same/2,901m 2,901m	.70sec/same/718m 3,619m	1.56sec/3.6± 6,450m .5(1) /2,831m	.85sec/same/2,338m 8,788m
1	2300	4.05sec/same/3,005 3,005m	.85sec/same/871m 3,876m	1.63sec/same/2,958m 6,834m	.95sec/same/2,613m 9,447m
1	2400	4.45sec/same/3,302m 3,302m	.64sec/1.97±.14(1)/630m 3,932m	1.61sec/3.2±.2(1)/2,576m 6,508m	.37sec/4.1±.1(1)/759m 7,267m
1	2500	4.68sec/same/3,473m 3,473m	.57sec/same/561m 4,034m	1.72sec/same/2,752m 6,786m	.57sec/same/1,169m 7,955m
1	2600	4.90sec/same/3,636m 3,636m	.62sec/same/611m 4,247m	1.69sec/same/2,704m 6,951m	.75sec/same/1,538m 8,489m
1	2700	5.11sec/same/3,792m 3,792m	.54sec/same/532m 4,324m	1.69sec/same/2,704m 7,028m	.36sec/same/738m 7,766m
1	2800	5.30sec/same/3,933m 3,933m	.52sec/same/512m 4,445m	1.68sec/same/2,688m 7,133m	.23sec/same/472m 7,605m
1	2900	5.43sec/same/4,029m 4,029m	.60sec/same/591m 4,630m	1.54sec/same/2,464m 7,094m	.29sec/same/595m 7,689m
1	3000	5.55sec/same/4,118 4,118m	.59sec/same/581m 4,699m	1.61sec/same/2,576m 7,275m	.48sec/same/984m 8,259m
1	3100	5.65sec/same/4,192m 4,192m	.62sec/same/611m 4,803m	1.49sec/same/2,384m 7,187m	.31sec/same/636m 7,823m
1	3200	5.73sec/same/4,252m 4,192m	.67sec/same/660m 4,912m	1.45sec/same/2,320m 7,232m	.39sec/same/800m 8,032m
1	3300	5.80sec/same/4,304m 4,304m	.67sec/same/660m 4,969m	1.43sec/same/2,288m 7,252m	.57sec/same/1,169m 8,421m
1	3400	5.88sec/same/4,363m 4,363m	.62sec/same/611m 4,974m	1.50sec/same/2,400m 7,374m	.53sec/same/1,087m 8,461m
1	3500	6.00sec/same/4,452m 4,452m	.53sec/same/522m 4,974m	1.01sec/same/1,616m 6,590m	.95sec/same/1,948m 8,538m

Table I (continued)

Line/ Reel (SB)	Time (SP)	Bottom-"X" B to 1 (Δ) 1 to "X" (\square)	"X"-2 (1-2)	2-3	3-"Z"	3-4	4-"Z"	"Z"- "K"	"K"- Basement
4	100	*2.15 \pm .25 (.23sec/247m)	-	-	-	-	-	- Tot. to "K"= 247 m	*3.5 \pm .1 (T _r Basin) (2.48sec/4,340m) Tot. to "B"= 4,587m
4	200	*1.9 \pm ? (.31sec/294m)	-	-	-	-	-	*2.4 \pm .1 (.11sec/132m)	-0- Tot. to "B"= 426m
4	300	*1.9 \pm ? (.32sec/304m)	-	-	*2.4 \pm .1 (.14sec/168m)	-	-	2.4 \pm .1 (.20sec/240m) Tot. to "K"= 712m	3.4 \pm .1 (.37sec/629m) Tot. to "B"= 1,341m
4	400	(Δ)1.9 \pm ? (.15sec/142m) (\square)1.9 \pm ? (.12sec/114m)	*1.9 \pm ? (.13sec/124m)	-	2.4 \pm .1 (.26sec/312m)	-	-	2.4 \pm .1 (.42sec/504m) Tot. to "K"= 1,196m	3.7 \pm .6 (.16sec/296m) Tot. to "B"= 1,492m
4	500	1.9 \pm ? (.26sec/247m)	*1.9 \pm ? (.19sec/180m)	-	2.4 \pm .1 (.61sec/732m)	-	-	2.4 \pm .1 (.53sec/636m) Tot. to "K"= 1,795m	3.7 \pm .6 (.26sec/481m) Tot. to "B"= 2,276m
4	600	2.0 \pm .1 (.33sec/330m)	*2.0 \pm .1 (.16sec/160m)	-	3.1 \pm .3 (.67sec/1,038m)	-	-	3.1 \pm .3 (.88sec/1,364m) Tot. to "B"= 4,557m	3.7 \pm .6 (.45sec/832m) 4.9 \pm .8 (.34sec/833m)
4	700	2.0 \pm .1 (.37sec/370m)	*2.0 \pm .1 (.20sec/200m)	-	3.1 \pm .3 (.62sec/961m)	-	-	3.1 \pm .3 (.63sec/976m) Tot. to "K"= 2,507m	3.7 \pm .6 (.65sec/1,202m) Tot. to "B"= 3,709m
4	800	2.0 \pm .1 (.40sec/400m)	2.0 \pm .1 (.21sec/210m)	2.0 \pm .1 (.02sec/20m)	-	3.1 \pm .3 (.71sec/1,100m)	3.1 \pm .3 (.19sec/294m)	3.1 \pm .3 (.20sec/310m) Tot. to "K"= 2,334m	4.1 \pm .4 (.31sec/636m) Tot. to "B"= 2,970m
4	900	2.0 \pm .1 (.40sec/400m)	2.0 \pm .1 (.24sec/240m)	2.0 \pm .1 (.06sec/60m)	-	3.1 \pm .3 (.60sec/930m)	3.1 \pm .3 (.28sec/434m)	3.1 \pm .3 (.20sec/310m) Tot. to "K"= 2,374m	4.1 \pm .4 (.57sec/1,168m) Tot. to "B"= 3,542m
4	1000	2.3 \pm .1 (.44sec/506m)	2.3 \pm .1 (.25sec/288m)	2.3 \pm .1 (.05sec/58m)	-	3.7 \pm .3 (.60sec/1,110m)	4.7 \pm .3 (.30sec/705m)	4.7 \pm .3 (.13sec/306m)	-0- Tot. to "B"= 2,973m
4	1100	2.3 \pm .1 (.43sec/494m)	2.3 \pm .1 (.29sec/334m)	2.3 \pm .1 (.07sec/80m)	-	3.7 \pm .3 (.60sec/1,110m)	4.7 \pm .3 (.31sec/728m)	4.7 \pm .3 (.15sec/352m)	-0- Tot. to "B"= 3,098m
	1200	2.3 \pm .1 (.48sec/552m)	2.3 \pm .1 (.32sec/368m)	2.3 \pm .1 (.15sec/172m)	-	3.7 \pm .3 (.56sec/1,036m)	4.7 \pm .2 (.30sec/705m)	4.7 \pm .3 (.70sec/1,645m) (?)	-0- Total to "B"= 4,478m
4	1300	2.3 \pm .1 (.53sec/610m)	2.3 \pm .1 (.33sec/380m)	2.3 \pm .1 (.21sec/242m)	-	3.7 \pm .3 (.56sec/1,036m)	4.7 \pm .3 (.33sec/776m)	4.7 \pm .3 (2.01sec/4,724m)	-0-(?) Tot. to "B"= 7,768m
4	1400	2.3 \pm .1 (.51sec/586m)	2.3 \pm .1 (.41sec/472m)	2.3 \pm .1 (.23sec/264m)	-	3.7 \pm .3 (.60sec/1,110m)	4.7 \pm .3 (.38sec/893m)	4.7 \pm .3 (4.40sec/10,340m)	-0-(?) Tot. to "B"= 13,665m
4	1500	2.3 \pm .1 (.48sec/552m)	2.3 \pm .1 (.42sec/483m)	2.3 \pm .1 (.20sec/230m)	-	3.7 \pm .3 (.53sec/980m)	4.7 \pm .3 (.38sec/893m)	4.5 \pm .3 (2.75sec/6,462m)	-0-(?) Tot. to "B"= 9,600m
4	1600	2.3 \pm .1 (.67sec/770m)	2.3 \pm .1 (.21sec/242m)	2.3 \pm .1 (.14sec/161m)	-	3.7 \pm .3 (.47sec/870m)	4.7 \pm .3 (.18sec/423m) Tot. to "K"= 2,466m	-(?)-	-(?)-

Table I (continued)

Line	SP	Depth of water	Bottom-"A _c " Depth to "A _c "	"A _c " - "J ₁ " Depth to "J ₁ "		"J ₁ " - Basement Depth to Basement
				"A _c " - "β"	"β" - "J ₁ "	
4	1800	(assumption) 2.54sec/1.500/1,905m 1,905m	.78sec/1.8±.1(4)/702m 2,607m	.71sec/2.8±.5(4)/994m 1,526m	.28sec/3.8±.6(4)/532m 4,133m	.39sec/3.8±.6(4)/741m 4,874m(?) [R(?)]
4	1900	3.10sec/same/2,325m 2,325m	1.04sec/same/936m 3,261m	.79sec/same/1,501m 2,109m	.32sec/3.8±.2(4)/608m 5,370m	.47sec/5.3±.6(4)/1,246m 6,616m (?) [R(?)]
4	2000	3.52sec/same/2,640m 2,640m	1.05sec/same/945m 3,580m	"A _c " - "A*" .84sec/same/1,176m 2,107m	"A*" - "J ₁ " .49sec/same/931m 5,687m	.58sec/same/1,537m 7,224m
4	2100	3.92sec/same/2,940m 2,940m	.88sec/same/792m 3,732m	.78sec/same/1,092m 2,346m	.66sec/same/1,254m 6,078m	.56sec/same/1,484m 7,562m
4	2200	4.12sec/same/3,090m 3,090m	1.06sec/same/954m 4,044m	.69sec/2.3±.1(4)/794m 1,770m	.61sec/3.2±.2(4)/976m 5,814m	.54sec/4.6±.2/1,242m 7,056m
4	2300	4.30sec/same/3,225m 3,225m	1.12sec/same/1,008m 4,233m	.79sec/same/909m 1,757m	.53sec/same/848m 5,990m	.64sec/same/1,472m 7,462m
4	2400	4.55sec/same/3,412m 3,412m	1.01sec/same/909m 4,321m	.82sec/same/943m 1,695m	.47sec/same/752m 6,016m	.55sec/same/1,265m 7,281m
4	2500	4.74sec/same/3,555m 3,555m	.88sec/same/792m 4,347m	.89sec/same/1,024m 1,936m	.57sec/same/912m 6,283m	.44sec/same/1,012m 7,295m

Table I (continued)

Line/ Reel (SB)	Time (SP)	Bottom-"X" B to 1 1 to "X"	*"X" - 3 "X" - 2 (1-2)	2-3	*3 - "K" 3 - "Z"	3 - 4	4 - "Z"	"Z" - "K"	"K" - Basement
5	107	1.9±.1 (.11sec/104m)	*1.9±.1 (.16sec/152m)	-	*2.4±.2 (.10sec/120m)	-	-	- Tot. to "K"= 376m	3.2±.5 (*1.17sec/1,872m) Tot. to "B"=2,248m
5	200	1.9±.1 (.11sec/104m)	*1.9±.1 (.20sec/190m)	-	*2.4±.2 (.09sec/108m)	-	-	- Tot. to "K"= 402m	3.2±.5 (1.83sec/2,928m) Tot. to "B"=3,330m
5	300	1.9±.1 (.09sec/86m)	*1.9±.1 (.25sec/238m)	-	*2.4±.2 (.19sec/228m)	-	-	- Tot. to "K"= 552m	3.2±.5 (2.10sec/3,360m) Tot. to "B"=3,912m
5	400	1.9±.1 (.10sec/95m)	*1.9±.1 (.34sec/323m)	-	*2.4±.2 (.14sec/168m)	-	-	- Tot. to "K"= 586m	3.2±.5 (1.06sec/1,696m) Tot. to "B"=2,282m
5	500	1.9±.1 (.11sec/104m)	*1.9±.1 (.37sec/352m)	-	*2.4±.2 (.27sec/324m)	-	-	- Tot. to "K"= 780m	3.2±.5 (1.12sec/1,792m) Tot. to "B"=2,572m
5	600	1.9±.1 (.15sec/142m)	*1.9±.1 (.38sec/361m)	-	*2.4±.2 (.45sec/540m)	-	-	- Tot. to "K"= 1,043m	3.2±.5 (1.38sec/2,208m) Tot. to "B"=3,231m
5	700	1.9±.1 (.14sec/133m)	*1.9±.1 (.44sec/418m)	-	2.4±.2 (.38sec/456m)	-	-	3.1±.3 (.22sec/341m) Tot. to "K"= 1,348m	3.2±.5 (2.57sec/4,112m) Tot. to "B"= 5,460m
5	800	1.9±.1 (.25sec/238m)	1.9±.1 (.05sec/48m)	1.9±.1 (.38sec/361m)	2.4±.1 (.42sec/504m)	-	-	3.1±.3 (.50sec/775m)	3.2±.5 (-0-) Tot. to "B"=1,926m
5	900	1.9±.1 (.32sec/304m)	1.9±.1 (.12sec/114m)	1.9±.1 (.41sec/390m)	2.4±.1 (.48sec/576m)	-	-	3.1±.3 (.50sec/775m)	-0- Tot. to "B"=2,159m
5	1000	1.9±.1 (.35sec/332m)	1.9±.1 (.17sec/162m)	1.9±.1 (.46sec/437m)	2.4±.1 (.51sec/612m)	-	-	3.1±.3 (.40sec/620m) Tot. to "K"= 2,163m	4.0±.6 (.48sec/960m) Tot. to "B"= 3,123m
5	1100	1.9±.1 (.36sec/342m)	1.9±.1 (.19sec/180m)	1.9±.1 (.44sec/418m)	2.4±.1 (.64sec/768m)	-	-	3.1±.3 (.50sec/775m) Tot. to "K"= 2,483m	4.9±.4 (.39sec/956m) Tot. to "B"= 3,439m
5	1200	2.0±.1 (.41sec/410m)	2.0±.1 (.27sec/270m)	2.0±.1 (.40sec/400m)	3.0±.2 (.73sec/1,095m)	-	-	4.0±.4 (.65sec/1,300m) Tot. to "K"= 3,475m	4.9±.4 (.98sec/2,401m) Tot. to "B"= 5,876m
5	1300	2.0±.1 (.49sec/490m)	2.0±.1 (.28sec/280m)	2.0±.1 (.43sec/430m)	3.0±.2 (.81sec/1,215m)	-	-	4.0±.4 (.90sec/1,800m) Tot. to "K"= 4,215m	4.9±.4 (2.00sec/4,900m) Tot. to "B"= 9,115m
5	1400	2.0±.1 (.53sec/530m)	2.0±.1 (.29sec/290m)	2.0±.1 (.42sec/420m)	-	3.0±.2 (.50sec/750m)	4.0±.4 (.37sec/740m)	4.0±.4 (1.16sec/2,320m) Tot. to "K"= 5,050m	4.9±.4 (.39sec/956m) Tot. to "B"= 6,006m
5	1500	2.0±.1 (.55sec/550m)	2.0±.1 (.28sec/280m)	2.0±.1 (.40sec/400m)	-	3.0±.2 (.53sec/795m)	4.0±.4 (.38sec/760m)	4.0±.4 (1.32sec/2,640m)	-0- Tot. to "B"=5,425m
5	1600	2.0±.1 (.63sec/630m)	2.0±.1 (.30sec/300m)	2.0±.1 (.35sec/350m)	-	3.0±.2 (.53sec/795m)	4.7±.5 (.41sec/964m)	4.7±.5 (1.44sec/3,384m)	-0- Tot. to "B"=6,423m
5	1700	2.0±.1 (.61sec/610m)	2.0±.1 (.23sec/230m)	2.0±.1 (.40sec/400m)	-	3.0±.2 (.47sec/705m)	4.7±.5 (.45sec/1,058m)	4.7±.5 (1.48sec/3,478m)	-0- Tot. to "B"=6,481m
5	1800	2.0±.1 (.23sec/230m)	2.5±.2 (.97sec/1,213m)	-0-	-	-0-	4.7±.5 (.48sec/1,128m)	4.7±.5 (2.28sec/5,358m)	-0- Tot. to "B"=7,929m

Table I (continued)

Line	SP	Depth of Water	Bottom - "Ac" Depth to "Ac"	"Ac" - "J ₁ " Depth to "J ₁ "		"J ₁ " - Basement Depth to Basement
				"Ac" - "β"	"β" - "J ₁ "	
5	1900	(assumption) 2.62sec/1.500/1,965m 1,965m	.93sec/1.9±.1(5)884m 2,849m	.85sec/2.5±.2(5)/1,063m 1,896m	.49sec/3.4±.2(5)/833m 4,745m	3.30sec/4.8±.5(5)/7,920m 12,665m
5	2000	2.74sec/same/2,055 2,055m	1.42sec/same/1,349m 3,404m	.96sec/same/1,200m 2,356m	.68sec/same/1,156m 5,760m	1.85sec/same/4,440m 10,200m
5	2100	3.05sec/same/2,288m 2,288m	1.39sec/same/1,321m 3,609m	1.13sec/same/1,413m 2,501m	.64sec/same/1,088m 6,110m	1.47sec/same/3,528m 9,638m
5	2200	3.12sec/same/2,340m 2,340m	1.56sec/same/1,482m 3,822m	1.13sec/same/1,413m 2,739m	.78sec/same/1,326m 6,561m	1.42sec/same/3,408m 9,969m
5	2300	3.29sec/same/2,468m 2,468m	1.67sec/same/1,587m 4,055m	1.06sec/same/1,325m 2,430m	.65sec/same/1,105m 6,485m	1.45sec/same/3,480m 9,965m
5	2400	3.47sec/same/2,602m 2,602m	1.71sec/same/1,625m 4,227m	.98sec/same/1,225m 2,364m	.67sec/same/1,139m 6,591m	1.46sec/same/3,504m 10,094m
5	2500	3.66sec/same/2,745m 2,745m	1.71sec/1.8±(5)/1,539m 4,284m	.97sec/same/1,213m 2,302m	.66sec/3.3±.3(5)/1,089m 6,586m	1.26sec/4.5±.5(5)/2,835m 9,421m
5	2600	3.87sec/same/2,902m 2,902m	1.65sec/same/1,485m 4,387m	.94sec/same/1,175m 2,231m	.64sec/same/1,056m 6,673m	1.05sec/same/2,363m 9,036m
5	2700	4.04sec/same/3,030m 3,030m	1.63sec/same/1,467m 4,497m	.91sec/same/1,138m 2,260m	.68sec/same/1,122m 6,757m	1.29sec/same/2,903m 9,660m
5	2800	4.16sec/same/3,120m 3,120m	1.61sec/same/1,449m 4,569m	.91sec/same/1,138m 2,260m	.68sec/same/1,122m 6,829m	.68sec/same/1,530m 8,359m
5	2900	4.26sec/same/3,195m 3,195m	1.62sec/same/1,458m 4,653m	.91sec/same/1,138m 2,227m	.66sec/same/1,089m 6,880m	.71sec/same/1,598m 8,478m
5	3000	4.34sec/same/3,255m 3,255m	1.60sec/same/1,440m 4,695m	.84sec/same/1,050m 2,321m	.77sec/same/1,271m 7,016m	.72sec/same/1,620m 8,636m
5	3100	4.42sec/same/3,315m 3,315m	1.60sec/same/1,440m 4,755m	.76sec/same/950m 2,303m	.82sec/same/1,353m 7,058m	.53sec/same/1,193m 8,251m
5	3200	4.50sec/same/3,375m 3,375m	1.75sec/same/1,575m 4,950m	.59sec/same/738m 2,190m	.88sec/same/1,452m 7,140m	.46sec/same/1,035m 8,175m
5	3300	4.61sec/same/3,458m 3,458m	1.75sec/same/1,575m 5,033m	.58sec/same/725m 2,161m	.87sec/same/1,436m 7,194m	.35sec/same/788m 7,982m
5	3400	4.75sec/same/3,562m 3,562m	1.76sec/same/1,584m 5,126m	.53sec/same/663m 1,967m	.79sec/same/1,304m 7,093m	.44sec/same/990m 8,083m

Table II. Time-To-Depth Conversions, AII-91 CDP Profiles.

Reel (SB)	Time	Bottom - "X" B to 1 1 to "X"	"X" - 2 (1 - 2)	2 - 3	3 - "Z"	3 - 4	4 - R 4 - "Z"	assuming *an over- all sediment sec- tion of 5.0sec(tt) (R)="reef-ridge"	*Taken from Ballard and Uchupi (1975) "K" - Basement
7	2305Z (CDP)	1.961 (CDP) (.59sec/578m)	2.675 (CDP) (.46sec/615m)	3.225 (CDP) (.53sec/855m)	-	5.2±.3 (Line 1) (.41sec/1,066m)	5.2±.3 (Line 1) (.19sec/494m)	(R) (?)	Tot. to "R" top=3,114m
8	0128Z (CDP)	1.766 (av, CDP) (.72sec/636m)	2.375 (CDP) (.37sec/439m)	2.978 (av, CDP) (.46sec/685m)	-	4.874 (CDP) (.65sec/1,584m)	5.2±.3 (Line 1) (.46sec/1,196m)	5.9±0.6 (Line 1) (1.01sec/2,980m)	-0- Tot. to "B"= 7,520m
8	0405Z (CDP)	1.743 (CDP) (.72sec/627m)	2.197 (CDP) (.43sec/472m)	3.4±0.1 (Line 1) (.47sec/799m)	-	4.7±0.4 (Line 1) (.63sec/1,480m)	4.7±0.4 (Line 1) (.52sec/1,222m)	5.9±0.6 (Line 1) (.95sec/2,802m)	*3.8±0.8 (.73sec(?)/1,387m) Tot. to "K"=7,402m Tot. to "B"=8,789m
9	0628Z (CDP)	1.627 (CDP) (.64sec/521m)	2.205 (av, CDP) (.44sec/485m)	3.445 (CDP) (.46sec/792m)	-	4.162 (CDP) (.55sec/1,145m)	4.7±0.4 (Line 1) (.56sec/1,316m)	5.9±0.6 (Line 1) (.83sec/2,448m)	-0- Tot. to "B"= 6,707m
9	0828CDP)	1.620 (CDP) (.58sec/470m)	2.584 (CDP) (.36sec/465m)	3.173 (CDP) (.41sec/650m)	4.2±0.3 Line 1 (1.07sec /2,247m)	-	-	5.6±0.8 (Line 1) (1.00sec/2,800m)	-0- Tot. to "B"= 6,632m
10	1616Z (CDP)	1.630 (CDP) (.60sec/489m)	2.180 (CDP) (.34sec/371m)	2.205 (?) (CDP) (.36sec/397m)	-	4.431 (av, CDP) (.58sec/1,285m)	4.7±0.4 (Line 1) (.45sec/1,058m)	5.9±0.6 (Line 1) (.73sec/2,154m)	-0- Tot. to "B"= 5,754m
11	1846Z (CDP)	1.817 (CDP) (.70sec/636m)	2.181 (av, CDP) (.32sec/349m)	2.974 (av, CDP) (.38sec/565m)	-	3.574 (CDP) (.62sec/1,108m)	4.7±0.4 (Line 1) (.42sec/987m)	5.9±0.6 (Line 1) (.74sec/2,183m)	-0- (?) Tot. to "B"=5,828m
17	0040Z (CDP)	2.009 (av, CDP) (.74sec/743m)	2.616 (CDP) (.27sec/353m)	3.079 (CDP) (.36sec/554m)	-	5.2±0.3 (Line 1) (.51sec/1,326m)	5.2±0.3 (Line 1) (.42sec/1,092m)	5.9±0.6 (Line 1) (1.32sec/3,894m)	-0- (?) Tot. to "B"=7,962m
18	0341Z (CDP)	1.631 (CDP) (.64sec/522m)	1.989 (CDP) (.31sec/308m)	2.312 (CDP) (.35sec/405m)	-	3.744 (CDP) (.50sec/936m)	4.7±0.4 (Line 1) (.42sec/987m)	5.9±0.6 (Line 1) (1.25sec/3,688m)	-0- Tot. to "B"= 6,846m
19	0804Z (CDP)	1.742 (CDP) (.68sec/592m)	2.154 (CDP) (.22sec/237m)	2.389 (CDP) (.15sec/179m)	-	3.788 (CDP) (.78sec/1,477m)	4.2±0.3 (Line 1) (.30sec/630m)	5.6±0.8 (Line 1) (.49sec/1,372m)	-0- Tot. to "B"= 4,487m
20	1041Z (CDP)	1.627 (CDP) (.61sec/496m)	2.304 (CDP) (.24sec/276m)	2.367 (CDP) (.10sec/118m)	-	4.2±0.3 (Line 1) (.67sec/1,407m)	4.2±0.3 (Line 1) (.34sec/714m)	5.6±0.8 (Line 1) (.44sec/1,232m)	-0- Tot. to "B"= 4,243m
21	1313Z (CDP)	1.752 (CDP) (.59sec/517m)	2.320 (CDP) (.25sec/290m)	2.320 (CDP) (.15sec/174m)	-	3.196 (CDP) (.54sec/863m)	3.354 (CDP) (.28sec/470m)	4.7±0.3 (Line 4) (.14sec/329m)	-0- Tot. to "B"= 2,643m
22	1702Z (CDP)	1.626 (CDP) (.59sec/480m)	2.153 (CDP) (.42sec/452m)	2.573 (CDP) (.24sec/309m)	-	3.323 (CDP) (.45sec/748m)	3.740 (CDP) (.44sec/823m)	4.7±0.3 (Line 4) (.1.12sec/2,632m)	-0- Tot. to "B"= 5,444m
23	2030Z (CDP)	1.628 (CDP) (.68sec/554m)	2.534 (CDP) (.39sec/494m)	2.562 (CDP) (.31sec/397m)	-	3.026 (CDP) (.48sec/726m)	3.469 (CDP) (.48sec/833m)	4.7±0.3 (Line 4) (.2.48*sec/5,828m)	-0- (?) Tot. to "B"=8,832m
31	0314Z (CDP)	1.503 (CDP) (.52sec/391m)	1.933 (CDP) (.37sec/358m)	2.683 (CDP) (.12sec/161m)	-	3.104 (CDP) (.68sec/1,055m)	3.433 (CDP) (.33sec/566m)	4.7±0.3 (Line 4) (.2.78sec/6,533m) extrapolation, Line 4	-0- (?) Tot. to "B"=9,064
31	0730Z (CDP)	1.623 (CDP) (.44sec/357m)	1.623 (CDP) (.33sec/268m)	2.544 (CDP) (.11sec/140m)	-	3.578 (CDP) (.66sec/1,181m)	4.147 (CDP) (.28sec/581m)	4.644 (CDP) (.10sec/232m)	-0- Tot. to "B"= 2,759m
32	0932Z (CDP)	1.619 (CDP) (.49sec/397m)	1.619 (CDP) (.27sec/219m)	1.619 (CDP) (.05sec/40m)	-	3.328 (CDP) (.63sec/1,048m)	3.328 (CDP) (.16sec/266m)	3.588 (CDP) (.17sec/305m)	*3.8±.8 (.14sec/266m) Tot. to "K"=2,275m Tot. to "B"=2,541m

Table II (continued)

Reel (SB)	Time	*Bottom-Tert. unc. (G. of M.) Bottom - "x" B to 1 1 to "x"	"x" - 2 (1 - 2)	2 - 3	3 - "z"	3 - 4	4 - "z"	Tert. unc. - "k" "z" - "k"	*Tert. unc. - "B" "k" - Basement
32	1206Z (CDP)	1.629(CDP) (.42sec/342m)	2.497(CDP) (.25sec/312m)	2.497(CDP) (.04sec/50m)	3.245(CDP) (.78sec/1,266m)	-	-	3.245(CDP) (.27sec/357m)	4.1±.4(Line 4) (.19sec/390m) Tot. to "K"=2,327m Tot. to "B"=2,717m
33	1339Z (CDP)	1.503(CDP) (.35sec/263m)	1.503(CDP) (.12sec/90m)	-	2.699(av,CDP) (.72sec/972m)	-	-	3.273(CDP) (.21sec/344m)	3.273(CDP) (.13sec/213m) Tot. to "K"=1,669m Tot. to "B"=1,882m
34	1553Z (CDP)	1.630(CDP) (.38sec/310m)	1.630(CDP) (.26sec/212m)	2.561 (.03sec/38m)	2.706(av,CDP) (.56sec/758m)	-	-	3.457(CDP) (.31sec/536m)	-0- Tot. to "B"= 1,854m
35	1951Z (CDP)	1.628(CDP) (.49sec/399m)	2.465(av,CDP) (.66sec/813m)	2.465(av,CDP) (.17sec/210m)	-	3.7±.3(4) (.44sec/814m)	4.7±.3(4) (.27sec/634m)	4.7±.3(4) (2.07sec/4,864m)	-0- (?) Tot. to "B"=7,734
36	2200Z (CDP)	1.747(CDP) (.46sec/402m)	2.358(CDP) (.62sec/731m)	3.397(av,CDP) (.18sec/306m)	-	3.397(av,CDP) (.60sec/1,019m)	4.729(CDP) (.37sec/875m)	*4.729(CDP) (2.59sec/6,124m)	-0- (?) Tot. to "B"=9,457m
37	0034Z (CDP)	1.502(CDP) (.45sec/338m)	2.060(CDP) (.44sec/453m)	2.632(CDP) (.16sec/211m)	-	3.747(av,CDP) (.59sec/1,105m)	4.862(CDP) (.31sec/754m)	(?)4.862(CDP) (2.05sec/4,984m) (?)	-0- (?) Tot. to "B"=7,845
38	0530Z (CDP)	1.860(CDP) (.54sec/502m)	1.860(CDP) (.30sec/279m)	2.724(CDP) (.23sec/313m)	-	3.304(CDP) (.52sec/859m)	3.770(CDP) (.29sec/547m)	5.034(CDP) (1.06sec/2,668m) (?)	-0- (?) Tot. to "B"=5,168m
38	0839Z (CDP)	1.628(CDP) (.54sec/440m)	2.415(CDP) (.34sec/411m)	2.997(av,CDP) (.30sec/450m)	-	3.800(CDP) (.50sec/950m)	4.761(av,CDP) (.54sec/1,285m)	4.761(av,CDP) (.82sec/1,952m)	-0- (?) Tot. to "B"=5,488m
39	1026Z (CDP)	1.502(CDP) (.60sec/451m)	2.419(CDP) (.29sec/351m)	2.449(av,CDP) (.31sec/380m)	-	3.410(av,CDP) (.53sec/904m)	3.641(CDP) (.51sec/928m)	5.9±.06(Line 1) (.72sec/2,124m)	-0- (?) Tot. to "B"=5,138m
39	1250Z (CDP)	1.742(CDP) (.55sec/479m)	2.551(av,CDP) (.41sec/523m)	3.143(CDP) (.26sec/409m)	-	3.792(av,CDP) (.60sec/1,138m)	4.512(CDP) (.58sec/1,308m)	5.9±0.6(Line 1) (.84sec/2,478m)	-0- (?) Tot. to "B"=6,335m
42	2234Z (CDP)	2.062(av,CDP) (.99sec/1,021m)	3.043(CDP) (.41sec/624m)	4.396(CDP) (.56sec/1,231m)	4.7 0.4(Line 1) (.71sec/1,668m)	-	-	5.9±0.6(Line 1) (.47sec/1,386m)	-0- (?) Tot. to "B"=5,930m
42	0010Z (CDP)	1.962(av,CDP) (.87sec/853m)	2.263(CDP) (.37sec/419m)	3.139(CDP) (.45sec/706m)	4.555(CDP) (.67sec/1,526m)	-	-	5.6±0.8(line 1) (.44sec/1,232m)	-0- (?) Tot. to "B"=4,736m
43	0225Z (CDP)	1.742(av,CDP) (.69sec/601m)	2.376(CDP) (.43sec/511m)	2.685(CDP) (.34sec/456m)	5.284(CDP) (.52sec/1,374m)	-	-	5.284(CDP) (.28sec/740m)	*3.8±.8 (.30sec/570m) Tot. to "K"=3,682m Tot. to "B"=4,252m
44	0817Z (CDP)	*1.891(CDP) (.33sec/312m)	-	-	-	-	-	*2.245(CDP) (.47sec/528m)	3.372(CDP) (1.04sec/1,753m) Tot. to "K"=640m Tot. to "B"=2,593m
45	1111Z (CDP)	*1.596(CDP) (.46sec/367m)	-	-	-	-	-	-	*2.092(CDP) (.97sec/1,015m) Tot. to Tert. unc=367m Tot. to "B"=1,382m
37	0253Z (CDP)	1.503(CDP) (.46sec/346m)	1.503(CDP) (.32sec/240m)	2.939(CDP) (.23sec/338m)	-	3.401(CDP) (.59sec/1,003m)	3.472(CDP) (.39sec/677m)	5.039(CDP) (1.87sec/4,711m)	-0- (?) Tot. to "B"=7,315m

Table II (continued)

Reel (SB)	Time	*Bottom-Tert.unc **Bottom-"B" Bottom - "X" B to 1 1 to "X"	* "X" - 3 "X" - 2 (1 - 2)	*Tert.unc.- 3 2 - 3	* -Tert. unc.- "Z" 3 - "Z"	3 - 4	4 - "Z"	*assuming overall sed. thickness of 5.0 sec. (tt) "Z" - "K"	*Tert. unc. - "B" "K" - Basement
46	1446Z (CDP)	**1.931(av, CDP) (.08sec/77m)	-	-	-	-	-	-	- Tot. to "B"=77m
48	NO	DATA							
51	NO	DATA							
52	NO	DATA							
56	2337Z (CDP)	*1.785(CDP) (.20sec/178m)	-	-	-	-	-	-	±.879(CDP) *3.018(av) (Tr basin) (.98sec/1,479m) Tot. to "B"=1,657m Tot. to unc.=178m
57	0225Z (CDP)	*1.840(CDP) (.33sec/304m)	-	-	*2.060(CDP) (.16sec/165m)	-	-	2.060(CDP) (.12sec/124m)	2.971±.585(av, CDP) (.41sec/609m) Tot. to "K"=593m Tot. to "B"=1,202m
58	0902Z (CDP)	1.626(av, CDP) (.35sec/285m)	1.626(av, CDP) (.14sec/114m)	1.830(CDP) (.17sec/156m)	2.498(av, CDP) (.87sec/1,087m)	-	-	3.779(CDP) (.47sec/888m)	3.7±.6 (Line 4) (.35sec/648m) Tot. to "K"=2,530m Tot. to "B"=3,178m
59	1122Z (CDP)	1.674(av, CDP) (.38sec/318m)	1.674(av, CDP) (.20sec/167m)	1.674(av, CDP) (.24sec/201m)	-	2.388(CDP) (.56sec/669m)	2.890(CDP) (.32sec/462m)	3.1±.3(Line 4) (.37sec/574m)	4.1±.4 (Line 4) (.33sec/676m) Tot. to "K"=2,391m Tot. to "B"=3,067m
60	1354Z (CDP)	1.771(av, CDP) (.42sec/372m)	2.037(CDP) (.20sec/204m)	2.260(CDP) (.23sec/260m)	-	2.667(CDP) (.60sec/800m)	3.715(CDP) (.32sec/594m)	4.7±.3(Line 4) (.60sec/1,410m)	-0- Tot. to "B"=3,630m
61	1854Z (CDP)	1.635(CDP) (.49sec/401m)	2.376(CDP) (.27sec/321m)	3.257(CDP) (.32sec/521m)	-	3.388(CDP) (.57sec/966m)	3.388(CDP) (.32sec/542m)	4.7±.3(Line 4) (2.08sec/4,888m)	-0- Tot. to "B"=7,639m
62	2106 (CDP)	1.874(av, CDP) (.57sec/534m)	2.761(CDP) (.18sec/248m)	3.460(CDP) (.58sec/1,003m)	-	4.214(CDP) (.53sec/1,117m)	4.214(CDP) (.21sec/442m)	*4.7±.3(Line 4) (2.77sec/6,510m)	-0- (?) Tot. to "B"=9,854m
68	0205Z (CDP)	1.634(av, CDP) (.67sec/547m)	2.901(av, CDP) (.42sec/609m)	2.901(av, CDP) (.23sec/334m)	-	3.375(CDP) (.55sec/928m)	3.375(CDP) (.33sec/557m)	*4.7±.3(Line 4) (2.55sec/5,992m)	-0- (?) Tot. to "B"=8,967m
69	0726Z (CDP)	1.502(CDP) (.42sec/315m)	1.502(CDP) (.41sec/308m)	2.427(CDP) (.11sec/133m)	-	3.160(CDP) (.62sec/980m)	3.160(CDP) (.18sec/284m)	4.7±.3(Line 4) (.09sec/212m)	-0- Tot. to "B"=2,232m
70	1338Z (CDP)	1.503(CDP) (.39sec/293m)	*1.503(CDP) (.16sec/120m)	-	2.528(CDP) (.66sec/834m)	-	-	2.969(CDP) (.12sec/178m)	-0- Tot. to "B"=1,425m
71	1602Z (CDP)	*1.649(CDP) (.46sec/379m)		*2.057(CDP) (.08sec/82m)	2.747(CDP) (.44sec/604m)	-	-	2.747(CDP) (.19sec/261m)	3.416(av, CDP) (.95sec/1,623m) Tot. to "K"=1,326m Tot. to "B"=2,949m

Table II (continued)

Reel (SB)	Time	*Bottom-Tert. unc. (Gulf of Maine)	"X" - 2 (1 - 2)	*2 - Basement 2 - 3	*3 - Basement 3 - "Z"	3 - 4	4 - "Z"	"Z" - "X"	*Tert. unc. - Basement "X" - Basement
		Bottom - "X" B to 1 1 to "X"		-0- *2.256(CDP) (Not Tr-3"Z" interval) (.30sec/338m) Tot. to unc=176m "B" Vp(CDP)=5.658(?) Tot. to "B"=514m					
72	1934Z (CDP)	*1.752(CDP) (.20sec/176m)	-	-	-	-	-	-	
72	2301Z (CDP)	1.524(CDP) (.23sec/175m)							*3.382(av,CDP)Tr basin (2.45sec/4,143m) Tot. to unc= 175m. Tot. to "B"=4,318m
73	0154Z (CDP)	*1.506(CDP) (.26sec/196m)	-	-	-	-	-	-	*3.975(av,CDP)Tr basin (1.17sec/2,325m) Tot. to unc= 196m. Tot. to "B"=2,521m
74	0527Z (CDP)	**1.502(CDP) (.12sec/90m)							Tot. to "B"=90m
75	0831Z (CDP)	**1.506(CDP) (.18sec/136m)	-	-	-	-	-	-	Tot. to "B"=136m
76	0536Z (CDP)	*1.504(CDP) (.27sec/203m)							*3.675(av,CDP)Tr basin (1.86sec/3,418m) Tot. to unc= 203m. Tot. to "B"=3,621m
77	1030Z (CDP)	1.578(av,CDP) (.36sec/284m)	2.421(CDP) (.15sec/182m)	*2.434(CDP) (.13sec/158m)	2.434(CDP) (.19sec/231m)	-	-	-	-0- Tot. to "B"=855m
78	1248Z (CDP)	1.755(av,CDP) (.47sec/412m)	2.336(CDP) (.41sec/479m)	3.118(av,CDP) (.13sec/203m)	-	3.118(av,CDP) (.50sec/780m)	4.7±.3(Line 4) (.50sec/1,175m)	*4.7±.3(Line 4) (2.63sec/6,180m)	-0- (?) Tot. to "B"=9,229m
No picks Reel #79		-	-	-	-	-	-	-	-
95	0840Z (CDP)	1.511(CDP) (.38sec/287m)	2.234(CDP) (.51sec/570m)	2.234(CDP) (.11sec/123m)	-	4.432(av,CDP) (.39sec/864m)	4.7±.3(Line 4) (.38sec/893m)	*4.7±.3(Line 4) (2.81sec/6,604m)	-0- (?) Tot. to "B"=9,341m
95	1119Z (CDP)	1.515(CDP) (.41sec/311m)	2.242(CDP) (.23sec/258m)	2.918(CDP) (.17sec/248m)	-	4.134(av,CDP) (.36sec/744m)	4.134(av,CDP) (.27sec/558m)	4.7±.3(Line 4) (.16sec/376m)	-0- Tot. to "B"=2,495m
96	1344Z (CDP)	1.508(CDP) (.24sec/181m)	2.310(CDP) (.22sec/254m)	*2.532(CDP) (.05sec/63m)	-	-	-	-	-0- Tot. to "B"=498m
97	1729Z (CDP)	*1.539(CDP) (.19sec/146m)	-	-	-	-	-	-	*1.836(CDP) (.17sec/156m) Tot. to "B"=302m
98	1945Z (CDP)	*1.508(CDP) (.18sec/136m)							*4.035(av,CDP)Tr basin (1.80sec/3,632m) Tot. to unc.= 136m. Tot. to "B"=3,768m
98	2148Z (CDP)	*1.510(CDP) (.15sec/113m)	-	-	-	-	-	-	*3.498(av,CDP)Tr basin (.90sec/1,574m) Tot. to unc= 113m. Tot. to "B"=1,687m

Table II (continued)

Reel (SB)	Time	Bottom - "X" (Δ) B to 1 (□) 1 to "X"	(Φ) 1 - Basement "X" - 2 (1 - 2)*	2 - 3	3 - "Z"	3 - 4	4 - "Z"	"Z" - "K"	"K" - Basement
99	0242Z (CDP)	**1.506(CDP) (.24sec/181m)	-	-	-	-	-	-	- Tot. to "B"=181m
No Picks (Reel #100)									
101	0844Z (CDP)	(Δ)1.506(CDP) (.35sec/264m) (□)1.791(CDP) (.19sec/170m)	2.087(CDP) (.25sec/261m)	2.080(CDP) (.11sec/114m)	-	2.080(CDP) (.08sec/83m)	2.973(av, CDP) (.39sec/580m)	3.353(CDP) (.29sec/486m)	-0- Tot. to "B"=1,958m
102	1020Z (CDP)	(Δ)1.834(av, CDP) (.45sec/413m) (□)2.021(CDP) (.14sec/141m)	2.064(CDP) (.39sec/402m)	2.454(CDP) (.06sec/74m)	-	2.454(CDP) (.15sec/184m)	3.388(CDP) (.48sec/813m)	3.388(CDP) (.30sec/508m)	-0- Tot. to "B"=2,535m
110	1739Z (CDP)	(Δ)2.636(av, CDP) (.55sec/450m)	*2.446(av, CDP) (.31sec/379m)	2.753(CDP) (.09sec/124m)	-	2.773(CDP) (.18sec/250m)	2.819(CDP) (.25sec/352m)	2.819(CDP) (.19sec/268m)	-0- Tot. to "B"=1,823m
111	2208Z (CDP)	(Δ)1.512(CDP) (.12sec/91m)	(Φ)1.675(CDP) (.17sec/142m)	-	-	-	-	-	-0- Tot. to "B"=233m
112	0420Z (CDP)	**1.654(av, CDP) (.21sec/174m)	-	-	-	-	-	-	-0- Tot. to "B"=174m
113	0851Z (CDP)	(Δ)1.512(CDP) (.16sec/121m) (□)1.975(CDP) (.12sec/118m)	1.975(CDP) (.34sec/336m)	1.975(CDP) (.13sec/128m)	-	1.975(CDP) (.04sec/40m)	1.975(CDP) (.18sec/178m)	3.642(CDP) (.05sec/91m)	-0- Tot. to "B"=1,012m
115	1408Z (CDP)	(Δ)2.004(av, CDP) (.78sec/782m)	*2.830(CDP) (.61sec/863m)	2.830(CDP) (.06sec/85m)	-	2.830(CDP) (.07sec/99m)	3.554(CDP) (.36sec/640m)	3.788(CDP) (.22sec/417m)	-0- Tot. to "B"=2,886m
122	2001Z (CDP)	(Δ)1.507(CDP) (.36sec/271m) (□)2.052(CDP) (.17sec/174m)	2.052(CDP) (.57sec/585m)	2.292(CDP) (.06sec/69m)	-	2.636(CDP) (.12sec/158m)	3.846(CDP) (.22sec/423m)	3.846(CDP) (.16sec/308m)	-0- Tot. to "B"=1,988m
123	0313Z (CDP)	(Δ)1.508(CDP) (.35sec/264m) (□)1.964(CDP) (.15sec/147m)	1.964(CDP) (.50sec/491m)	4.027(CDP) (.03sec/60m)	-	4.027(CDP) (.10sec/201m)	4.027(CDP) (.20sec/403m)	4.027(CDP) (.14sec/282m)	-0- Tot. to "B"=1,848m
124	0637Z (CDP)	(Δ)1.648(av, CDP) (.77sec/634m)	*1.740(CDP) (.33sec/287m)	1.900(CDP) (.04sec/39m)	-	1.900(CDP) (.13sec/124m)	2.124(CDP) (.32sec/340m)	3.002(CDP) (.27sec/405m)	-0- Tot. to "B"=1,828m
126	1431Z (CDP)	(Δ)1.742(av, CDP) (.42sec/366m) (□)1.980(av, CDP) (.06sec/59m)	1.980(av, CDP) (.36sec/356m)	1.980(av, CDP) (.10sec/99m)	-	2.282(CDP) (.47sec/536m)	4.743(SB#27) (.45sec/1,067m)	4.743(SB#27) (.2,80sec/6,640m)	-0-(?) Tot. to "B"=9,123m
127	1746Z (CDP)	1.844(av, CDP) (.43sec/396m)	1.888(CDP) (.18sec/170m)	1.888(CDP) (.12sec/113m)	1.888(CDP) (.54sec/510m)	-	-	3.500(CDP) (.18sec/315m)	-0- Tot. to "B"=1,504m
129	0457Z (CDP)	1.624(av, CDP) (.42sec/341m)	1.624(CDP) (.18sec/146m)	1.983(CDP) (.12sec/119m)	2.103(CDP) (.76sec/799m)	-	-	2.892(CDP) (.35sec/506m) Tot. to "K"= 2.207m	3.117(av, CDP) (1.19sec/1,855m) Tot. to "B"= 4.062m
131	0739Z (CDP)	1.632(av, CDP) (.39sec/318m)	1.985(CDP) (.22sec/218m)	2.054(CDP) (.18sec/185m)	-	2.298(av, CDP) (.53sec/609m)	3.143(av, CDP) (.47sec/739m)	3.143(av, CDP) (.26sec/409m) Tot. to "K"= 2.478m	3.828(CDP) (.33sec/631m) Tot. to "B"= 3,109m

Table II (continued)

Reel (SB)	Time	Bottom - "X" B to 1 (Δ) 1 to "X" (□)	*"X" - 3			3 - "Z"	3 - 4	4 - "Z"	"Z" - "K"	*Taken from Ballard and Uchupi (1975) "K" - Basement
			"X" - 2 (1 - 2)	2 - 3						
135	0103Z (CDP)	1.636 (av, CDP) (.57sec/466m)	2.068 (CDP) (.40sec/414m)	2.293 (CDP) (.35sec/401m)	-	2.471 (CDP) (.54sec/667m)	3.343 (CDP) (.34sec/568m)	4.7±.3 (Line 4) (2.64sec/6,204m)	-0-(?) Tot. to "B"=8,720m	
136	0657Z (CDP)	1.628 (CDP) (.50sec/407m)	2.390 (CDP) (.30sec/358m)	2.390 (CDP) (.03sec/36m)	-	3.346 (CDP) (.63sec/ 1,054m)	4.7±.3 (Line 4) (.38sec/893m)	4.7±.3 (Line 4) (.06sec/141m) Tot. to "K"= 2,889m	3.8±.8* (.46sec/874m) Tot. to "B"= 3,763m	
137	0915Z (CDP)	1.618 (CDP) (.39sec/316m)	1.618 (CDP) (.37sec/299m)	1.618 (CDP) (.07sec/57m)	-	3.152 (CDP) (.64sec/ 1,009m)	4.7±.3 (Line 4) (.36sec/846m)	4.7±.3 (Line 4) (.10sec/235m)	-0- Tot. to "B"= 2,762m	
138	1137Z (CDP)	1.503 (CDP) (.42sec/316m)	2.010 (av, CDP) (.61sec/613m)	2.010 (av, CDP) (.10sec/100m)	-	3.275 (CDP) (.63sec/ 1,032m)	4.7±.3 (Line 4) (.36sec/846m)	4.7±.3 (Line 4) (.11sec/258m)	-0- Tot. to "B"= 3,165m	
139	1507Z (CDP)	1.849 (CDP) (.49sec/453m)	2.248 (av, CDP) (.72sec/809m)	2.248 (av, CDP) (.08sec/90m)	-	3.204 (CDP) (.65sec/ 1,041m)	4.7±.3 (Line 4) (.38sec/893m)	4.7±.3 (Line 4) (.09sec/212m)	-0- Tot. to "B"= 3,498m	
140	1940Z (CDP)	1.507 (CDP) (.44sec/332m)	*2.602 (CDP) (.71sec/924m) (approx. 859m) (approx. 65m)		-	3.000 (av, CDP) (.64sec/960m)	4.672 (SB#23) (.38sec/888m)	4.672 (SB#23) (2.46sec/5,747m)	-0-(?) Tot. to "B"= 8,851m	
141	0036Z (CDP)	(Δ) 1.504 (CDP) (.46sec/346m) (□) 2.058 (CDP) (.21sec/216m)	2.158 (CDP) (.36sec/388m)	2.184 (CDP) (.12sec/131m)	-	2.184 (CDP) (.13sec/142m)	3.532 (CDP) (.38sec/671m)	3.532 (CDP) (1.00sec/1,766m)	-0- Tot. to "B"= 3,660m	
141	0407Z (CDP)	(Δ) 1.858 (av, CDP) (.85sec/790m)	*2.736 (CDP) (.20sec/274m)	3.087 (CDP) (.12sec/185m)	-	3.087 (CDP) (.12sec/185m)	3.210 (CDP) (.32sec/514m)	(SB#30) 5.203±.291 (av) (.40sec/1,041m)	-0- Tot. to "B"= 2,989m	
No V-picks reel #142										
143	0909Z (CDP)	(Δ) 1.503 (CDP) (.34sec/256m) (□) 1.503 (CDP) (.20sec/150m)	2.130 (av, CDP) (.58sec/618m)	3.367 (CDP) (.08sec/135m)	-	3.494 (CDP) (.11sec/192m)	3.494 (CDP) (.28sec/489m)	5.118 (SB#36) (.18sec/461m)	-0- Tot. to "B"= 2,301m	
159	2359Z (CDP)	1.503 (CDP) (.59sec/443m)	2.544 (CDP) (.31sec/394m)	2.681 (CDP) (.37sec/496m)	-	2.681 (CDP) (.50sec/670m)	3.029 (CDP) (.37sec/560m)	4.7±.3 (Line 4) (1.59sec/3,736m)	-0- Tot. to "B"=6,229m	
159	0324Z (CDP)	1.502 (CDP) (.63sec/473m)	2.138 (CDP) (.36sec/385m)	3.025 (CDP) (.42sec/635m)	-	3.906 (CDP) (.47sec/918m)	4.7±.4 (Line 1) (.49sec/1,152m)	5.9±.6 (Line 1) (1.33sec/3,924m)	-0- Tot. to "B"=7,487	
160	0701Z (CDP)	1.747 (CDP) (.65sec/568m)	2.301 (CDP) (.29sec/334m)	2.530 (CDP) (.48sec/607m)	-	2.726 (CDP) (.51sec/695m)	4.7±.4 (Line 1) (.51sec/1,198m)	5.9±.6 (Line 1) (.95sec/2,802m) Tot. to "K"=6,204m	*3.8±.8 (.17sec/323m) Tot. to "B"=6,527m	
162	1301Z (CDP)	1.731 (av, CDP) (.95sec/822m)	2.045 (CDP) (.43sec/440m)	2.295 (CDP) (.53sec/608m)	-	3.144 (av, CDP) (.69sec/ 1,085m)	5.2±.3 (Line 1) (.46sec/1,196m)	5.9±.6 (Line 1) (.68sec/2,006m)	-0- Tot. to "B"= 6,157m	
163	2046Z (CDP)	2.112 (av, CDP) (1.12sec/1,183m)	3.144 (CDP) (.59sec/928m)	3.450 (av, CDP) (.49sec/845m)	-	5.2±.3 (Line 1) (1.06sec/ 2,756m)	5.2±.3 (Line 1) (.43sec/1,118m)	5.9±.6 (Line 1) (.51sec/1,504m)	-0- Tot. to "B"= 8,334m	
No V-picks reels #169-172										
173	0453Z (CDP)	1.727 (CDP) (.33sec/285m)	1.852 (av, CDP) (.26sec/241m)	1.969 (CDP) (.20sec/197m)	2.235 (CDP) (.37sec/413m)	-	-	2.606 (CDP) (.45sec/586m) Tot. to "K"=1,722m	2.866 (CDP) (.53sec/759m) Tot. to "B"=2,481m	

Table II (continued)

Reel (SB)	Time	Bottom-"X" B to 1 1 to "X"	"X"-2 (1-2)	2 - 3	3 - "Z"	3 - 4	4 - "Z"	"Z" - "K"	"K" - Basement
175	1011Z (CDP)	1.619 (CDP) (.35sec/283m)	1.619 (CDP) (.26sec/210m)	2.285 (CDP) (.48sec/548m)	3.231 (CDP) (.51sec/824m)	-	-	3.354 (CDP) (.83sec/1,392m) Tot. to "K"= 3,257m	3.939 (CDP) (1.46sec/2,875m) Tot. to "B"= 6,132m
177	1750Z (CDP)	1.791 (av, CDP) (.74sec/663m)	2.704 (av, CDP) (.58sec/784m)	2.891 (CDP) (.43sec/622m)	-	2.891 (CDP) (.17sec/246m)	3.892 (CDP) (.50sec/973m)	4.7±.5 (Lines) (1.69sec/3,972m)	-0- (?) Tot. to "B"= 7,260m
181	1039Z (CDP)	1.794 (av, CDP) (.69sec/619m)	2.177 (CDP) (.36sec/392m)	2.437 (CDP) (.40sec/487m)	-	2.954 (CDP) (.57sec/842m)	3.884 (CDP) (.35sec/680m)	4.7±.5 (Line 5) (1.40sec/3,290m)	-0- (?) Tot. to "B"= 6,310m

Table III. Time-to-Depth Conversions, Average All-91 CDP/Sonobuoy Results

Reel (SB)	Time	***Tert. unc. - "X" *Bottom-Tert. unc. **Bottom-Base-ment Bottom-"X" (Δ) B to 1 1 to "X"	**"X"-3 "X"-2 (1-2)*	*Tert. unc.-3 2 - 3	3 - "2"	3 - 4	4 - "2"	*Assuming Overall Sediment Section of 5.0 sec(tt) "2"- "K"	*Taken from Ballard and Uchupi (1975) "K"-Basement
10 (6)	1424Z	1.742 (CDP) (.60sec/523m)	2.102±.036(av) (.32sec/336m)	2.634±.162 (av) (.37sec/487m)	-	3.394±.148(av) (.51sec/866m)	3.811(SB) (.51sec/972m)	5.9±.6(Line 1) (.88sec/2,596m)	Total to "B" (-0-)5,780m
21 (8)	1521Z	1.724(CDP) (.55sec/447m)	2.685±.124(av) (.38sec/511m)	4.054(SB) (.24sec/486m)	-	4.054(SB) (.43sec/872m)	4.054(SB) (.42sec/851m)	4.7±.3(Line 4) (.82sec/1,927m)	Tot. to "B" (-0-)5,094±
34 (11)	1722Z	1.876(SB) (.37sec/347m)	2.157(SB) (.47sec/507m)	2.620±.098(av) (.11sec/144m)	-	2.620±.098(av) (.39sec/511m)	4.098(SB) (.20sec/410m)	4.7±.3(Line 4) (.49sec/1,152m)	-0- Tot. to "B"=3,071m
40 (12)	1453Z	1.713±.168(av) (.60sec/514m)	2.452±.086(av) (.46sec/564m)	3.504±.014(av) (.28sec/491m)	-	3.504±.014(av) (.54sec/946m)	4.7 0.4(Line 1) (.66sec/1,551m)	5.9±0.6(Line 1) (.96sec/2,832m)	-0- Tot. to "B"=6,898±
41 (13)	2029Z(CDP) 2046Z - 2252Z(SB)	(of averages) 2.085±.020(av) (1.05sec/ 1,095m)	2.634±.072(av) (.44sec/580m)	4.012(SB) (.60sec/1,204m)	-	4.012(SB) (.57sec/1,143m)	6.261(SB) (.53sec/1,659m)	6.261(SB)	-0-(?) Tot. to "B"=6,839m
43 (14)	0519Z	1.762(CDP) (.51sec/449m)	1.957±.018(av) (.19sec/186m)	2.642±.086(av) (.19sec/251m)	2.642±.086(av) (.41sec/542m)	-	-	3.344±.167(av) (.19sec/318m) Tot. to "K"= 1,746m	3.344±.167 (av)(.32sec/ 535m) Tot. to "B"=3,231m
47 (15)	(no CDP) 1537- 1719Z(SB)	**1.517(SB) (.07-.20sec/ 53-152m)	-	-	-	-	-	-	-0- Tot. to "B"=53-152m "Basement" Vp=5.692(SB)
49 (16)	0151Z(CDP) 0119- 0310Z(SB)	*1.523(CDP) (.22sec/168m)	-	1.727(CDP) (.14sec/121m)	3.232±.080(av) (.19sec/307m)	-	-	3.232±.080(av) (.08sec/129m) Tot. to "K"= 725m	3.278±.164 (av)(.56sec/ 918m) Tot. to "B"=1,643m
53 (17)	1416Z(CDP) 1332- 1557Z(SB)	*1.657(CDP) (.13sec/108m) ***1.935(CDP) (.14sec/135m)	*1.954±.116(av) (.25sec/244m)	-	1.954±.116(av) (.17sec/166m)	-	-	1.954±.116(av) (.13sec/127m) Tot. to "K"= 780m	1.954±.116 (av)(.36sec/ 352m) Tot. to "B"=1,132m
57- 58 (18)	0508Z	1.656±.018(av) (.35sec/290m)	2.064±.105(av) (.14sec/144m)	2.064±.105(av) (.13sec/134m)	2.494±.048(av) (.33sec/407m)	-	-	2.494±.048(av) (.26sec/324m)	-0- Tot. to "B"=1,299m "Basement" Vp=5.660(SB)
61 (19)	1653Z	1.633(CDP) (.46sec/376m)	2.229(CDP) (.23sec/256m)	2.666±.223(av) (.29sec/387m)	-	3.530±.220(av) (.59sec/1,041m)	5.235±.535(av) Line 4/SB#19 (.44sec/1,151m)	5.235±.535(av) Line 4/SB#19 (.86sec/2,251m) Tot. to "K"= 5,462m	*3,8±.8 (.39sec/741d 741m) Tot. to "B"=6,203±
68 (21)	0453Z	1.631(CDP) (.47sec/383m)	1.960(CDP) (.59sec/578m)	3.252±.124(av) (.19sec/309m)	-	3.252±.124(av) (.55sec/894m)	5.155(SB) (.29sec/748m)	5.155(SB) (3.21sec/8,274m)	-0- Tot. to "B"=11,186m
70 (22)	1138Z	2.029(SB) (.43sec/436m)	2.294(SB) (0.0-0m) just N of pinchout	2.294(SB) (.17sec/195m) (X-3 interval)	-	2.472±.489(av) (.55sec/680m)	3.034±.018(av) (.19sec/288m)	3.034±.018(av) (.05sec/76m)	*3,8±.15 sec/285m) Tot to "K"=1,675 m. Tot. to "B"=1,960m "Basement" Vp=6.536(SB)
78 (23)	1606Z	1.742±.066(av) (.46sec/401m)	2.180±.132(av) (.73sec/796m)	2.312±.090(av) (.12sec/139m)	-	4.672(SB) (.47sec/1,098m)	4.672(SB) (.54sec/1,261m)	4.672(SB) (=2.43sec/5,723m)	-0-(?) Tot. to "B"=9,418 m(1)
94 (27)	0546Z	1.798±.369(av) (.46sec/414m)	2.225±.094(av) (.64sec/712m)	3.314(SB) (.21sec/348m)	-	4.743(SB) (.30sec/711m)	4.743(SB) (.36sec/854m)	4.743(SB) (=2.67sec/6,332m)	-0-(?) Tot. to "B"=9,371
110 (30)	1203Z	2.092±.585(Δ) (1.25sec/1,308)	2.677±.071 (.07sec/94m)	2.677±.071 (.11sec/147m)	-	5.203±.291(av) (.20sec/520m)	5.203±.291(av) (.30sec/780m)	5.203±.291(av) (.36sec/937m)	-0- Tot. to "B"=3,786m

Table III (continued)

(SB)	Time	Bottom - "X" B to 1 (Δ) 1 to "X" (□)	"X" - 2 (1 - 2)	2 - 3	3 - "Z"	3 - 4	4 - "Z"	*Assuming an overall sediment section of 5.0sec(cc) "Z" - "X"	Taken from * Ballard (1974) "K" - Basement
111 (31)	1946Z (CDP) 2045Z (SB)	1.504±.006(av) (Δ) (.20sec/150m) 2.138±.126(av) (□) (.25sec/267m)	2.138±.126(av) (.17sec/182m)	3.126(SB) (.08sec/125m)	-	-	-	-	-0- Tot. to "B"= 574m "Basement" Vp=5.946(SB)
114 (32)	1218Z	1.794±.152(av) (Δ) .44sec/395m 1.794±.152(av) (□) (.10sec/90m)	2.349±.211(av) (.60sec/705m)	2.349±.211(av) (.11sec/129m)	-	4.334(SB) (.04sec/87m)	4.334(SB) (.28sec/607m)	4.334(SB) (.14sec/303m)	-0- Tot. to "B"= 2,316m
121 (35)	1743Z	1.753±.116(av) (Δ) (.73sec/640m) 1.911±.018(av) (□) (.09sec/86m)	1.945±.018(av) (.56sec/545m)	2.059±.029(av) (.11sec/113m)	-	2.948±.022(av) (.12sec/177m)	3.590±.573(av) (.24sec/431m)	4.114(SB) (.79sec/1,625m)	-0- Tot. to "B"= 3,617m
121 (36)	1813Z	1.730±.095(av) (Δ) (.51sec/441m) 1.934±.111(av) (□) (.25sec/242m)	2.738±.333(av) (.56sec/767m)	2.738±.333(av) (.11sec/151m)	-	3.939±.391(av) (.12sec/236m)	3.939±.391(av) (.21sec/414m)	5.118(SB) (.40sec/1,024m)	-0- Tot. to "B"= 3,275m "Basement" Vp=5.919(SB)
123 (37)	2257Z (CDP) 0004Z (SB)	(Δ) 1.700±.026(av) (.36sec/306m) 1.859 (CDP) (□) (.20sec/186m)	2.366±.246(av) (.68sec/804m)	2.534±.055(av) (.07sec/89m)	-	2.534±.055(av) (.07sec/89m)	2.534±.055(av) (.24sec/304m)	2.534±.055(av) (.19sec/241m)	-0- Tot. to "B"= 2,019m "Basement" Vp=4.764(SB)
125 (38)	0831Z	(Δ) 1.774±.156(av) (.54sec/479m) (□) 2.180±.138(av) (.08sec/87m)	2.452±.134(av) (.42sec/515m)	2.452±.134(av) (.10sec/123m)	-	2.700±.114(av) (.11sec/148m)	3.988±.876(av) (.41sec/818m)	4.559(SB) (.11sec/251m)	-0- Tot. to "B"= 2,421m
125 (39/ 40)	1049Z (CDP) 1120Z (SB)	(Δ) 1.892±.264(av) (.50sec/473m) 1.892±.264(av) (□) (.15sec/142m)	1.892±.264(av) (.33sec/312m)	2.384±.288(av) (.12sec/143m)	2.726±.082(av) (.68sec/927m)	-	-	2.726±.082(av) (.27sec/368m)	-0- Tot. to "B"= 2,365m "Basement" Vp=6.444(dips 117)
127 (41)	2025Z (CDP) (1844- 2001Z) (SB)	1.716±.086(av) (.46sec/395m) 2.125 (CDP) (.28sec/298m) "X"-2		2.102±.197(av) (.10sec/210m)	2.102±.197(av) (.60sec/631m)	-	-	4.631(SB) (.23sec/533m)	-0- Tot. to "B"= 2,067m
128 (42)	0103Z (CDP) (2245- 2351Z) (SB)	1.750±.189(av) (.43sec/376m)	1.856±.189(av) (.25sec/232m)	2.075 (CDP) (.08sec/83m)	(of averages) 2.946±.019(av) (.65sec/958m)	-	-	3.627±.152(av) (.21sec/381m)	*3.8±.8 (.72sec/1,368m) Tot. to "K"=2,030m Tot. to "B"=3,398m
129 (43)	0252Z	1.634±.131(av) (.40sec/327m)	2.042±.260(av) (.22sec/225m)	2.255±.240(av) (.09sec/102m)	-	2.519±.198(av) (.66sec/831m)	2.750±.185(av) (.18sec/248m)	2.972±.172(av) (.19sec/282m)	3.743(CDP) (.91sec/1,703m) Tot. to "K"=2,015m Tot. to "B"=3,718m
132 (44)	1259Z	1.742±.030(av) (.57sec/496m)	2.100±.092(av) (.19sec/200m)	2.723±.504(av) (.28sec/381m)	-	3.208±.660(av) (.50sec/802m)	3.346±.522(av) (.33sec/552m)	4.956(?) (CDP) (.86sec/2,131m)	-0- Tot. to "B"= 4,562m
133 (45)	1603Z	1.709±.075(av) (.58sec/496m)	2.436±.314(av) (.18sec/219m)	2.436±.314(av) (.41sec/499m)	-	2.436±.314(av) (.43sec/524m)	5.737(SB) (.36sec/1,033m)	5.737(SB) (2.89sec/8,290m) (?) Guess 1*	-0- (?) Tot. to "B"=11,061m
143 (46)	1318Z (CDP) 1120Z 1220Z (SB)	(Δ) 1.682±.050(av) (.32sec/269m) 1.682±.050(av) (□) (.19sec/160m)	2.349±.191(av) (.53sec/622m)	2.576±.161(av) (.07sec/90m)	-	4.185(SB) (.10sec/209m)	4.185(SB) (.26sec/544m)	4.185(SB) (.05sec/105m)	-0- Tot. to "B"= 1,999m

Table III (continued)

Reel (SB)	Time	Bottom-"X" B to 1 1 to "X"	"X" - 2 (1 - 2)	2 - 3	3 - "Z"	3 - 4	4 - "Z"	*assuming an overall sediment section of 5.0sec(tt) "Z" - "K"	*taken from Ballard and Uchupi (1975) "K" - Basement
158 (53)	2025Z	1.879(CDP) (.69sec/648m)	2.236±.208(av) (.26sec/291m)	2.781(CDP) (.29sec/403m)	-	3.326(CDP) (.44sec/732m)	3.796(SB) (.42sec/797m)	4.7±.3(Line 4) (2.70sec/6,345m)	-0-(?) Tot. to "B"=9,216m
158 (54)	2105Z(CDP) 2205-2303 (SB)	1.884(CDP) (.66sec/622m)	2.441(CDP) (.30sec/366m)	3.254±.107(av) (.32sec/521m)	-	4.378(SB) (.46sec/1,007m)	5.104(SB) (.38sec/970m)	4.7±.3(Line 4) (2.74sec/6,439m)	-0-(?) Tot. to "B"=9,925m
161 (55)	1100Z(CDP) 1146-1303Z (SB)	1.839±.021(av) (.82sec/754m)	2.491±.149(av) (.42sec/523m)	3.566±.230(av) (.48sec/856m)	-	4.7±.04(Line 1) (.66sec/1,551m)	4.7±.04(Line 1) (.47sec/1,104m)	5.9±0.6(Line 1) (.85sec/2,508m)	-0- Tot. to "B"= 7,296m
176 (56)	1346Z(CDP) 1447-1554Z (SB)	1.868±.146(av) (of averages) (.50sec/467m)	2.112±.044(av) (.38sec/401m)	2.406±.267(av) (.45sec/541m)	3.084±.368(av) (.63sec/972m)	-	-	4.000(SB) (.98sec/1,960m)	-0- Tot. to "B"= 4,341m
182 (59)	1516Z(CDP) 1301-1429Z (SB)	1.710 ±065(av) (.56sec/479m)	2.196±.040(av) (.19sec/209m)	2.196±.040(av) (.46sec/505m)	2.966±.822(av) (of averages) (.82sec/1,216m)	-	-	3.836±.084(av) (.93sec/1,784m)	-0- Tot. to "B"= 4,193m
183 (60)	1726Z(CDP) 1618-1730Z (SB)	1.642±.139(av) (.50sec/410m)	2.192±.018(av) (.17sec/186m)	2.192±.018(av) (.34sec/373m)	2.698±.375(av) (of averages) (.79sec/1,066m)	-	-	3.788±.039(av) (of averages) (.72sec/1,364m)	3.8±.8* (1.03sec/1,957m) Tot. to "K"=3,399m Tot. to "B"=5,356m
184 (61/ 62)	2020Z	1.624±.000(av) (.38sec/309m)	1.624±.000(av) (.12sec/97m)	2.306±.034(av) (.31sec/357m)	2.598±.331(av) (.61sec/792m)	-	-	3.108±.578(av) (.63sec/979m)	-0- "Basement" Vp=5.069 Tot. to "B"= 2,534m